PHASE TRANSITIONS

PROSEMINAR IN THEORETICAL PHYSICS
INSTITUT FÜR THEORETISCHE PHYSIK
ETH ZÜRICH

SS07

typeset & compilation by H. G. Katzgraber (with help from F. Hassler)

TABLE OF CONTENTS

Chapter 1

Symmetry and ergodicity breaking, mean-field study of the Ising model

Rafael Mottl
supervisor: Dr. Ingo Kirsch

We describe a ferromagnetic domain in a magnetic material by the Ising model using the language of statistical mechanics. By heuristic arguments we show that there is no spontaneous magnetization for the nearest-neighbour Ising model in one dimension and that there is spontaneous magnetization in two and three dimensions. Three solutions are presented: the transfer matrix method in one dimension and non-zero external magnetic field, some ideas of the Onsager solution for the two-dimensional case with zero external magnetic field and the mean-field theory for arbitrary dimension and non-zero external magnetic field. Symmetry and ergodicity breaking are introduced and applied to the Ising model. The restricted ensemble is used to describe the system with broken ergodicity.

1.1 Introduction

We describe a ferromagnetic domain with spontaneous magnetization. In a correlated state of spontaneous magnetization we have an ordered system whereas above some critical temperature we observe an unordered state: a phase transition occurs at the critical temperature T_C.

This phase transition is described by an order parameter which is zero above the critical temperature (zero order) and non-zero below the critical temperature: a measure of order which is in our case of a magnetic material the magnetization M of the material.
From a general Hamiltonian with all possible spin-interaction terms we make a couple of assumptions to get to the Ising model. This model was introduced by the German physicist Ernst Ising (1900 - 1998).

1.2 FORMALISM

The analysis of the Ising model makes use of the statistical mechanical description of the system. We remember the reader of the statistical mechanical basics to introduce afterwards the definitions of phases, phase transition and critical exponents.

1.2.1 STATISTICAL MECHANICAL BASICS

We describe a certain sample region Ω of volume $V(\Omega)$ which contains a number of particles $N(\Omega)$. The analysis is based on the canonical ensemble description. The corresponding partition function is given by:

$$Z_\Omega[\{K_n\}] = \mathrm{Tr}\exp^{-\beta \mathrm{H}_\Omega(\{\mathrm{K_n}\},\{\Theta_\mathrm{n}\})}, \tag{1.1}$$

$$\beta = \frac{1}{k_B T}, \tag{1.2}$$

where the trace operator is the sum over all possible states in phase space Γ. The Hamiltonian defined on the phase space depends on the degrees of freedom Θ_n of the system (in our case: spin variables) and certain coupling constants K_n (e.g. external magnetic field).
From the partition function we can calculate the free energy

$$F_\Omega[\{K_n\}] = F_\Omega[K] = -k_B T \log Z_\Omega[K]. \tag{1.3}$$

By taking the thermodynamical limit we get the bulk free energy per site

$$f_b[K] = \lim_{N(\Omega)\to\infty} \frac{F_\Omega[K]}{N(\Omega)}. \tag{1.4}$$

As we will see below, phase boundaries are defined as the regions of non-analyticity of the bulk free energy per site. We need the thermodynamic limit in order to describe phase transitions. As the bulk free energy per site is just a finite sum over exponential terms having non-singular exponents it would be analytic everywhere. Thus phase transitions are only observed in the thermodynamical limit. By applying partial derivatives to the bulk free energy we obtain the well-known thermodynamical properties: internal energy, heat capacity, magnetization and magnetic susceptibility:

$$\epsilon_{in}[K] = \frac{\partial}{\partial \beta}(\beta f_b[K]), \tag{1.5}$$

$$C[K] = \frac{\partial \epsilon_{in}[K]}{\partial T}, \tag{1.6}$$

$$M[K] = -\frac{\partial f_b[K]}{\partial H}, \tag{1.7}$$

$$\chi_T[K] = \frac{\partial M[K]}{\partial H}. \tag{1.8}$$

1.2.2 PHASES, PHASE TRANSITIONS AND CRITICAL EXPONENTS

A phase is a region of analyticity of the bulk free energy per site. Different phases are separated by phase boundaries which are singular loci of the bulk free energy per site of dimension d - 1. We distinguish between two different kinds of phase transitions:

1. first-order phase transition: one (or more) of the first partial derivatives of the bulk free energy per site is discontinuous
2. continuous phase transition: all first derivatives of the bulk free energy per site are continuous.

For a continuous phase transition we can introduce the critical exponents which describe the behaviour of the thermodynamical properties near the phase transition:

1. heat capacity $C \sim |t|^{-\alpha}$
2. order parameter $M \sim |t|^{\beta}$
3. susceptibility $\chi \sim |t|^{-\gamma}$

4. equation of state $M \sim H^{1/\delta}$.

The first three critical exponents are defined for zero external magnetic field and t describes the deviation of the temperature from the critical temperature:

$$t = \frac{T - T_C}{T_C}. \tag{1.9}$$

The notation $\sim$ means that the described value has a singular part proportional to the given value.

1.2.3 CORRELATION FUNCTION, CORRELATION LENGTH AND THEIR CRITICAL EXPONENTS

The definition of the correlation function looks as follows:

$$G(r) := \Big\langle \, (S(r) - \langle S(r) \rangle) \, (S(0) - \langle S(0) \rangle) \, \Big\rangle, \tag{1.10}$$

where r is the location of the spin variable $S(r)$. The correlation function measures the correlation between the fluctuations of the spin variables $S(r)$ and $S(0)$. Near the critical temperature T_C we assume that the correlation function has the so called Ornstein-Zernike form

$$G(r) \simeq r^{-p} e^{-r/\xi}. \tag{1.11}$$

ξ is the correlation length, i.e. the "length scale over which the fluctuations of the microscopic degrees of freedom are significantly correlated with each other" [1]. Cooling the system down near the critical temperature, we observe the divergence of the correlation length. Finally, the critical exponents ν and η for the correlation function are defined as

$$\xi \sim |t|^{-\nu}, \quad p = d - 2 + \eta. \tag{1.12}$$

1.3 THE MODEL SYSTEM: ISING MODEL

We introduce the Ising model and want to discuss the possibility of observing spontaneous magnetization in different dimensions.

1.3.1 Characterization of the Ising model

The properties of the general spin system are the follwing:

1. periodic lattice Ω in d dimensions
2. lattice contains $N(\Omega)$ fixed points called lattice sites
3. for each site: classical spin variable $S_i = \pm 1, i = 1, \ldots, N$, in a definite direction (degrees of freedom)
4. most general Hamiltonian

$$-H_\Omega = \sum_{i\in\Omega} H_i S_i + \sum_{i,j} J_{ij} S_i S_j + \sum_{i,j,k} K_{ijk} S_i S_j S_k + \ldots \tag{1.13}$$

In order to be able to solve the problem of calculating the partition function we have to make some assumptions:

1. $K_{ijk} = 0, \ldots$, we constrain the exchange interactions to two-spin interactions,
2. $H_i \equiv H$, we assume that the external magnetic field is constant over the lattice,
3. $\sum_{i,j} \to \sum_{<ij>}$, we assume that the two-spin interactions are very short-ranged by considering only nearest-neighbour interactions,
4. $J_{ij} \equiv J$, the exchange interactions should be spatially isotropic,
5. we descibe a hypercubic lattice for which each lattice site has $z = 2d$ nearest neighbours,
6. by choosing $J > 0$, we want to describe a ferromagnetic material, whereas assuming $J < 0$ would describe an antiferromagnetic material (without changing anything in the following description and calculus).

With these six assumptions we end up with the following nearest-neighbour Ising model Hamiltonian:

$$-H_\Omega = H \sum_{i\in\Omega} S_i + J \sum_{<i,j>} S_i S_j. \tag{1.14}$$

The number of possible configurations is $2^{N(\Omega)}$ and the trace operator in the partition function Z_Ω looks as:

$$\mathrm{Tr} \equiv \sum_{\mathrm{S_1=\pm1}} \sum_{\mathrm{S_2=\pm1}} \cdots \sum_{\mathrm{S_{N(\Omega)}=\pm1}} \equiv \sum_{\mathrm{\{S_i=\pm1\}}} . \tag{1.15}$$

1.3.2 ARGUMENTS FOR/AGAINST PHASE TRANSITION IN ONE, TWO DIMENSIONS

By a simple argument we can show that in the nearest-neighbour Ising model there is no phase transition in one dimension for non-zero temperature . A phase transition in two dimensions is however possible. Since we are looking for spontaneous magnetization, we set the external magnetic field to zero. The free energy can be calculated if we know the internal energy and the entropy:

$$F_\Omega[K] = E_{in,\Omega}[K] - TS_\Omega[K] = -J \sum_{<i,j>} S_i S_j - Tk_B \log\left(\sharp(states)\right). \tag{1.16}$$

The internal energy $E_{in,\Omega}$ is just equal to the Hamiltonian and the entropy S_Ω equals Boltzmann's constant times the logarithm of the number of possible realizations of a certain state.

ONE DIMENSION

We describe two different states:

1. phase A: all spins up
2. phase B: a domain wall separates a region with spins up and a region with spins down.

The number of possibilities of setting the domain wall is $N-1$, placing it at some of the $N-1$ bonds between the N spin variables. We get:

state	internal energy	entropy	free energy
state A	$-NJ$	0	$-NJ$
state B	$-NJ+2J$	$k_B \log(N-1)$	$-NJ+2J-k_BT\log(N-1)$

The difference in free energy is

$$F_{N,B} - F_{N,A} = 2J - k_B T \log(N-1). \tag{1.17}$$

This implies that for the limit $N \to \infty$ the energy difference goes to minus infinity which means that the building of a domain wall is energetically more favourable. More and more domain walls are built and we will not observe a state with all spins up (or down). Thus there is on phase transition in one dimension (for $T \neq 0$).

TWO DIMENSIONS

Again we describe two different states:

1. phase A: all spins up
2. phase B: a domain wall separates a region with spins up and a region with spins down where we suppose that the domain wall contains n bonds.

We use an upper bound for the number of possibilities of setting the domain wall: coming from a bond between two lattice sites there are 3 possibilities of choosing the next bond (the one where we are coming from is forbidden). As we assumed that the number of bonds is n, the number of possible domain walls is 3^n. In this case we get:

state	internal energy	entropy	free energy
state A	E_0	0	E_0
state B	$E_0 + 2Jn$	$\sim k_B n \log 3$	$E_0 + 2Jn - k_B T n \log 3$

The difference in the free energy is

$$F_{N,B} - F_{N,A} = [2J - k_B T \log 3]n, \tag{1.18}$$

which now depends in the limit $n \to \infty$ on the factor standing in front of the n. There are two cases:

1. $T > T_C = \frac{2J}{k_B \log 3}$: the free energy difference goes to minus infinity and the system is unstable towards the formation of domains: we do not observe spontaneous magnetization.
2. $T < T_C$: state A is energetically favourable and we will observe long range order leading to spontaneous magnetization.

So in two dimensions we observe a phase transition at some critical temperature.

1.3.3 SHORT AND LONG RANGE ORDER

We want to discuss the question if the impossibility of a phase transition in one dimension is generally true or if it is just a consequence of the assumptions of the nearest-neighbour Ising model. Consider a general interaction term between two spins located at $\vec{r_i}$ and $\vec{r_j}$ of the form

$$J_{ij} = \frac{J}{|r_i - r_j|^\sigma}, \tag{1.19}$$

then one can show that we observe three different behaviour dependent on the value σ:

$\sigma < 1$	thermodynamic limit does not exist,
$1 \leqslant \sigma \leqslant 2$	short-range order persists for $0 < T < T_C$,
$2 < \sigma$	short-range interaction: no ferromagnetic state for $T > 0$.

So for the interaction (1.19) with $1 \leqslant \sigma \leqslant 2$ there exists a phase transition even in one dimension.

1.4 SOLUTIONS IN ONE AND MORE DIMENSIONS

There are several approaches to solve the nearest-neighbour Ising model:

$\mathbf{d = 1}$	$H = 0$	ad hoc methods, recursion method
	$H \neq 0$	transfer matrix method (Kramers, Wannier 1941)
$\mathbf{d = 2}$	$H = 0$	low temperature expansion, Onsager solution (1944)
$\mathbf{d = 1, 2, 3}$	$H \neq 0$	mean-field theory (Weiss)

In the following we give an introduction to the transfer matrix method, the Onsager solution and the mean-field theory.

1.4.1 TRANSFER MATRIX METHOD

We discuss the solution of a one-dimensional system with non-zero external magnetic field ($H \neq 0$). The idea of the transfer matrix method is to reduce the problem of calculating the partition function to the problem of finding the eigenvalues of a matrix.

BULK FREE ENERGY PER SITE

With

$$h = \beta H \quad \text{and} \quad K = \beta J \tag{1.20}$$

we get for the partition function:

$$\begin{aligned} Z_\Omega[h,K] &= \sum_{S_1}\dots\sum_{S_N} e^{h\sum_i S_i + K\sum_i S_i S_{i+1}} \\ &= \sum_{S_1}\cdots\sum_{S_N}[e^{h/2(S_1+S_2)+KS_1S_2}][e^{h/2(S_2+S_3)+KS_2S_3}]\dots[e^{h/2(S_N+S_1)+KS_NS_1}] \\ &= \sum_{S_1}\cdots\sum_{S_N} T_{S_1S_2}T_{S_2S_3}\dots T_{S_NS_1}, \end{aligned} \tag{1.21}$$

where the elements $T_{S_iS_{i+1}}$ form a matrix

$$\mathbf{T} = \begin{pmatrix} T_{11} & T_{1-1} \\ T_{-11} & T_{-1-1} \end{pmatrix} = \begin{pmatrix} e^{h+K} & e^{-K} \\ e^{-K} & e^{-h+K} \end{pmatrix}. \tag{1.22}$$

We can rewrite 1.21 by using standard matrix multiplication formula:

$$\sum_{S_1}\cdots\sum_{S_N} T_{S_1S_2}T_{S_2S_3}\dots T_{S_NS_1} = \sum_{S_1}\left(T^N\right)_{S_1S_1} = \mathrm{Tr}\left(\mathrm{T^N}\right), \tag{1.23}$$

which can be calculated by bringing the matrix T in its diagonal form D and using the cyclic property of the trace to get the following result

$$\begin{aligned} Z_\Omega[h,K] &= \mathrm{Tr}\left(\mathrm{T^N}\right) = \mathrm{Tr}\left((\mathrm{SDS^{-1}})^{\mathrm{N}}\right) = \mathrm{Tr}\left(\mathrm{SD^NS^{-1}}\right) = \mathrm{Tr}\left(\mathrm{S^{-1}SD^N}\right) \\ &= \mathrm{Tr}\left(\mathrm{D^N}\right) = \mathrm{Tr}\begin{pmatrix} \lambda_1 & 0 \\ 0 & \lambda_2 \end{pmatrix}^{\mathrm{N}} = \lambda_1^{\mathrm{N}} + \lambda_2^{\mathrm{N}} = \lambda_1^{\mathrm{N}}\left(1 + \left(\frac{\lambda_2}{\lambda_1}\right)^{\mathrm{N}}\right). \end{aligned} \tag{1.24}$$

The eigenvalues of T are

$$\lambda_{1,2} = e^K(\cosh h \pm \sqrt{\sinh^2 h + e^{-4K}}). \tag{1.25}$$

Using the eigenvalues of the matrix T, we get the bulk free energy per site:

$$\begin{aligned} f_b(h,K,T) &= \lim_{N\to\infty}\frac{F_N}{N} = -k_BT\lim_{N\to\infty}\frac{1}{N}\log\lambda_1^N - k_BT\lim_{N\to\infty}\frac{1}{N}\log\left[1+\left(\frac{\lambda_2}{\lambda_1}\right)^N\right] \\ &= -k_BT\log\lambda_1 = -J - k_BT\log\left[\cosh h + \sqrt{\sinh^2 h + e^{-4K}}\right]. \end{aligned} \tag{1.26}$$

SPATIAL CORRELATION

We look here only at the special case of zero external magnetic field. The case of non-zero magnetic field is treated as above by the use of the transfer matrix method, see [2]. The correlation function can be written as follows

$$G(i,i+j) = \langle (S_i - \langle S_i\rangle)(S_{i+j} - \langle S_{i+j}\rangle)\rangle = \langle S_i S_{i+j}\rangle - \langle S_i\rangle\langle S_{i+j}\rangle. \tag{1.27}$$

The second term is zero, as can be seen as follows. We write down the free energy and assume that we have a varying external magnetic field in order to do the calculation (afterwards it is set to zero)

$$F_\Omega = -\frac{1}{\beta}\log \mathrm{Tr}\left(\mathrm{e}^{-\beta[\sum_\mathrm{i} \mathrm{S_i H_i} - \mathrm{J}\sum_{<\mathrm{ij}>}\mathrm{S_i S_j}]}\right), \tag{1.28}$$

$$\begin{aligned} M = -\frac{\partial F_\Omega}{\partial H_i} &= \frac{1}{\beta}\frac{\mathrm{Tr}\left[\frac{\partial}{\partial \mathrm{H_i}}\left(\mathrm{e}^{-\beta \mathrm{H}_\Omega}\right)\right]}{\mathrm{Tr}\left[\mathrm{e}^{-\beta\mathrm{H}_\Omega}\right]} = \beta^{-1}\frac{\mathrm{Tr}\left[-\beta \mathrm{e}^{-\beta\mathrm{H}_\Omega}\frac{\partial \mathrm{H}_\Omega}{\partial \mathrm{H_i}}\right]}{Z} \\ &= -\frac{\mathrm{Tr}\left[\mathrm{e}^{-\beta\mathrm{H}_\Omega}(-\mathrm{S_i})\right]}{Z} = \frac{\mathrm{Tr}\left[\mathrm{S_i}\mathrm{e}^{-\beta\mathrm{H}_\Omega}\right]}{Z} = \langle S_i\rangle. \end{aligned} \tag{1.29}$$

Setting $H_i = H$, we get $\langle S_i\rangle = M = 0$ because of the earlier argument of having no magnetization in one dimension.
Let's now compute the expression $\langle S_i S_{i+1}\rangle$. We find

$$\begin{aligned} \langle S_i S_{i+1}\rangle &= \frac{1}{Z_N\{k_i\}}\sum_{S_1}\dots\sum_{S_N} S_i S_{i+1} e^{K_1 S_1 S_2 + K_2 S_2 S_3 + \ldots + K_{N-1}S_{N-1}S_N} \\ &= \frac{1}{Z_N}\frac{\partial}{\partial K_i}\sum_{S_N} e^{K_1 S_1 S_2 + K_2 S_2 S_3 + \ldots + K_{N-1}S_{N-1}S_N} = \frac{1}{Z_N}\frac{\partial}{\partial K_i} Z_N. \end{aligned} \tag{1.30}$$

The partition function can then be written as

$$Z_N\{K_i\} = 2^N \prod_{i=1}^{N-1}\cosh K_i \tag{1.31}$$

such that

$$\langle S_i S_{i+1}\rangle = \tanh K_i = \tanh \beta J_i. \tag{1.32}$$

Since

$$\frac{1}{Z_N}\frac{\partial}{\partial K_i}\frac{\partial}{\partial K_{i+1}} Z_N = \langle S_i S_{i+1} S_{i+1} S_{i+2}\rangle = \langle S_i (S_{i+1})^2 S_{i+2}\rangle = \langle S_i S_{i+2}\rangle, \tag{1.33}$$

where we have used $S_i^2 = 1$, we can proceed by induction and obtain

$$\begin{aligned} G(i, i+j) = \langle S_i S_{i+j} \rangle &= \frac{1}{Z_N} \frac{\partial}{\partial K_i} \frac{\partial}{\partial K_{i+1}} \dots \frac{\partial}{\partial K_{i+j-1}} Z_N \{K_i\} \\ &= \tanh K_i \tanh K_{i+1} \dots \tanh K_{i+j-1}. \end{aligned} \tag{1.34}$$

Setting all the $K_i = K$, we finally get the result:

$$G(i, i+j) = (\tanh K)^j = e^{-j \log(\coth K)}. \tag{1.35}$$

When - as we assumed - the K_i do not depend on i we obtain a translationally invariant correlation function. For zero temperature the correlation function equals one - a perfectly correlated state. By this result we also get an expression for the correlation length which we expand for small T:

$$\begin{aligned} \xi = \frac{1}{\log(\coth K)} &= \left(\log \frac{e^K + e^{-K}}{e^K - e^{-K}} \right)^{-1} \\ = \left(\log \left[1 + 2e^{-2K} + O(e^{-4K}) \right] \right)^{-1} &\cong \ 1/2 \ e^{J/(k_B T)}. \end{aligned} \tag{1.36}$$

This expression diverges for $T \to 0$, as we expected from 1.12.

1.4.2 ONSAGER SOLUTION

One can apply the ideas of the transfer matrix method to the two-dimensional case. As this procedure includes a rather tedious and long calculation we present here only some ideas. The full calculation can be found in [3].
We describe a square lattice in two dimensions and write for the spin variables in the α's row

$$\mu_\alpha = \{s_1, s_2, \dots, s_n\}_{\alpha th\ row}. \tag{1.37}$$

We suppose periodic boundary conditions:

$$s_{n+1} = s_1 \ , \ \mu_{n+1} = \mu_1. \tag{1.38}$$

We separate the energy terms belonging to the spin interactions in a row and those belonging to row-row interactions as

$$E(\mu) = -\epsilon \sum_{k=1}^{n} s_k s_{k+1} \tag{1.39}$$

and

$$E(\mu,\mu') = -\epsilon \sum_{k=1}^{n} s_k s'_k. \tag{1.40}$$

The second one is only defined for nearest rows (nearest-neighbour interactions). The partition function then reads

$$\begin{aligned} Z_\Omega[H=0,T] &= \sum_{\{\mu_i\}} e^{-\beta \sum_{\alpha=1}^{n} [E(\mu_\alpha,\mu_{\alpha+1})+E(\mu_\alpha)]} \\ &= \sum_{\{\mu_i\}} \prod_{\alpha=1}^{n} e^{-\beta[E(\mu_\alpha,\mu_{\alpha+1})+E(\mu_\alpha)]} = \sum_{\{\mu_i\}} \prod_{\alpha=1}^{n} \langle \mu_\alpha | P | \mu_{\alpha+1} \rangle. \end{aligned} \tag{1.41}$$

Similarly to the transfer matrix method, we may think of P as some $2^n \times 2^n$ matrix. As before we can show by similar arguments that the knowledge of the largest eigenvalue of P is enough for calculating the partition function:

$$\begin{aligned} Z_\Omega[H=0,T] &= \sum_{\{\mu_i\}} \langle \mu_1|P|\mu_2\rangle\langle \mu_2|P|\mu_3\rangle \dots \langle \mu_n|P|\mu_1\rangle \\ &= \sum_{\{\mu_i\}} \langle \mu_1|P^n|\mu_1\rangle = TrP^n = \sum_{\alpha=1}^{2^n} (\lambda_\alpha)^n. \end{aligned} \tag{1.42}$$

For detailson the calculation of the eigenvalues λ_α see [3]. It is possible to show that at large N Z_Ω depends only on the largest eigenvalue λ_{max}, i.e.

$$\lim_{N\to\infty} \frac{1}{N} \log Z_\Omega = \lim_{n\to\infty} \frac{1}{n} \log \lambda_{max}, \tag{1.43}$$

where $N = n^2$ is the number of sites. Then, the bulk free energy per site turns out to be [3]

$$\beta f_b[0,T] = -\log(2\cosh 2\beta\epsilon) - \frac{1}{2\pi}\int_0^\pi d\phi \log\left[\frac{1}{2}\left(1+\sqrt{1-\kappa^2\sin^2\phi}\right)\right], \tag{1.44}$$

where

$$\kappa = 2[\cosh 2\phi \coth 2\phi]^{-1}\ ,\ k_B T_C = (2.269185)\epsilon. \tag{1.45}$$

For the specific heat near the transition temperature $T \simeq T_C$ one gets

$$\frac{1}{k_B}C[O,T] \approx \frac{2}{\pi}\left(\frac{2\epsilon}{k_B T_C}\right)^2 \left[-\log\left|1-\frac{T}{T_C}\right| + \log\left(\frac{k_B T_C}{2\epsilon}\right) - \left(1+\frac{\pi}{4}\right)\right], \quad (1.46)$$

which fulfills no power-law, but just exhibits a logarithmical behaviour as $|T - T_C| \to 0$. The specific heat is continuous, the phase transition does not involve latent heat.

The computation of the spontaneous magnetization is again rather complicated and can be found in a paper by Yang [4]:

$$M[H=0,T] = \begin{cases} 0 & , \ T > T_C \\ \{1 - [\sinh 2\beta\epsilon]^{-4}\}^{\frac{1}{8}} & , \ T < T_C \end{cases} \quad (1.47)$$

1.4.3 MEAN-FIELD THEORY

Having discussed two exact solutions we now present an approximation method which can be used to make model predictions in an arbitrary dimension for non-zero external magnetic field.

BULK FREE ENERGY PER SITE AND SPONTANEOUS MAGNETIZATION

Our starting point is again the Hamiltonian given by equation (1.14). The idea of mean-field theory is to approximate the interactions between the spins by the introduction of a mean-field due to neighbouring spins.

$$J\sum_{j\ n.n.} S_j = J\sum_{j\ n.n.} \langle S_j\rangle + J\sum_{j\ n.n.} (S_j - \langle S_j\rangle) \cong J\sum_{j\ n.n.} \langle S_j\rangle = 2dJM, \quad (1.48)$$

where the first term after the first equality sign describes the mean-field and the second one describes the fluctuations in the mean-field which will be neglected. In the following we introduce an effective external magnetic field H_{eff} and can easily calculate the partition function, the bulk free energy per site and the magnetization:

$$Z_\Omega[H,T] = (2\cosh\beta H_{eff})^N = (2\cosh\beta[H+2dJM])^N, \quad (1.49)$$

$$f_b[H,T] = -k_B T \log(2\cosh\beta[H+2dJM]), \quad (1.50)$$

$$M[H,T] = -\frac{\partial f_b[H,T]}{\partial H} = \tanh\frac{H+2dJM}{k_B T}. \quad (1.51)$$

Therefore we got a formula determining M. As we look for spontaneous magnetization we want to solve the equation (setting $H = 0$)

$$M = \tanh \frac{2dJM}{k_B T}. \tag{1.52}$$

If the slope of the tangens hyperbolicus at the point zero is greater than one, the above equation has three possible solutions else only one possible solution. This condition defines the critical temperature

$$T_C = \frac{2dJ}{k_B}. \tag{1.53}$$

For $T > T_C$ the only solution is $M = 0$. However if $T < T_C$ the equation allows two other non-zero solutions which describe spontaneous magnetization.

CRITICAL EXPONENTS

For the calculation of the critical exponents one expands the formula (1.51) for small H, M and uses the definition

$$\tau = \frac{T_C}{T}. \tag{1.54}$$

This leads to the formula

$$\frac{H}{k_B T} = M(1-\tau) + M^3(\tau - \tau^2 + \frac{\tau^3}{3} + \ldots) + \ldots \quad . \tag{1.55}$$

From this we can easily get the desired critical exponents:

	defining property	critical exponent
$H = 0$	$M \sim \sqrt{\frac{T-T_C}{T_C}} \sim t^{\beta}$	$\beta = \frac{1}{2}$
$\tau = 1$	$M \sim H^{1/3} \sim H^{1/\delta}$	$\delta = 3$
$M = 0$	$\chi \sim (T - T_C)^{-1} \sim t^{-\gamma}$	$\gamma = 1$

1.5 SYMMETRY AND ERGODICITY BREAKING

Having discussed some solution methods of the nearest-neighbour Ising model we now analyse the model from some more general perception by looking at two things: symmetry breaking in the Ising model and broken ergodicity. We will see that broken symmetry is a special case of broken ergodicity.

1.5.1 Broken symmetry

From the form of our Hamiltonian (1.14) it is obvious that for $H = 0$ (zero magnetic field) the Hamiltonian has the symmetry

$$H_\Omega(\{-S_i\}) = H_\Omega(\{S_i\}), \tag{1.56}$$

the time-reversal symmetry. It is broken in the thermodynamical limit as one recognizes in the expression for the spontaneous magnetization:

$$M \;=\; \langle S_i \rangle \;\neq\; 0. \tag{1.57}$$

1.5.2 Broken ergodicity

The ergodic hypothesis predicts that the following two expressions are equal: the time average of some quantity A

$$\langle A \rangle_{ta} \;:=\; \lim_{t\to\infty} \frac{1}{t} \int_0^t dt' A(\{\eta_i(t')\}), \tag{1.58}$$

and its expectation value calculated with the Boltzmann distribution

$$\langle A \rangle_{eqm} \;:=\; \mathrm{Tr}\;[\mathrm{P}_\Omega(\{\eta_\mathrm{i}\})\mathrm{A}(\{\eta_\mathrm{i})\})]. \tag{1.59}$$

Thus the ergodic hypothesis states

$$\langle A \rangle_{ta} = \langle A \rangle_{eqm}. \tag{1.60}$$

This means that for infinitely long time the system comes arbitrarily close to every possible configuration described by the Boltzmann distribution.
Is the ergodic hypothesis fulfilled for our model? Let's assume that the Boltzmann factor describes the probability distribution in the thermodynamical limit. Then one gets

$$M \;=\; \langle S_i \rangle \;=\; \mathrm{Tr}[\mathrm{P}_\Omega(\{\mathrm{S_i}\})\mathrm{S_i}] \;=\; \mathrm{Tr}[\frac{\exp{(-\beta \mathrm{H}_\Omega(\{\mathrm{S_i}\}))}}{\mathrm{Z}_\Omega[\mathrm{K}]}\mathrm{S_i}] \;=\; 0. \tag{1.61}$$

This is because we sum over a symmetric and an antisymmetric summand. This result contradicts to the calculated solutions with $M \neq 0$ (e.g. Onsager solution). What went wrong? The reason is that the Boltzmann distribution is not valid anymore in the thermodynamic limit. In order to keep the idea of the ergodic hypothesis we need a new probability distribution in the thermodynamic limit as it is done by the restricted ensemble presented in the next section.

The restricted ensemble

The idea is to separate the phase space in components

$$\Gamma \;=\; \bigcup_{\alpha} \Gamma_\alpha \;=\; \bigcup_{\alpha(\{K_n\})} \Gamma_\alpha. \tag{1.62}$$

We state to assumptions on this composition of the phase space:

1. Confinement: there is a cumulative probability for escape from some component $\Gamma_\alpha \, : \, P_\alpha$.
2. If the system is confined to a component we can apply internal ergodicity to it to get any expectation value of some quantities.

So we separate our phase space of the spin variables in our magnetic model system in the following two components

$$\Gamma = \{\{S_i\} \in \Gamma : M(\{S_i\}) > 0\} \cup \{\{S_i\} \in \Gamma : M(\{S_i\}) < 0\}. \tag{1.63}$$

A calculation in [2] shows that a measure for the transition probability is

$$(P^\alpha)' \;\sim\; \exp\left(-\beta N^{(d-1)/d}\right), \tag{1.64}$$

which leads in the thermodynamic limit to

$$\lim_{N\to\infty} (P^\alpha)'(N) \;=\; \begin{cases} \neq 0 & , \quad \text{for } d = 1 \\ 0 & , \quad \text{for } d > 1. \end{cases} \tag{1.65}$$

This shows that in the one-dimensional case the transition probability is non-zero: we have to sum over all possible states (not the restricted states) and therefore get by the argument 1.61 no spontaneous magnetization. For the other dimensions the transition probability is zero and we can use the restricted ensemble to get the prediction of spontaneous magnetization.

1.5.3 What is special about a broken symmetry?

Symmetry breaking implies ergodicity breaking. Ergodicity breaking does not imply symmetry breaking. So broken symmetry is a special case of broken ergodicity. There are two properties which are only observed when broken ergodicity is due to broken symmetry:

1. Different components are mapped on each other by the symmetry mapping which is broken: the time-reversal mapping ($\{S_i\} \to \{-S_i\}$) maps states of positive magnetization in one component to states of negative magnetization in the other component.

2. We can introduce an order parameter M with three properties: $|M|$ contains the information of the amount of order, $M/|M| = \pm 1$, the "direction" of the order parameter identifies the components and $|M| \to 0$ for $T \nearrow T_C$, as it also observes in our analytical solutions.

1.6 Concluding remarks

Let us now compare the calculated critical exponents with experimental values.

1.6.1 Critical exponents in two dimensions

crit.exp.	mean-field	Onsager	$Rb_2CoF_4^*$	$Rb_2MnF_4^*$
α	$0(disc.)$	$0(log)$	$\simeq 0.8$	4.7×10^{-3}
β	0.5	0.125	0.122 ± 0.008	0.17 ± 0.03

* values from [5]. Therefore two-dimensional magnetic system are realized in nature.

1.6.2 Critical exponents in three dimensions

crit. exp.	mean-field	Monte Carlo**	$CrBr_3^*$	$RbMnF_3^*$
β	0.5	0.3258 ± 0.0044	0.368 ± 0.005	0.316 ± 0.008
δ	3	4.8030 ± 0.0558	4.28 ± 0.1	

* from [5] and ** from [6]. The Monte-Carlo simulation gives the best theoretical predictions for the critical exponents.

1.6.3 Concepts to remember

Phase transitions occur in the thermodynamical limit where we have to adapt the Boltzmann distribution by the introduction of the restricted ensemble. The broken symmetry in the Ising model is the time-reversal symmetry.

BIBLIOGRAPHY

[1] J. Cardy, *Scaling and Renormalization in Statistical Physics* (Cambridge University Press, Cambridge, 1996).

[2] N. Goldenfeld, *Lectures on phase transitions and the renormalization group* (Westview Press, Boulder, Colorado, 1992).

[3] K. Huang, *Statistical Mechanics* (John Wiley & Sons, New York, 1987).

[4] C. Yang, *The spontaneous magnetization of a two-dimensional ising model*, Phys. Rev. **85**, 808 (1952).

[5] L. J. De Jongh and A. R. Miedema, *Experiments on simple magnetic model systems*, Adv.Phys. **23**, 1 (1974).

[6] A. Ferrenberg and D. Landau, *Critical behaviour of the three-dimensional ising model: A high-resolution monte carlo study*, Phys.Rev. B **44**, 5081 (1991).

CHAPTER 2

CRITICAL PHENOMENA IN FLUIDS

SEVERIN ZIMMERMANN
SUPERVISOR: DAVIDE BATIC

In this chapter, we discuss the critical phenomena at the liquid-gas transition, with particular emphasis on the description given by the Van der Waals equation. Furthermore we will calculate some critical exponents and look at difficulties of measurements near the critical point.

2.1 REPETITION OF THE NEEDED THERMODYNAMICS

2.1.1 THERMODYNAMIC POTENTIALS AND THEIR DIFFERENTIALS

The energy

$$E = E(S, V, N)$$

$$dE = TdS - pdV + \mu dN$$

The Helmholtz free energy

$$F = F(T, V, N) = E - TS$$

$$dF = -SdT - pdV + \mu dN$$

The Gibbs free energy

$$G = G(T, p, N) = F + pV = \mu N$$

$$dG = -SdT - Vdp + \mu dN$$

All these relations follow from the First Law of Thermodynamics, from them we can read off thermodynamic identities and Maxwell-Relations.

2.1.2 PHASE DIAGRAM

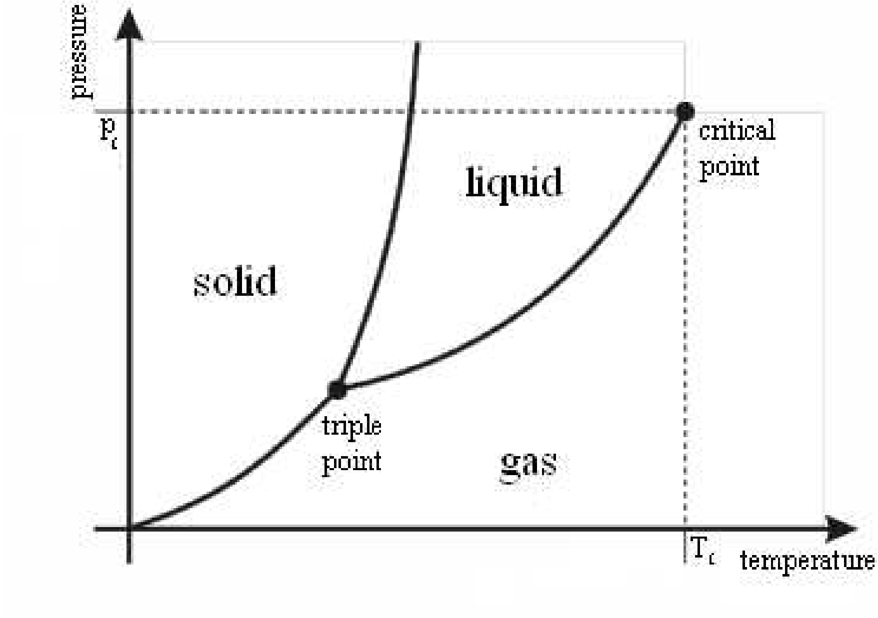

Phase diagram in the p-V plane

In this chapter we will only look at first order transitions, such as melting, vaporizing etc.

From the extremal principle for the Gibbs free energy we know that the realized phase is always the one with the lowest G. Therefore the coexistence line between two phases indicates that $G_I = G_{II}$ i.e. $\mu_I = \mu_{II}$.

Consider now the coexistence line between liquid and solid in the p - T plane:

$$G_l(T, p, N) = G_s(T, p, N)$$

Now we move along the line: $T \to T + \delta T$, $p \to p + \delta p$ and expand G to first order:

$$G_{l,s}(T + \delta T, p + \delta p, N) = G_{l,s}|_{T,p} + \left.\frac{\partial G_{l,s}}{\partial T}\right|_{T,p} \delta T + \left.\frac{\partial G_{l,s}}{\partial p}\right|_{T,p} \delta p$$

Using thermo-dynamical identities given by the differentials above we come to an important consequence: the Clausius-Clapeyron relation.

$$\left.\frac{dp}{dT}\right|_{transition} = \frac{S_l - S_s}{V_l - V_s}$$

Normally $\frac{\partial p}{\partial T} > 0$, because $V_l > V_s$ and $S_l < S_s$. However there are exceptions like H_2O ($V_l < V_s$) due to hydrogen bonds and ^{3}He ($S_l > S_s$) due to spin disorder present in the solid phase.

From the Clausius-Clapeyron relation we also see that if $S_l \neq S_s$ latent heat will be released in this first order transition which corresponds to the chemical enthalpie. If we get close to a critical point the latent heat will become vanishingly small.

2.1.3 Landau's Symmetry Principle

We saw in the phase diagram that two phases of matter must be separated by a line of (first order) transitions due to the the fact that one can't continuously change symmetry. A symmetry is either present or absent.

The existence of the critical point on liquid gas transition line tells you that there is no symmetry difference between those two phases.

2.2 Two-phase Coexistence

2.2.1 Fluid at constant pressure

If we keep the pressure in a fluid constant and apply heat, the liquid will start expanding and at a certain temperature it will start boiling. During the boiling the temperature remains constant while the volume increases. When all the matter has become gaseous further heating will cause the gas to expand.

The whole process corresponds to moving along a horizontal line in the figure below. During the entire time that the liquid is turned into gas the system remains at the intersection point of the horizontal and the transition line, afterwards the system will move again horizontally.

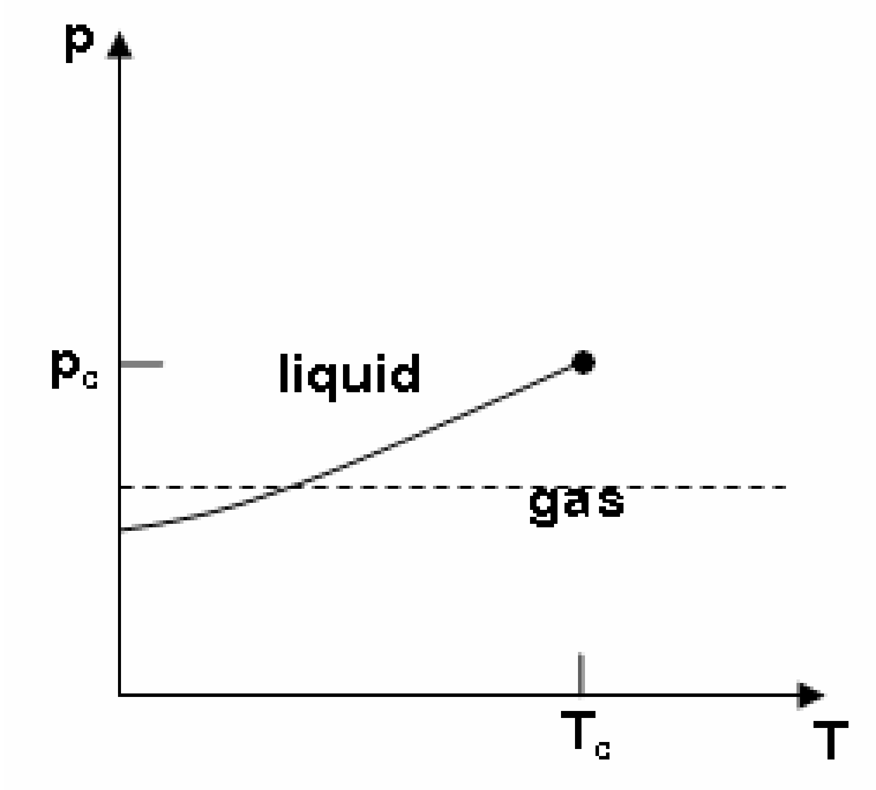

Figure 2.2: Coexistence curve in the p - T plane

2.2.2 Fluid at Constant Temperature

If we look at isotherms in figure 2.3 we see that at $T > T_c$ the isotherms are well approximated by the ideal gas law (and small corrections). As T $\rightarrow T_c^+$ the isotherms become flatter until they have a horizontal tangent at the top of the two-phase region. At $T < T_c$ as we move to the left (meaning: decreasing V and increasing p) we will reach point A where we have equilibrium vapor pressure and equilibrium volume $v_g(T)$. Under further compression the gas starts condensing at constant pressure. Eventually we reach point B where all gas is liquefied, then the pressure will rise again.

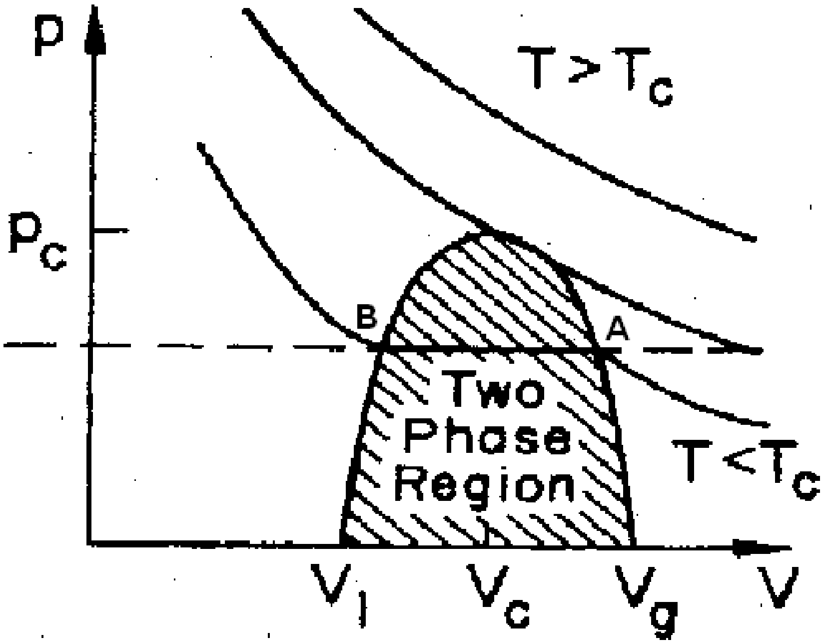

Figure 2.3: Isotherms above and below the critical temperature

2.2.3 Maxwell's Equal Area Rule

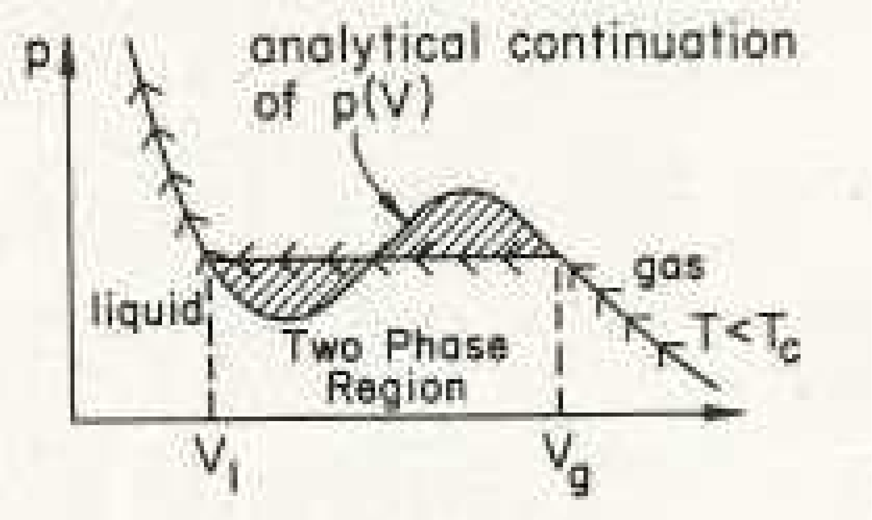

Figure 2.4: Maxwell's equal area construction

Although model equations of state (like due to Van der Waals) are analytic through the two-phase coexistence region. However isotherms exhibit a non-analytic behavior at the boundaries of the two-phase region. This reflects that the model equations of state can't ensure that at the equilibrium state the Gibbs free energy is globally minimized.

So in the two-phase coexistence region the Gibbs free energy is the same for both phases. An equivalent statement to this is that the chemical potentials are equal. In addition to thermal equilibrium we also need mechanical equilibrium (which implies that the pressure in the liquid phase is equal to the pressure in gas phase). Hence the isotherm must be horizontal in the two-phase coexistence region.

$$dG = \mu dN + N d\mu$$

$$\begin{aligned} d\mu = \frac{1}{N}dG - \frac{\mu}{N}dN &= \frac{1}{N}(-SdT + Vdp + \mu dN) - \frac{\mu}{N}dN \\ &= -\frac{S}{N}dT + \frac{V}{N}dp \end{aligned}$$

We can drop the dT because we are looking at isotherms, so $dT = 0$.

$$\mu_l - \mu_g = \int_{gas}^{liq} d\mu = \int_{gas}^{liq} \frac{V}{N} dp = 0$$

The geometrical interpretation of this is that the horizontal must be drawn such that the two bounded areas sum to zero.

2.3 VAN DER WAALS EQUATION

If we look at an ideal gas we have the following equation:

$$pV = Nk_BT$$

Van der Waals made two significant changes to that equation. He introduced the parameter a due to the attractive interaction between the atom and he introduced the parameter b to take care of the hard-core potentials of atoms (atoms have a non-zero radius). Van der Waals proposed the following equation:

$$p = \frac{Nk_BT}{V - Nb} - \frac{N^2a}{V}$$

The parameter a and b can be determinated by fitting the equation to experimental data (e.g. $a = 3.45\ kPa \cdot dm^6/mol^2$, $b = 0.0237\ dm^3/mol$ for Helium)

2.3.1 DETERMINATION OF THE CRITICAL POINT

We can rewrite the Van der Waals equation to obtain a cubic polynomial for the volume.

$$V^3 - \left(Nb + \frac{Nk_BT}{p}\right)V^2 + \frac{N^2a}{p}V - \frac{N^3ab}{p} = 0$$

Solving this equation we get 2 imaginary and 1 real solution for T $> T_c$ and 3 real solutions at T $< T_c$. Hence at T $= T_c$ the three solutions merge and we get:

$$(V - V_c)^3 = 0$$

By comparing the coefficients of these two cubic polynomials we get:

$$3V_c = Nb = \frac{Nk_BT_c}{p_c}; \quad 3V_c^2 = \frac{N^2a}{p_c}; \quad V_c^3 = \frac{N^3ab}{p_c}$$

this leads to

$$V_c = 3Nb; \quad p_c = \frac{a}{27b^2}; \quad k_BT_c = \frac{8a}{27b}$$

Using a high temperature fit for a and b you can predict T_c, p_c and T_c and get quite good results, this theory also predicts an universal number.

$$\frac{p_cV_c}{Nk_BT_c} = \frac{3}{8}$$

2.3.2 Law of Corresponding States

We can rescale the Van der Waals equation defining reduced pressure, volume and temperature.

$$\pi = \frac{p}{p_c}; \quad \nu = \frac{V}{V_c}; \quad \tau = \frac{T}{T_c}$$

This rescaling leads to:

$$\left(\pi + \frac{3}{\nu^2}\right)(3\nu - 1) = 8\tau$$

This equation is called law of corresponding states. It is the same for all fluids with no other parameter involved, so all properties which follow from this equation are universal.
Experimentally it's also well-satisfied even for fluids which don't obey the Van der Waals equation.

2.3.3 Vicinity of the critical point/ critical exponents

Now we want to calculate some critical exponents of important quantities like

the specific heat	$C_V \propto \lvert T - T_c\rvert^{-\alpha}$
the width of the two-phase coexistence region	$V_g - V_l \propto \lvert T_c - T\rvert^{\beta}$
the compressibility	$k_T = -\frac{1}{V}\left(\frac{\partial V}{\partial p}\right)_T \propto \lvert T - T_c\rvert^{-\gamma}$
and the shape of the critical isotherm	$\lvert p - p_c\rvert \propto \lvert V - V_c\rvert^{\delta}$ To calculate

the exponent α we need the Helmholtz free energy due to the Van der Waals equation:

$$p = \frac{\partial F}{\partial V}$$

$$F = \int p dV = \int \left(\frac{N k_B T}{V - Nb} - \frac{aN^2}{V^2} \right) dV$$

$$F = N k_B T log(V - Nb) + \frac{aN^2}{V} + f(T)$$

$$C_V = T \frac{\partial S}{\partial T} = T \frac{\partial^2 F}{\partial T^2}$$

Now if we look at the free energy we see that C_V depends just on the constant of integration. Therefore it's the same as for an ideal gas (a = 0, b = 0).
For an ideal gas we know that U = $\frac{3}{2}$ Nk_BT due to Boltzmann, then the heat capacity C_V is given by:

$$C_V^{VdW} = C_V^{ideal} = \left(\frac{\partial U}{\partial T} \right)_V = \frac{3}{2} N k_B$$

We see that C_V does not diverge at the critical point and $\alpha = 0$.
To calculate the exponent β we start with the law of corresponding states and rewrite it using:

$$t \equiv \tau - 1 \frac{T - T_c}{T}, \quad \phi \equiv \nu - 1 = \frac{V - V_c}{V}$$

this leads to

$$\pi = \frac{8(1+t)}{3(1+\phi) - 1} - \frac{3}{(1+\phi)^2}$$

Now we expand this equation using a Taylor series around the critical point (π = τ = ν = 1).

$$\pi|_{t,\phi=0} + \left.\frac{d\pi}{dt}\right|_{t,\phi=0} \cdot t + \left.\frac{d\pi}{d\phi}\right|_{t,\phi=0} \cdot \phi + \left.\frac{d^2\pi}{dt d\phi}\right|_{t,\phi=0} \cdot t\phi + \frac{1}{2} \left.\frac{d^2\pi}{dt^2}\right|_{t,\phi=0} \cdot t^2 + \frac{1}{2} \left.\frac{d^2\pi}{d\phi^2}\right|_{t,\phi=0} \cdot \phi^2 + ...$$

Note that $\pi \propto t$ so all higher derivatives in t are zero and the first derivative in ϕ is zero as well. Therefore we get:

$$1 + 4t - 6t\phi - \frac{3}{2}\phi^3 + O(t\phi^2, \phi^4)$$

We want to find the coexistence volumes V_l(p), V_g(p) or their corresponding values ϕ_l and ϕ_g. Therefore we use Maxwell's construction for a fixed t < 0 (T < T_c)

$$\oint \frac{V}{N} dp = 0$$

and make a substitution due to $\pi = \frac{p}{p_c}$

$$dp = p_c \cdot d\pi = p_c \left[-6t - \frac{9}{2}\phi^2 \right] d\phi$$

this leads to

$$\int_{\phi_l}^{\phi_g} \phi(-6t - \frac{9}{2}\phi^2) d\phi = 0$$

The function in the integral is odd in ϕ. Hence we conclude that $\phi_g = -\phi_l$, because the integral has to be zero for all values of t.

By going back to our expansion of the law of corresponding states we get

$$\pi = 1 - 4t - 6t\phi_g - \frac{3}{2}\phi_g^3$$

$$\pi = 1 - 4t - 6t\phi_l - \frac{3}{2}\phi_l^3 = 1 - 4t + 6t\phi_g + \frac{3}{2}\phi_g^3$$

Now we subtract and get

$$\phi_g = 2\sqrt{-t}$$

$$|\phi_g - \phi_l| = |2\phi_g| \propto \left(\frac{T_c - T}{T_c} \right)^{\frac{1}{2}}$$

$$\Rightarrow \quad \beta = \frac{1}{2}$$

To calculate the critical exponent γ of the compressibility k_T we start with the definition and switch the derivatives.

$$k_T = -\frac{1}{V}\frac{\partial V}{\partial p} = -\frac{1}{V}\left(\frac{\partial p}{\partial V} \right)^{-1}$$

Then we use the Van der Waals equation to get p(V) and calculate the derivative.

$$k_T = \frac{1}{V}\left(\frac{Nk_BT}{(V - Nb)^2} - \frac{2aN^2}{V^3} \right)^{-1}$$

$$= \frac{V^2(V - Nb)^2}{Nk_BTV^3 - 2aN^2(V - Nb)^2}$$

We want to look at the critical point so we use $V = V_c =$ 3Nb

$$k_T = \frac{36N^4b^4}{27N^4b^3k_BT - 8aN^4b^2} = \frac{36b^2}{27bk_BT - 8a}$$

$$= \frac{36b^2/27bk_B}{T - \underbrace{\frac{8a}{27bk_B}}_{T_c}}$$

Now we see that $k_T \propto (T-T_c)^{-1}$, so $\gamma = 1$
As a result we know that the compressibility diverges at $T \to T_c$ which means that the system becomes extremely sensitive to an applied pressure at the critical point. As we approach the critical temperature the system is thermodynamically unstable towards phase separation.

We can determine the shape of the critical isotherm by doing the same as for the exponent β, but now we set t = 0 (T = T_c)

$$\pi = 1 - \frac{3}{2}\phi^3$$

$$\pi - 1 = \frac{p-p_c}{p_c} = -\frac{3}{2}\left(\frac{V-V_c}{V_c}\right)^3$$

$$\propto (V-V_c)^3 \ \Rightarrow \ \delta = 3$$

2.4 Spatial correlations

In fluid the two point correlation function describes the statistical fluctuations in the density.
We consider a volume of space V embedded in a bigger volume Ω. Then particles of a fluid in Ω will wander through V and cause a number fluctuation in the volume V. The mean Number of particles in V is given by:

$$\langle N \rangle = k_B T \left. \frac{\partial log \Xi}{\partial \mu} \right|_{T,V} = k_B T \frac{1}{\Xi} \left. \frac{\partial \Xi}{\partial \mu} \right|_{T,V}$$

where Ξ is the trace of the grand partition function

$$\Xi = Tr\left(e^{-\beta(H-\mu N)}\right)$$

Similarly we define

$$\left\langle N^2 \right\rangle \equiv \frac{Tr\left(N^2 e^{-\beta(H-\mu N)}\right)}{Tr\left(e^{-\beta(H-\mu N)}\right)} = k_B T \frac{1}{\Xi}\frac{\partial^2 \Xi}{\partial \mu^2}$$

Now we can relate this to $\langle N \rangle$

$$\frac{1}{\beta^2}\frac{\partial^2 log \Xi}{\partial \mu^2} = \frac{1}{\beta^2}\frac{\partial}{\partial \mu}\left(\frac{1}{\Xi}\frac{\partial \Xi}{\partial \mu}\right) = \frac{1}{\beta^2}\left(-\frac{1}{\Xi^2}\left(\frac{\partial \Xi}{\partial \mu}\right)^2 + \frac{1}{\Xi}\frac{\partial^2 \Xi}{\partial \mu^2}\right)$$

$$= \frac{1}{\beta^2}\frac{1}{\Xi}\frac{\partial^2 \Xi}{\partial \mu^2} - \langle N \rangle^2$$

The fluctuation of N is given by

$$\Delta N^2 = \left\langle N^2 \right\rangle - \left\langle N \right\rangle^2 = \frac{1}{\beta^2} \left. \frac{\partial^2 log \Xi}{\partial \mu^2} \right|_{T,V} = \frac{1}{\beta} \frac{\partial}{\partial \mu} \left. \left\langle N \right\rangle \right|_{T,V} = \frac{k_B T}{\left(\frac{\partial \mu}{\partial N}\right)_{T,V}}$$

$\left(\frac{\partial \mu}{\partial N}\right)_{T,V}$ is not very useful so we try to express it in measurable quantities. We do this by using Jacobians:

$$\frac{\partial(u,v)}{\partial(x,y)} = det \begin{pmatrix} \frac{\partial u}{\partial x} & \frac{\partial u}{\partial y} \\ \frac{\partial v}{\partial x} & \frac{\partial v}{\partial y} \end{pmatrix}$$

$$\left. \frac{\partial \mu}{\partial N} \right|_{V,T} = \frac{\partial(\mu,V)}{\partial(N,V)} = \frac{\partial(\mu,V)}{\partial(N,p)} \cdot \frac{\partial(N,p)}{\partial(N,V)} = \left(\left. \frac{\partial \mu}{\partial N} \right|_{p,T} \left. \frac{\partial V}{\partial p} \right|_{N,T} - \left. \frac{\partial \mu}{\partial p} \right|_{N,T} \left. \frac{\partial V}{\partial N} \right|_{p,T} \right) \left(\left. \frac{\partial V}{\partial p} \right|_{N,T} \right)^{-1}$$

The first bracket can be simplified by using $\left.\frac{\partial \mu}{\partial N}\right|_{p,T} = 0$ for the first term and the Maxwell-Relation $\left.\frac{\partial \mu}{\partial p}\right|_{N,T} = \left.\frac{\partial V}{\partial N}\right|_{T,p}$ for the second term. Whereas the second bracket is related to the compressibility.
Finally we get:

$$\Delta N^2 = k_B T \rho^2 V k_T$$

2.4.1 Number fluctuations and the correlation function

The dimensionless two-point correlation function is given as

$$G(r - r') = \frac{1}{\rho^2} \left(\langle \rho(r), \rho(r') \rangle - \rho^2 \right)$$

Here we expect two widely separated points to be uncorrelated ($G(r-r') \to 0$ as $|r - r'| \to \infty$)
We perform an integration to write

$$\int d^d r d^d r' G(r-r') = \frac{1}{\rho^2} \left(\left\langle N^2 \right\rangle - \left\langle N \right\rangle^2 \right)$$

$$= k_B T V k_T$$

On the other hand we have translational invariance for our two-point correlation function which implies

$$\int d^d r d^d r' G(r - r') = V \int d^d r G(r)$$

Using all of the above we get

$$\int d^d r G(r) = k_B T k_T$$

In d-dimensions the correlation function is of the form

$$G(r) \propto \frac{e^{\frac{-|r|}{\xi}}}{|r|^{\frac{d-1}{2}} \xi^{\frac{d-3}{2}}}$$

$\xi(T)$ is called the correlation length and represents the regions that have fluctuations about the equilibrium state.

2.4.2 CRITICAL OPALESCENCE

In a fluid the two-point correlation function measures the density fluctuations which are able to scatter light. The Intensity of the scattered light is proportional to the structure factor

$$I \propto S(k) = \rho \int d^d r e^{-ik\cdot r} G(r) = \frac{k_B T k_T \rho}{1 + k^2 \xi^2(T)}$$

At the critical point the correlation length diverges which implies that the system exhibits fluctuations of all length scales. As a result the light is strongly scattered and multiple scattering becomes important. Therefore the light can't be transmitted through the medium and it becomes milky or opaque.

2.5 DETERMINATION OF THE CRITICAL POINT/ DIFFICULTIES IN MEASUREMENT

The critical exponent occurs at a certain temperature (T_c), so we introduced the reduced temperature:

$$t = \frac{T - T_c}{T_c}$$

Then the critical exponent can be defined as limiting power law

$$k = lim_{t \to 0} \frac{log f(t)}{log(t)}$$

In general these exponents only describe the leading behavior, so there will be sub-dominant corrections. These are known a corrections to scaling.
e.g. the heat capacity can be written as

$$C_V(t) = A\,|t|^{-\alpha} \left(1 + B\,|t|^{\theta} + ...\right) \qquad \theta > 0$$

These corrections vanish at the critical point, but they can make a significant difference for $|t| > 0$. If we want reliable values for the actual critical exponents in practise those corrections can't be neglected.
There are also other constants of proportionality

$$C_V(t) = \begin{cases} At^{-\alpha} & t > 0 \\ A'(-t)^{-\alpha'} & t < 0 \end{cases}$$

A, A' are called critical amplitudes and α, α' are called critical exponents. The exponents are the same above and beneath the critical temperature ($\alpha = \alpha'$), but the amplitudes are different for both sides. However the ratio $\frac{A}{A'}$ is universal.

2.5.1 Measurement

It's actually quite difficult to measure critical exponents for various reasons.
Suppose we want to measure $C_V(T)$ to read off α. Theoretically it can be plotted versus the reduced temperature t to read off α, practically $C_V$is measured by putting ΔE into the system and measuring the change ΔT. This works rather fine in areas which aren't too close to the critical temperature. $|t| >> \frac{\delta T}{T_c}$ (where δT is the limiting sensitivity), so we require very high resolution thermometry if we want to go close to the critical temperature. Today one uses paramagnetic salt (e.g. $GdCl_3$) or alloys (e.g. Pd(Mn)) because they have a sub-nanokelvin resolution. Another problem is the background, in addition to the critical behavior there is normally a slightly varying background which has no singular behavior at T_c. So we need to subtract it to determine the critical exponent, this requires curve fitting.
Other problems are impurity effects or the finite size of the system which causes a rounding of the divergence.
The last big problem is called critical slowing down. As $T \rightarrow T_c$ it takes longer and longer for the system to equilibrate. At the critical point the correlation length diverges, so the regions, which show fluctuations about the equilibrium state get bigger and bigger. Therefore the system takes longer to relax (the relaxation time diverges).

BIBLIOGRAPHY

[1] N. Goldenfeld, *Lectures on Phase Transitions and the Renormalization Group* (Westview Press, New York, 1992).

[2] H. E. Stanley, *Introduction to Phase Transitions and Critical Phenomena* (Clarendon Press, Oxford, 1971).

CHAPTER 3

LANDAU THEORY, FLUCTUATIONS AND BREAKDOWN OF LANDAU THEORY

RAPHAEL HONEGGER
SUPERVISOR: DR. ANDREY LEBEDEV

Describing phase transitions of second order with an order parameter, that is zero for the phase of higher symmetry and growing continuously in the other phase, one could expand the free energy about the critical point in a power series in this order parameter. This somehow doesn't seem to make much sense, because we know, that at the critical point, we don't find analytic behavior, which is the requirement for such an expansion. However, we will show, that assuming the existence of such a power series, makes us able to qualitatively calculate the behavior of thermodynamic quantities near the critical point.

3.1 INTRODUCTION

3.1.1 SECOND ORDER PHASE TRANSITIONS

Because of their different behavior in the change of symmetry, we distinguish between different types of phase transitions. First order phase transitions are the ones, we encounter every day, as for example when boiling or freezing water. The important property of such phase transitions is, that the transition occurs as an abrupt change in symmetry.

On the other hand, second order phase transitions have the property, that the symmetry is changed in a continuous way. As example, we could think of a body center cubic lattice, where at a certain critical temperature, the centered particle starts to move towards one of the corners. As soon as this particle isn't placed anymore in the middle of the cube, the body center cubic symmetry is broken and the lattice has to be described by another symmetry. While in this case, the displacement of the centered particle is a continuous function of the temperature, there can't be found such a continuous parameter when melting ice or boiling water (or any other substance).[1]

3.1.2 Order Parameter

As described before, a second order phase transition is connected with a continuous change of symmetry. Besides the change of the relative positions in a lattice, this could also be the probability of finding one kind of atom at a given lattice position or the magnetization in a ferromagnet or something else. It then is sensible to introduce a parameter η, called the order parameter, that describes this continuous change of symmetry in the following way:

- η is zero for the phase of higher symmetry,
- η takes non-zero values (positive or negative) for the “asymmetric” phase,
- for second order phase transitions, η is a continuous function of temperature.

3.1.3 Bragg-Williams Theory

Before we get to the concept of Landau Theory, we discuss a simplified version of the Ising model, that somehow might give us an idea of why expanding the free energy in a power series in the order parameter makes sense.
In the Ising Model, the internal Energy $U = \langle H \rangle$ is assumed to be of the form

$$U = \langle H \rangle = \sum_i H_i S_i - \sum_{i,j} J_{ij} S_i S_j - \sum_{i,j,k} K_{ijk} S_i S_j S_k - ... \tag{3.1}$$

where $S_i = \pm 1$ represents the spin at lattice site i and $H_i, J_{ij}, H_{ijk}, ...$ are the spin interaction constants. In Bragg-Williams Theory we assume, that all the spin interaction constants besides the J_{ij} are zero. Furthermore, we assume that only nearest neighbor sites interact with each other and this in the same way. As additional simplification, we replace the S_i by their position independent average

$m = \langle S \rangle =: \eta$, which will be the order parameter. Then we can write the internal energy as

$$U = -J \sum_{\langle i,j \rangle} \eta^2 = -J \, \frac{Nz\eta^2}{2} \tag{3.2}$$

denoting with $\langle i, j \rangle$ the sum over nearest neighbors and therefore with z the number of nearest neighbor sites.

The entropy for a given $\eta = m$ is the logarithm of the number of configurations with a given number $N_\uparrow$ of sites with spin up and $N_\downarrow$ of sites with spin down

$$S = \ln \binom{N}{N_\uparrow} = \ln \left(\frac{N!}{(N(1+\eta)/2)!(N(1-\eta)/2)!} \right) \tag{3.3}$$

where we used that $\eta = (N_\uparrow - N_\downarrow)/N$ and $N_\downarrow = N - N_\uparrow$. Using Sterling's Approximation for large N

$$\ln(N!) \approx N(\ln(N) - 1) \tag{3.4}$$

wo obtain

$$S \approx N \left(\ln(2) - \frac{1+\eta}{2} \ln(1+\eta) - \frac{1-\eta}{2} \ln(1-\eta) \right) \tag{3.5}$$

For small η, we expand in powers of η, to get

$$\frac{S}{N} \approx \ln(2) - \frac{1}{2}\eta^2 - \frac{1}{12}\eta^4 - ... \tag{3.6}$$

Now, we are ready to write down the Bragg-Williams free energy density per site

$$\frac{F(T,\eta)}{N} = \frac{U - TS}{N} = -T\ln(2) + \frac{1}{2}(T - T_c)\,\eta^2 + \frac{1}{12}T\eta^4 + ... \tag{3.7}$$

Here we set $zJ =: T_c$, the transition temperature. The reason why we did this is, that minimizing $F(T, \eta)/N$ with respect to η leads exactly to the conditions for the order parameter described above, if we take T_c as critical temperature. That means, for $T > T_c$, we have a minimum at $\eta = 0$, which corresponds to the phase of higher symmetry. For $T < T_c$ however, we get a maximum at $\eta = 0$ and two equivalent minima at $\eta \neq 0$, which corresponds to the low symmetry phase.

Looking at the Bragg-Williams free energy, generalizing the idea of expanding the free energy in a power series in η doesn't look so strange anymore and that's exactly what's done in Landau Theory.[2]

3.2 Landau Theory

In the following sections, we assume that the high symmetry phase corresponds to $T > T_c$, which is true for most cases.

3.2.1 Power Series about the critical Point

We consider the free energy as function $F(P, T, \eta)$ of the pressure P, the temperature T and the order parameter η. While P and T can be any sensible values, η is given by the condition, that it minimizes the free energy at given P and T. Looking at the region near the critical point, we use the fact that η must be small there and expand in a power series

$$F(P, T, \eta) \;=\; F_0 + \alpha\eta + A\eta^2 + C\eta^3 + B\eta^4 + ... \tag{3.8}$$

where F_0, α, A, C, B are functions of P and T. Here, we simply assumed that this expansion is allowed. We will discuss later, under which conditions this is valid. In the further discussions we won't take into account the terms of higher order than η^4.

Because $\eta = 0$ has to be a minimum of F for the high symmetry phase ($T > T_c$), α must be zero (at least in this phase). If α would not be zero in the low symmetry phase, the effect would be like the one shown in figure 3.1b in the following chapter. But in general, there is no reason, why negative or positive η should be preferred, without an external field. Therefore, we assume α to be zero for both phases.

In addition to this, it must be $A(P, T) > 0$ for $T > T_c$ in order to get a minimum at $\eta = 0$ and also $A(P, T) < 0$ for $T < T_c$ in order to get a non-zero minimum of F. Therefore, $A(P, T)$ can only vanish at the critical point to satisfy continuity. If we look at the critical point itself and require it to be stable, which means that $\eta = 0$ has to be a minimum, then it is clear, that it must be $C(P, T) = 0$ and $B(P, T) > 0$ at this point. Then, $B(P, T) > 0$ for sure in a neighborhood of the critical point. To go on, we distinguish two cases:

1) $C(P, T) \equiv 0$: In this case, the condition $A(P, T) = 0$ at the critical point defines a line in the (P, T)-space, that describes the phase transition.

2) $C(P, T) \not\equiv 0$: At the critical point, we have an additional condition, namely $C(P, T) = 0$, which together with $A(P, T) = 0$ generally results in points in the (P, T)-space, at which the "phase transition" occurs.

It is only the first case, we're interested in. That's why we assume $C(P,T) \equiv 0$ and therefore write the free energy as

$$F(P,T,\eta) \;=\; F_0(P,T) + A(P,T)\eta^2 + B(P,T)\eta^4 \tag{3.9}$$

If $A(P,T)$ has no singularity at the transition point, we can expand it in terms of $(T - T_c)$, at least in a region of the critical point $T_c = T_c(P)$. Near the critical point, we can then write

$$F(P,T,\eta) \;=\; F_0(P,T) + a(P)(T-T_c)\eta^2 + B(P)\eta^4 \tag{3.10}$$

where we assumed, that we can write $B(P,T) \sim B(P,T_c) = B(P)$.
This is the form of the free energy, with which we can predict qualitatively the behavior of thermodynamic quantities near the critical point. But first we want to describe what happens, if we apply an external field.[1]

3.2.2 External Field

If we apply a small external field h, which could be a magnetic field for a ferromagnet, we have to apply in first order approximation a term of the form $-\eta h V$ in equation (3.10). That is

$$F_h(P,T,\eta) \;=\; F_0(P,T) + a(P)t\eta^2 + B(P)\eta^4 - \eta h V \tag{3.11}$$

where we replaced $t := (T - T_c(P))$. Even if the field h is small, but non-zero, the Minimum in η will be non-zero, to minimize F.[1]

3.2.3 The Minima

Lets go one step further and explicitly discuss the minima of the free energy without (3.10) and with an external field (3.11).
For $T \geq T_c$, by definition, the free energy (3.10) has a single minimum at $\eta = 0$. As soon as T gets smaller than T_c, $\eta = 0$ will be a maximum and the two equivalent minima can be obtained by requiring the derivative to be zero

$$\frac{\partial F(P,T,\eta)}{\partial \eta} \;=\; (2a(P)t + 4B(P)\eta^2)\eta \;=\; 0 \tag{3.12}$$

So, we have two minima at

$$\eta \;=\; \pm\sqrt{\frac{a}{2B}(T_c - T)} \tag{3.13}$$

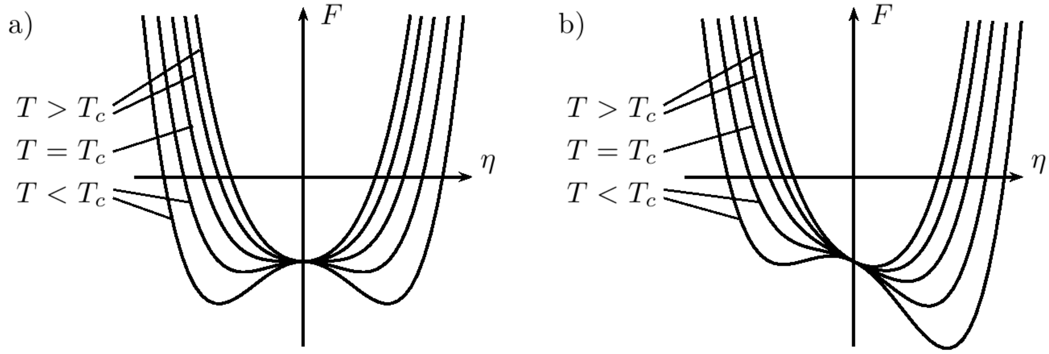

Figure 3.1: a) Free energy as function of η a) without external field, b) with $h > 0$.

To see how the free energy as function of η for different temperatures looks like, see figure 3.1a.

With an external field h applied, the free energy is somehow weighted in the direction of the field (see figure 3.1b). The minima we find by setting

$$\frac{\partial F_h(P,T,\eta)}{\partial \eta} = (2a(P)t + 4B(P)\eta^2)\eta - hV = 0 \tag{3.14}$$

The explicit solutions can be found using Cardano's Method, but we won't need them to understand what happens qualitatively. However, the character of the roots η, depending on the external field h is different for T bigger or smaller than T_c. This can be seen quite well by looking for the solutions of

$$hV = 2at\eta + 4B\eta^3 \tag{3.15}$$

which is equivalent to equation (3.14). Like that, we can interpret hV as function of η and this function then shows the relationship between the external field h and η. The two cases are sketched out in figure 3.2.

For $T > T_c$, the function $(hV)(\eta)$ is monotonically increasing and therefore, there is a unique and non-zero solution for η, which is bigger than zero if $h > 0$ and vice versa. This means, that the external field lowers the symmetry of the high symmetry phase, such that there is no more difference between the to phases. Therefore, there is no more discrete transition point, in fact, the transition is spread out over an interval of temperature.

For $T < T_c$, in an interval $-h_t < h < h_t$, there is three solutions for η. The η, that corresponds to h_tV can be found by calculating the extrema of $(hV)(\eta)$

$$\frac{\partial}{\partial \eta}\left(2at\eta + 4B\eta^3\right) = 2at + 12B\eta^2 = 0 \tag{3.16}$$

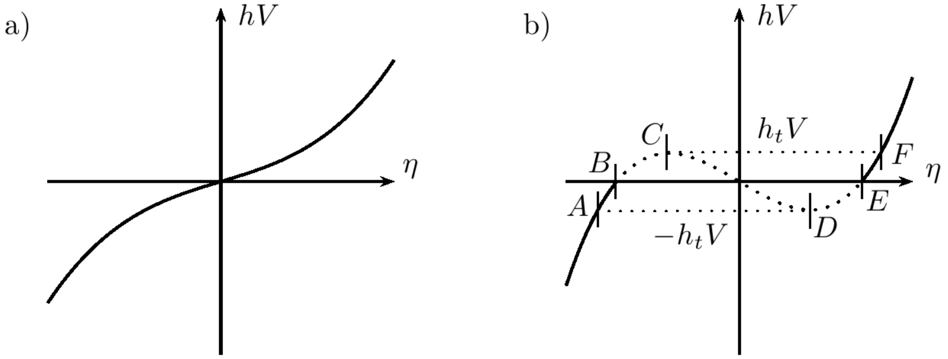

Figure 3.2: a) Relation between h and η for a) $T > T_c$ and b) $T < T_c$.

So there is one negative and one positive solution for η, given by

$$\eta = \pm\sqrt{\frac{2a(-t)}{12B}} = \pm\sqrt{\frac{a(-t)}{6B}} \tag{3.17}$$

Therefore we find for h_t

$$h_t = 2at\left(\frac{a|t|}{6B}\right)^{1/2} + 4B\left(\frac{a|t|}{6B}\right)^{3/2} = \left(\frac{2}{3}\right)^{2/3}\frac{a^{3/2}|t|^{3/2}}{B^{1/2}} \tag{3.18}$$

Only one of the three solutions is the one, that corresponds to the global minimum. To determine, which one it is, we look at the sections AB, BC, CD, DE and EF as drawn in figure 3.2 and we use

$$\left.\frac{\partial}{\partial h}\right|_T \left(2at\eta + 4B\eta^3\right) = \left(\frac{\partial\eta}{\partial h}\right)_T \left(2at + 12B\eta^2\right) = V \tag{3.19}$$

which we can write as

$$\left(\frac{\partial\eta}{\partial h}\right)_T \left(\frac{\partial^2 F_h(P,T,\eta)}{\partial\eta^2}\right) = V \tag{3.20}$$

Therefore, because in the section CD, we have $(\partial\eta/\partial h)_T < 0$, it follows that the solutions in that section correspond to a maximum and not to a minimum. For $h > 0$, the remaining possible sections are BC and EF. They both correspond to minima, because $(\partial\eta/\partial h)_T > 0$. But as we can see in figure 3.1b, it's the solutions in the section EF, that lead to the global minimum. In the same way we find that for negative h, the solutions in section AB are the global minimum ones. So, we can simply replace the dotted region by a horizontal line connecting the points B and E.[1]

3.2.4 CRITICAL BEHAVIOR

The Entropy near the critical point is given by

$$S = -\frac{\partial F(P,T,\eta)}{\partial T} = S_0 - \frac{\partial A(P,T)}{\partial T}\eta^2 \tag{3.21}$$

where we used that in equilibrium, $\frac{\partial F}{\partial \eta} = 0$. Using (3.13), we get

$$S = \begin{cases} S_0 + \frac{a^2}{2B}(T - T_c), & T < T_c \\ S_0, & T > T_c \end{cases} \tag{3.22}$$

We can see that the entropy is a continuous function. Using Maxwell's relations, we can now calculate the specific heat for constant pressure

$$C_P = T\left(\frac{\partial S}{\partial T}\right)_P = \begin{cases} C_{P0} + \frac{a^2}{2B}T, & T < T_c \\ C_{P0}, & T > T_c \end{cases} \tag{3.23}$$

So Landau Theory predicts a discontinuity in C_P at $T = T_c$, namely a negative jump of $(a^2 T_c/2B)$. Similar results we can find for quantities like the heat capacity at constant volume V, the coefficient of thermal expansion or the compressibility. And in fact, such discontinuities have been measured in nature.
With equation (3.19), we find for the susceptibility

$$\chi := \left(\frac{\partial \eta}{\partial h}\right)_{T;h\to 0} = \lim_{h\to 0} \frac{V}{2at + 12B\eta^2} \tag{3.24}$$

Using $\lim_{h\to 0}\eta^2 = 0$ for $T > T_c$ and equation (3.13), we get

$$\chi = \begin{cases} \frac{V}{2a(T-T_c)}, & T > T_c \\ \frac{V}{4a(T_c-T)}, & T < T_c \end{cases} \tag{3.25}$$

This result can be explained by looking at figure 3.1a. The minima of the free energy curve get very flat, the closer we get to the critical temperature. A small perturbation of the equilibrium then results in a big change in η.[1]

3.3 FLUCTUATIONS

3.3.1 FLUCTUATIONS IN THE ORDER PARAMETER

So far, we assumed the order parameter to be spatially uniform, that is independent of the position $\mathbf{r}$. More realistic is the case, in which we allow at least small deviations from the equilibrium value $\overline{\eta}$. The work, which is needed to bring a system out of equilibrium at given pressure P and temperature T is just the change of the free energy ΔF. Therefore, the probability ω for a fluctuation for constant P and T is given with the Gibbs distribution

$$\omega \ \sim \ e^{-\frac{\Delta F}{k_B T}} \tag{3.26}$$

For small deviations from the equilibrium value $\overline{\eta}$, we use that $(\partial F/\partial \eta)_{\eta=\overline{\eta}} = 0$ and write

$$\Delta F \ = \ \frac{1}{2}(\eta - \overline{\eta})^2 \left(\frac{\partial^2 F}{\partial \eta^2}\right)_{P,T} \tag{3.27}$$

Using the definition of the susceptibility (3.24) and equation (3.20), we get for temperatures $T \sim T_c$

$$\omega \ \sim \ e^{-\frac{(\eta-\overline{\eta})^2 V}{2\chi k_B T_c}} \quad \Rightarrow \quad \left\langle (\Delta\eta)^2 \right\rangle \ = \ \frac{k_B T_c \chi}{V} \tag{3.28}$$

which is a Gaussian distribution with the mean square fluctuation $\langle (\Delta\eta)^2 \rangle$. From (3.25) we see that χ goes like $1/t$ as $T \to T_c$, so $\langle (\Delta\eta)^2 \rangle$ also goes like $1/t$ for $T \to T_c$, which means that the fluctuations grow anomaly much near the critical point. So, the actual critical behavior of the free energy potential at the critical point is due to the already discussed flat minima of F.[1]

For an inhomogeneous body, we have to introduce the free energy density $\mathcal{F}$, where $F = \int \mathcal{F} \mathrm{d}\mathbf{r}$. We use the expansion (3.11) as for F, just with the coefficients divided by the volume V and add the spacial derivatives, such that changes in the free energy due to deviations from the equilibrium value are considered. Assuming that we have only fluctuations with long wave length, it is enough to add terms up to second derivatives, that is terms proportional to

$$\frac{\partial \eta}{\partial x_i}, \qquad \eta \frac{\partial \eta}{\partial x_i}, \qquad \eta \frac{\partial^2 \eta}{\partial x_i \partial x_k}, \qquad \frac{\partial \eta}{\partial x_i} \frac{\partial \eta}{\partial x_k} \tag{3.29}$$

By integrating over the volume, the first two terms transform to surface effects, which we're not interested in and the third term reduces to the form of the fourth term, just by integrating by parts. Therefore, we can write the additional terms in the form

$$g_{ik}(P,T) \frac{\partial \eta}{\partial x_i} \frac{\partial \eta}{\partial x_k} \tag{3.30}$$

In the following, we will use the simplification $g_{ik} = g\delta_{ik}$. Finally, we write the free energy density as

$$\mathcal{F}(P,T,\eta) \ = \ \mathcal{F}_0(P,T) + \alpha t \eta^2 + b\eta^4 + g\left(\frac{\partial \eta}{\partial \mathbf{r}}\right)^2 - \eta h \tag{3.31}$$

where $\eta \equiv \eta(\mathbf{r})$ and $\alpha = a/V$, $b = B/V$ with the coefficients a, B from expansion (3.11). The coefficient g must be bigger than zero in order to make sure that the non-fluctuating case is the energetically most favorable.[1]

3.3.2 THE CORRELATION RADIUS

We have to use some concepts of Statistical Mechanics. We use that the Helmholz free energy is given by

$$A = -k_B T \ln\left[Z(h(\mathbf{r}))\right] \tag{3.32}$$

where $Z(h(\mathbf{r}))$ is the partition function, given by

$$Z(h(\mathbf{r})) = \mathrm{Tr}\, \exp\left[-\frac{1}{k_B T}\left(H(\eta(\mathbf{r})) - \int \mathrm{d}^d\mathbf{r}\, h(\mathbf{r})\eta(\mathbf{r})\right)\right] \tag{3.33}$$

where $H(\eta(\mathbf{r}))$ is the part of the Hamiltonian, that doesn't depend on the external field $h(\mathbf{r})$ and d is the dimension of the system. The expectation value of $\eta(\mathbf{r})$ then can be obtained by the functional derivative

$$\langle \eta(\mathbf{r}) \rangle = -\frac{\delta A}{\delta h(\mathbf{r}')} = \lim_{\varepsilon \to 0} \frac{A(h(\mathbf{r}) + \varepsilon\delta(\mathbf{r} - \mathbf{r}')) - F(h(\mathbf{r}))}{\varepsilon} \tag{3.34}$$

We then define the generalized isothermal susceptibility

$$\chi_T(\mathbf{r}, \mathbf{r}') = \frac{\delta \langle \eta(\mathbf{r}) \rangle}{\delta h(\mathbf{r}')} \tag{3.35}$$

To find the relation

$$\begin{aligned}
\chi_T(\mathbf{r}, \mathbf{r}') &= -\frac{\delta^2 A}{\delta h(\mathbf{r})\delta h(\mathbf{r}')} \\
&= k_B T \left(\frac{1}{Z}\frac{\delta^2 Z}{\delta h(\mathbf{r})\delta h(\mathbf{r}')} - \frac{1}{Z}\frac{\delta Z}{\delta h(\mathbf{r})} \cdot \frac{1}{Z}\frac{\delta Z}{\delta h(\mathbf{r}')}\right) \\
&= \frac{1}{k_B T}\left(\langle \eta(\mathbf{r})\eta(\mathbf{r}') \rangle - \langle \eta(\mathbf{r}) \rangle \langle \eta(\mathbf{r}') \rangle\right) \\
&= \frac{1}{k_B T} G(\mathbf{r}, \mathbf{r}')
\end{aligned} \tag{3.36}$$

where $G(\mathbf{r}, \mathbf{r}')$ is the correlation function. Now we take the functional derivative of the Landau free energy and require it to be zero, that means, we require it to be stationary

$$\frac{\delta F}{\delta \eta(\mathbf{r})} = 2\alpha t \eta(\mathbf{r}) + 4b\eta^3(\mathbf{r}) + 2g\nabla^2\eta(\mathbf{r}) - h(\mathbf{r}) = 0 \tag{3.37}$$

This differential equation has to be satisfied by the expectation value $\langle\eta(\mathbf{r})\rangle$, because the Trace, with which the expectation value is calculated, is nothing else than the functional integral over all possible $\eta(\mathbf{r})$ that satisfy equation (3.37). If we now substitute $\eta(\mathbf{r})$ in equation (3.37) with this expectation value $\langle\eta(\mathbf{r})\rangle$ and use the definition of the generalized isothermal susceptibility χ_T (3.35), we obtain

$$\left(2\alpha t + 12b\eta^2(\mathbf{r}) - 2g\nabla^2\right)\chi_T(\mathbf{r},\mathbf{r}') - \delta(\mathbf{r}-\mathbf{r}') \;=\; 0 \tag{3.38}$$

With equation (3.36) we then find for the correlation function

$$\frac{1}{k_B T}\left(2\alpha t + 12b\eta^2(\mathbf{r}) - 2g\nabla^2\right)G(\mathbf{r}-\mathbf{r}') \;=\; \delta(\mathbf{r}-\mathbf{r}') \tag{3.39}$$

where we assumed that we have a translationally invariant system and therefore wrote $G(\mathbf{r},\mathbf{r}') = G(\mathbf{r}-\mathbf{r}')$. With equation (3.39), we see that $G(\mathbf{r}-\mathbf{r}')$ actually is a Green's Function. To calculate it, we go back to the case where we have a spatially uniform η and use the equilibrium values for $h = 0$, we calculated in the last chapter (that is $\eta^2 = 0$ for $t > 0$ and $\eta^2 = -at/2b$ for $t < 0$). This leads to the new equation

$$\left(\frac{1}{\xi^2(t)} - \nabla^2\right)G(\mathbf{r}-\mathbf{r}') \;=\; \frac{k_B T}{2g}\,\delta(\mathbf{r}-\mathbf{r}') \tag{3.40}$$

where we introduced the temperature dependent quantity

$$\xi(t) \;=\; \begin{cases} \left(\frac{g}{\alpha t}\right)^{1/2} & T > T_c \\ \left(\frac{g}{2\alpha(-t)}\right)^{1/2} & T < T_c \end{cases} \tag{3.41}$$

To resolve this, we use the Fourier Transform which makes us able to write

$$\hat{G}(k) \;=\; \frac{k_B T}{2g}\,\frac{1}{k^2 + \xi^{-2}} \tag{3.42}$$

That is simply the Fourier Transform of the Yukawa Potential, multiplied by $k_B T/8\pi g$. It follows directly

$$G(\mathbf{r}) \;=\; \frac{k_B T}{8\pi g}\,\frac{e^{-\frac{r}{\xi}}}{r} \tag{3.43}$$

This is why we call $\xi(t)$ the correlation length. It gives the order of magnitude, at which the fluctuations fall off.[3]

3.3.3 THE GINZBURG CRITERION

The criterion for Landau Theory to be valid is that the mean square fluctuation of the order parameter, averaged over the correlation volume ξ^3, is small with respect to the characteristic value given by (3.13). That is

$$\frac{k_B T_c \chi}{\xi^3} \ll \frac{\alpha|t|}{2b} \tag{3.44}$$

Using the calculation for χ (3.25) and the correlation radius ξ (3.39), wo obtain the Ginzburg Criterion

$$\alpha|t| \gg \frac{k_B T_c^2 b^2}{g^3} \tag{3.45}$$

While we built up our theory, we assumed that we can expand in terms of t. So we require t to be small with respect to T_c as well. If we apply this property to (3.45), we get the validity condition

$$\frac{k_B^2 T_c b^2}{\alpha g^3} \ll 1 \tag{3.46}$$

Only if (3.46) is valid, there exists a temperature interval at which Landau Theory can be applied. From (3.45) we see, that the theory, that was built up for temperatures near the critical temperature T_c, so for small $|t|$, is not valid for small $|t|$! We expect the right-hand side of (3.45) to be small, such that Landau Theory can be applied for small $|t|$, but not for very small $|t|$. There is always a region near the critical temperature, the fluctuation region, at which the theory is not valid.[1]

3.3.4 LANDAU THEORY IN HIGHER DIMENSIONS

As we derived the correlation length $\xi(t)$ for any dimension d, we can also reformulate the Ginzburg criterion for this dimension. We take

$$\frac{T_c \chi}{\xi^3} \ll \frac{\alpha|t|}{2b} \quad \rightarrow \quad \frac{T_c \chi}{\xi^d} \ll \frac{\alpha|t|}{2b} \tag{3.47}$$

which, replacing χ and ξ as before, leads to

$$\frac{b}{g^{d/2}}\, k_B T_c \left(\alpha|t|\right)^{d/2-2} \ll 1 \tag{3.48}$$

This condition is always satisfied for temperatures near the critical point, if $d > 4$ and it can be satisfied for $d = 4$. In fact, the case $d = 4$ can be used to approximate real systems of dimension $d = 3$.[4]

3.4 Conclusive Words

We started with Bragg-Williams Theory, a very simplified version of the Ising Model, to make an example of a case, where it makes sense to expand the free energy in a potential series in the order parameter. We then generalized this idea and derived the Landau free energy, applying phenomenological properties. Only by leaving mean field theory and considering fluctuations in the order parameter, we could find a criterion for Landau theory to be valid, the Ginzburg criterion. We found that due to the flatness of the free energy near the critical point, the fluctuations grow up to infinity. That's why Landau theory, at least in 3 dimensions, can't be valid for temperatures very close to the critical point. Because of this effect, Landau theory makes quantitatively wrong predictions, like for example for the critical indices, but it describes the phase transitions very well in a phenomenological way.

Bibliography

[1] L. D. Landau and E. M. Lifschitz, *Lehrbuch der theoretischen Physik, Statistische Physik* (Akademie-Verlag Berlin, Berlin, Leipziger Strasse 3-4, 1979).

[2] P. M. Chaikin and T. C. Lubensky, *Principles of Condensed Matter Physics* (Cambridge University Press, 2000).

[3] N. D. Goldenfeld, *Lectures on Phase Transitions and the Renormalisation Group* (Addison-Wesley, 1992).

[4] T. Fließbach, *Statistische Physik, Lehrbuch zur Theoretischen Physik IV* (Spektrum Akademischer Verlag, Heidelberg, 2007).

CHAPTER 4

SCALING THEORY

ROGER HERRIGEL
SUPERVISOR: HELMUT KATZGRABER

Near the critical temperature of a continuous phase transition the singularity of the thermodynamic quantities, such as the specific heat or the magnetization are controlled by critical exponents. These exponents are not independent of each other. In this chapter we show, that only two critical exponents are independent and the rest can be derived from scaling relations. Furthermore, we study polymer statistics and see that the above exponents also describe the behavior of the spatial extent of a chain-molecule.

4.1 CRITICAL EXPONENTS

We define the reduced temperature t and the reduced external magnetic field h, which are dimensionless quantities via:

$$t = \frac{T - T_c}{T_c} \qquad h = \frac{H}{k_B T_c}. \tag{4.1}$$

The critical exponent λ of a function $f(t)$ is defined as

$$\lambda = \lim_{t \to 0} \frac{\ln f(t)}{\ln t} \tag{4.2}$$

Thus the function $f(t)$ near the critical temperature T_C is dominated by t^{λ}. For a magnetic system the critical exponents are listed in Table 4.1.
In principle, we should consider two different exponents α for $t > 0$ and α' for $t < 0$. Likewise for the exponents γ and ν. But we show that $\alpha = \alpha'$ and we

Exponent	Definition	Description
α	$C_H \sim \lvert t\rvert^{-\alpha}$	specific heat at $H = 0$
β	$M \sim \lvert t\rvert^{\beta}$	magnetization at $H = 0$, $t < 0$
γ	$\chi \sim \lvert t\rvert^{-\gamma}$	isothermal susceptibility at $H = 0$
δ	$M \sim h^{\frac{1}{\delta}}$	critical isotherm
ν	$\xi \sim \lvert t\rvert^{-\nu}$	correlation length
η	$G\left(r\right) \sim \lvert r\rvert^{-(d-2+\eta)}$	correlation function

Table 4.1: Critical exponents of a magnetic system

will therefore not distinguish between them. The amplitudes, however, are not necessarily the same, in general if $c_H \sim A|t|^{\alpha}$ then $A \neq A'$.
There are exponent inequalities which follow from fundamental thermodynamic considerations. One example is the Rushbrooke inequality [1]:

$$\alpha + 2\beta + \gamma \geq 2. \tag{4.3}$$

Using the scaling hypothesis in the next section we show that these inequalities are in fact equalities.

4.2 Scaling hypothesis

4.2.1 Definition of a homogeneous function

A function $f(r)$ is homogeneous if for all values of λ

$$f(\lambda r) = g(\lambda) f(r) \tag{4.4}$$

$g(\lambda)$ is called the scaling function which must be of the form $g(\lambda) = \lambda^p$.
In n dimensions the variables may scale with different factors. Therefore we define the generalized homogeneous function by the condition

$$\lambda f(x, y) = f(\lambda^a x, \lambda^b y) \Leftrightarrow \lambda^c f(x, y) = f(\lambda^a x, \lambda^b y). \tag{4.5}$$

4.2.2 Scaling hypothesis

The scaling hypothesis states that the singular part of the free energy density $f(t, h)$ is a homogeneous function near a second-order phase transition. Furthermore, the reduced temperature t and the order parameter h rescale by different factors:

$$f(t,h) = b^{-d} f(b^{y_t} t, b^{y_h} h). \tag{4.6}$$

A short calculation shows that if $f(t,h)$ is a generalized homogeneous function then the Legendre transform is also a homogeneous function. If follows that in the vicinity of a second-order phase transition all thermodynamic potentials are generalized homogeneous functions.

4.2.3 DERIVATION OF THE SCALING RELATIONS

If we choose $b = |t|^{\frac{1}{y_t}}$ Equation (4.6) of the free energy density becomes

$$f(t,h) = |t|^{\frac{d}{y_t}} f(\pm 1, |t|^{-\frac{y_h}{y_t}} h). \tag{4.7}$$

The function f on the right-hand-side is now a function of only one variable and we write it as

$$f(t,h) = |t|^{\frac{d}{y_t}} \phi(|t|^{-\frac{y_h}{y_t}} h). \tag{4.8}$$

In fact, there are two different scaling functions ϕ_+ for $t > 0$ and ϕ_- for $t < 0$. From Equation (4.8) the critical exponent can be easily derived.

1. **Magnetization** $M \sim |t|^{\beta}$ at $H = 0$

$$M = \frac{1}{k_B T} \left.\frac{\partial f}{\partial h}\right|_{h=0} = \frac{1}{k_B T} |t|^{\frac{d-y_h}{y_t}} \left.\phi'\right|_{h=0} \sim |t|^{\frac{d-y_h}{y_t}} \Rightarrow \beta = \frac{d-y_h}{y_t} \tag{4.9}$$

2. **Heat capacity** $C \sim |t|^{-\alpha}$ at $H = 0$

$$C = \left.\frac{\partial^2 f}{\partial t^2}\right|_{h=0} \sim |t|^{\frac{d}{y_t}-2} \Rightarrow \alpha = \frac{d}{y_t} - 2 \tag{4.10}$$

   In principle, for the different exponents α and α' we must use different scaling functions ϕ_+ and ϕ_-. We see that this has no effect on the scaling an therefore $\alpha = \alpha'$.

3. **Magnetic susceptibility** $\chi \sim |t|^{\gamma}$ at $H = 0$

$$\chi = \frac{1}{k_B T} \left.\frac{\partial M}{\partial h}\right|_{h=0} = \frac{1}{(k_B T)^2} \left.\frac{\partial^2 f}{\partial h^2}\right|_{h=0} \sim |t|^{\frac{d-2y_h}{y_t}} \Rightarrow \gamma = \frac{d-2y_h}{y_t} \tag{4.11}$$

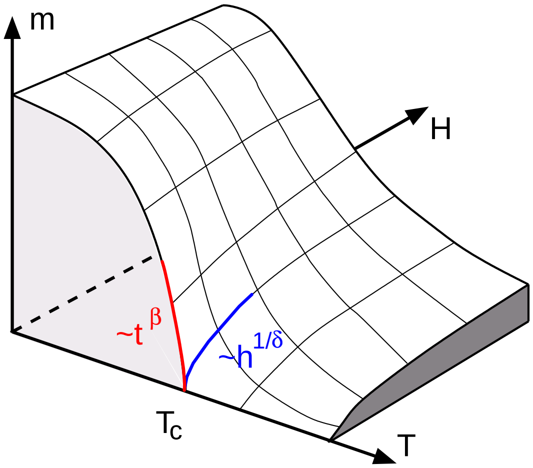

Figure 4.1: Shape of the magnetization and the critical isotherm

4. **Critical isotherm** $M \sim h^{\frac{1}{\delta}}$
   We have

$$M = \frac{1}{k_B T}\frac{\partial f}{\partial h} = |t|^{\frac{d-y_h}{y_t}}\ \phi'(|t|^{-\frac{y_h}{y_t}}\ h). \tag{4.12}$$

   But M should remain finite as $t \to 0$. Therefor $\phi'(x)$ must scale like $\phi'(x) \sim x^{\frac{d}{y_h}-1}$ such that

$$M \sim |t|^{\frac{d-y_h}{y_t}}\ \frac{h^{\frac{d-y_h}{y_h}}}{|t|^{\frac{y_h(d-y_h)}{y_h y_t}}} = h^{\frac{d-y_h}{y_h}}. \tag{4.13}$$

   The t dependence cancels out and it follows that

$$\delta = \frac{y_h}{d-y_h}. \tag{4.14}$$

The shape of the magnetization and the critical isotherm are shown in Figure 4.1.

4.2.4 HYPERSCALING

The correlation function G has also a homogeneous form which is given by

$$G(r) = b^{-2(d-y_h)}G(\frac{r}{b}, b^{y_t}t). \tag{4.15}$$

Using the same technique as for the free energy we can rewrite Equation (4.15) to obtain:

$$G(r) = |t|^{\frac{2(d-y_h)}{y_t}} \Phi\left(\frac{r}{|t|^{-\frac{1}{y_t}}}\right). \tag{4.16}$$

1. **Correlation length** $\xi \sim |t|^{-\nu}$
   We know that the correlation function has the form $G \sim e^{\frac{r}{\xi}}$ for all t, also for $t \neq 0$. The only r/ξ dependence can be found in the argument of Φ and thus

$$\xi \sim |t|^{-\frac{1}{y_t}} \Rightarrow \nu = \frac{1}{y_t}. \tag{4.17}$$

2. **Correlation function** $G \sim |r|^{-(d-2-\eta)}$
   We start form Equation (4.15) were we choose $b = r$ and $t = 0$ to obtain

$$G\left(r\right) \sim r^{-2(d-y_h)} \Rightarrow \eta = d + 2 - 2y_h \tag{4.18}$$

4.2.5 Scaling Relations

From the eight equations of the exponents α, β, γ, δ, ν,η, y_t, and y_h one obtains the following identities:

$$\begin{array}{cc} \alpha + 2\beta + \gamma = 2 & \text{Rushbrook's Identity} \\ \delta - 1 = \frac{\gamma}{\beta} & \text{Widom's Identity} \\ 2 - \alpha = d\nu & \text{Josephson's Identity} \\ \gamma = \nu\left(2 - \eta\right) & \end{array}$$

The scaling relations which involve the spatial dimension d of a system are also called hyperscaling relations. It follows that given two independent exponents all other can be obtained using the four scaling relations above.

4.2.6 Ising model

Every theory should be validated by experimental data. For the two-dimensional Ising Hamiltonian [2] the exact values from the Onsager solution $\alpha = 0$, $\beta = 1/8$, $\gamma = 7/4$, $\delta = 15$, $\nu = 1$, $\eta = 1/4$ solves our set of equation. Thus the Onsager solution fulfills the scaling relations.

4.3 DERIVING THE HOMOGENEOUS FORMS

Kadanoff presented in 1966 a heuristic argument that provides intuitive support for the scaling hypothesis [1]. His work also was the beginning of the renormalization group theory.

4.3.1 SCALING OF THE FREE ENERGY

Consider an Ising model [3] of N spin $s_i = \pm 1$ situated on an d-dimensional hypercubic lattice. We consider only nearest neighbor interactions. The lattice constant is a. The Hamiltonian is given by

$$H_\Omega = -J \sum_{\langle ij \rangle}^{N} s_i s_j - H \sum_{i}^{N} s_i. \tag{4.19}$$

We partition the lattice into cells of length ba. Thus there are N/b^d blocks each containing b^d sites. Figure 4.2 shows such a partition with $b = 3$ in a two-dimensional system.

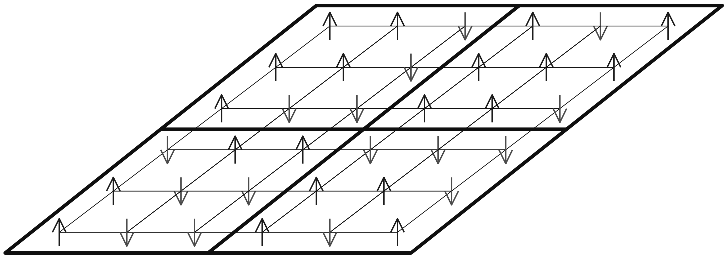

Figure 4.2: Block spin transformation

We now want to define a **block spin** $\tilde{s}$ for each cell. We do this by setting $\tilde{s}$ to the direction of the majority of the original spins in the cell. Alternatively it is also possible to set the block spin equal to the spin in the middle of the cell or equal to the spin in the left upper corner of the cell. Important is, that all block spins have the same magnitude.

The original spins interacting only with their nearest neighbors and the external field. We make the assumption that the block spin also interacts only with nearest-neighbor block spins and an effective external field. Thus we define new coupling constants $\tilde{J}$ and $\tilde{H}$ and the Hamiltonian for the block spin is given by

$$\tilde{H}_\Omega = -\tilde{J} \sum_{\langle ij \rangle}^{Nb^{-d}} \tilde{s}_i \tilde{s}_j - \tilde{H} \sum_{i}^{Nb^{-d}} \tilde{s}_i. \tag{4.20}$$

Since the Hamiltonian has the same structure for both the block spins and the original spins, we may expect that also the thermodynamic functions are similar, but with different parameters. For the free energy density f it follows

$$f(t,h) = b^{-d} f(\tilde{t},\tilde{h}). \tag{4.21}$$

The new parameters $\tilde{t}$ and $\tilde{h}$ depend on t and h as well as the scaling parameter b. This means we have that $\tilde{h} = \tilde{h}\,(h,b)$ and $\tilde{t} = \tilde{t}\,(t,b)$. From Equation (4.21) we conclude that $\tilde{h} \propto h$ and $\tilde{t} \propto t$. For the dependence of b Kadanoff assumed that

$$\tilde{h} = b^{y_h} h \qquad \tilde{t} = b^{y_t} t, \tag{4.22}$$

which leads to

$$f(t,h) = b^{-d} f(b^{y_t} t, b^{y_h} h). \tag{4.23}$$

Equation (4.23) is identical to Equation (4.5) and thus we obtained the homogeneity of the free energy density f.

4.3.2 SCALING FOR THE CORRELATION FUNCTION

For a given partition function $Z = \mathrm{Tr} e^{-\beta H_\Omega}$ where $\beta = 1/k_B T$ the free energy is given by $F = -\beta^{-1} \ln Z$.
If we consider a system with a non-uniform magnetic field

$$\beta H_\Omega = \beta H_{\Omega 0} - \sum_r h(r) s(r), \tag{4.24}$$

we obtain the 2-point correlation function by taking the derivative of βF with respect to $h(r)$

$$\begin{aligned} G(r_1 - r_2, H_\Omega) &= \langle s(r_1) s(r_2) \rangle - \langle s(r_1) \rangle \langle s(r_2) \rangle & (4.25) \\ &= \left. \frac{\partial^2}{\partial h(r_1) \partial h(r_2)} \ln Z \right|_{h(r)=0}. & (4.26) \end{aligned}$$

We demand that $h(r)$ does not vary significantly over a distance ba of a block. Thus we can assume it transforms in the same manner as a uniform field $h = h(r)$. Setting $\tilde{r} = r/b$ we obtain

$$\beta\tilde{H}_\Omega(\tilde{s}) = \beta\tilde{H}_{\Omega 0}(\tilde{s}) - \sum_{\tilde{r}} \tilde{h}(\tilde{r})\tilde{s}(\tilde{r}). \tag{4.27}$$

The free energy of the original and the block spin systems are the same. Thus we obtain

$$\frac{\partial^2}{\partial\tilde{h}(\tilde{r}_1)\partial\tilde{h}(\tilde{r}_2)} \ln \tilde{Z}(\tilde{h}) = \frac{\partial^2}{\partial\tilde{h}(\tilde{r}_1)\partial\tilde{h}(\tilde{r}_2)} \ln Z(h). \tag{4.28}$$

The left-hand-side is the correlation function of the the block spin system $G(\tilde{r}_1 - \tilde{r}_2, \tilde{H}_\Omega)$. From $\tilde{h}(\tilde{r}) = b^{y_h} h(r)$ we obtain the infinitesimal change $\delta\tilde{h}(\tilde{r}) = b^{y_h}\delta h(r)$. It is crucial that a change in $\tilde{h}(\tilde{r})$ correspond to all fields $h(r_i)$ with r_i in the block of $\tilde{r}$. Thus we obtain for the right-hand-side:

$$b^{-2y_h} \left\langle \left(s_1^{(1)} + ... + s_{b^d}^{(1)}\right) \left(s_1^{(2)} + ... + s_{b^d}^{(2)}\right) \right\rangle = b^{-2y_h} \sum_i^{b^d} \sum_j^{b^d} \left\langle s_i^{(1)} s_j^{(2)} \right\rangle. \tag{4.29}$$

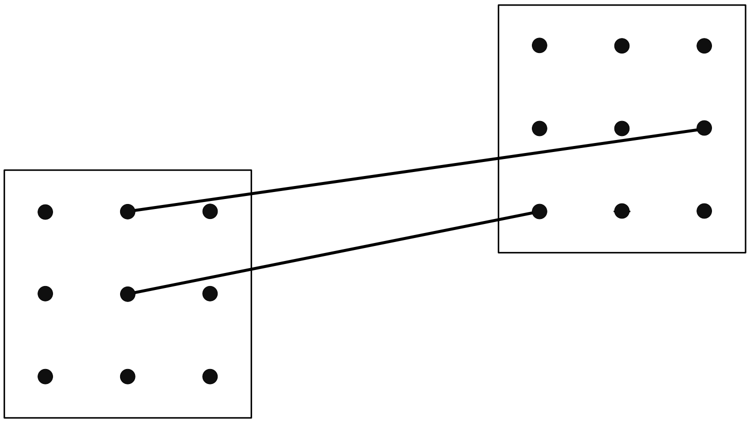

Figure 4.3: Correlation between spins of two distant blocks

The spins of the block 1 corresponding to $\tilde{r}_1$ are labeled by $s_i^{(1)}$ while the spins of block 2 corresponding to $\tilde{r}_2$ are labeled by $s_i^{(2)}$. If $r = |r_1 - r_2| \gg ba$ the term under the sum, as can be seen in Figure 4.3, is almost the same for all i and j and we obtain

$$G(\frac{r}{b}, \tilde{H}_\Omega) = b^{2d-2y_h} G(r, H_\Omega) \tag{4.30}$$

Taking b^{2d-2y_h} to the other side of the equation and using the relation (4.22) we see that this is exactly the same homogeneous Equation as (4.15).

4.4 UNIVERSALITY CLASSES

Universality is a prediction of the renormalization group theory. There we have some renormalization group fixed point and two systems are in the same universality class if they flow into the same renormalization group fixed point [3]. Systems in the same Universality class have the same critical exponents but can have different transition temperatures. According to renormalization group two systems require only a few common features to be in the same universality classes. They must have the same

- spatial dimension
- symmetries of the order parameter
- range and symmetries of Hamiltonian

The details of the form and magnitude of interactions is irrelevant. Therefore, if the above properties of a system are the same of an other (well known) system, we already known its critical exponents!

4.4.1 FINITE SIZE SCALING

Experiments on real systems and numerical calculations like Monte Carlo simulations [4] use finite systems. By observing how the quantities C, M, χ vary for different lattices sizes it its possible to calculate the values for the critical exponents. For example, we have for the specific heat C that

$$C_L = L^{\frac{\alpha}{\nu}} \widetilde{C}(L^{\frac{1}{\nu}} t), \tag{4.31}$$

where $\widetilde{C}$ is independent of the lattice size while T_c, α and ν depends on it. If these three parameters are chosen correctly and $C_L L^{-\alpha/\nu}$ is plotted against $L^{\frac{1}{\nu}} t$ the curve of different lattice sizes will collapse onto a universal curve.

4.4.2 RANDOM SYSTEMS

A real system will inevitably contain impurities. We will now study there influence on the critical behavior. Since random inhomogeneities tend to disorder a system, it is possible that the ordered phase is completely eliminated. But it is also possible that systems remain ordered and only the universality class may be modified.

The Harris criterion [5], [3] says that the critical behavior of a quenched disordered system does not differ from that of the pure systems if

$$d\nu > 2. \tag{4.32}$$

This is equivalent to $\alpha < 0$. The exponent of Equation (4.32) are thus of the pure fixed point. For most three-dimensional systems the criterion is satisfied, and therefore a weak randomness has no effect on the critical exponents.

4.5 POLYMER STATISTICS

A polymer is a chain of monomers. A large class of natural and synthetic materials are polymers. Examples are plastic such as PVC PE and PET but also our RNA DNA and proteins are polymers.

4.5.1 RANDOM WALK

A flexible polymer chain can be idealized by a random walk on a periodic lattice. We consider random walks on a hypercubic grid. This means the distance from one point to the next is a constant, the direction from one point to the next is chosen at random and no direction is more probable than another. Figure 4.4 shows a random and a self-avoiding random walk for a two-dimensional system.

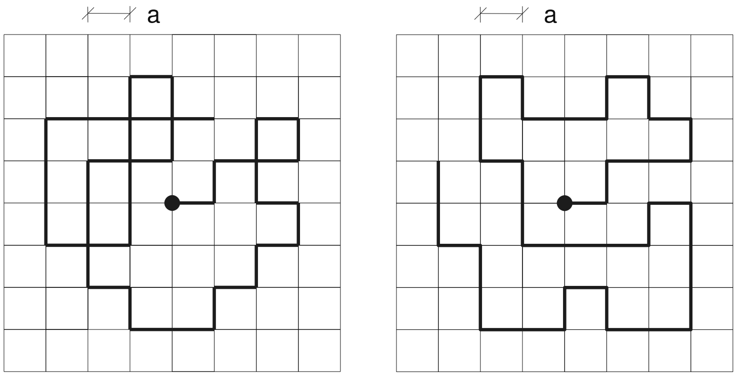

Figure 4.4: A random and a self-avoiding random walk

Let $c_N(\vec{r})$ be the number of distinct walks from 0 to $\vec{r}$ in N steps. The end-to-end vector is the sum of n jump vectors:

$$\vec{r} = \sum_n \vec{a}_n. \tag{4.33}$$

The average square distance is then given by

$$\left\langle r^2 \right\rangle = \sum_{n=m} \langle \vec{a}_n \vec{a}_m \rangle + \underbrace{\sum_{n\neq m} \langle \vec{a}_n \vec{a}_m \rangle}_{=0} = Na^2. \tag{4.34}$$

Since two pieces of the polymer cannot be at the same place, a more accurate description is given by the self-avoiding random walk. The goal of the following sections is to find a scaling behavior for the average square distance of a self-avoiding random walk.

4.5.2 $O(n)$ vector model

We consider the n vector model. This model describes a hypercubic lattice of dimension d where each site i of the lattice caries a spin $\vec{S}_i$ with n components $S_i^1, S_i^2, .., S_i^n$. We chose the following normalization

$$\sum_\alpha \left(\vec{S}^\alpha\right)^2 = n. \tag{4.35}$$

We consider only nearest-neighbor interaction. Thus the Hamiltonian of the system is

$$H_\Omega = -K \sum_{\langle ij\rangle,\alpha} S_i^\alpha S_j^\alpha. \tag{4.36}$$

We want to expand the exponential of the Hamiltonian in a power series

$$\begin{aligned} \exp(-\beta H_\Omega) &= \exp(-\beta K \sum_{\langle ij\rangle,\alpha} S_i^\alpha S_j^\alpha) = \prod_{\langle ij\rangle} \exp(-\beta K \sum_\alpha S_i^\alpha S_j^\alpha) \qquad (4.37) \\ &= \prod_{\langle ij\rangle} (1 - \beta K \sum_{\langle ij\rangle,\alpha} S_i^\alpha S_j^\alpha + \frac{1}{2}(\beta K)^2 (\sum_{\langle ij\rangle,\alpha} S_i^\alpha S_j^\alpha)^2 - ...). \end{aligned}$$

The trace of this term is the partition function form which we construct a link to the self-avoiding random walk.

4.5.3 Moment Theorem

We denote by $\langle ... \rangle_0$ the average of all possible orientation of the n-dimensional spin space. If we choose the normalization Equation (4.35) and take the limit

$n \to 0$ only one of these averages is nonvanishing while all other momentum are 0, i.e.,

$$\left\langle S_i^{\alpha} S_i^{\beta} \right\rangle_0 = \delta_{\alpha\beta} \tag{4.38}$$

Proof: We start with $n \in \mathbb{N}\backslash\{0\}$. The spins are normalized like in Equation (4.33). The characteristic function $f(\vec{k})$ of S^{α} is given by

$$f(\vec{k}) = \left\langle \exp(i\vec{k}\vec{S}) \right\rangle_0 . \tag{4.39}$$

It follows that the moments are calculated in the following manner

$$\left\langle S^{\alpha} S^{\beta} S^{\gamma} \right\rangle_0 = \left(-i\frac{\partial}{\partial k_{\alpha}}\right)\left(-i\frac{\partial}{\partial k_{\beta}}\right)\left(-i\frac{\partial}{\partial k_{\gamma}}\right) f(\vec{k})|k = 0. \tag{4.40}$$

Let $k = |\vec{k}|$. If we use our normalization condition (4.35) we obtain

$$\nabla^2 f = -\sum_{\alpha} \left\langle (S^{\alpha})^2 \exp\left(i\vec{k}\right)\vec{S} \right\rangle_0 = -fn. \tag{4.41}$$

Using the chain rule $\frac{\partial f}{\partial k_{\alpha}} = \frac{f_{\alpha}}{k}\frac{df}{dk}$ we can write the Laplacian as

$$\nabla^2 f = \sum_{\alpha} \frac{\partial^2 f}{\partial k_{\alpha}^2} = \frac{n-1}{k}\frac{df}{dk} + \frac{d^2 f}{dk^2}. \tag{4.42}$$

From Equation (4.41) and Equation (4.42) we obtain the differential equation

$$\frac{n-1}{k}\frac{df}{dk} + \frac{d^2 f}{dk^2} = -nf. \tag{4.43}$$

The solution of this differential equation for $n = 0$ is $f(k) = a + bk^2$. Considering the boundary conditions from Equation (4.39), $f(0) = 1$ and $df/dk(0) = 0$, we obtain

$$f(k) = 1 - \frac{1}{2}k^2. \tag{4.44}$$

This implies that all moment except of $\langle S_i^{\alpha} S_i^{\alpha} \rangle_0 = 1$ vanish.

4.5.4 MAPPING TO $n \to 0$ MODEL OF A MAGNETIC SYSTEM

Using Equation (4.38) the partition function at a zero external field has the form

$$\begin{aligned} Z &= \operatorname{Tr}\exp\left(-\beta H_\Omega\right) \qquad (4.45) \\ &= \Omega \left\langle \prod_{\langle ij\rangle} \left(1 - \beta K \sum_\alpha S_i^\alpha S_j^\alpha + \frac{1}{2}(\beta K)^2 \left(\sum_\alpha S_i^\alpha S_j^\alpha \right)^2 \right) \right\rangle_0 . \end{aligned}$$

Note that the trace and the average $\langle ... \rangle_0$ differ only by a factor $\Omega = \prod_i \int d\Omega_i$. All higher terms of the power series are zero due to the moment theorem. Now we can expand the product over $\langle ij \rangle$. This gives us 3^B terms. Each of this terms is represented by a diagram on the lattice. To obtain a certain term of the expansion we have to choose for each factor either 1, $\beta K \sum_\alpha S_i^\alpha S_j^\alpha$ or $(\beta K)^2 \left(\sum_\alpha S_i^\alpha S_j^\alpha\right)^2$. If we choose $\beta K \sum_\alpha S_i^\alpha S_j^\alpha$ we draw a line form i to j in our lattice, if we choose 1 we do nothing. The term $(\beta K)^2 \left(\sum_\alpha S_i^\alpha S_j^\alpha\right)^2$ will correspond to a closed loop from the lattice site i and j and back. We thus obtain 3^B diagrams of the form shown in Figure 4.5.

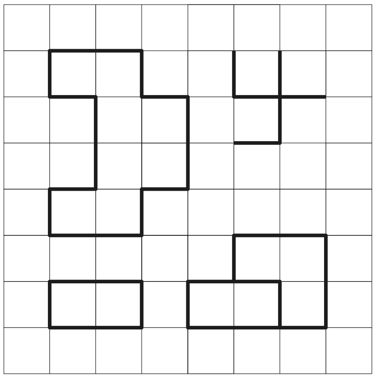

Figure 4.5: Diagram of a typical term in the expansion.

On taking the average any vertex with more than two lines running into it, is associated to a power grater than two of that spin variable and will according the moment theorem vanish. Vertices with only one line also vanish because the average is invariant under the parity transformation $\vec{S}_i \to -\vec{S}_i$.

We are left with diagrams consisting of closed, mutually self-avoiding loops like in Figure 4.6. If we take the average around such a loop we force the spin index to be the same

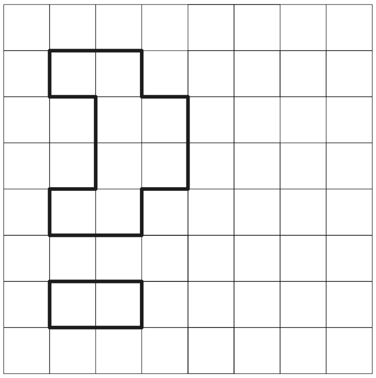

Figure 4.6: Diagram that survives taking the average.

$$\langle\sum_{\alpha\beta\ldots} S_i^\alpha S_j^\alpha\ S_j^\beta S_k^\beta\ \ldots\ S_q^\theta S_i^\iota\rangle_0 = \sum_{\alpha\beta\ldots}\delta_{\alpha\beta}\delta_{\beta\gamma}\ldots\delta_{\alpha\iota} = \sum_{\alpha}^{n} 1 = n. \tag{4.46}$$

Thus the partition function is given by the formula

$$Z = \sum_{\text{loop conf}} n^{\text{number of loops}} \left(\beta K\right)^{\text{number of bounds}}. \tag{4.47}$$

For $n \to 0$ it follows that $Z = \Omega$.
More interesting is the correlation function defined by

$$G\left(i, j, H\right) = \left\langle S_i^1 S_j^1 \right\rangle \tag{4.48}$$
$$= Z^{-1}\mathrm{Tr}\prod_{\langle ij\rangle} S_i^1 S_j^1 \left(1 - \beta K \sum_\alpha S_i^\alpha S_j^\alpha + \frac{1}{2}\left(\beta K^2\right)\left(\sum_\alpha S_i^\alpha S_j^\alpha\right)^2\right)$$

Apart from the normalization condition the correlation function defined in Equation (4.49) is the same as the common correlation function. With the same consideration as before the only non-empty diagram must have a single line form the vertex i to j. Taking the average will fix the spin-index of this line to be 1. Letting $n \to 0$ all other surviving loops will disappear. If we denote by r the distance between two point we have obtained

$$\sum_N c_N(r)(\beta K)^N = \lim_{n\to 0} G(r, \beta K). \tag{4.49}$$

This formula gives us a connection between self-avoiding random walks and the correlation function of the Heisenberg model for $n \to 0$.

4.5.5 Critical behavior

We denote $x = \beta K = \frac{K}{k_B T}$ and $x_c = \frac{K}{k_B T_c}$. The total number of self-avoiding walks of N steps is

$$c_N = \sum_r c_N\left(r\right). \tag{4.50}$$

From Equation (4.49) it follows that

$$\sum_N c_N x^N = \sum_N \sum_r c_N(r) x^N = \lim_{n\to 0} \sum_r G(r,x) = \chi \sim |x - x_c|^{-\gamma}. \tag{4.51}$$

The series on the left-hand-side should (according to the right-hand-side) diverge as x reaches the critical value x_c. This suggests the following value for c_N:

$$c_N = \text{const} \cdot x_c^{-N} N^{\gamma - 1} \tag{4.52}$$

such that

$$\begin{aligned}\sum_N c_N x^N &= \int_0^\infty dN N^{\gamma-1} \left(\frac{x}{x_c}\right)^N \\ &= \text{const}(\gamma) \ln\left(\frac{x}{x_c}\right)^{-\gamma} \sim |x - x_c|^{-\gamma}\end{aligned} \tag{4.53}$$

where we used the approximation $\ln\left(\frac{x}{x_c}\right) = \ln\left(1 + \frac{(x-x_c)}{x_c}\right) \approx \frac{x-x_c}{x_c}$ for $x - x_c \ll 1$. We are also interested in the scaling behavior of $\langle r^2 \rangle$. We have

$$\left\langle r^2 \right\rangle = \sum_{\vec{R}} r^2 \frac{c_N(r)}{c_N} \tag{4.54}$$

$$\begin{aligned}\sum_{\vec{r}} r^2 G\left(r,x\right) &= \sum_{\vec{r}} \sum_N c_N\left(r\right) x^N r^2 \\ &= \sum_N \left(\sum_{\vec{r}} c_N\left(r\right) R^2\right) x^N = \sum_N a_N x^N,\end{aligned} \tag{4.55}$$

where we defined $a_N = \sum_{\vec{r}} c_N\left(r\right) r^2$ which scales like

$$\begin{aligned}\sum_{\vec{r}} r^2 G\left(r,x\right) &\sim \int_{\mathbb{R}^d} r^2 r^{d-1} r^{-(d-2+\eta)} \exp\left(\frac{r}{\xi}\right) dr d\Omega \\ &= \int_0^\infty r^{3-\eta} \exp\left(\frac{r}{\xi}\right) dr \int_\Omega d\Omega \\ &\sim \xi^{4-\eta}\Gamma\left(d-\eta\right) \sim \left|x_c - x\right|^{\gamma-2\nu}.\end{aligned} \tag{4.56}$$

Here we used that $G\left(r,x\right) = r^{-(d-2+\eta)}\exp\left(-\frac{r}{\xi}\right)$. Like above we have that

$$\sum_N a_N x^N \sim \left|x_c - x\right|^{\gamma-2\nu} \Rightarrow a_N \sim x_c^{-N} N^{\gamma-2\nu-1}. \tag{4.57}$$

We conclude that

$$\left\langle r^2\right\rangle \sim \frac{a_N}{c_N} = \frac{x_C^{-N} N^{2\nu+\gamma-1}}{x_C^{-N} N^{\gamma-1}} \sim N^{2\nu}. \tag{4.58}$$

Summarizing we have found that for a simple random walk $\langle r^2\rangle \sim N$ and for a self-avoiding random walk $\langle r^2\rangle \sim N^{2\nu}$. In three dimension $\gamma = 7/6$ and $\nu = 3/5$.

4.6 CONCLUSIONS

Near the critical point of a second-order phase transition the thermodynamic potentials are assumed to be homogeneous functions. It follows that only two of the six critical exponents are independent of each other and the other four can be derived from the scaling relations.

Furthermore we can group systems into universality classes. All system in the same universality class have the same critical exponents. Impurities can destroy the ordered phase. The Harris criterion says that the critical behavior of a quenched disordered system does not differ form that of the pure systems if $d\nu > 2$.

Finally we found that spatial extent of a random and self-avoiding random walk can be scaled with the critical exponents of the $O(n)$ $n \to 0$ model. We have that for a simple random walk $\langle r^2\rangle \sim N$ and for a self-avoiding random walk $\langle r^2\rangle \sim N^{2\nu}$, where N is the number of steps.

Bibliography

[1] H. E. Stanley, *Introduction to Phase Transitions and Critical Phenomena* (Oxford University Press, 1971).

[2] K. Huang, *Statistical Mechanics* (John Wiley, 1987).

[3] N. Goldenfeld, *Lectures on Phase Transitions and the Renormalization Group* (Addison-Wesley, 1992).

[4] D. P. Laundau, *A Guide to Monte Carlo Simulations in Statistical Physics* (Cambridge University Press, 2005).

[5] J. Cardy, *Scaling and Renormalization in Statistical Physics* (Cambridge University Press, Cambridge, 1996).

[6] P. G. de Gennes, *Scaling Concepts in Polymer Physics* (Cornell University Press, 1979).

CHAPTER 5

THE RENORMALIZATION GROUP

THOMAS COUTANDIN
SUPERVISORS: DR. CH. INIOTAKIS, DR. M. MATSUMOTO

5.1 INTRODUCTION

Given a macroscopic physical system near a critical point. A renormalization group (RG) for our system is a set of *symmetry transformations* which are defined to act on an appropriate space of states of our system. These symmetry transformations are called **RG transformations**. The idea of symmetry transformations is here in principle the same as the one we know from atomic physics, for example. But there are some differences: first the whole system will not be simply invariant under an RG transformation, second it is not so easy to *find* an RG and third the RG is *not* a group. Besides that recall that carrying out a symmetry transformation does not mean the same as solving a particular model.

Our job: Find an RG for our system (there may be many). **The idea:** Study the behavior of our system under a change of scale. **What do we get from RG theory?** First we get a connection to QFT. Second the **critical exponents appear as symmetry properties** of the RG transformations: (a) as a direct consequence of having found an RG for our system we get the **scaling relations** corresponding to our system; (b) there is a way to **calculate critical exponents**.

In this text the RG will be treated in the framework of *Classical Statistical Mechanics* restricted to *lattice spin systems*, having applications in condensed matter physics in mind[1].

---

[1] This text is mainly based on a paper of J. Fröhlich and T. Spencer [1].

It should be emphasized that RG methods are not restricted to statistical mechanics; far from it, the idea underlying the RG has many applications in other parts of physics. Definitely included is for example astrophysics and *Quantum Field Theory*.

5.2 CLASSICAL LATTICE SPIN SYSTEMS

In the following we will only look at the simplest, classical spin systems, namely lattice ones. For the treatment below we should justify the following: (i) the use of **classical** spin systems, (ii) considering **infinitely large** lattice systems and (iii) considering only the **(hyper-) cubic** lattice.
As physical systems we will only consider classical spin systems with a mathematical structure described by four properties defining 1. the lattice, 2. the spin, 3. the energy and 4. the equilibrium state of the lattice system.

Classical spin system (summarized[2]): **lattice**: $\mathbb{Z}^{\mathbf{d}}$; **classical spin**: $\varphi(j) \in \mathbb{R}^N_{(j)} \simeq \mathbb{R}^N$, $j \in \mathbb{Z}^d$ (N: dimension of spin space); **spin configuration on $\boldsymbol{\Lambda} \subset \mathbb{Z}^d$**: $\varphi_\Lambda := \{\varphi(j) : j \in \Lambda\} \in K_\Lambda := \prod_{j\in\Lambda} \mathbb{R}^N_{(j)}$; **a priori distribution of the spin** $\varphi(j)$: probability measure $d\lambda(\varphi(j))$. For a *finite* sublattice $\Lambda \subset \mathbb{Z}^d$: **a priori distribution of a spin configuration on $\boldsymbol{\Lambda}$**: probability measure $\prod_{j\in\Lambda} d\lambda(\varphi(j))$; **energy/hamilton function** on Λ: $H_\Lambda(\varphi_\Lambda)$ (continuous); for $\Lambda_n \nearrow \mathbb{Z}^d$, $n \to \infty$ (Λ_n: finite), there exist the **interaction energy** between Λ and Λ^c, $W_{\Lambda,\Lambda^c} \equiv \lim_{n\to\infty} W_{\Lambda,\Lambda_n\setminus\Lambda} \equiv \lim_{n\to\infty} \{H_{\Lambda_n} - (H_\Lambda + H_{\Lambda_n\setminus\Lambda})\}$, and the **free energy**, $f(\beta,\lambda)$, **per unit volume** defined by $\beta f(\beta,\lambda) \equiv \lim_{n\to\infty} -\frac{1}{|\Lambda_n|} \log Z_\beta(\Lambda_n)$, where $Z_\beta(\Lambda_n) \equiv \int_{K_{\Lambda_n}} exp[-\beta H_{\Lambda_n}(\varphi_{\Lambda_n})] \prod_{j\in\Lambda_n} d\lambda(\varphi(j))$, for all $\beta \geq 0$.

An **equilibrium state at inverse temperature** β of the *infinite* lattice spin system is given by a probability measure, $d\mu_{\beta,\lambda}(\varphi)$, on $K_{\mathbb{Z}^{\mathbf{d}}}$ with the following *defining property*: for every bounded measurable function A on K_Λ, where Λ is an *arbitrary* finite sublattice, the following holds:

$$\boxed{\langle A\rangle_{\beta,\lambda} \equiv \int\limits_{K_\infty} A(\varphi_\Lambda) d\mu_{\beta,\lambda}(\varphi) = \int\limits_{K_{\Lambda^c}} d\rho(\varphi_{\Lambda^c}) \int\limits_{K_\Lambda} e^{-\beta\left(W_{\Lambda,\Lambda^c}(\varphi)\ +\ H_\Lambda(\varphi_\Lambda)\right)} A(\varphi_\Lambda) \prod_{j\in\Lambda} d\lambda(\varphi(j))\ ,} \tag{5.1}$$

where $d\rho(\varphi_{\Lambda^c})$ is a finite measure on K_{Λ^c}. These are the so called **Dobrushin-Lanford-Ruelle equations**. **Note:** For simplicity we will consider a one-component spin field $\varphi : \mathbb{Z}^d \to \mathbb{R}$ in the following, i.e. $N = 1$.

---

[2] For more details see [1] or a more detailed version available from me.

Correlation function ("correlating" the spins of a finite number of lattice sites $x_1, \ldots, x_n$):

$$\langle\, \varphi(x_1)\ \cdots\ \varphi(x_n)\,\rangle_\beta \equiv \left\langle \prod_{k=1}^{n} \varphi(x_k) \right\rangle_\beta = \int_{K_\infty} \prod_{k=1}^{n} \varphi(x_k)\ d\mu_\beta(\varphi)\ . \tag{5.2}$$

Inverse correlation length (mass): $m(\beta) := -\lim_{|x|\to\infty} \frac{1}{|x|} \log\ \langle \varphi(0)\varphi(x)\rangle^c_\beta$, measures the exponential decay rate of $\langle\varphi(0)\varphi(x)\rangle^c_\beta$; **susceptibility**: $\chi(\beta) := \sum\limits_{x\in\mathbb{Z}^d} \langle\varphi(0)\varphi(x)\rangle^c_\beta$, where $\langle\varphi(0)\varphi(x)\rangle^c_\beta := \langle\varphi(0)\varphi(x)\rangle_\beta - \langle\varphi(0)\rangle^2_\beta$.
In the following we will only consider phase transitions at a critical point. $\beta = \beta_c$ is defined to be a **critical point** if $m(\beta) \searrow 0$ as $\beta \nearrow \beta_c$, or $\beta \searrow \beta_c$. **Scaling laws**: $\tilde{m}(t) \sim t^\nu$ and $\tilde{\chi}(t) \sim t^{-\gamma}$ as $t \to 0$, where $\tilde{m}(t) := m(\beta)$, $\tilde{\chi}(t) := \chi(\beta)$, $t := \frac{\beta_c - \beta}{\beta_c}$ and $a(t) \sim b(t)$, $t \to 0$ $:\Leftrightarrow$ $\lim_{t\to 0+} \frac{\log a(t)}{\log b(t)} = 1$. The exponents ν and γ, occurring in the scaling laws, are called **critical exponents**.

5.3 SCALING LIMIT

5.3.1 SCALED LATTICE SYSTEMS, RENORM. CONDITION

For the following we consider the case in which $\beta < \beta_{\mathbf{c}}$. In order to simplify the discussion we make some other **assumptions (equilibrium state, inverse correlation length)**:

- The equilibrium state $d\mu_\beta(\varphi)$ is *invariant under lattice translations* , i.e.

$$\forall x \in \mathbb{Z}^d : \quad d\mu_\beta(\varphi_x) = d\mu_\beta(\varphi)\ , \text{with } \varphi_x(j) = \varphi(j+x)\ ,\ x, j \in \mathbb{Z}^d\ . \tag{5.3}$$

- Furthermore for $\beta < \beta_c$, the equilibrium state $d\mu_\beta$ is extremal (w.r.t. translation invariance), i.e. ergodic under the action of lattice translations. Physically this means that $d\mu_\beta$ is a "macrostate"; see [4].
- The inverse correlation length $m(\beta)$ is *positive*, i.e. $\langle\varphi(x)\varphi(y)\rangle_\beta$ tends to 0 exponentially fast, as $|x-y| \to \infty$ (with decay rate $m(\beta)$: by a trivial re-definition of φ it is always possible to assume that $\langle\varphi(x)\rangle_\beta = 0$).
- Furthermore $\beta \mapsto m(\beta)$ is continuous and $m(\beta) \searrow 0$, as $\beta \nearrow \beta_c$.

Due to the divergence of the correlation length, $\xi \equiv m(\beta)^{-1}$, at a critical point we are interested in the **large scale behavior of the correlation functions**

$$\langle\varphi(z_1)\cdots\varphi(z_n)\rangle_\beta \quad , \quad \beta \text{ near to } \beta_c \qquad (z_i \in \mathbb{Z}^d, 1 \le i \le n)\ ; \tag{5.4}$$

more precisely we are interested in the long distance limit of (5.4), in which

$$|z_i - z_j| \to \infty \quad , \quad \text{whenever } i \neq j \ . \tag{5.5}$$

In order to realize such a limit we consider a **scale transformation**

$$\mathbb{Z}^d \to \mathbb{Z}^d_{\vartheta^{-1}} := \{y \in \mathbb{R}^d \ : \ \vartheta y \in \mathbb{Z}^d\} \quad , \qquad z \mapsto \vartheta^{-1} z \tag{5.6}$$

where $\vartheta \in [1, \infty[$ is called a **scale parameter**. Then, for given points $x_k \in \mathbb{Z}^d \subset \mathbb{R}^d$, $1 \leq k \leq n$, we choose for every $\vartheta \in [1, \infty[$ functions $\vartheta \mapsto x_i(\vartheta) \in \mathbb{Z}^d_{\vartheta^{-1}} \subset \mathbb{R}^d$, $1 \leq i \leq n$, in such a way that

$$x_i(\vartheta) = x_i + O(\vartheta^{-1}) \quad , \quad (\vartheta \to \infty) \ . \tag{5.7}$$

In particular we get $|x_i(\vartheta) - x_j(\vartheta)| = |x_i - x_j| + O(\vartheta^{-1})$, $(\vartheta \to \infty)$. Then in the **scaling limit**, in which $\vartheta \to \infty$ the corresponding points $z_i = z_i(\vartheta) := \vartheta x_i(\vartheta) \in \mathbb{Z}^d$ satisfy (5.5). The scaling limit is also called **continuum limit**. One reason is certainly that the *lattice spacing* of $\mathbb{Z}^d_{\vartheta^{-1}}$, namely ϑ^{-1}, vanishes in the scaling limit.

The general strategy is now to *construct* from our *real* lattice system in some way, including the above scale transformation with scale parameter ϑ, an "effective" one. The first step in doing this is the *construction* of a **scaled lattice system**, "naturally" determined by the scale transformation (5.6). The second step is the construction of an effective lattice system of $\mathbb{Z}^d$. The transformation mapping the original state of our real system to the effective state is then an **RG transformation**. Crucial is the *construction* of the RG transformation itself, i.e. that the transformation is actually realized as a *symmetry transformation*. Note that this (scaled) "effective" lattice system will only be a *construction*; the motivation for doing this is only to *extract* the effective large scale behavior of the correlation functions from our physical lattice system $\mathbb{Z}^d$.

In order to specify this new scaled lattice system we have to make clear in particular what we mean by a spin in this new system. So we define the **scaled spin**, $\varphi^{(\vartheta)}$, on $\mathbb{Z}^d_{\vartheta^{-1}}$ as

$$\varphi^{(\vartheta)} : \mathbb{Z}^d_{\vartheta^{-1}} \to \mathbb{R}^d \quad , \quad y \mapsto \varphi^{(\vartheta)}(y) := \alpha(\vartheta) \ \varphi(\vartheta y) \ , \tag{5.8}$$

where $\alpha(\vartheta)$ is a *positive* rescaling factor. Similarly, one has to *bring in* **scaled parameters** (w.r.t. $\mathbb{Z}^d_{\vartheta^{-1}}$), dependent on the scale parameter ϑ, corresponding to just these (thermodynamic) parameters, which determine the equilibrium state (defined by the DLR-equations (5.1)) of our real lattice system $\mathbb{Z}^d$. One such parameter is the inverse temperature β.

Since we want the transformation, mapping the real lattice system to a scaled "effective" one, to be realized as an *RG transformation* and think of the latter being a *symmetry transformation*, it would be rather disadvantageous to allow any ("non-natural") *"symmetry breaking"*. Therefore we require, due to $\beta < \beta_c$, the "**scaled inverse temperature**", $\beta(\vartheta)$, to satisfy $\beta(\vartheta) < \beta_c \ , \ \forall \vartheta \in [1, \infty[$. Intuitively expecting but also motivated by the fact that (free) energy has **scale dimension** 0 (see [3]) we set (with obvious notation):

$$H^{(\vartheta)}_{\vartheta^{-1}\Lambda}(\varphi^{(\vartheta)}) := H_\Lambda(\varphi) \quad , \quad d\lambda^{(\vartheta)}\left(\varphi^{(\vartheta)}(\vartheta^{-1}j)\right) := d\lambda(\varphi(j)) \quad , \ j \in \mathbb{Z}^d \ . \tag{5.9}$$

This enables us to define the **scaled equilibrium state** of $\mathbb{Z}^d_{\vartheta^{-1}}$, denoted by $d\mu^{(\vartheta)}_{\beta(\vartheta)}$, to be the probability measure which solves the DLR-equations (5.1), wherein all expressions are replaced by their scaled counterparts. The corresponding (expectation value) functional on the set of observables is denoted by $\langle\cdot\rangle^{(\vartheta)}_{\beta(\vartheta)}$. Note that due to (5.9) $d\mu^{(\vartheta)}_{\beta(\vartheta)}$ differs from $d\mu_\beta$ only in respect thereof that the scaled parameters have to be brought in, instead of the unscaled ones. Therefore

$$d\mu^{(\vartheta)}_{\beta(\vartheta)}(\varphi^{(\vartheta)}) = d\mu_{\beta(\vartheta)}(\varphi) \ . \tag{5.10}$$

Define the **scaled correlations** for points $y_i \in \mathbb{Z}^d_{\vartheta^{-1}}$ $(1 \leq i \leq n, \ \vartheta \in [1, \infty[)$:

$$G_\vartheta(y_1, \ldots, y_n) := \left\langle \varphi^{(\vartheta)}(y_1) \cdots \varphi^{(\vartheta)}(y_n) \right\rangle^{(\vartheta)}_{\beta(\vartheta)} \ \underset{(5.10)}{\overset{(5.8)}{=}} \ \alpha(\vartheta)^n \ \langle \varphi(\vartheta y_1) \cdots \varphi(\vartheta y_n) \rangle_{\beta(\vartheta)} \tag{5.11}$$

(also called **rescaled correlation function**). This finally enables us to state the **renormalization condition**:

$$\begin{aligned} &\text{For } x_1, \ldots, x_n \in \mathbb{Z}^d: \qquad 0 < |x_i - x_j| < \infty \ , \ n \geq 2 \\ &\qquad \Rightarrow \qquad 0 < \ G^*(x_1, \ldots, x_n) := \lim_{\vartheta \to \infty} G_\vartheta\left(x_1(\vartheta), \ldots, x_n(\vartheta)\right) \ < \infty \quad , \end{aligned} \tag{5.12}$$

where $x_i(\vartheta)$ satisfies (5.7), $1 \leq i \leq n$. $G^*(x_1, \ldots, x_n)$ is called **limiting correlation function**.

Now it has to be emphasized that the condition (5.12) is only the renormalization condition for an RG transformation which ends up with the "scaled" state $d\mu_{\beta(\vartheta)}$ (see (5.10)) as effective state of $\mathbb{Z}^d$. In general, where the RG transformation ends up with just any effective state of $\mathbb{Z}^d$, the **general renormalization condition** is obtained by considering the scaling limit of the correlation function with respect to the effective state.

5.3.2 CONSEQUENCES OF THE RENORMALIZATION CONDITION

The renormalization condition yields a **connection to QFT**. The statement is: **the limiting correlation functions of a classical lattice spin system may**

be the Euclidean Green's functions of a relativistic quantum field theory satisfying the Wightman axioms. For more information, see [1] and references given there.

The renormalization condition implies non-trivial **scaling relations** between critical exponents (see below). From (5.11), (5.12), $m(\beta) \searrow 0$ as $\beta \nearrow \beta_c$ and the definition of the inverse correlation length it follows that

$$\beta(\vartheta) \nearrow \beta_c \quad , \quad \text{as} \;\; \vartheta \to \infty \; . \tag{5.13}$$

In order to get a scaling relation between the critical exponents η, ν and γ, it suffices to show a **second "renormalization condition"** (in addition to (5.12)):

$$\vartheta m(\beta(\vartheta)) \to m^* > 0 \quad , \quad \text{as} \;\; \vartheta \to \infty \; . \tag{5.14}$$

Together with the definitions of the critical exponents, (5.14) implies

$$\boxed{\beta_c - \beta(\vartheta) \;\sim\; \vartheta^{-\frac{1}{\nu}} \quad , \quad \vartheta \to \infty} \; . \tag{5.15}$$

as well as the *scaling relation* between the critical exponents η, ν and γ (to see this use[3] in particular (5.11), the definition of the susceptibility and (5.13)):

$$\boxed{(2-\eta)\nu - \gamma = 0} \; . \tag{5.16}$$

(Determination of critical exponents) An explicit construction of the renormalization condition, i.e. having found a choice for the functions $\alpha(\vartheta)$ and $\beta(\vartheta)$, determines, in principle, the critical exponents ν, γ and η: (i) $\alpha(\vartheta)$ determines η via equation (5.31) and (ii) $\beta(\vartheta)$ determines ν by (5.15).

5.4 RENORMALIZATION GROUP TRANSFORMATIONS

Here we only study the *static* (time-averaged) case but there exists an RG theory for *dynamics* as well. The ultimate ambition of RG theory is the *construction* of a non-trivial limiting correlation function, i.e. the accomplishment of a *renormalization condition.*

As it was already stated in 5.3.1 an RG transformation is a combination of a scale transformation and some **coarse graining** process, leading finally to an effective state. Now we will consider a typical example of RG transformations, namely the RG block spin transformations.

---

[3] **Fact**: From (5.12) and (5.14) it follows that the quantity $\chi_\vartheta := \sum_{y \,\in\, \mathbb{Z}^d_{\vartheta^{-1}}} \vartheta^{-d}\, G_\vartheta(0,y)$ has the property that $0 \;<\; \lim_{\vartheta\to\infty} \chi_\vartheta \;<\; \infty$.

5.4.1 Kadanoff (RG) block spin transformations

An RG block spin transformation consists of two transformations: a scale transformation and a block spin transformation. As stated above, a scale transformation is somehow incorporated in every RG transformation.
Starting point: our lattice *system* as described in the preliminaries + assumptions from last section.
First we let act a **scale transformation** on our lattice (system) $\mathbb{Z}^d$. Since we are interested in the large scale behavior of our lattice system, we choose a scale transformation

$$\mathbb{Z}^d \to \mathbb{Z}^d_{\vartheta^{-1}} \quad , \quad z \mapsto \vartheta^{-1} z \tag{5.17}$$

where $\vartheta \in [1, \infty[$. (intuitively speaking: zooming out).

As a consequence of scaling the *lattice*, all the quantities which can be associated with our lattice get rescaled in some way (see last section). In particular we expect that the spin as well as all the thermodynamic parameters which determine the equilibrium state (especially the inverse temperature) become non-trivially rescaled. For the spin we therefore introduced the rescaling factor $\alpha(\vartheta)$ (see (5.8)); the scaled inverse temperature we denote by $\beta(\vartheta)$.

Second we will do a **block spin transformation**, which is a (linear) transformation in spin (configuration) space $K_{\mathbb{Z}^d}$. The construction is described below.
Characteristic to any block spin transformation is a number

$$L \in \mathbb{N} \quad : \qquad L > 1 \quad , \tag{5.18}$$

called **block size**. For the following we fix it. The main idea is now to "divide" the scaled lattice $\mathbb{Z}^d_{\vartheta^{-1}}$, $\vartheta \in [1, \infty[$, into (hyper-) cubic blocks with side length $\epsilon := \vartheta^{-1} L$, then to take an average of all the spins contained in a block – this average one might call **block spin** – and identifying each block with a site in $\mathbb{Z}^d$; with this site is then associated the block spin.
Depending on how big ϑ was chosen in the scale transformation one might want to average over a bigger block with side length $\epsilon := \vartheta^{-1} L^m$. The question which then automatically arises is: How big do we want to have ϵ ? Since we want to identify each block with a site in $\mathbb{Z}^d$, a good answer is certainly $\epsilon \approx 1$. Therefore define

$$m \equiv m(\vartheta) := \min \{ j \in \mathbb{N} \ : \ \vartheta \leq L^j \} \tag{5.19}$$

and set the **scaled "block" size** to be

$$\epsilon := \vartheta^{-1} L^{m(\vartheta)} \ . \tag{5.20}$$

Hence $1 \leq \epsilon < L$. Note that therefore

$$\vartheta \to \infty \qquad \Leftrightarrow \qquad m \to \infty \quad . \tag{5.21}$$

When we use the latter as scaling limit we write ϑ_m instead of ϑ in order to remind of (5.21).

Now we want to understand how we can construct from the scaled lattice (system) $\mathbb{Z}^d_{\vartheta^{-1}}$ a new *effective* lattice (system) $\mathbb{Z}^d$; effective in the sense that we extract only relevant information from $\mathbb{Z}^d_{\vartheta^{-1}}$.

- First we specify *how* we want to divide the lattice $\mathbb{Z}^d_{\vartheta^{-1}}$ into ϵ-blocks (blocks with side length ϵ): we want to do it in that way that the ϵ-blocks are centered in exactly these points which are contained in $C := \{y \in \mathbb{Z}^d_{\vartheta^{-1}} \mid \exists x \in \mathbb{Z}^d : y = \epsilon x\}$.

- Realizing that $\mathbb{Z}^d$ is naturally contained in $\mathbb{Z}^d_{L^{-m}}$ we do the following "identification map"
$$\mathbb{Z}^d_{\vartheta^{-1}} \to \mathbb{Z}^d_{L^{-m}} \quad , \quad y \mapsto \epsilon^{-1} y \ , \tag{5.22}$$
which maps any ϵ-block centered in $y := \epsilon x \in C \subset \mathbb{Z}^d_{\vartheta^{-1}}$, $x \in \mathbb{Z}^d$, to an 1-block centered in $x \in \mathbb{Z}^d \subset \mathbb{Z}^d_{L^{-m}}$.

- Then we associate with each site $x \in \mathbb{Z}^d \subset \mathbb{Z}^d_{L^{-m}}$ a **block spin** $(r^{(\vartheta)}\varphi)(x)$, which is the average of all spins that are "contained" in the ϵ-block centered in $\epsilon x \in \mathbb{Z}^d_{\vartheta^{-1}}$. It follows the ultimate **block spin transformation**, a linear transformation in spin configuration space $K_{\mathbb{Z}^d}$, transforming the measure $\mu_{\beta(\vartheta)}$ into a measure $R^{(\vartheta)}\mu_{\beta(\vartheta)}$, which means intuitively establishing the block spin as a "real" spin on $\mathbb{Z}^d$. To what extent the measure $R^{(\vartheta)}\mu_{\beta(\vartheta)}$ really describes an ("effective") equilibrium state on $\mathbb{Z}^d$ will then be discussed.

- Note that after having constructed the block spin we "forget" the points contained in $\mathbb{Z}^d_{L^{-m}} \setminus \mathbb{Z}^d$. What we regard as relevant information has been absorbed into the block spin.

In order to introduce the notions of *block spin* and *block correlation function* we define a function $\kappa \equiv \kappa^\epsilon : \mathbb{Z}^d_{\vartheta^{-1}} \to \mathbb{R}$ as follows:

$$\kappa^\epsilon(y) := \begin{cases} \epsilon^{-d} & \|\epsilon^{-1} y\|_\infty \leq \dfrac{1}{2} \\ 0 & \text{otherwise} \end{cases} \tag{5.23}$$

So this function, where ϵ is defined by (5.20), assigns to exactly those points in $\mathbb{Z}^d_{\vartheta^{-1}}$ a non-vanishing value, which are after being subject to a "scale transformation" ("identification map" !) $\mathbb{Z}^d_{\vartheta^{-1}} \to \mathbb{R}^d_{\epsilon^{-1}\vartheta^{-1}} = \mathbb{Z}^d_{L^{-m}}$, $y \mapsto \epsilon^{-1} y$, contained in a closed box in $\mathbb{Z}^d_{L^{-m}}$ centered in 0 with edge length 1. And the non-vanishing value is just the inverse volume of the unscaled box. Next define:

$$\kappa^\epsilon_x(y) := \kappa^\epsilon(y - \epsilon x) = \begin{cases} \epsilon^{-d} & \|\epsilon^{-1} y - x\|_\infty \leq \dfrac{1}{2} \\ 0 & \text{otherwise} \end{cases} \quad , \quad x \in \mathbb{Z}^d \, . \tag{5.24}$$

Compared to the original function, here the role of 0 (center of the "scaled box") is played by the point $x \in \mathbb{Z}^d$ understood as a point in $\mathbb{Z}^d_{L^{-m}}$.

Now define the **block spin**, $(r^{(\vartheta)}\varphi)(x)$, at site $x \in \mathbb{Z}^d$ to be

$$(r^{(\vartheta)}\varphi)(x) := \vartheta^{-d} \sum_{y \, \in \, \mathbb{Z}^d_{\vartheta^{-1}}} \kappa^\epsilon_x(y) \; \varphi^\vartheta(y) \tag{5.25a}$$

$$\overset{(5.24)}{=} \frac{1}{(L^m)^d} \sum_{\substack{y \, \in \, \mathbb{Z}^d_{\vartheta^{-1}} \\ \|\epsilon^{-1} y - x\|_\infty \leq \frac{1}{2}}} \varphi^\vartheta(y) \tag{5.25b}$$

$$\overset{(5.8)}{=} \frac{1}{(L^m)^d} \sum_{\substack{y \, \in \, \mathbb{Z}^d_{\vartheta^{-1}} \\ \|\epsilon^{-1} y - x\|_\infty \leq \frac{1}{2}}} \alpha(\vartheta) \; \varphi(\vartheta y) \tag{5.25c}$$

$$\underset{\substack{\uparrow \\ z := \vartheta y}}{=} \alpha(\vartheta) \; \frac{1}{(L^m)^d} \sum_{\substack{z \, \in \, \mathbb{Z}^d \\ \|L^{-m} z - x\|_\infty \leq \frac{1}{2}}} \varphi(z) \; . \tag{5.25d}$$

The average is taken in dividing by $(L^m)^d = (\vartheta\epsilon)^d$ instead of ϵ^d. We do this because we get then the right average in the trivial case, where $\vartheta = 1$.
At this point we recall why we want to construct an RG (block spin) transformation: we hope to accomplish the renormalization condition ! Therefore the following definition becomes important:

For $x_i \in \mathbb{Z}^d$, $1 \leq i \leq n$, define the **block correlation function**, $G_\vartheta(\kappa_{x_1}, \ldots, \kappa_{x_n})$, to be

$$G_\vartheta(\kappa_{x_1}, \ldots, \kappa_{x_n}) := \sum_{y_1, \ldots, y_n \, \in \, \mathbb{Z}^d_{\vartheta^{-1}}} \prod_{k=1}^{n} \left(\vartheta^{-d} \; \kappa^\epsilon_{x_k}(y_k)\right) \; G_\vartheta(y_1, \ldots, y_n) \tag{5.26a}$$

$$\overset{(5.24)}{=} \left(\frac{1}{(L^m)^d}\right)^n \sum_{\substack{y_1, \ldots, y_n \, \in \, \mathbb{Z}^d_{\vartheta^{-1}} \\ \|\epsilon^{-1} y_i - x_i\|_\infty \leq \frac{1}{2} \; , \; 1 \leq i \leq n}} G_\vartheta(y_1, \ldots, y_n) \tag{5.26b}$$

$$\overset{(5.11)}{=} \left(\frac{1}{(L^m)^d}\right)^n \sum_{\substack{y_1,\ldots,y_n \,\in\, \mathbb{Z}^d_{\vartheta^{-1}} \\ \|\epsilon^{-1}y_i - x_i\|_\infty \leq \frac{1}{2}\ ,\ 1\leq i\leq n}} \alpha(\vartheta)^n \ \langle \varphi(\vartheta y_1)\cdots\varphi(\vartheta y_n)\rangle_{\beta(\vartheta)} \tag{5.26c}$$

$$\underset{z_i:=\vartheta y_i}{\underset{\uparrow}{=}} \alpha(\vartheta)^n \left(\frac{1}{(L^m)^d}\right)^n \sum_{\substack{y_1,\ldots,y_n \,\in\, \mathbb{Z}^d_{\vartheta^{-1}} \\ \|L^{-m}z_i - x_i\|_\infty \leq \frac{1}{2}\ ,\ 1\leq i\leq n}} \langle \varphi(z_1)\cdots\varphi(z_n)\rangle_{\beta(\vartheta)} \ . \tag{5.26d}$$

$G_\vartheta(\kappa_{x_1},\ldots,\kappa_{x_n})$ describes the *average correlation* between ϵ-blocks, centered in points $\epsilon x_i \in C \subset \mathbb{Z}^d_{\vartheta^{-1}}$, $1 \leq i \leq n$, with respect to the *scaled equilibrium state.* Then:

$$\begin{aligned} G_\vartheta(\kappa_{x_1},\ldots,\kappa_{x_n}) &\overset{(5.26b)}{=} \left(\frac{1}{(L^m)^d}\right)^n \sum_{\substack{y_1,\ldots,y_n \,\in\, \mathbb{Z}^d_{\vartheta^{-1}} \\ \|\epsilon^{-1}y_i - x_i\|_\infty \leq \frac{1}{2}\ ,\ 1\leq i\leq n}} G_\vartheta(y_1,\ldots,y_n) \\ &\overset{(5.11)}{=} \left(\frac{1}{(L^m)^d}\right)^n \sum_{\substack{y_1,\ldots,y_n \,\in\, \mathbb{Z}^d_{\vartheta^{-1}} \\ \|\epsilon^{-1}y_i - x_i\|_\infty \leq \frac{1}{2}\ ,\ 1\leq i\leq n}} \alpha(\vartheta)^n \ \langle \varphi(\vartheta y_1)\cdots\varphi(\vartheta y_n)\rangle_{\beta(\vartheta)} \\ &\overset{(5.25c)}{=} \left\langle (r^{(\vartheta)}\varphi)(x_1)\cdots(r^{(\vartheta)}\varphi)(x_n)\right\rangle_{\beta(\vartheta)} && (5.27) \\ &= \int\limits_{K_{\mathbb{Z}^d}} \prod_{k=1}^n (r^{(\vartheta)}\varphi)(x_k) \ d\mu_{\beta(\vartheta)}(\varphi) && (5.28) \end{aligned}$$

Intuitively (5.27) says that the *average correlation* between the spins contained in ϵ-blocks, centered in points $\epsilon x_i \in C \subset \mathbb{Z}^d_{\vartheta^{-1}}$, $x_i \in \mathbb{Z}^d$, with respect to the *scaled equilibrium state* is just the *correlation* between the *block spins* in $x_i \in \mathbb{Z}^d$, $1 \leq i \leq n$, with respect to the state $d\mu_{\beta(\vartheta)}$ on $\mathbb{Z}^d$.
Since $d\mu_{\beta(\vartheta)}$ is a translation-invariant (finite) probability measure on $K_{\mathbb{Z}^d}$ there is a unique (finite) probability measure $R^{(\vartheta)}\mu_{\beta(\vartheta)}$ on $K_{\mathbb{Z}^d}$ such that:

$$\int\limits_{K_{\mathbb{Z}^d}} \prod_{k=1}^n (r^{(\vartheta)}\varphi)(x_k) \ d\mu_{\beta(\vartheta)}(\varphi) = \int\limits_{K_{\mathbb{Z}^d}} \prod_{k=1}^n \varphi(x_k) \ d(R^{(\vartheta)}\mu_{\beta(\vartheta)})(\varphi) \quad , \tag{5.29}$$

for all $x_i \in \mathbb{Z}^d$, $(1 \leq i \leq n)$, and $n \in \mathbb{N} \setminus \{0\}$.

Having defined the measure $R^{(\vartheta)}\mu_{\beta(\vartheta)}$, we have to check if

1. there is a lattice system (described by the four properties stated in 5.2) with an equilibrium state given by our new measure $R^{(\vartheta)}\mu_{\beta(\vartheta)}$.
2. $R^{(\vartheta)}\mu_{\beta(\vartheta)}$ satisfies the assumptions stated in 5.3.1 .

Important points: $R^{(\vartheta)}\mu_{\beta(\vartheta)}$ is

- invariant under lattice translations ? Yes!
- extremal invariant ? Yes!
- a Gibbs measure (i.e. a measure which satisfies the DLR-equations (5.1) for some Hamilton function H) ? *Unfortunately*, this is *not true in general*! See [4]. The proceeding is now to choose an *appropriate* space of Gibbs states which is *closed* under the action of any RG block spin transformation.

Finally from (5.28) and (5.29) we get

$$\boxed{G^*(\kappa_{x_1},\ldots,\kappa_{x_n}) := \lim_{\vartheta\to\infty} G_\vartheta(\kappa_{x_1},\ldots,\kappa_{x_n}) = \lim_{\vartheta\to\infty} \int\limits_{K_{\mathbb{Z}^d}} \prod_{k=1}^{n} \varphi(x_k)\ d(R^{(\vartheta)}\mu_{\beta(\vartheta)})(\varphi)} \quad , \tag{5.30}$$

provided the limit exists.

In order to arrive at an interesting concept we now assume that $\alpha(\vartheta)$ is "proportional" to some power of ϑ, or, consistent with $\alpha(1) = 1$, that

$$\alpha(\vartheta)^2 = \vartheta^{d-2+\eta} \quad , \quad \vartheta \to \infty \ , \tag{5.31}$$

for some η (this includes the *definition* of η). Then define

$$(r\varphi)(x) := L^{(\eta-d-2)/2} \sum_{\substack{z\ \in\ \mathbb{Z}^d \\ \|L^{-1}z-x\|_\infty \le \frac{1}{2}}} \varphi(z) \ . \tag{5.32}$$

Then

$$(r^{(\vartheta)}\varphi)(x) = \alpha(\epsilon^{-1})\ (r^{m(\vartheta)}\varphi)(x) \ . \tag{5.33}$$

Analogous to (5.29) define $R\mu_{\beta(\vartheta)}$ to be the unique measure on $K_{\mathbb{Z}^d}$ such that:

$$\int\limits_{K_{\mathbb{Z}^d}} \prod_{k=1}^{n} (r\varphi)(x_k)\ d\mu_{\beta(\vartheta)}(\varphi) = \int\limits_{K_{\mathbb{Z}^d}} \prod_{k=1}^{n} \varphi(x_k)\ d(R\mu_{\beta(\vartheta)})(\varphi) \quad , \tag{5.34}$$

for all $x_i \in \mathbb{Z}^d$, $(1 \le i \le n)$, and $n \in \mathbb{N} \setminus \{0\}$. Then

$$\int\limits_{K_{\mathbb{Z}^d}} \prod_{k=1}^{n} (r^{(\vartheta)}\varphi)(x_k)\ d\mu_{\beta(\vartheta)}(\varphi) = \int\limits_{K_{\mathbb{Z}^d}} \prod_{k=1}^{n} \varphi(x_k)\ d(R^{m(\vartheta)}\mu_{\beta(\vartheta)})(\alpha(\epsilon)\varphi) \ . \tag{5.35}$$

Due to uniqueness we get

$$d(R^{(\vartheta)}\mu_{\beta(\vartheta)})(\varphi) = d(R^{m(\vartheta)}\mu_{\beta(\vartheta)})(\alpha(\epsilon)\varphi) \ . \tag{5.36}$$

So we can write (5.30) alternatively

$$\boxed{G^*(\kappa_{x_1}, \ldots, \kappa_{x_n}) := \lim_{m\to\infty} G_{\vartheta_m}(\kappa_{x_1}, \ldots, \kappa_{x_n}) = \lim_{m\to\infty} \int\limits_{K_{\mathbb{Z}^d}} \prod_{k=1}^{n} \varphi(x_k) \ d(R^m \mu_{\beta(\vartheta_m)})(\alpha(\epsilon)\varphi) \ .} \tag{5.37}$$

Note that by (5.31), (5.32) and (5.34) the transformation $R \equiv R_\eta$ depends on the exponent η.

5.4.2 Fixed points, critical exponents

Definitions

Let M be some appropriately chosen cone of finite measures, μ, on the space, $K_{\mathbb{Z}^d}$, of spin configurations and R_η be an RG block spin transformation, defined by (5.31), (5.32) and (5.34), *acting* on M ($R_\eta : M \to M$). Furthermore we assume that the action of R_η on M is smooth. Then, a **fixed point** of R_η is a point $\mu^* \in M$ which is invariant under the action of R_η, i.e. $R_\eta \ \mu^* = \mu^*$. Obviously, if the scaling limit of a state $d\mu$, $d\mu^*(\varphi) := d(\lim_{m\to\infty} R^m \mu)(\varphi)$, exists, then $d\mu^*$ is a fixed point.

General strategy: For the following we assume that we already know η, corresponding to a specific class of spin systems; this means that we already made a choice of $\alpha(\vartheta)$. In particular we assume the existence of a fixed point of R_η.
Then the strategy is to find *all* fixed points of R_η. Having a specific spin system in mind, the state of this system (assumed to be contained in M) will be driven to one of those fixed points (this has to be checked!).
Having found one (some or all) fixed point(s) of R_η we calculate the critical exponents, corresponding to this (these) fixed point(s), as it is described below. The idea here is to study how R_η behaves in the vicinity of a fixed point. This is done in considering the linearization of R_η.
When we know ν then we know how to choose $\beta(\vartheta)$ (see (5.15)) and the RG transformation is constructed (we assumed to know $\alpha(\vartheta)$ already).

Now we *choose* a fixed point, μ^*, of R_η. We define $M_{f.p.} \equiv M_{f.p.}(R_\eta, \mu^*)$ to be the manifold of all fixed points of R_η passing through μ^*. Under suitable conditions on M and R_η one can *decompose* M in the vicinity of μ^* into a **stable manifold**, $M_s(\mu^*)$, and an **unstable manifold**, $M_u(\mu^*)$, defined as follows: states on $M_s(\mu^*)$ are driven towards μ^* and states on $M_u(\mu^*)$ are driven away from μ^*. Finally we introduce the following tangent spaces ($\mathcal{C}$, $\mathcal{I}$, $\mathcal{R}$, $\mathcal{M}$) at the point μ^*:

	tangent space at μ^* (to)	called space of	vector space spanned by eigenvectors of $DR_\eta(\mu^*)$ corresponding to eigenvalues of modulus
$\mathcal{C}$	$M_{f.p.}(R_\eta, \mu^*)$		
$\mathcal{I}$	$M_s(\mu^*)$	"irrelevant perturb."	< 1
$\mathcal{R}$	$M_u(\mu^*)$	"relevant perturbations"	> 1
$\mathcal{M}$		"marginal perturb."	1

DETERMINATION OF THE CRITICAL EXPONENTS ν AND γ

The important statement is: **The critical exponents ν and γ are determined by the spectrum of $DR_\eta(\mu^*)$, more precisely by the relevant eigenvalues (which have modulus > 1) of $DR_\eta(\mu^*)$.**

Assumption: The tangent space at μ^* splits into a *one-dimensional* space of *relevant* perturbations and a *co-dimension-one* space of *irrelevant* perturbations, which means in particular that there are no further marginal perturbations.

Since the space of relevant perturbations is 1-dimensional there exists exactly one simple relevant eigenvalue $\lambda = \lambda(L)$. One can proof[4] that

$$\boxed{\nu = \frac{\log L}{\log \lambda(L)}} \tag{5.38}$$

This holds for every choice of $L > 1$. The critical exponent γ is then determined by η and ν via the scaling relation (5.16).

5.5 EXAMPLE: THE GAUSSIAN FIXED POINT

Primary aim of this (very brief) example is to point out the connection of the theory stated above towards a formalism often found in literature.

One big difference lies in the treatment of the thermodynamic limit. Regarding the RG transformation this point is basically ignored, one just considers a

---

[4] For a sketch of the proof see [1] or a more detailed version available from me.

"macroscopic" but finite sublattice of $\mathbb{Z}^d$. Furthermore spins are no longer confined to the discrete lattice sites but defined to be continuously distributed over the subset of $\mathbb{R}^d$ "filling up" this macroscopic sublattice.

Let us consider a Hamilton function which has the Ginzburg-Landau form, i.e.

$$\mathcal{K} := \beta H[\varphi] := \frac{1}{2}\int (r\varphi^2 + \frac{1}{4}u\varphi^4 + c(\nabla\varphi)^2)\; d^dx \;. \tag{5.39}$$

The above Hamilton function can be described by a point in a parameter space, defined with respect to the parameters r, u and c: $\mu := (r, u, c)^T$.
The **Gaussian model** is obtained by setting $u = 0$ in the above expression (5.39) for the Hamilton function. Equation (5.39) can be expressed in Fourier-transformed space (φ_k: Fourier components of φ; $u = 0$) as

$$\mathcal{K}|_{u=0} = \frac{1}{2}\sum_{|k|<2\pi} (r + ck^2)\; |\varphi_k|^2 \;. \tag{5.40}$$

The cutoff-parameter corresponds to the distinguished minimal distance, namely the lattice constant (here 1 $\rightsquigarrow$ cutoff-parameter: $\frac{2\pi}{\text{lattice constant}} = \frac{2\pi}{1}$).

Above we have defined an RG transformation to transform equilibrium states. This corresponds in principle to a transformation between parameters which determine the equilibrium state (or to a transformation between Hamilton functions). The link between these two formulations are the DLR-equations: to every equilibrium state corresponds a(n) (equivalence class of) Hamilton function(s) (DLR) and the latter one can be described by a point in parameter space.
The RG-transformed "Hamilton function" $\mathcal{K}'$, defined to include no additive constant, is obtained from $\mathcal{K}$ by

$$\text{const.}\; e^{-\mathcal{K}'} = \left[\int e^{-\mathcal{K}} \prod_{2\pi\vartheta^{-1} \;\leq\; |q| \;<\; 2\pi} d\varphi_q\right]_{\varphi_k \;=\; \vartheta^{1-\frac{\eta}{2}}\varphi'_{\vartheta k}} \;. \tag{5.41}$$

The [...]-term can be interpreted as a block spin transformation (w.r.t. a block size $\vartheta \equiv L^m$). Here all the degrees of freedom in a block with side length ϑ are integrated out. Due to the simple form of $\mathcal{K}|_{u=0}$, see (5.40), this step becomes trivial in the case $u = 0$. The next and last step of our RG transformation – essentially an RG block spin transformation, only carried out in k-space – is to express [...] in terms of the scaled quantities (w.r.t. ϑ again as in the integration process before).

Carrying out the RG transformation in the Gaussian model gives immediately:

$$\begin{aligned}\mathcal{K}'|_{u=0} &= \frac{1}{2} \sum_{|k| \, < \, 2\pi\vartheta^{-1}} (r + ck^2) \; |\varphi_k|^2 \\ &= \frac{1}{2} \sum_{|k| \, < \, 2\pi\vartheta^{-1}} (r + ck^2) \; \vartheta^{2-\eta} \; |\varphi'_{\vartheta k}|^2 \\ &\underset{k' := \vartheta k}{\underset{\uparrow}{=}} \; \frac{1}{2} \sum_{|k'| \, < \, 2\pi} (\vartheta^{2-\eta} r + \vartheta^{-\eta} c k'^2) \; |\varphi'_{k'}|^2 \; . \end{aligned} \tag{5.42}$$

We notice that $\mathcal{K}'|_{u=0}$ has the same form as $\mathcal{K}$, i.e. $\mathcal{K}'|_{u=0}$ can be represented by a point in the parameter space defined above, namely:

$$R_{(\vartheta)} \mu|_{u=0} \equiv (\vartheta^{2-\eta} r, 0, \vartheta^{-\eta} c)^T \tag{5.43}$$

($R_{(\vartheta)}$: RG transformation on the parameter space).

Now we can discover fixed points of $R_{(\vartheta)}$: for $\eta = 0$ we find the fixed point $\mu_0^* := (0, 0, c)^T$, and for $\eta = 2$ we obtain another fixed point $(r, 0, 0)^T$. μ_0^* is called the **Gaussian fixed point** and corresponds to the "hamilton function" $\mathcal{K}^* := \frac{1}{2} \sum_{|k|<2\pi} ck^2 \; |\varphi_k|^2$. The next question arising is how $R_{(\vartheta)}$ behaves in the vicinity of a Gaussian fixed point. For the case $u = 0$ we have already found out (see (5.43)). If one wants to study the vicinity of μ_0^* more detailed one includes the parameter u. Then it is advantageous to consider only the linearized $R_{(\vartheta)}$, denoted by $R^L_{(\vartheta)}$. This means that we linearize $\mathcal{K}'$ with respect to $\mathcal{K} - \mathcal{K}^*$; $\mathcal{K}'^L :=$ linearization of $\mathcal{K}'$. One finds[5] that $\mathcal{K}'^L$ has the same form as $\mathcal{K}$ and can be represented by the following point in parameter space:

$$R^L_{(\vartheta)} \mu \equiv \begin{pmatrix} \vartheta^2 & * & 0 \\ 0 & \vartheta^{4-d} & 0 \\ 0 & 0 & 1 \end{pmatrix} \begin{pmatrix} r \\ u \\ c \end{pmatrix} \tag{5.44}$$

Note that only the second row of the matrix above gives new information. ϑ^2 is the relevant eigenvalue, ϑ^{4-d} has to be the irrelevant and 1 is the marginal one. The new information is essentially that μ_0^* is only stable whenever $d > 4$. From the relevant eigenvalue we get, setting $\vartheta := L$ and using (5.38):

$$\nu = \frac{\log(L)}{\log(L^2)} = \frac{1}{2} \; . \tag{5.45}$$

Summary: The Gaussian fixed point is stable only for $d > 4$ and the critical exponents corresponding to the Gaussian fixed point are $\eta = 0$ and $\nu = \frac{1}{2}$, ($\gamma = 1, \ldots$).

---

[5] See [3], p. 169-175; the * in (5.44) denotes a term which is irrelevant for our discussion.

Bibliography

[1] J. Fröhlich and T. Spencer, *Some recent rigorous results in the theory of phase transitions and critical phenomena*, Séminaire BOURBAKI (1981/82).

[2] J. Fröhlich, ed., *Scaling and Self-Similarity in Physics: Renormalization in Statistical Mechanics and Dynamics* (Birkhäuser, 1983).

[3] S. Ma, *Modern Theory of Critical Phenomena* (Benjamin, 1976).

[4] A. van Enter, R. Fernández, and A. Sokal, *Regularity Properties and Pathologies of Position-Space Renormalization-Group Transformations: Scope and Limitations of Gibbsian Theory*, Journal of Statistical Physics **72** (1993).

[5] D. Ruelle, *Statistical mechanics: Rigorous Results* (Imperial College Press, 1999).

[6] K. Wilson and J. Kogut, Phys. Rep. **12C**, 75 (1974).

[7] C. Domb and M. Green, eds., *Phase Transitions and Critical Phenomena*, vol. 6 (1976).

[8] R. Israel, *Convexity in the Theory of Lattice Gases* (Princeton University Press, 1979).

[9] P. Pfeuty and G. Toulouse, *Introduction to the Renormalization Group and to Critical Phenomena* (John Wiley, 1977).

CHAPTER 6

CRITICAL SLOWING DOWN AND CLUSTER UPDATES IN MONTE CARLO SIMULATIONS

RUBEN ANDRIST
SUPERVISOR: DR. MUNEHISA MATSUMOTO

As a critical temperature T_c is approached, a (nearest neighbor correlated) Ising system develops large spatial correlations which have long temporal correlations associated with them. Hence the characteristic time scale diverges at T_c. This chapter seeks to give an introduction to critical slowing down as observed in the 2-dimensional Ising model and to explain how this divergence in time scale can be counteracted in simulations using cluster update schemes.

6.1 INTRODUCTION

6.1.1 MOTIVATION

Mean-field theory often gives a qualitatively correct picture of a given model's phase diagram. And for certain problems such as the Ising Model in one or two dimensions, exact solutions have been found[1]. However, a close comparison of the aforementioned shows some inaccuracy, which gives rise to the need for accurate predictions both for problems being discussed and such that remain unsolved.

Monte Carlo simulations provide means of acquiring numerical predictions for the behavior of a given model. Through extensive use of random numbers, these simulations seek to probe phase space in a stochastic manner to determine the equilibrium state of the underlying system. This is done by constructing a Markov Chain of states, where every new state of the system is generated from the previous one. The generation itself is non deterministic, as one of the possible new states is picked randomly on every step.
If the choosing of the new state can be implemented in a way to ensure a tendency towards the equilibrium state of the system, then relaxation to this equilibrium state is guaranteed if the system is left untouched for some time.

6.1.2 Historical notes

Estimations making use of random numbers have been known as far back as the 19th century. For instance, Laplace was able to estimate the number π by throwing a set of needles randomly onto a board with lines.
The first work on Monte Carlo simulations was published in 1949 by N. Metropolis et al.[2]. Ever since, the simulations have not only grown along with the computer industry but have also enabled a whole new field of research by providing reference data and investigating new models numerically.
One model which has been of particular interest is the Ising model in two dimensions. We shall also use it in this context to outline and discuss the application of a Monte Carlo simulation.

6.1.3 Ising model in two dimensions

This Ising model consists of spins with only two states ($\sigma \in \{\pm 1\}$) arranged in a plane. For simplification we will only look at nearest neighbor interactions. This results in the following Hamiltonian[3]:

$$\mathcal{H} = -\mathcal{J} \sum_{NN} \sigma_i \sigma_j - H \sum_i \sigma_i,$$

where $\mathcal{J}$ is some interaction constant and H represents the magnetic field. Also, theory predicts the critical temperature to be $T_c = 2.269$ and the following power law relation for the correlation length ξ:

$$\xi \propto \varepsilon^{-\nu},$$

where ν is termed critical exponent and $\varepsilon = |1 - T/T_c|$ is the reduced temperature.

6.1.4 CONDITIONS FOR VALIDITY

To ensure the validity of the simulation data, we must show that the simulation really does converge to the equilibrium state. Sufficient conditions for convergence are given by Ergodicity and the Detailed Balance relation.

ERGODICITY

Ergodicity means that every point in phase space must be reachable. This is a requirement, as the system may otherwise be trapped in a non-equilibrium state. We write the probability for the system to be in state i as:

$$P_i(t+1) = P_i(t) - \sum_{j \neq i} w_{i \to j} + \sum_{i \neq j} w_{j \to i}, \tag{6.1}$$

where $w_{i \to j}$ is the probability of getting from state i to state j. We can rewrite this equation in matrix form by defining the following:

$$\begin{aligned} L_{ij} &= w_{j \to i} \quad (\text{for } i \neq j) \\ L_{ii} &= 1 - \sum_{j \neq i} w_{i \to j} \end{aligned}$$

Equation 6.1 then translates to:

$$P_i(t+1) = \sum_j L_{ij} P_i(t) \tag{6.2}$$

And we want to show that $P_i(t)$ converges to some equilibrium distribution $P_i(\infty)$. This can be done by looking at the properties of the probability matrix L. Suppose ergodicity is given, then any state can be reached within a finite number of steps. By choosing n to be the number of steps required to be able to reach any state we can assure that $(L^n)_{ij} > 0 \ \forall i, j$.

The theorem by Perron and Frobenius states that any matrix with strictly positive elements has a non degenerate largest eigenvalue. Since we are dealing with a probability matrix, the largest possible eigenvalue is 1. Therefore, if we can show that a stable distribution exists, then we know that it is unique.

Supposing such a unique state with non degenerate, largest eigenvalue 1 exists, we can show convergence by taking the limit

$$\lim_{s \to \infty} (L^n)^s P_i(t) \longrightarrow P_i(\infty)$$

Taking this limit results in all distributions with an eigenvalue below 1 to vanish, whereas the equilibrium distribution with eigenvalue remains.

Detailed Balance

In order for the above argument to hold, we must show that an equilibrium distribution exists. Such an equilibrium distribution should satisfy the Balance Relation:

$$\sum_{j\neq i} P_j^{eq} w_{j\to i} \overset{!}{=} \sum_{j\neq i} P_i^{eq} w_{i\to j} \tag{6.3}$$

One way to satisfy this is by requiring detailed balance:

$$P_j^{eq} w_{j\to i} \overset{!}{=} P_i^{eq} w_{i\to j} \tag{6.4}$$

□

6.2 Critical slowing down

6.2.1 Metropolis algorithm

The algorithm introduced by N. Metropolis et al.[4] incorporates so-called local updates, which flip only a single spin according to a certain probability, which depends only on the nearest neighbors. Several such updates form a Markov chain where successive states differ only in at most one single site that was potentially updated.
The flipping probability proposed with was:

$$w_{b\to a} = \begin{cases} e^{-\Delta E/k_B T} & \Delta E > 0 \\ 1 & \Delta E < 0 \end{cases}, \tag{6.5}$$

where $\Delta E = E_{after} - E_{before}$, k_B is the Boltzmann constant and T is the temperature. Note that for a negative ΔE, the probability for flipping the spin is 1 (always flipped), since there is a gain in energy associated with this transition.
When implementing the Metropolis Algorithm, the sites can be chosen either in a specific order or randomly.

Ergodicity

If we choose the sites for the local updates randomly, then ergodicity can be shown very easily: To get from a given state to any other state, we simply need to update all the sites which differ between these states. Since there is a non-vanishing probability for all of the attempted flips, there is also a non-vanishing probability to construct a Markov chain to the other state. As this holds for any two states, ergodicity is given. □

DETAILED BALANCE

It is instructive to verify that the detailed balance relation (Eq. 6.4) holds. To do this, we compare the probability of flipping one site back and forth:

$$P_b w_{b\to a} \overset{!}{=} P_a w_{a\to b} \tag{6.6}$$

W.l.o.g. the energy difference is $\Delta E = E_a - E_b > 0$. Therefore, the transition probability to the state of lower energy E_b becomes 1. Hence we get the relation

$$e^{-E_b/k_BT} \cdot e^{-(E_a-E_b)/k_BT} \overset{!}{=} e^{-E_a/k_BT} \cdot 1 \tag{6.7}$$

And from this we get the relation $-E_b - E_a + E_b = -E_a$. □

6.2.2 MEASURED PROPERTIES

The fact that only very small changes occur in each step suggests the interpretation that the simulation time is somehow related to real time. Thus not only can the Metropolis Algorithm be used to find the equilibrium state, it also gives some insight in the evolution of the system over time. For numerical comparison, the magnetization M is a good choice, as it is also the order parameter of a 2D Ising ferromagnet. The n-th measurement is taken by calculating the average magnetization per site:

$$M_n = \frac{1}{S}\sum_{i=1}^{S} \sigma_i,$$

where S is the total number of spins in the system and the sum is taken over all of these. To reduce the impact of random noise, this property is then averaged over time:

$$\langle M\rangle = \frac{1}{N}\sum_{n=1}^{N} M_n,$$

where N is the number of states considered in the measurement. To reduce the impact of the set of random numbers, the simulation ought to be repeated several times using different sets of random numbers.

When visualizing the system during the simulation, several observations can be made: While at high temperatures, the system is mainly dominated by noise, one can clearly see the formation of domains at low temperatures. Introducing a magnetic field favors one state over the other, which results in (nearly) all spins aligning at low temperatures. By sweeping this magnetic field H (i.e. from a negative to a positive value), one can clearly observe a phase transition. The fact

that this transition exhibits a metastable state – the orientation of the magnetization does not immediately follow a change in the orientation of the magnetic Field – suggests this transition to be first order.
The other interesting change happens as we continuously cool down from the high temperature state (with small correlated domains). As we approach a certain point T_c, we start to see all sizes of clusters emerge. Further cooling gradually creates percolating clusters growing to a completely ordered state.

6.2.3 DIVERGENCE OF TIME SCALE

In order for the simulation to yield numerical results for the equilibrium state, we must allow time for the system to relax to this equilibrium state. This means we have to omit the first $\mathcal{N}_0$ configurations obtained during the simulation, where $\mathcal{N}_0$ must be chose sufficiently large to ensure relaxation.
However, the relaxation time of the system depends on T, and at the critical temperature T_c it diverges. The fact that this is a physical effect, which is not only seen in simulations, suggests that the Metropolis dynamics do in fact nicely capture the properties of the physical system.
This slow relaxation is termed "Critical Slowing Down" and the divergence is associated with a long correlation length. As the correlation of the spins is not local any more, the local updates of the Metropolis algorithm become very ineffective. This can be shown by measuring the magnetization against time M/t at different temperatures T.

RELAXATION FROM HIGH ENERGY STATE

When starting from a high energy state (Fig. 6.1), i.e. checkerboard pattern, we can see that for low temperatures, there is a relaxation to a fixed average magnetization per site, which is close to 1 (most spins are aligned). At high temperatures some random noise prevails and the system shows next to no alignment of the spins. For a simulation at T_c, the results are, however, inconclusive as the system is unable to relax to the equilibrium state within the given time span of the measurements.

RELAXATION FROM LOW ENERGY STATE

A very similar picture is obtained when doing the same measurements starting from a low energy state (Fig. 6.2), i.e. when all spins are aligned: While the simulations at low temperatures maintain the high magnetization, those at high

temperatures drop to a state dominated by noise which exhibits next to no total magnetization. The results for T_c show, once again, no signs of relaxation.
This long relaxation time results in most of the gathered data being discarded as $\mathcal{N}_0$ must be larger than the steps required for the system to relax. This is very ineffective and makes it difficult to acquire reliable data around the critical temperature T_c. Therefore some other methods must be sought to probe the system around the critical temperature.

6.3 CLUSTER UPDATES

The basic idea of cluster updates is to flip several spins in a common domain at once rather than attempting to do single flips. This allows for changes which correspond in scale to the current correlation length of the system and therefore do not become ineffective as T approaches T_c (and the correlation length diverges). First steps in this were taken by Kasteleyn and Fortuin,[5] who showed that the ferromagnetic two state Potts model could be mapped to a percolation problem. This is done by mapping the "bonds" of the Ising model onto a corresponding lattice, where there is a non zero probability for aligned nearest neighbors to be in the same cluster. Therefore, domains of aligned spins are grouped into clusters. The importance of this discovery lies in the fact that, even though the Potts model suffers from critical slowing down, the percolation problem does not.
The cluster probability suggested by Swendson and Wang[6] was:

$$p = 1 - e^{-\frac{2\mathcal{J}}{k_B T}\,\delta_{\sigma_i \sigma_j}}, \tag{6.8}$$

where $\mathcal{J}$ is some interaction constant, k_B and T are the Boltzmann constant and temperature respectively. Note that the delta function results in a non-zero probability only in the case of aligned spins.
The method suggested with this cluster probability was to

1. Iterate through all bonds and try placing them
2. Identify all clusters created in step 1
3. Randomly assign a new value to the clusters

Thus each newly generated state differs substantially from the previous one. The method introduced by Wolff[7] proceeds to build clusters sequentially by starting from a random site and growing them recursively. Contrary to the Swendson-Wang method, all grown clusters are flipped, which is a slight improvement.

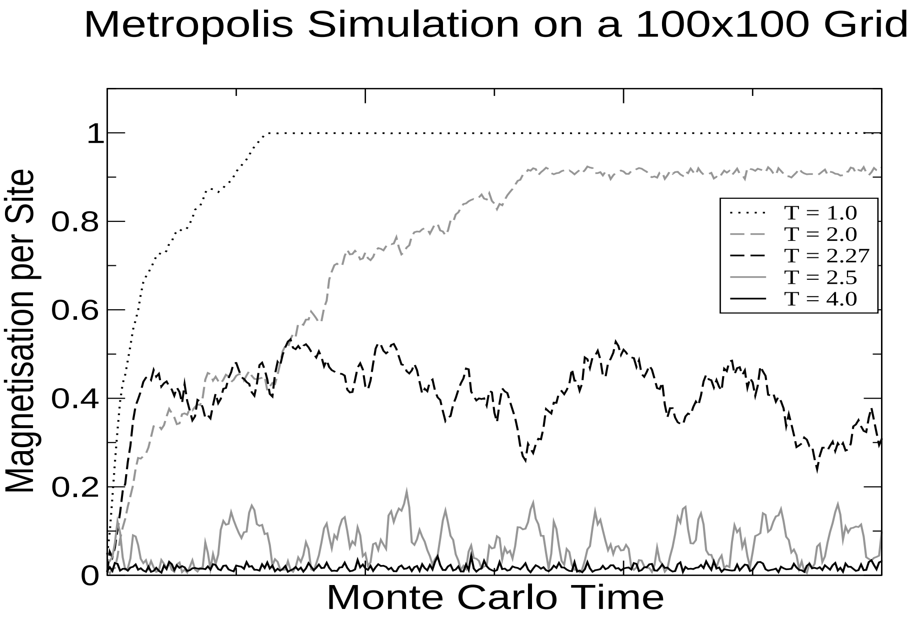

Figure 6.1: Relaxation from high energy state under metropolis dynamics

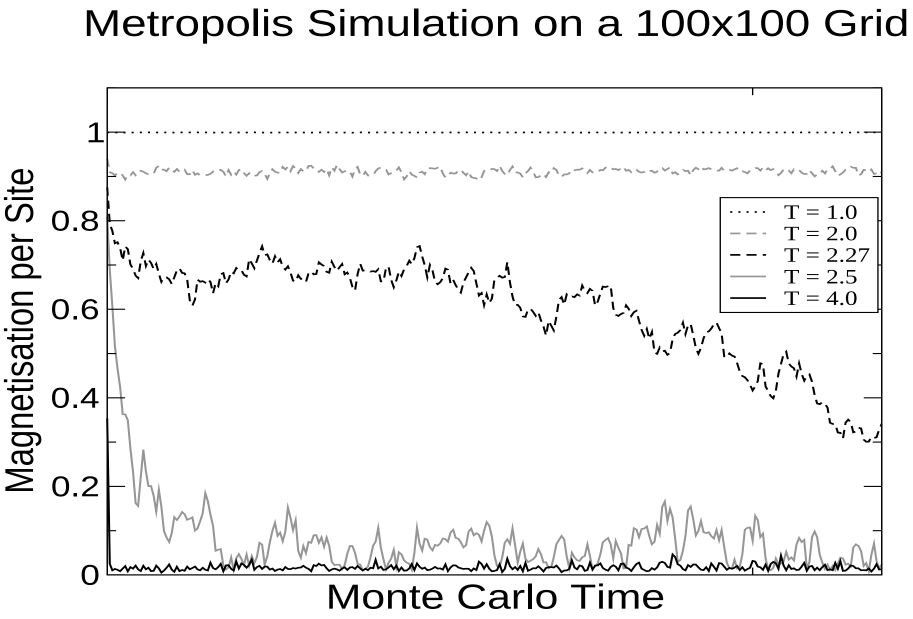

Figure 6.2: Relaxation from low energy state under metropolis dynamics

Ergodicity

Ergodicity can be seen immediately since there is always a non vanishing probability of building a single site cluster. Such single site updates correspond to the Metropolis update scheme, which was already shown to be ergodic. □

Detailed balance

To show detailed balance we look at a specific cluster and show that the probabilities of flipping it back and forth are equal.
The probability of constructing a certain cluster is given by the probability to place the inner bonds and the probability not to place the outer ones. Since when constructing the very same cluster in two situations, the inner part will be the same, we only need to look at the non-placed bonds outlining the cluster.
Suppose we have a cluster with n (m) spins aligned (not aligned) on the border (respectively). In the cluster grown before the flip (state b), we must not include n spins which would be aligned with the cluster. Likewise in the state a, when looking at the inverse transition, we must not include m such spins:

$$P_b(1-p)^n \overset{!}{=} P_a(1-p)^m \tag{6.9}$$

From this, we get the following relation

$$e^{-E_b/k_BT}e^{-\frac{2n}{k_BT}} = e^{-E_a/k_BT}e^{-\frac{2m}{k_BT}},$$

Which requires $-E_b - 2n = -E_a - 2m$ to hold. Since all the difference in energy between the states originates from the change on the border of the cluster, we can also use n and m to calculate the difference in energy:

$$\Delta E = E_b - E_a = (m-n) - (n-m) = 2m - 2n,$$

which clearly satisfies the requirement. □

6.3.1 Measured properties

Again a visualization shows some interesting properties of the simulation. At high temperatures, the picture corresponds to the one observed with Metropolis dynamics. At low temperatures, however, the system starts to oscillate wildly. This can easily be understood since at low temperatures, there is a good chance of building a percolating cluster (or even one that fills the whole system) every time. The oscillation allows the system to populate both states of lowest energy

in phase space, whereas in Metropolis dynamics, the system would be trapped in one of the two degenerate states.
As the temperature is swept though T_c, we see a (remarkably quick) change in size of the clusters. In particular, at T_c all sizes of clusters emerge. Similarly as for the Metropolis method, we can obtain a visual picture of the relaxation by plotting the magnetization per site against time.
Both simulations starting from a high energy state (Fig. 6.3) as well as from a low energy state (Fig. 6.4) exhibit fast relaxation to the equilibrium state for all temperatures. This initial relaxation is followed by random oscillations around that state. Even though this oscillation is stronger around T_c, averaging over time allows for accurate results even at the critical temperature.

6.3.2 Relaxation compared to local updates

The advantage of the cluster updates over Metropolis dynamics become very obvious when comparing the evolution of a system under each of the two simulation methods (Fig. 6.5). The local update scheme converges only gradually to the equilibrium state, whereas the cluster update scheme exhibits very fast relaxation. The fact that the two methods do find the same equilibrium state nicely outlines that the cluster updates really do catch the main properties of the relaxing system.
At the critical temperature (Fig. 6.6), the difference is even more dramatic: The local updates do not show a tendency to converge, whereas the cluster update scheme quickly finds the equilibrium state and proceeds by oscillating there. Hence, this allows us to gather reliable data.

6.3.3 Drawbacks of cluster updates

However, the cluster update scheme also has drawbacks: At temperatures away from T_c, performance can be worse than for local updates, since extensive effort is put into constructing clusters which do not greatly affect the evolution of the system.
Another major drawback is the fact that the cluster update scheme does not include ways to handle a magnetic field. This is due to the fact that the dynamics are dictated by the cluster probability which does not depend on a magnetic field. One could try to implement the cluster flipping such that it is influenced by the magnetic field similarly as for local updates. However, this results in freezing at the critical temperature because the probability for a successful flip becomes very small.

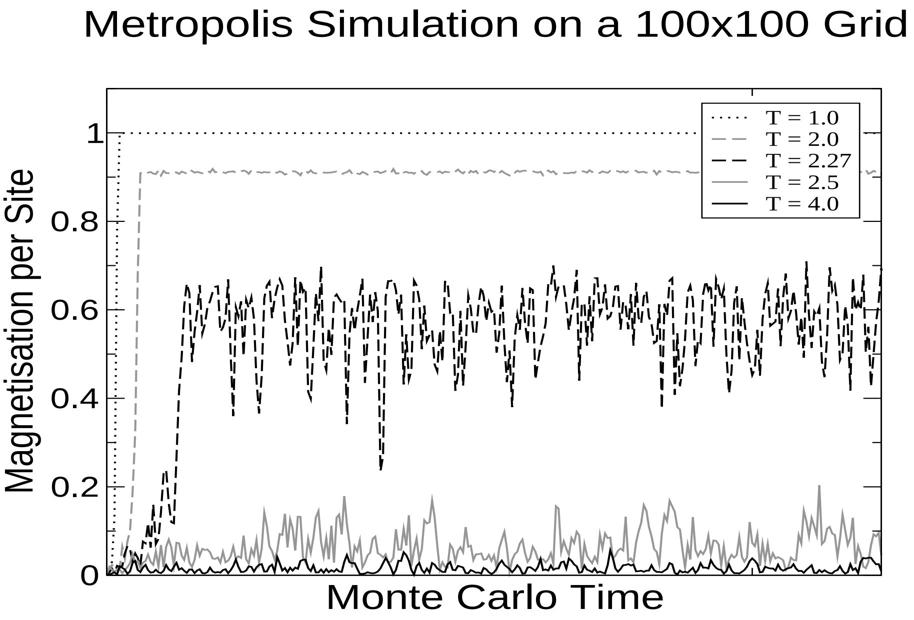

Figure 6.3: Relaxation from high energy state using cluster updates

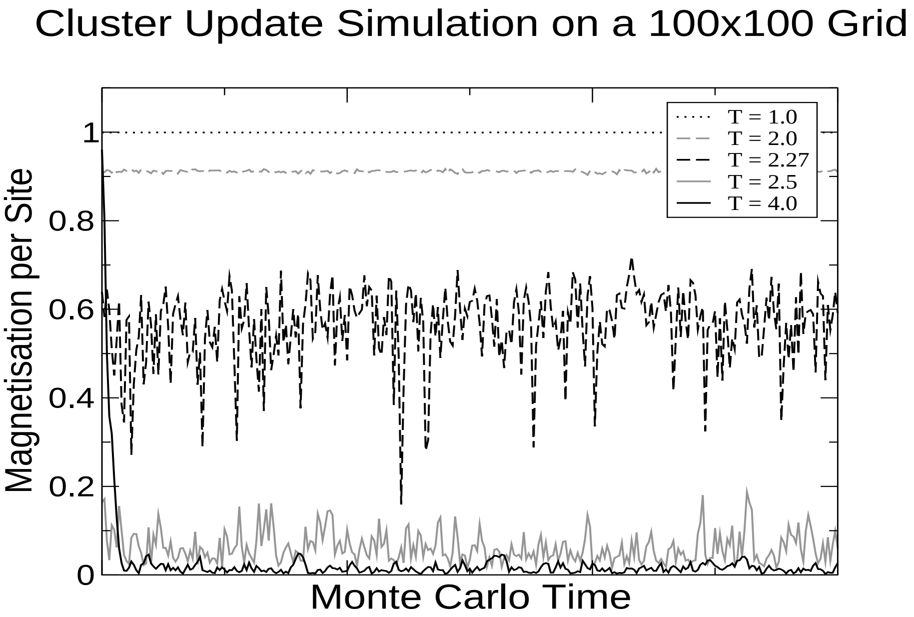

Figure 6.4: Relaxation from high energy state using cluster updates

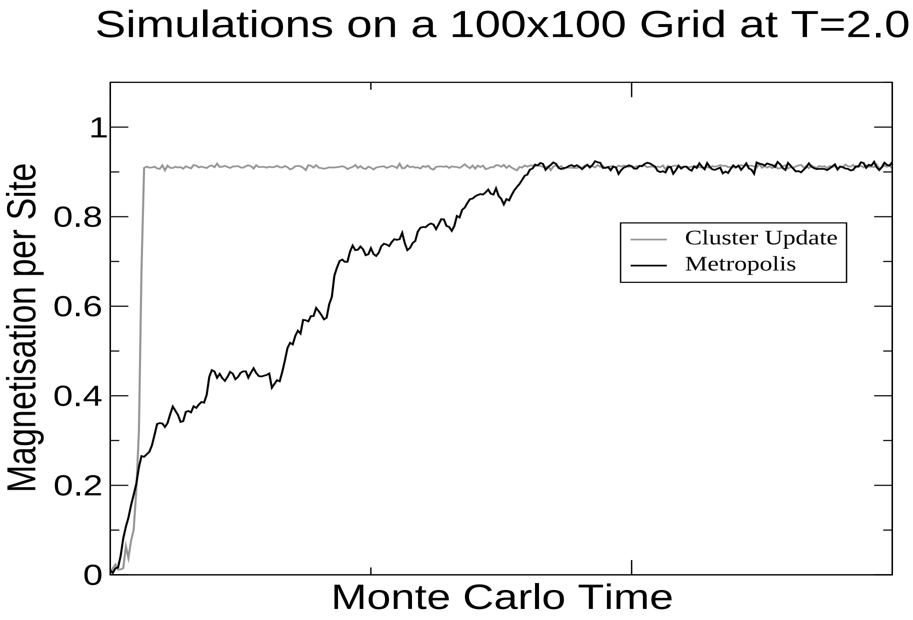

Figure 6.5: Comparison of local and cluster updates at $T = 2.0$

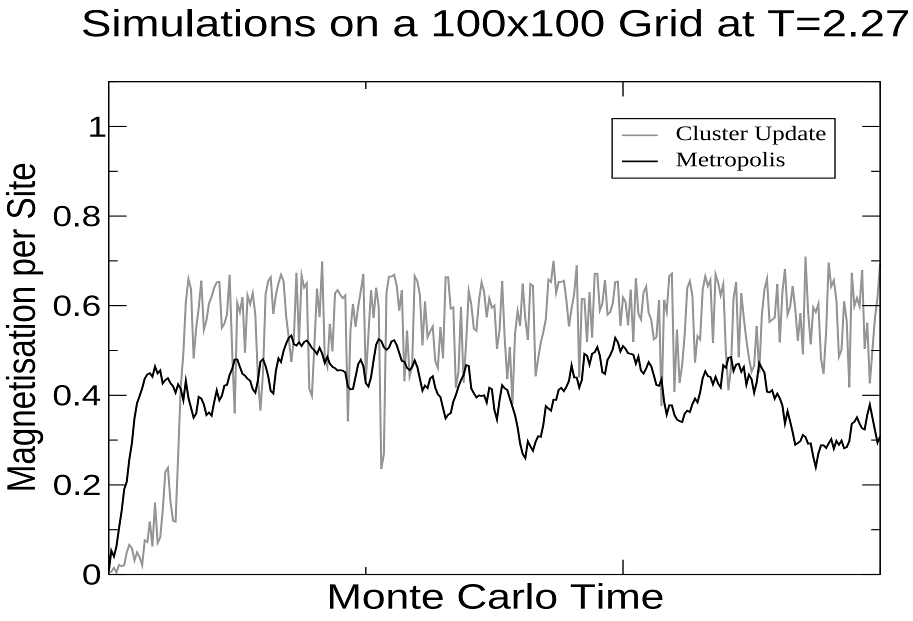

Figure 6.6: Comparison of local and cluster updates at $T = T_c$

What is more, the fast relaxation was achieved by giving up the close modeling of the physical system present in the local update scheme. Therefore, cluster updates should not be used to investigate the dynamics of the system, but only to probe the equilibrium state.

6.4 CONCLUDING REMARKS

The results of the simulations show that good predictions can be achieved using Monte Carlo methods. In particular, it was shown that cluster updates provide a means to overcome the difficulties around the critical temperature T_c. However, this cluster update scheme has drawbacks as well, which gives rise to the need for other methods to simulate specific properties of a system that cannot be handled by such cluster updates.

BIBLIOGRAPHY

[1] L. Onsager, Phys. Rev. **65**, 117 (1944).

[2] N. Metropolis and S. Ulam, Journal of the American Statistical Association **44**, 335 (1949).

[3] D. P. Landau and K. Binder, *A Guide to Monte Carlo Simulations in Statistical Physics* (Cambridge University Press, 2000).

[4] N. Metropolis, A. W. Rosenbluth, M. N. Rosenbluth, A. H. Teller, and E. Teller, J. of Chem. Phys. **21**, 1087 (1953).

[5] P. W. Kasteleyn and C. M. Fortuin, Journal of the Physical Society of Japan Supplement **26s**, 11 (1969).

[6] R. H. Swendsen and J.-S. Wang, Phys. Rev. Lett. **58**, 86 (1987).

[7] U. Wolff, Phys. Rev. Lett. **62**, 361 (1989).

CHAPTER 7

FINITE-SIZE SCALING

DARKO PILAV
SUPERVISOR: MUNEHISA MATSUMOTO

We discuss - by looking at the Ising Model - how one can use finite-size scaling in order to extract crucial information of an infinite system out of a finite system. We also see different possible ways of distinguishing between 1st and 2nd order phase transitions.

7.1 INTRODUCTION

There are two options to get the right behaviour of certain quantities of a thermodynamic system. Either by exact analysis or by simulations of the system. Both ways have their drawbacks. The downside of exact analysis is evidently the inability to solve complicated systems, so solutions are available only for very limited cases. On the other hand, if we look at simulations, certain difficulties arise there as well. We can not simulate the infinite system due to finite processing time and finite memory. This is why we need to look at finite systems. But finite systems behave differently than infinite ones. So if we manage to extract the size dependence of our quantities, we can deduce the behaviour of the thermodynamic system.

Let us look at the difference in behaviour between finite and infinite systems. Taking the Ising model as an example we have the following Hamiltonian

$$H = -J \sum_{\langle i,j \rangle} \sigma_i \sigma_j \qquad \sigma_n \in \{\pm 1\}. \tag{7.1}$$

As you can see, we neglect the three and more site interactions and since we want to look at the 2nd order phase transition we also have no magnetic field (See Fig. 7.1).

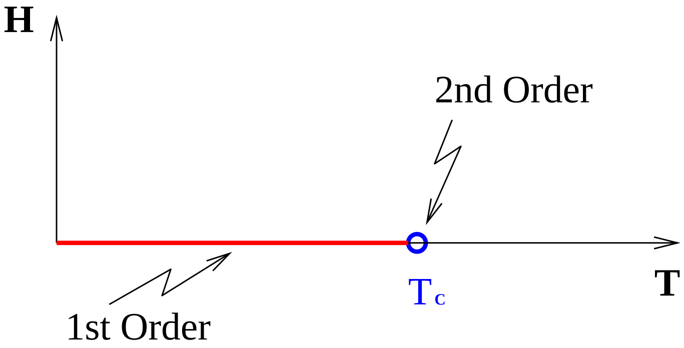

Figure 7.1: Phase diagram of the Ising model ($D \geq 2$)

Consider the magnetisation, the order parameter of the system. By definition the order parameter vanishes in one phase and is finite in the other. If we however consider the finite system, the absolute value of the magnetisation will never completely disappear and the transition will be smeared out (See Fig. 7.2). The reason why we look at the absolute value of the magnetisation in finite systems is that the system is able to flip the whole magnetisation and the positive and negative contributions will cancel out.

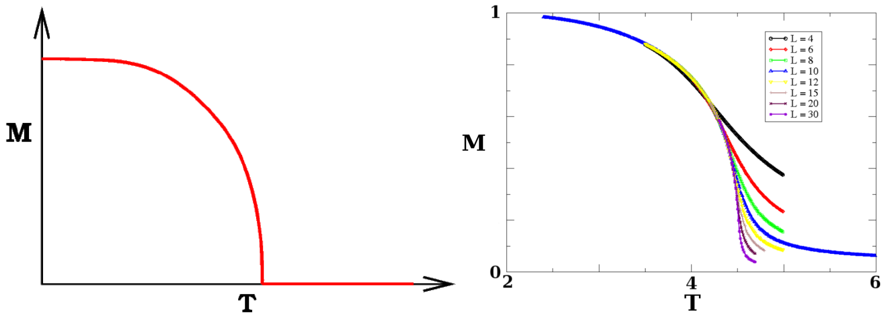

Figure 7.2: Left: Magnetisation in the thermodynamic limit. Right: Magnetisation in a finite size system with different system sizes.

7.2 SCALING FUNCTION HYPOTHESIS

Our goal is to know how we can extract the correct values for the interesting quantities of the infinite system out of the finite system. It is reasonable to introduce a scaling function and merge it with the theoretical scaling behaviour of the infinite system. Of course we can do this for any thermodynamic quantity, in this chapter however we will be using the example of magnetic susceptibility. Now we should talk about how this scaling function should look like. But first a few facts should be mentioned. The magnetic susceptibility can be defined by the fluctuation of magnetisation as follows

$$k_bT\chi_M = \sum_{\langle i,j \rangle} \langle \sigma_i \sigma_j \rangle - \langle \sigma_i \rangle \langle \sigma_j \rangle. \tag{7.2}$$

This definition can be understood quite intuitively after a short hand waving argument. The right hand side is the fluctuation of the magnetisation. If the fluctuations are high the system must be limp and a small magnetic field results in an large magnetisation of the system, therefore the magnetic susceptibility is high. On the other hand a system with low fluctuations is stiff and even a large magnetic field will have only little impact.

Another important fact is that when we approach the critical temperature, the correlation length ξ will diverge as $|t|^{-\nu}$ and the magnetic susceptibility will saturate when $\xi \sim L$ since all the sites of the lattice will be correlated.

Including this into the scaling theory gives us

$$\chi(L,T) = |t|^{-\gamma} g\left(\frac{L}{\xi(t)}\right), \tag{7.3}$$

where $t = (T - T_c)/T_c$ [1]. The scaling function $g(x)$ should also satisfy

- $g(x) \longrightarrow$ const. as $x \longrightarrow \infty$,
- $g(x) \propto x^{\gamma/\nu}$ as $x \longrightarrow 0$.

The first of these two constraints ensures correct power law behaviour in the thermodynamic limit. The other ensures, that the magnetic susceptibility becomes independent of the temperature if $\xi \gg L$ since

$$\begin{aligned} \chi(L,T) &= |t|^{-\gamma} g\left(\frac{L}{\xi(t)}\right) \\ &\overset{\xi \gg L}{\propto} |t|^{-\gamma}\left(\frac{L}{\xi(t)}\right)^{\gamma/\nu} \\ &\propto |t|^{-\gamma}(L|t|^{\nu})^{\gamma/\nu} \\ &\propto L^{\gamma/\nu}. \end{aligned} \tag{7.4}$$

The side product of this calculation is that the maximum of our thermo dynamical quantity grows as $L^{\gamma/\nu}$.
There are different consistent ways of parametrising the scaling function. When using numerical analysis one mostly uses the following

TD limit	FS system
$M \propto \|t\|^{-\beta}$	$M = L^{-\beta/\nu} g_M(tL^{1/\nu}),$
$\chi \propto \|t\|^{\gamma}$	$\chi = L^{\gamma/\nu} g_\chi(tL^{1/\nu}),$
$C \propto \|t\|^{\alpha}$	$C = L^{\alpha/\nu} g_C(tL^{1/\nu}).$

These two notations are equivalent, since

$$\begin{aligned}\chi(L,T) &= |t|^{-\gamma} g\left(\frac{L}{\xi(t)}\right)\\ &\propto \xi^{\gamma/\nu} g(Lt^{\nu})\\ &\propto L^{\gamma/\nu} g'(L^{1/\nu}t).\end{aligned}$$

The proportionality constant can be plugged into g' and so we will get the new scaling function. All we need to know for this calculus is that near T_c the correlation length diverges like $|t|^{-\nu}$ and the measured correlation length behaves like L. Therefore this approach is only valid for temperatures close enough to the critical temperature T_c and for sufficient large system sizes L. The reason behind the system size dependence is, that the distance between two lattice sites compared to the system size itself gets too large for small systems.
Now that we know on what our universal scaling function depends, we can plot the measured quantities so that the measured data collapses if we plug in the correct exponents. Thus if we measure and plot $\chi(L,T)L^{-\gamma/\nu}$ versus $tL^{1/\nu}$ for different system sizes, we can apply numerical data fitting algorithms in order to extract the correct parameters γ and ν. In the plot the data curves for different System sizes should collapse on a single curve - the universal scaling function (See Fig. 7.3).
Of course the same can be done for other thermodynamic quantities like the heat capacity (See Fig. 7.4). The important thing is to collect all the parameters at once, since e.g. ν is the same for all thermodynamic quantities and in this way the error resulting from the numerical fitting can be reduced.

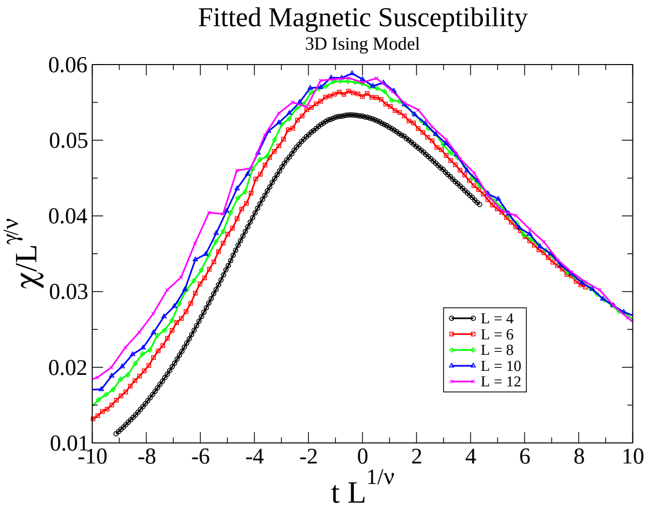

Figure 7.3: Fitted Magnetic Susceptibility. If we go away from T_c or go to small system sizes, the data collapse does not work too well anymore.

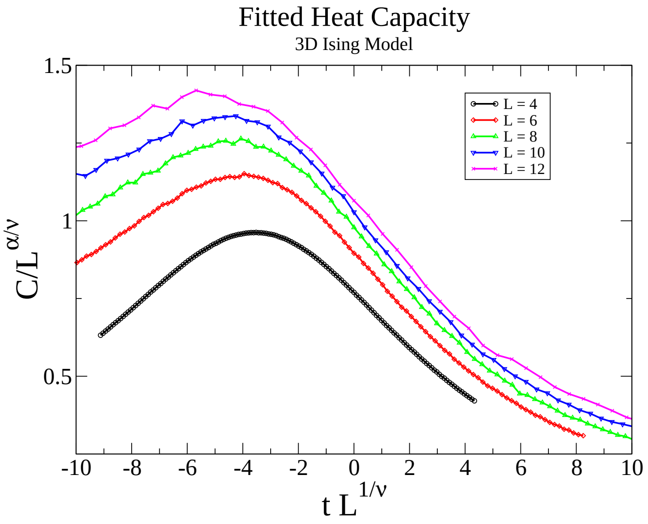

Figure 7.4: Fitted Heat Capacity. If we go away from T_c or go to small system sizes, the data collapse does not work too well anymore.

7.3 CRITICAL TEMPERATURE T_c

The extraction of the critical temperature T_c should be emphasised since knowing where the phase transition exactly is enables making more samples around the critical point and getting more reliable data.

As mentioned before, the problem of getting the critical temperature lies in the smeared out transition due to finite size (See Fig. 7.2). Another contribution to this problem is the lack of divergence of correlation length or any thermodynamic quantity at T_c (See Fig. 7.5).

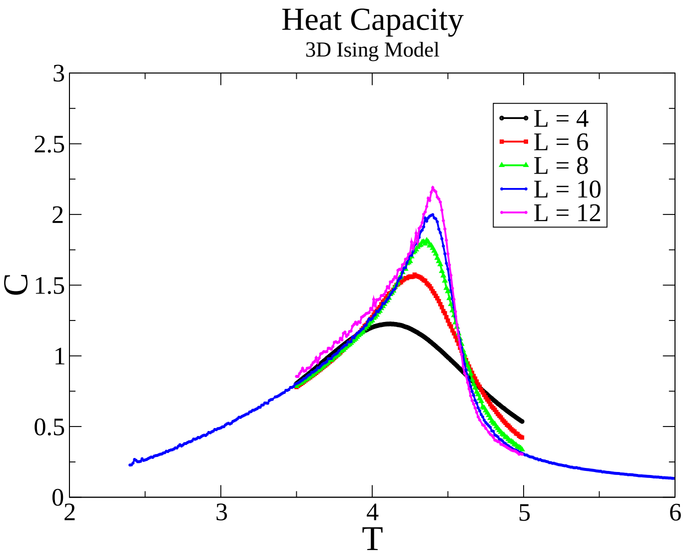

Figure 7.5: Heat Capacity for different system sizes. Notice the lack of divergence at T_c and the shift of the maxima towards T_c with increasing system size.

There are three major solutions for this problem:

- Analysis of behaviour of TD quantities
- Binder Cumulant
- Analysis of behaviour of correlation length

7.3.1 Behaviour of thermodynamic quantities

As shown in Figure 7.5 the maxima of the thermodynamic quantities for different system sizes are not exactly at T_c.
Denote the temperature where the quantity has its maximum by $T_c(L)$. One can make the following first order assumption

$$\xi(T_c(L) - T_c) = aL. \tag{7.5}$$

Since $\xi(x) \propto |x|^{-\nu}$ solving for $T_c(L)$ gives us

$$T_c(L) = T_c + bL^{-1/\nu}. \tag{7.6}$$

With (7.6) we can apply numerical fitting algorithms to get the correct values for T_c, ν and b. The problem is that even with a first order assumption we have three tunable parameters. If we use higher order assumptions instead of (7.5) there will be even more. This requires very good statistical accuracy of the data. For this method, it is important to use measurements of different quantities, since all have the same T_c and ν [2].

7.3.2 BINDER CUMULANT

Another possibility of extracting the critical temperature out of a finite system is the very often used Binder Cumulant

$$U_L := 1 - \frac{\langle M^4 \rangle_L}{\langle M^2 \rangle_L^2}. \tag{7.7}$$

The crucial property of the Binder Cumulant is that it does not depend on the lattice size at the critical temperature as can easily be seen in (7.8).

$$\begin{aligned} \frac{\langle M^4 \rangle_L}{\langle M^2 \rangle_L^2} &= \frac{L^{-4\beta/\nu} g_{M^4}(tL^{1/\nu})}{(L^{-2\beta/\nu} g_{M^2}(tL^{1/\nu}))^2} \\ &= g_c(tL^{1/\nu}) \end{aligned} \tag{7.8}$$

The distribution of the magnetisation is a Gaussian around zero for $T > T_c$ and a sum of two Gaussians for $T < T_c$. With this knowledge it is possible to calculate the following two limits

$$U_L = 1 - \frac{\langle M^4 \rangle_L}{\langle M^2 \rangle_L^2} \xrightarrow{L \to \infty} \begin{cases} \frac{2}{3} & \text{for } T < T_c \\ 0 & \text{for } T > T_c \end{cases} . \tag{7.9}$$

The transition from 2/3 to 0 will happen faster for larger systems and at the critical temperature all lines should intersect at T_c since there the Binder Cumulant does not depend on L (See Fig. 7.6). Due to finite size effects, numerical roundoff errors etc., this intersection will not be exactly in one point.
If the Finite Size Scaling approach is applied on the Binder Cumulant it is possible to get a good value for ν. Since the β is cancelled out (As seen in (7.8)), the only tunable parameter is ν.

7.3.3 BEHAVIOUR OF CORRELATION LENGTH

Very similarly to the Binder Cumulant method we can derive T_c with the correlation length ξ. The scaling ansatz for the correlation length is

$$\xi_L = L g_\xi(tL^{1/\nu}). \tag{7.10}$$

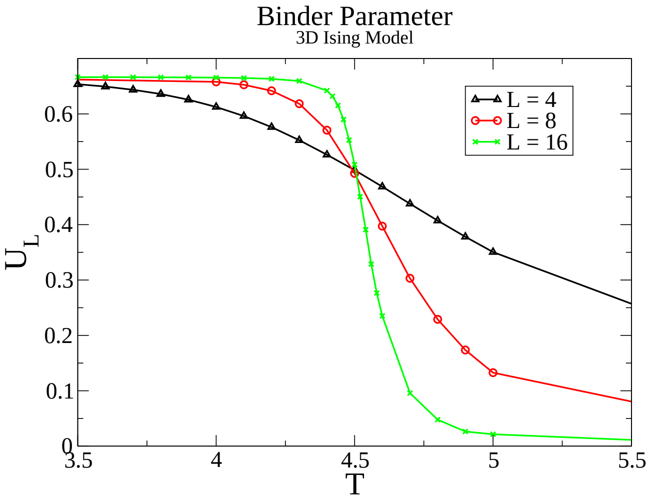

Figure 7.6: The Binder Cumulants for different system sizes intersect at T_c.

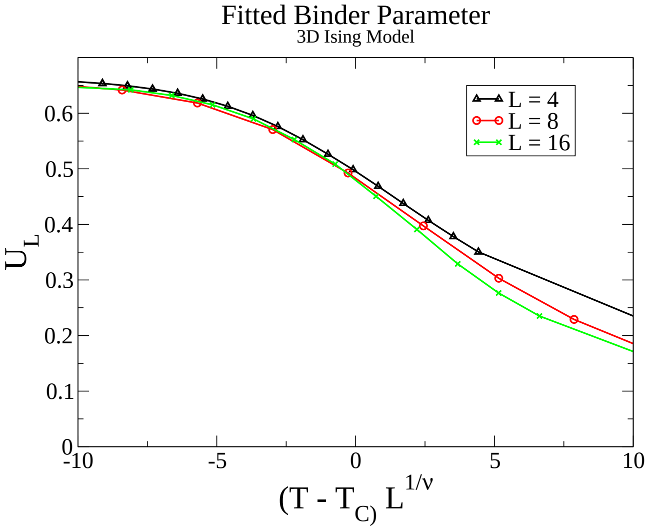

Figure 7.7: Finite Size Scaling applied on the Binder Cumulant gives us ν.

If we go to critical temperature (7.10) can be written as

$$\xi_L / L = g_\xi(0). \tag{7.11}$$

So here too, the ξ/L curves for different system sizes should intersect at nearly the same point.
Naturally Finite Size Scaling can be applied on ξ too and again the only tunable parameter will be ν.

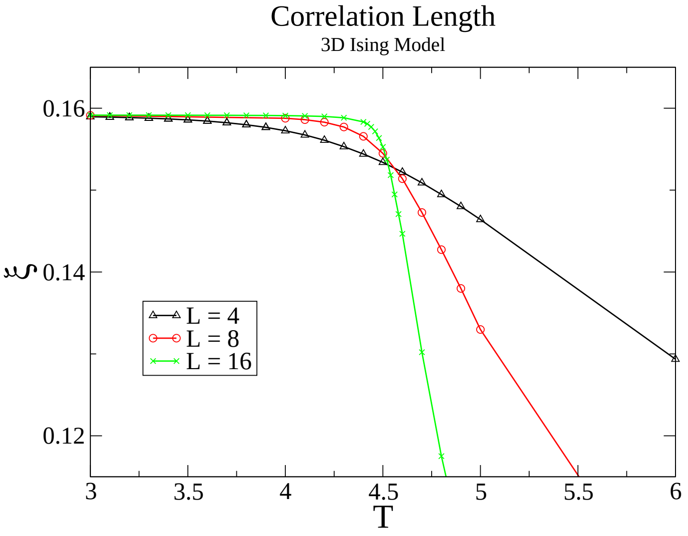

Figure 7.8: The intersection point gives the critical temperature T_c.

7.4 DISTINGUISHING BETWEEN 1ST AND 2ND ORDER PHASE TRANSITIONS

In this chapter we will see why it is difficult to distinguish between 1st and 2nd order phase transitions and what we can do to overcome this problem. We will consider three ways of distinguishing these two types of transitions

- Failure of Finite Size Scaling,
- Lack of Merging of Histogram Peaks,
- Behaviour of thermodynamic Maxima at T_c

7.4.1 FAILURE OF FINITE SIZE SCALING

If we apply the Finite Size Scaling, as we have seen in this chapter, on a 1st order phase transition we will not be able to get good values for critical exponents and the data will not collapse.

The Binder Cumulant as well as the Correlation Length divided by system size ξ/L will not intersect in a single point, even if system size is increased.

Such a behaviour is a good indicator of an 1st order phase transition.

7.4.2 Behaviour of Histogram Peaks

Another way of distinguishing between the different types of phase transitions is to look at the histogram of the order parameter.
If there are two peaks that merge with increasing system size, we know that it is a 2nd order transition. If, however, the peaks stay in the same place after increasing system size, we know that it is a 1st order transition.

7.4.3 Behaviour of thermodynamic Maxima at T_c

The third approach that will be discusses in this chapter is nothing else than applying a Finite Size Scaling approach that is designed for 1st order phase transitions on the measured data. If it gives reasonable results, we will know, that it is a 1st order transition.
All one has to do is to look at the maxima of thermodynamic quantities at T_c. Scaling as we have seen in (7.4) indicates a 2nd order transition, whereas scaling of the maximum as L^d, where d is the dimension of the lattice, indicates a 1st order transition.

7.4.4 Problem of Weak 1st Order Phase Transitions

A weak 1st order transition is a major problem, since all the approaches we discussed beforehand might fail. For example the Finite Size Scaling as we have seen in section 7.4.3 might work quite well for a weak first order transition. It will yield completely wrong exponents, but the data will collapse fairly nice.
The problem is the correlation length ξ. In a first order transition it will not diverge, but if it gets larger than the system size we can not be sure if it diverges or not. So if ξ gets very large near T_c the system will behave as if it were a second order transition unless the system size exceeds the correlation length.

7.5 Concluding remarks

With the Finite Size Scaling, it is possible to gather correct values for the critical exponents of a thermodynamic system and to differentiate between first and second order phase transitions. Nevertheless weak first order phase transitions are and will stay a problem that can only be handled with simulations of large enough systems. But with invention of clever techniques and faster algorithms, one can overcome this problem as well.

BIBLIOGRAPHY

[1] M. Plischke and B. Bergersen, *Equilibrium Statistical Physics* (World Scientific, Singapore, 1994).

[2] D. P. Landau and K. Binder, *A Guide to Monte Carlo Simulations in Statistical Physics* (Cambridge University Press, 2000).

CHAPTER 8

BEREZINSKII-KOSTERLITZ-THOULESS TRANSITION

ROLAND BAUERSCHMIDT
SUPERVISOR: DR. ANDREY LEBEDEV

The two-dimensional XY model is introduced and the phenomenological features are outlined. Then, the relation to the Villain model is established and equivalence to a two-dimensional gas of point defects, interacting via a Coulomb potential, is shown. Finally, the Kosterlitz-Thouless renormalization group equations are motivated and the critical features analyzed.

8.1 INTRODUCTION

The XY model refers to a d-dimensional lattice with two-component (classical) unit vectors $\mathbf{S}_x$ at each site of the lattice (referred to as spin or rotor). Exhibiting $O(2)$ symmetry, it is a special case of the general $O(n)$ model. We consider the two-dimensional XY model a the quadratical two-dimensional lattice $(a_0\mathbb{Z})^2$. The interaction between neighboring spins is given by the potential

$$V(\mathbf{S}_x, \mathbf{S}_y) := -J\,\mathbf{S}_x \cdot \mathbf{S}_y = -J\ \cos(\theta_x - \theta_y) =: V(\theta_x - \theta_y). \tag{8.1}$$

Dimensions one and two are distinguished by the fact that long-range order is impossible (Mermin-Wagner theorem). Nonetheless there is a transition of vortex unbinding, whose explaination is due to Kosterlitz and Thouless.
To second order, the interaction reduces to $\frac{J}{2}(\theta_x - \theta_y)^2$ (neglecting a constant contribution); the corresponding model is sometimes also referred to as the *spin-wave*

theory. However, the feature of periodicity that is responsible for the formation of vortices, and thus ultimately for the Kosterlitz-Thouless transition, is lost in this approximation.

8.1.1 ABSENCE OF LONG-RANGE ORDER IN TWO DIMENSIONS

Before explaining the Kosterlitz-Thouless transition, however, we recall a result from Landau theory (chapter 3): Long-range order is destroyed by fluctuations in dimensions less than or equal to two. The treatment roughly follows lecture notes from Simons[1].

Unlike in the following sections, we assume the quadratic approximation of the $O(n)$ model here and consider a lattice of arbitrary dimension d (the non-linear σ-model, a special case of the Ginzburg-Landau Hamiltonian),

$$H = \frac{J}{2} \sum_{xy} (\mathbf{S}_x - \mathbf{S}_y)^2 \tag{8.2}$$

Assuming without loss of generality that the axis of the order parameter is $\mathbf{S}_0 = (0, \ldots, 0, 1)$, we consider deviations from this direction,

$$\mathbf{S}_0 = (\mathbf{\Pi}_1, \ldots, \mathbf{\Pi}_{n-1}, \sqrt{1 - \mathbf{\Pi}^2}), \tag{8.3}$$

where the ground state corresponds to $\mathbf{\Pi} = 0$. The $\mathbf{\Pi}_i$ are *Goldstone modes* (or spin-waves). If we consider only Gaussian order, the Hamiltonian becomes

$$\begin{aligned} H &= \frac{J}{2} \sum_{xy} (\mathbf{\Pi}_x - \mathbf{\Pi}_y)^2 + \left(\sqrt{1 - \mathbf{\Pi}_x^2} - \sqrt{1 - \mathbf{\Pi}_y^2} \right)^2 && (8.4) \\ &\approx \frac{J}{2} \sum_{xy} (\mathbf{\Pi}_x - \mathbf{\Pi}_y)^2 = \frac{J}{2} \sum_{xy} \mathbf{\Pi}_x (-\triangle) \mathbf{\Pi}_y && (8.5) \end{aligned}$$

where $\triangle$ is the lattice Laplacian. Recall that the correlation function $\langle \mathbf{\Pi}(x) \mathbf{\Pi}(y) \rangle$ of a Gaussian ensemble is given by the Green's function (of the lattice Laplacian in this case), which goes approximately like $\log(x - y)$ in two-dimensions and like $|x - y|^{d-2}$ in more than two dimensions. In the two-dimensional case, the correlation function diverges for $|x| \to \infty$, whereas it is finite in dimensions greater than two. (The Green's function of the lattice Laplacian will be discussed in more detail later.)

In fact, this is a general result, the *Mermin-Wagner-Hohenberg theorem*: There is no phase with spontaneous breaking of a continuous symmetry for $T > 0$, in $d \leq 2$ dimensions. The Kosterlitz-Thouless transition, however, is an example that the absence of spontaneous symmetry breaking does not forbid the existence of criticality. In particular, the Kosterlitz-Thouless transition cannot be described within the Landau model, for there is no order parameter!

8.2 Vortices

We begin with a field of spins $\mathbf{S}_x$ on the lattice $\Lambda \subset \mathbb{Z}^2$. The angle between two neighboring spins $\mathbf{S}_x$ and $\mathbf{S}_y$ is $\psi_{xy} = \arccos(\mathbf{S}_x \cdot \mathbf{S}_y) \in [0, 2\pi)$. We can now consider arbitrary paths on the lattice. Adding the angles between neighboring spins around a closed loop $\gamma \subset \mathbb{Z}^2$, the sum

$$\psi_\gamma = \sum_{xy \in \gamma} \psi_{xy} = 2\pi k, \tag{8.6}$$

must be an integer multiple of 2π, where xy denotes the *bond* between two nearest neighbors x and y in γ. This is a consequence of the fact that a sum of angles is only meaningful up to the addition of a multiple of $2\pi k$[1], and that the angle of a spin with itself must obviously vanish. A *vortex* with vorticity (or topological charge) k is a square (or plaquette) $p \subset \mathbb{Z}^2$ of the lattice such that the closed loop around the boundary of the square ∂p has a sum of angles $\psi_{\partial p} = 2\pi k$.

8.2.1 Continuum extension

We can now extend the field of spins (initially only defined on $\mathbb{Z}^2$) to $\mathbb{R}^2$, continuously everywhere except within vortex squares $p \subset \mathbb{Z}^2$, which is necessary to simulate the "topological" properties of the lattice model in the continuum version. We require the curve integral around a vortex to be an integer multiple of 2π, meaning that the resulting space is not simply connected. Besides that, we do not go into detail on how the continuum continuation should look in detail; in fact, the explicit form is insignificant because only the values on the lattice are of physical significance when working with the lattice model.

If $\gamma_{xy} : [0,1] \to \mathbb{R}^2$ is a curve connecting a curve connecting nearest neighbors x and y (meaning that $\gamma(0) = x$ and $\gamma(1) = y$), the angle can be expressed as

$$\psi_{xy} = \int_0^1 \mathrm{d}t \, \frac{\mathrm{d}}{\mathrm{d}t} \theta(\gamma_{xy}(t)), \tag{8.7}$$

where $\theta(x)$ is a local choice of angle (with respect to some fixed axis) associated with x such that $t \mapsto \theta(\gamma(t))$ is differentiable (and in particular, continuous).

---

[1] Angles can be thought of a as equivalence classes, where $a \sim b$ iff $a = b + 2\pi k, \quad k \in \mathbb{Z}$. Only this identification of angles makes the sum is a well-defined operation, sending two angles to a another angle.

Our notation corresponds to local coordinates of S^1 as a manifold, where all smooth 2π-periodic functions on $\mathbb{R}$ are smooth with respect to the differentiable structure of S^1 if identified in the obvious way, meaning in particular that cos is smooth at every angle. However, it is important to note that two charts are required to cover S^1, which is the reason that vortices can appear.

Note, however, that if we make a global choice of such an angle for all x, $\theta(\gamma(t))$ cannot be continuous for every curve γ because 0 and 2π have to be identified.[2]

Remark. There are other physical models that can be modeled after the XY model; however, many of the models consider a field of spins on a continuum rather than a lattice. The introduction of a lattice of finite spacing can be seen as a mathematical regularization of those models. For simplicity, this discussion is restricted to the lattice model.

8.2.2 FREE ENERGY ARGUMENT

The most simple realization of a vortex of charge k is given by the spin field

$$\phi(x, y) = k \arctan\left(\frac{y}{x}\right). \tag{8.8}$$

The field is singular at $r = |x^2+y^2| = 0$. In fact, vorticity is a homotopy invariant, hence the domain must be homotopically non-trivial.

In the continuum approximation of the Gaussian model, the sum over the nearest neighbor interactions $\sum_{\langle x,y\rangle}(\phi_x - \phi_y)^2$ is replaced by the integral $\int_{\tilde{\Lambda}}(\nabla\phi(x))^2 \, \mathrm{d}^2x$ over the continuum extension of the spin field; here $\tilde{\Lambda} \subset \Lambda \subset \mathbb{R}^2$ denotes the lattice, take away subsets of diameter of the order of the lattice spacing centered at each vortex. This is necessary because at a vortex, the angle rotates very rapidly, making the continuum approximation of the energy very bad; due to the discrete nature of the lattice, the cores do not contribute at all in the original model. We furthermore have to assume that the continuum extension of the spin field is chosen so that both terms agree reasonably well far away from the vortex center, as mentioned before. For the circular field defined above this condition seems to be well satisfied.

In this approximation, the energy of the above vortex is given by

$$\frac{J}{2}\int_{S_L\setminus S_a} (\nabla\phi)^2 \, \mathrm{d}^2x = \frac{J}{2}\int_0^{2\pi} \mathrm{d}\phi \int_a^L \left(\frac{1}{r}\right)^2 r \, \mathrm{d}r = J\pi \log\left(\frac{L}{a}\right), \tag{8.9}$$

in the approximation that the region of the lattice is spherical.

In this approximation for the energy of an isolated vortex, the phase transition can already be predicted: We assume that we add a single vortex to a given configuration of spins. The number of sites the vortex can occupy is approximately

---

[2] This corresponds to a $U(1)$-principal bundle which can only be covered with more than one chart. For two neighboring spins (on the lattice), we require that there is always a chart covering both, though.

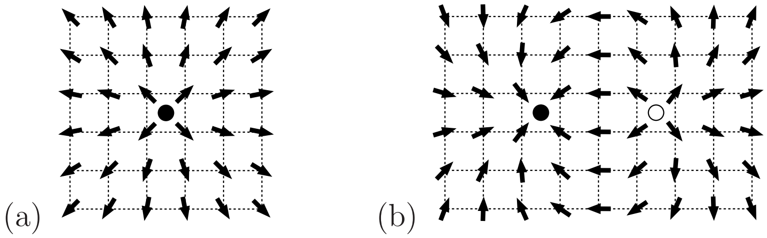

Figure 8.1: Simple configurations with vortices: (a) One vortex of charge +1, (b) Two vortices with charges ±1

$\left(\frac{L}{a}\right)^2$, hence the entropy can be estimated to be $S = -2\,\log\left(\frac{L}{a}\right)$ (units such that $k = 1$) and the Helmholtz free energy is

$$F = U - TS = \log\left(\frac{L}{a}\right)(J\pi - 2T). \tag{8.10}$$

Thus, for $T > \frac{J\pi}{2}$ (or with $\beta = T^{-1}$ and $K = \beta J$, $K < \frac{2}{\pi}$), the formation of vortices seems favorable.

8.3 VILLAIN AND COULOMB GAS MODELS

We will now establish a better picture of how vortices arise in the model, meaning that the approximations seem natural from first principles. In the first step of the analysis, we will replace the rotor model by the so-called Villain model, whose qualitative features are the same. Subsequently, it will be shown that the partition function of the Villain model decouples exactly into a part for a two-dimensional Coulomb gas and a part for spin-waves.

8.3.1 VILLAIN MODEL

Following José et al.[2], we can perform a duality transformation of an arbitrary potential by doing Fourier transformations in the angle variable. In particular, we are obviously interested in the interaction between two spins, given by

$$V(\theta - \theta') = -K(1 - \cos(\theta - \theta')), \tag{8.11}$$

where the irrelevent constant term $-K$ is introducted for later convenience. Note that we now denote with $V(\theta)$ what was $-\beta V(\theta)$ in (8.1), where $K = \beta J$ in order to keep the notation simple. This will lead to the Villain model.

Clearly, $V(\theta)$ is a 2π-periodic function and so is $e^{V(\theta)}$. It can therefore be expanded as a Fourier series,

$$e^{V(\theta)} = \sum_{s=-\infty}^{\infty} e^{\tilde{V}(s)}\, e^{is\theta} =: \sum_{s=-\infty}^{\infty} f(s), \tag{8.12}$$

where the Fourier coefficient is written as $e^{\tilde{V}(s)}$. Now the sum over all integers

$$S(t) = \sum_{s=-\infty}^{\infty} f(t+sT) \tag{8.13}$$

of any function f (that is regular enough) is obviously T-periodic and can thus be written as a Fourier sum,

$$S(t) = \sum_{m=-\infty}^{\infty} f_m e^{im\frac{2\pi}{T}t}, \tag{8.14}$$

where the Fourier coefficient f_m can be expressed in terms of the Fourier transform $\hat{f}$ of f as $f_m = \frac{1}{T}\hat{f}(\frac{2\pi}{T}m)$ which can be verified by a straight-forward calculation. The Fourier transform of the potential is a special case of this with $t = 0$ and $T = 0$, therefore $e^{im\frac{2\pi}{T}t} = 1$ and (8.12) is equal to

$$e^{V(\theta)} = \sum_{m=-\infty}^{\infty} \hat{f}(2\pi m), \quad \hat{f}(\omega) = \int_{-\infty}^{\infty} \mathrm{d}t\; e^{\tilde{V}(t)+it(\theta-\omega)}. \tag{8.15}$$

Writing

$$e^{V_0(\theta)} = \int_{-\infty}^{\infty} \mathrm{d}t\; e^{\tilde{V}(t)+it\theta}, \tag{8.16}$$

this becomes

$$e^{V(\theta)} = \sum_{m=-\infty}^{\infty} e^{V_0(\theta+2\pi m)}. \tag{8.17}$$

Note that if we modify V_0 and define $e^{V(\theta)}$ by the last equation, it will still be periodic automatically. A good approximation of the rotor model is given by

$$V_0(\theta) := -\frac{1}{2}K\theta^2, \tag{8.18}$$

which is the expansion of the original potential V up to second order (see figure 8.2). Compared to the ordinary expansion, however, the Villain model is periodic which we have seen to be the crucial feature in the formation of vortices. In fact, it has been shown that result of this approximation is actually the same as for the original cos-potential model[3].

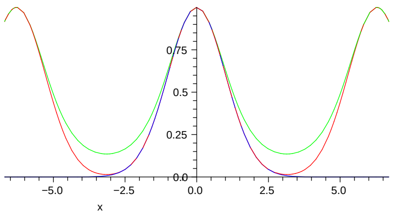

Figure 8.2: (Reduced) Boltzmann factor for (1) the rotor model $e^{\cos(\theta)-1}$, (2) the Villain model $V_0(\theta) = -\frac{1}{2}\theta^2$, and (3) the spin-wave approximation $e^{-\frac{1}{2}\theta^2}$. In the vicinity of the origin, all of the potentials are very similar. However, unlike the Gaussian approximation, the original rotor and the Villain model are periodic.

8.3.2 Coulomb gas model

In this section, the equivalence of the Villain model obtained in the previous section and the model of a gas of point defects, interacting via a two-dimensional Coulomb potential shall be established, following a treatment by Fröhlich and Spencer[3] that emphasizes the analogies with exterior calculus.

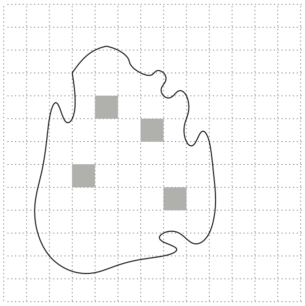

Figure 8.3: Continuous extension of a loop in $\mathbb{Z}^2$ to $\mathbb{R}^2$. The field of spins is considered continuous everywhere except within plaquettes, which are greyly shaded.

We assume an extension of the spin field to $\mathbb{R}^2$ as described before. The sum of angles around a closed loop is then (by construction) the same as the curve integral around that loop, where two points are connected by an arbitary curve (due to homotopy invariance):

$$\sum_{xy \in \gamma} \psi_{xy} = 2\pi n_\gamma \tag{8.19}$$

The vorticity n_γ is a property of the curve γ. Using Stokes' theorem, it can be decomposed as the sum of vorticities due to the enclosed vortices, where each of them corresponds to a lattice square p,

$$n_\gamma = \sum_{p \in S, \gamma = \partial S} n_p, \tag{8.20}$$

and

$$2\pi n_p = \sum_{xy \in \partial p} \psi_{xy}. \tag{8.21}$$

Here, ψ_{xy} refers to the angle between the two sites the bond xy connects.

DIGRESSION: DISCRETE EXTERIOR CALCULUS

We can now use discrete analogues of the standard notions of exterior calculus, such as k-forms or exterior derivatives, which allows to rewrite the problem conveniently. An extensive treatment can be found in [4], for example.

Let the lattice be denoted by Λ.

An oriented *k-cell* can be thought of as the lattice version of an oriented k-dimensional unit volume. It is defined as follows: A 0-cell is a single lattice site x with a choice of orientation, a 1-cell is an oriented bond xy between two neighboring lattice sites, and a 2-cell is an oriented plaquette (square) p. With each k-cell c_k, we associate a set of $k-1$ cells ∂c_k, the *boundary* of c_k and the cell of *reversed orientation* c_k^{-1}. We denote the set of k-cells by C_k.

The boundary of a 0-cell is empty and the orientation is defined intrinsically. The boundary of a 1-cell is defined by $\partial xy = \{x, y^{-1}\}$, where x and y are the sites connected by the bond, and for a 2-cell by $\partial p = \{x_1x_2, x_2x_3, x_3x_4, x_4x_1\}$, where the x_i are the sites at the corner of the square and the x_ix_j the bonds between neighboring corners. Oriention means a choice of the order of the elements in the boundary. Orientation reserval of c_k is defined by requiring that $\partial c_k^{-1} = \bigcup_{s \in \partial c_k} s^{-1}$.

A *k-chain* is a function $\omega : C_k \to \mathbb{R}$ such that $\omega(c_k^{-1}) = -\omega(c_k)$, where c_k^{-1} denotes orientation reversal of the k-cell c_k. It can be thought of as the integral of a k-form over a volume corresponding to c_k. We denote the set of k-chains by Ω_k.

Analogues of the *exterior derivative* $\mathrm{d} : \Omega_k \to \Omega_{k+1}$ and the *codifferential* $\delta : \Omega_k \to \Omega_{k-1}$ can be defined as follows:

$$(\mathrm{d}\omega)(c_{k+1}) = \sum_{c_k \in \partial c_{k+1}} \omega(c_k). \tag{8.22}$$

$$(\delta\omega)(c_{k-1}) = \sum_{c_k :\, c_{k-1} \in \partial c_k} \omega(c_k), \tag{8.23}$$

Note that the definition of the exterior derivative defines the analogue of Stoke's theorem. It is easily verfied that with respect to the scalar product $(\cdot,\cdot) : \Omega_k \times \Omega_k \to \mathbb{R}$ defined by

$$(\omega,\phi) := \frac{1}{2} \sum_{c_k \subset \mathbb{Z}^2} \omega(c_k)\phi(c_k), \tag{8.24}$$

δ and d are actually adjoints of each other, meaning that $(\omega, \mathrm{d}\phi) = (\delta\omega, \phi)$. The *Laplacian* on k-chains can be defined as

$$-\triangle := \delta\mathrm{d} + \mathrm{d}\delta, \tag{8.25}$$

which is analoguous to the definition of the Laplacian of differential k-forms[3]. Similar properties as for the differential versions of the notions hold:

$$\mathrm{d}^2 = 0, \quad \delta^2 = 0, \tag{8.27}$$

and if α is a k-chain such that $\mathrm{d}\alpha = 0$, there is $(k-1)$-chain β such that $\alpha = \mathrm{d}\beta$ (and similarly for δ), which corresponds to *Poincaré's Lemma* [Verify!].

Going back to the model, we can use the definition (8.22) of the lattice exterior derivative d to rewrite the constraint equation (8.21) as

$$2\pi n_p = \sum_{xy \in \partial p} \psi_{xy} = \mathrm{d}\psi_p. \tag{8.28}$$

This implies that

$$\mathrm{d}n = \mathrm{d}^2\psi = 0. \tag{8.29}$$

By Poincaré's Lemma, there is a 1-chain (function on bonds) m_b, such that

$$n_p = \mathrm{d}m_p, \tag{8.30}$$

which allows us to rewrite (8.28) as

$$2\pi\mathrm{d}m_p = \mathrm{d}\psi_p, \tag{8.31}$$

---

[3] Note that in the case of a 0-form (function) f in the differential case or 0-chain f in the discrete case, the Laplacian reduces to $-\delta\mathrm{d}$ because $\delta f = 0$. Observing that $\partial xy = \{x, y^{-1}\}$, this means

$$-(f, \triangle f) = (\mathrm{d}f, \mathrm{d}f) = \sum_{xy \subset \Lambda} (\mathrm{d}f_{xy})^2 = \sum_{xy \subset \Lambda} \left(\sum_{z \subset \partial xy} f_z \right)^2 = \sum_{xy \subset \Lambda} (f_x - f_y)^2, \tag{8.26}$$

which agrees with what one would expect for the discrete Laplacian of a function.

meaning that $\mathrm{d}(2\pi m - \psi)_p = 0$, and thus there is a 0-chain (function on sites) θ_x such that

$$2\pi m_b - \psi_b = -\mathrm{d}\theta_b \quad \text{or} \quad \psi_b = \mathrm{d}\theta_b + 2\pi m_b. \tag{8.32}$$

However, θ and m are not unique; there is still a freedom of gauge. We will consider two possible choices:

1. Writing $\psi_b = \mathrm{d}\theta_b + 2\pi m_b$, we require $\theta_x \in (-\pi, \pi]$, and consider all integer valued 1-chains m (that is, $m_b \in \mathbb{Z}$ for all bonds b). This way, we obtain all configurations compatible with the constraint (8.21).
2. Writing $\psi_b = \mathrm{d}\theta_b^{\mathbb{R}} + 2\pi m_b^{\mathbb{R}}$, we do not impose restrictions on $\theta_x^{\mathbb{R}} \in \mathbb{R}$, requiring that $m_b^{\mathbb{R}} = -(\delta \triangle^{-1} n)_b$, with the discrete Laplacian's Green's function $\triangle^{-1}$ and suitable boundary conditions.[4]

With these preparations, it will now turn out that the canonical ensemble described by the Hamiltonian

$$H(\psi) = -J\,(\psi, \psi) = -\frac{J}{2} \sum_{xy \subset \Lambda} \psi_{xy}^2, \tag{8.33}$$

is equivalent to the Villain model using choice (1) $\psi_b = \mathrm{d}\theta_b + 2\pi m_b$, while it is also equivalent to a two-dimensional Coulomb gas model choice (2) $\psi_b = \mathrm{d}\theta_b^{\mathbb{R}} + 2\pi m_b^{\mathbb{R}}$ is used, establishing the equivalence of the two models.
We consider the canonical ensemble with inverse temperature β

$$\mathrm{d}\mu_\beta(\psi) = Z_\beta^{-1} e^{-\beta H(\psi)} \prod_{p \subset \Lambda} \delta(\mathrm{d}\psi_p - 2\pi n_p) \prod_{xy \subset \Lambda} \mathrm{d}\lambda(\psi_{xy}), \tag{8.34}$$

where the Kronecker-$\delta(\mathrm{d}\psi_p - 2\pi n_p)$ enforces the constraint (8.21), and $\mathrm{d}\lambda(\psi_{xy})$ is the usual Lebesque measure with variable ψ_{xy}. Only in this section, the Lebesque measure is denoted explicitly to avoid confusion with the exterior derivative. The partition function Z_β is defined as usual.

---

[4] Actually, the Green's function is $(G_y)_x$, satisfying $(\triangle_x G_y)_x = \delta_{xy}$, meaning that $(\triangle f)_x = \rho_x$ is solved by $f_x = \sum_{y \in \mathbb{Z}^2} (G_y)_x \rho_y$, for

$$(\triangle f)_x = \left(\triangle_x \sum_{y \in \mathbb{Z}^2} (G_y)_x \rho_y \right)_x = \left(\sum_{y \in \mathbb{Z}^2} \delta_{xy} \rho_y \right)_x = \rho_x.$$

However, we write $(\triangle^{-1} \rho)_x = \sum_{y \in \mathbb{Z}^2} (G_y)_x \rho_y$.

Using choice (1), we obtain the partition function (with $K := \beta J$)

$$\begin{aligned} Z_K &= \sum_{m\subset\Lambda:\, m_{xy}\in\mathbb{Z}} \int_{-\pi}^{\pi}\cdots\int_{-\pi}^{\pi}\prod_{x\in\Lambda}\mathrm{d}\lambda(\theta_x)\; e^{-\frac{K}{2}\sum_{xy\subset\Lambda}(\mathrm{d}\theta_{xy}+2\pi m_{xy})^2} && (8.35)\\ &= \sum_{m\subset\Lambda:\, m_{xy}\in\mathbb{Z}} \int_{-\pi}^{\pi}\cdots\int_{-\pi}^{\pi}\prod_{x\in\Lambda}\mathrm{d}\lambda(\theta_x)\;\prod_{xy\subset\Lambda} e^{-\frac{K}{2}(\mathrm{d}\theta_{xy}+2\pi m_{xy})^2}. && (8.36)\end{aligned}$$

Because $\mathrm{d}\theta_{xy} = \theta_x - \theta_y$ and for every combination of x and y, m_{xy} assumes all possible integers[5], the partition sum can be rewritten as

$$Z_K = \int_{-\pi}^{\pi}\cdots\int_{-\pi}^{\pi}\prod_{x\in\Lambda}\mathrm{d}\lambda(\theta_x)\;\prod_{xy\subset\Lambda} g(\theta_x-\theta_y), \tag{8.37}$$

where

$$g(\theta) = \sum_{m=-\infty}^{\infty} e^{-\frac{K}{2}(\theta+2\pi m)^2}. \tag{8.38}$$

But we know this expression: It is the partition function for the Villian model!

On the other hand, we might as well use choice (2) to rewrite the partition function as

$$\begin{aligned} Z_K &= \int_{-\infty}^{\infty}\cdots\int_{-\infty}^{\infty}\prod_{x\in\Lambda}\mathrm{d}\lambda(\theta_x)\; e^{-\frac{K}{2}(\mathrm{d}\theta^{\mathbb{R}}+2\pi m^{\mathbb{R}},\mathrm{d}\theta^{\mathbb{R}}+2\pi m^{\mathbb{R}})} && (8.39)\\ &= \int_{-\infty}^{\infty}\cdots\int_{-\infty}^{\infty}\prod_{x\in\Lambda}\mathrm{d}\lambda(\theta_x)\; e^{-\frac{K}{2}(\mathrm{d}\theta^{\mathbb{R}},\mathrm{d}\theta^{\mathbb{R}})+(2\pi m^{\mathbb{R}},2\pi m^{\mathbb{R}})} && (8.40)\end{aligned}$$

because $\delta^2 = 0$ implies that

$$(m^{\mathbb{R}},\mathrm{d}\theta^{\mathbb{R}}) = (\delta m^{\mathbb{R}},\theta^{\mathbb{R}}) = (\delta(-\delta\triangle^{-1}n),\theta^{\mathbb{R}}) = 0. \tag{8.41}$$

This means, however, that the partition function decouples into a spin-wave and a vortex part,

$$Z_K = \underbrace{\left(\int_{-\infty}^{\infty}\cdots\int_{-\infty}^{\infty}\prod_{x\in\Lambda}\mathrm{d}\lambda(\theta_x)\; e^{-\frac{K}{2}(\mathrm{d}\theta^{\mathbb{R}},\mathrm{d}\theta^{\mathbb{R}})}\right)}_{Z_K^{\mathrm{SW}}}\underbrace{\left(\sum_{n\subset\Lambda:\, n_p\in\mathbb{Z}} e^{-\frac{K}{2}(2\pi m^{\mathbb{R}},2\pi m^{\mathbb{R}})}\right)}_{Z_K^{\mathrm{V}}}, \tag{8.42}$$

while due to

$$(m^{\mathbb{R}},m^{\mathbb{R}}) = (-(\delta\triangle^{-1}n),-(\delta\triangle^{-1}n)) = (n,\triangle^{-1}n) = \sum_{p\subset\Lambda} n_p(\triangle^{-1}n)_p, \tag{8.43}$$

---

[5] Note that actually, it assumes all possible integers many times. But since the number of times is equal for all terms, we can assume that it is unity.

the vortex part is equivalent to a two-dimensional lattice Coulomb gas:

$$Z_K^{\mathrm{V}} = \sum_{n\subset\Lambda:\, n_p\in\mathbb{Z}} e^{2\pi^2 K \sum_{p\subset\Lambda} n_p(\triangle^{-1}n)_p}. \tag{8.44}$$

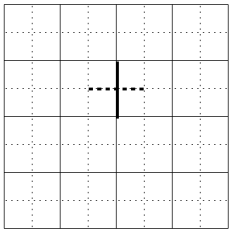

Figure 8.4: The dual lattice $(\mathbb{Z}^2)^*$ (dotted) is the lattice of squares of the original lattice $\mathbb{Z}^2$ (solid). Sites are identified with squares, and bonds with bonds. The dual identification corresponds to the Hodge operation.

Note that n is defined on lattice squares (plaquettes) which we can consider a dual lattice $(\mathbb{Z}^2)^*$. However, we can identify squares with sites of the lattice, as indicated in figure 8.4. We shall furthermore identify bonds of the dual lattice with the corresponding perpendicular bonds on the real lattice: $xy \cong x^*y^*$. Recalling the constraint (8.21) $\mathrm{d}n = 0$, one observes that $\triangle n = \mathrm{d}\delta n$. With these considerations, we obtain

$$(n, \triangle n) = (\delta n, \delta n) = \sum_{xy\subset\Lambda}\left(\sum_{p:\, xy\in\partial p} n_p\right)^2 = \sum_{x^*y^*\subset\Lambda^*}(n_{x^*} - n_{y^*})^2\,, \tag{8.45}$$

meaning that the Laplacian of a 2-chain does indeed look like the Laplacian of a function (0-chain) on the dual lattice.

8.4 EFFECTIVE INTERACTION

We have thus seen that the rotor model is equivalent to a two-dimensional lattice gas of point defects, interacting via a Coulomb potential. In order to understand the critical properties of the rotor model, we therefore need to understand the criticial properties of the Coulomb gas. The qualitative picture is that at low temperatures, particles of opposite charge form closely bound pairs, while at higher temperatures the pairs unbind and a transition to a plasma takes place.
Under assumption of the Villain model, all of the previous calculations were exact. In this section, we will state a number of approximations and further assumptions that we will then use in the renormalization group analysis of the criticial features

in the next section. Note that the results can as well be established in a rigorous way as shown by Fröhlich and Spencer[3, 5], which we shall not consider here, however.

8.4.1 Generalized Villain model

In order to construct a (perturbative) renormalization group procedure for the Villain model (or Coulomb gas) in the next section, it is necessary to modify the partition function by introducing an energy cost for the creation of vortices, corresponding to a chemical potential. Hence, in the generalized Villain model, the vortex part of the partition function is modified by substituting $e^{-\beta E}$ with $e^{-\beta(E+N\cdot E_c)} =: y_0^N e^{-\beta E}$, where y_0 is called the fugacity. $N \equiv N(n)$ is a measure for the number of vortices of the vortex configuration n. We can choose

$$N(n) = \sum_{p\subset\Lambda} n_p^2. \tag{8.46}$$

The exact form is insignificant, however. The generalized partition function is

$$Z_K^{\mathrm{V}} = \sum_{n\subset\Lambda:\, n_p\in\mathbb{Z}} y_0^{N(n)}\, e^{2\pi^2 K \sum_{p\subset\Lambda} n_p(\triangle^{-1}n)_p}. \tag{8.47}$$

The fugacity y_0 controls the fluctuations: A small value of y_0 corresponds to a large energy associated with a vortex, making the creation of vortices unfavorable. In the limit $y_0 \to 0$, the energy associated with a vortex becomes infinite such that vortices disappear and the system is described only by the spin-wave part of the partition function.
The original Villain model is obtained for $y_0 = 1$.

8.4.2 Approximation of the Green's function

In the following, we will generally approximate the Green's function of the lattice Laplacian by the normal Laplacian's Green's function

$$\triangle_{xy}^{-1} \approx C(x-y) := \log\left(\frac{|x-y|}{a_0}\right), \tag{8.48}$$

which makes sense for large $|x-y|$.

8.4.3 Dielectric constant

An effective description corresponding of the Coulomb gas can be obtained in a perturbative way. This section follows the heuristic derivation given by Kardar[6].

We assume the approximation that the dominant contribution to the partition function is given by the configurations n with none or two charges of opposite sign:

$$Z_K^{\mathrm{V}} = \sum_n {y_0}^{\sum_{p\subset\Lambda} n_p^2}\, e^{2\pi^2 K \sum_{p\subset\Lambda} n_p(\triangle^{-1}n)_p} = 1 + {y_0}^2 \sum_{y,y'} e^{-2\pi^2 K \triangle^{-1}_{yy'}} + \mathcal{O}({y_0}^4) \tag{8.49}$$

We have excluded the possiblity of charge configurations where the total charge is odd, for we have seen before that the energy of an isolated charge diverges.
The additional reduced energy (βH) if two additional (external) charges are added to a given configuration n (internal charges) is

$$E(x,x';n) = 2\pi K(+1)C(x-x')(-1) + 2\pi K D(x,x';n) \tag{8.50}$$

where

$$D(x,x';n) = \sum_y (+1)C(x-y)n_y + \sum_y (-1)C(x'-y)n_y \tag{8.51}$$

is the interaction term between the external and the internal charges.
The Boltzmann factor of the effective interaction between the two further charges x and x' is now *assumed* to be the ensemble average

$$e^{-\beta V(x-x')} = \langle e^{-E(x,x';n)} \rangle \tag{8.52}$$

of the Boltzmann factor corresponding to the additional energy of the two external charges with the system.
Making use of

$$\frac{1+u}{1+v} = 1 + u - v + \mathcal{O}((u+v)^2), \tag{8.53}$$

this can be approximated to order y_0^2 by

$$e^{-\beta V(x-x')} = e^{-2\pi^2 K C(x-x')} \cdot \\ \Big[1 + y_0^2\, e^{-2\pi^2 K C(y-y')} \,\Big(e^{2\pi^2 K \sum_{y,y'} D(x,x';n^{(2)})} - 1\Big)\Big] + \mathcal{O}(y_0^4). \tag{8.54}$$

In center of mass coordinates $R = (y+y')/2$ and $r = y'-y$, and under the assumption that r is small, meaning that the dipoles are tightly bound, we obtain

$$D_{xx';yy'} = -r\cdot\nabla_R C(x-R) + r\cdot\nabla_R C(x'-R) + \mathcal{O}(r^3) \tag{8.55}$$

We can further use the approximation

$$e^{2\pi^2 K D_{xx';yy'}} - 1 = 2\pi^2 K D_{xx';yy'} + 4\pi^4 K^2 D^2_{xx';yy'} + \mathcal{O}((x+y)^3) \tag{8.56}$$

in this order.

Approximating sums by integrals, and putting everything together, the effective potential can now be evaluated to obtain

$$e^{-\beta V_{xx'}} = e^{-2\pi^2 KC(x-x')} \left[1 + 4\pi^5 K^2 {y_0}^2 C(x-x') \int_a^\infty \mathrm{d}r \; r^3 e^{-2\pi K \log(r/a)} \right] + \mathcal{O}({y_0}^4), \tag{8.57}$$

or

$$e^{-\beta V_{xx'}} = e^{-2\pi^2 K_{\text{eff}} C(x-x')}, \tag{8.58}$$

with

$$K_{\text{eff}} = K - 2\pi^3 K^2 {y_0}^2 a^{2\pi K} \int_a^\infty \mathrm{d}r \; r^{3-2\pi K} + \mathcal{O}({y_0}^4). \tag{8.59}$$

The term $a^{2\pi K}$ may be combined with y_0 to define a new fugacity y.

Remark. Note that this heuristic derivation only suggests the renormalization of the coupling constant in the Coulomb gas part of the partition function. However, as can be seen by a more careful argument by José et al.[2], which considers the spin-spin correlation function instead of the partition function, the same renormalization should be carried out in the spin-wave part of the partition function as well.

8.5 KOSTERLITZ-THOULESS TRANSITION

We have thus motivated an effective coupling constant for a the two-dimensional Coulomb gas. In this section, we shall apply the method of the renormalization group to this result to determine the critical features of the model.

8.5.1 RECURSION RELATIONS

The effective coupling constant K_{eff} that suggested by a perturbative analysis is

$$K_{\text{eff}} = K - 4\pi^3 K^2 y^2 \int_a^\infty \mathrm{d}r \; r^{3-2\pi K}. \tag{8.60}$$

Unfortunately, the integral on the right hand side diverges for $K < \frac{2}{\pi}$, that is $T > \frac{\pi J}{2}$, which is exactly the temperature where the contribution of vortices becomes favorable in the Free Energy (see section 8.2.2). However, it can still be made sense of by the means of renormalization using a procedure described by José et al.[2]. Absorbing a finite part of the integral into a new bare coupling constant K',

$$K' := K - 4\pi^3 K^2 y^2 \int_a^{a(1+l)} \mathrm{d}r \; r^{3-2\pi K}, \tag{8.61}$$

and rescaling the divergent part of the integral,

$$\int_{a(1+l)}^{\infty} \mathrm{d}r\, r^{3-2\pi K} = (1+l)^{4-2\pi K} \int_{a}^{\infty} \mathrm{d}r\, r^{3-2\pi K}, \tag{8.62}$$

equation (8.60) can be restarted as

$$K_{\text{eff}} = K' - 4\pi^3 K'^2 y'^2 \int_{a}^{\infty} \mathrm{d}r\, r^{3-2\pi K'}, \tag{8.63}$$

when the rescaled fugacity is defined by

$$y' := y(1+l)^{2-\pi K}. \tag{8.64}$$

We have also made a further replacement of K with K' which is valid in the same order of y_0 as the original equation. In the limit $l \to 0$, the iteratation of this transformation is described by the differential equations,

$$\begin{aligned} \frac{\mathrm{d}K}{\mathrm{d}l} &= -4\pi^3 K^2 y^2 + \mathcal{O}(y^4) && (8.65) \\ \frac{\mathrm{d}y}{\mathrm{d}l} &= (2-\pi K)y + \mathcal{O}(y^3), && (8.66) \end{aligned}$$

known as Kosterlitz renormalization group (RG) equations or recursion relations.

8.5.2 RENORMALIZATION GROUP FLOW

It is readily observed that $(K_c, y_c) = (\frac{2}{\pi}, 0)$ is a fixed point (in this order), which we shall later identify as the critical point. For the subsequent discussion, we adapt rescaled and shited variables

$$\begin{aligned} X &:= \frac{1}{4}(2-\pi K) && (8.67) \\ Y &:= \pi^2 y && (8.68) \\ L &:= 2l, && (8.69) \end{aligned}$$

such that the recursion relations simplify to

$$\begin{aligned} \frac{\mathrm{d}X}{\mathrm{d}L} &= 2Y^2 + \mathcal{O}((X+Y)^4) && (8.70) \\ \frac{\mathrm{d}Y}{\mathrm{d}L} &= 2XY + \mathcal{O}((X+Y)^3) && (8.71) \end{aligned}$$

in the vicinity of the fixed point $(X, Y) = (0, 0)$.
Note that $-X \sim K \sim T^{-1}$, meaning that low temperatures correspond to low X and vice versa, and that $\mathrm{d}X/\mathrm{d}L \geq 0$; hence X is a relevant scaling field (in

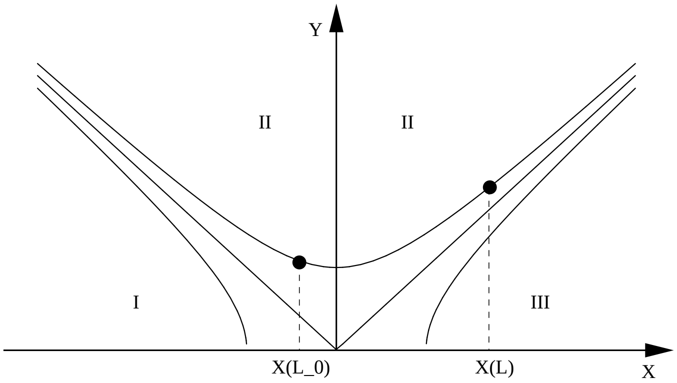

Figure 8.5: Renormalization group flow in the vinicity of the critical point $(X, Y) = (0, 0)$. The separatices $Y = |X|$ divide the parameter space into three regions I, II, and III.

the sense of renormalization), as is Y for high temperatures $X > 0$. For low temperatures $X < 0$, however, Y is irrelevant.
The hyperbolae $h_\alpha : L \mapsto (X(L), Y(L))$, $\alpha \in \mathbb{R}$ implicitly defined by

$$X(L)^2 - Y(L)^2 = \alpha \tag{8.72}$$

solve the recursion relations (8.70, 8.71).

As can be seen in figure 8.5, parameter space in divided into three regions which are separated by the critical trajectory, corresponding to the degenerate hyperbola with $\alpha = 0$.
In region I (low temperatures), the flows terminate on the fixed line $Y = 0$ and $X < 0$. This can be interpreted as follows: The points in region I are effectively described by the renormalized values of the parameters, given by the points on the flow passing through the initial point. All flows terminate at $Y = 0$; recalling the interpretation $y_0 = e^{-\beta E_c}$, this means that the energy associated to the creation of a vortex diverges and vortices disappear. Hence region I describes a (renormalized) spin-wave theory with a finite values for X or K_{eff}. In the picture of charges, the dielectric constant $\varepsilon = K_{\text{eff}}/K$ corresponds to an insulating phase.
In region II (high temperatures), in contrast, flows do not terminate on fixed points, and X and Y proceed to infinity — this is where perburbation theory breaks down. However, the points are clearly described by non-zero Y, meaning that the formation of vortices becomes likely. This is a phase of free vortices, which we can also think of as a metallic phase.

We can now think of physical changes of a system as trajectories in parameter space. The previous considerations suggest that the effective partition function is not analytic as a function in parameter space when the separatix is crossed. We will thus associate the separatix with the critical temperature.

SCREENING LENGTH

Recall that the renormalization group transformation corresponds to an infinitsimal change of length scale from a to $a(1+l)$, meaning that $\frac{\mathrm{d}}{\mathrm{d}l}a(l) = a(l)$, thus

$$a(l) = a\exp(l). \tag{8.73}$$

For parameters with $X(L) \approx 1$, that is high temperature, we assume that there is an abundance of vortices, suggesting that the screening length is only of the order of the lattice spacing. In the original variables this means $\lambda(l) \sim a$. We further assume that the screening length scales as follows (refer to a textbook for motivation)

$$\frac{\lambda(l_0)}{a} = \frac{\lambda(l)}{a(l)} \quad \text{i.e.} \quad \lambda(l_0) \sim a\exp(l), \tag{8.74}$$

where $(X(L_0), Y(L_0))$ is a point in parameter space describing the actual lattice spacing a.
In region II, the solution of the recursion relations (8.72) can be used to integrate them and obtain

$$L - L_0 = \frac{1}{2\sqrt{|\alpha|}}\left[\arctan\left(\frac{X(L)}{\sqrt{|\alpha|}}\right) - \arctan\left(\frac{X(L_0)}{\sqrt{|\alpha|}}\right)\right]. \tag{8.75}$$

The parameter α parameterizing the hyperbolae is negative for the vortex phase (region II) and vanishes at the critical temperature (separatix). Approaching the critical temperature from below, we thus approximate α linearly by

$$\alpha = -b^2(T_C - T), \quad b > 0. \tag{8.76}$$

Close to the critical temperature, we can now consider $X(L) \approx 1$ and $X(L_0) < 0$ to obtain (refer to figure 8.5 for visualization of the points):

$$L \approx \frac{\pi}{2\sqrt{|\alpha|}} \approx \frac{\pi}{2b\sqrt{T - T_C}} \tag{8.77}$$

Hence we can estimate the screening length to be

$$\lambda \sim a\exp(l) \approx a\exp\left(\frac{\pi}{4b\sqrt{T - T_C}}\right). \tag{8.78}$$

Note the remarkable feature that it has an essential singularity at $T = T_C$ (i.e. $(T_C - T)^n\lambda \to \infty$ as $T \to T_C$ for any $n \in \mathbb{N}$).

BIBLIOGRAPHY

[1] B. Simons, *Phase Transitions and Collective Phenomena*, Lecture Notes, University of Cambridge, 1997.

[2] J. V. José, L. P. Kadanoff, S. Kirkpatrick, and D. R. Nelson, *Renormalization, vortices, and symmetry-breaking perturbations in the two-dimensional planar model*, Phys. Rev. B **16**, 1217 (1977).

[3] J. Fröhlich and T. Spencer, *The Kosterlitz-Thouless Transition in Two-Dimensional Abelian Spin System and the Coulomb Gas*, Commun. Math. Phys. **81** (1981).

[4] M. Desbrun, A. N. Hirani, M. Leok, and J. E. Marsden, *Discrete Exterior Calculus* (2005), URL `http://www.citebase.org/abstract?id=oai:arXiv.org:math/0508341`.

[5] J. Fröhlich and T. Spencer, *The Berezinskii-Kostelritz-Thouless Transition. (Energy-Entropy Arguments and Renormalization in Defect Gases)* (1984), in Fröhlich, J. (Ed.): Scaling and Self-similarity In Physics, 29-138.

[6] J. Kardar, *Statistical Mechanics II: Statistical Mechanics of Fields*, Lecture Notes, MIT, Spring 2004.

CHAPTER 9

O(N) MODEL AND 1/N EXPANSION

MICHAEL KAY
SUPERVISOR: INGO KIRSCH

We introduce the Ginzburg-Landau-Wilson O(N) model which describes N-dimensional self-interacting spins on a lattice of arbitrary dimension d. We also develop the 1/N expansion of the partition function, analyze the existence of spontaneous symmetry breaking (for $d = 1, 2, 3, 4$) and calculate critical exponents by applying a general Renormalization Group procedure.

9.1 INTRODUCTION

The O(N) model is a field theoretical model used to describe a hypothetical system of N-dimensional spins in a lattice of arbitrary dimension. In particular O(N) refers to the invariance of the Hamiltonian of the system under isometries of the N-dimensional spin space. The peculiarity of this theory is that as N goes to infinity it becomes simpler and in fact exactly solvable. In the large N limit the magnitude of the spin vectors self averages thus giving rise to an effective average spin field with fluctuations of order 1/N [1]. This behavior motivates an expansion of all physical quantities of interest in powers of 1/N, away from the exact theory.

The ultimate goal of the 1/N expansion is that of obtaining physical quantities for $N = 3$. This turned out to be a very hard task and indeed is still a hot topic today.

The aim of this chapter is not that of presenting detailed calculations in the 1/N-expansion approximation, because it would only result in a strenuous mathematical effort, but that of discussing some important aspects of this theory.

After a brief description of the model, the mathematical background will be given with particular emphasis on the steepest descent method. Next we will investigate the existence of spontaneous symmetry breaking for space (lattice) dimensions $d = 1, 2, 3, 4$ at leading order in 1/N. We will then present a general renormalization group scheme that is applicable to any order in 1/N. The calculation of critical exponents will be outlined for leading order in 1/N, and results for next-to-leading order will also be given.

9.2 The Model

In order to define the system we need first to introduce a Hamiltonian expressed in terms of the spin configurations. Let us consider the spins to be located at discrete lattice sites. We can neglect the microscopic details of the system and thus let the lattice constant a vanish. Each spin configuration will be interpolated by a real smooth spin density field ϕ, which can be thought of as a (Fourier) superposition of waves. Divergences in the thermodynamic quantities resulting from the continuum limit, can be avoided by setting an upper bound Λ to the wavenumber of the order $\Lambda \sim 1/a$. This eliminates the unphysical spin density fluctuations within one lattice spacing. This simple idea is closely related to the (less intuitive) renormalization techniques that will be described in Sec. 9.4.
We require the Hamiltonian to be O(N) invariant. The Hamiltonian density corresponding to the simplest non-trivial O(N) model in a space of dimension d is the so-called Ginzburg-Landau-Wilson model. This is of the form

$$\mathcal{H}(\phi^a, \partial_\mu \phi^a) \equiv \frac{1}{2}(\partial_\mu \phi^a)^2 + \frac{1}{2}\mu_0^2 \phi^a \phi^a + \frac{\lambda_0}{8N}(\phi^a \phi^a)^2, \tag{9.1}$$

where $a = 1, ..., N$ runs over the spin components, $\mu = 1, ..., d$ and each $\phi^a = \phi^(x_\mu)$ is a scalar field. In the field theoretical framework the first term in the r.h.s of Eq. (9.1) corresponds to the relativistic kinetic term for bosons (Klein-Gordon), the second term is a mass term and the last term to corresponds to the first non-trivial O(N)-symmetric interaction. μ_0 and λ_0 are the bare mass and bare coupling constant, respectively. By "bare" we mean free parameters that do not coincide with the physical quantities yet to be defined. We stress that $\lambda_0 > 0$, otherwise the energy would be unbounded from below. Higher order interaction terms are neglected because they would lead to an unrenormalizable theory for $d \leqslant 4$ [2].
We consider the system described by the Hamiltonian (9.1) subject to a constant external magnetic field $\vec{J}$ at fixed temperature. The partition function, that is the sum of the probabilities that each configuration ϕ is realized under these

macroscopic conditions, is

$$\mathcal{Z}[\beta, J^a] = \mathcal{N} \int \mathcal{D}\phi^a \exp\left(-\int \left[\mathcal{H} - J^a(x)\phi^a(x)\right] d^dx\right), \tag{9.2}$$

where β is the inverse temperature and $\mathcal{N}$ a normalization constant.
It is now useful to introduce the functional $\mathcal{W}$,

$$\mathcal{W}[\beta, \vec{J}] = \ln \mathcal{Z}[\beta, \vec{J}], \tag{9.3}$$

which corresponds to the definition of the negative Gibbs free energy. All thermodynamic quantities can be derived from either of these two functionals.
Note that $\mathcal{Z}$ is the generating functional of the n-point correlation functions of ϕ^a, which in turn can be represented as the sum of all the Feynman diagrams of the theory with n external lines. On the other hand, $\mathcal{W}$ is the generating functional of the connected n-point correlation functions $G^{(n)}$, which in turn can be represented as the sum of all the connected Feynman diagrams of the theory with n external lines. For details on the computation on n-point correlation functions see Ref. [2].

9.3 MATHEMATICAL BACKGROUND

An exact solution of the functional integral (9.2) can be obtained only if the Hamiltonian is a quadratic form, that is if the interaction term in Eq. (9.1) is neglected. In this section we will outline two perturbative methods for the approximation of the partition function: the weak-coupling expansion (see e.g. [3]) and the steepest descent method [4]. It is important to stress that our aim is to obtain an expansion of $\mathcal{Z}$ in 1/N.

9.3.1 WEAK COUPLING EXPANSION

We assume that the interaction term of the Hamiltonian density (9.1) is a weak perturbation. After integrating by parts, the Hamiltonian is split into a free part

$$\int d^dx \mathcal{H}_0[\phi^a(x)] \equiv \frac{1}{2} \int d^dx d^dx' \phi^a(x)(-\nabla^2 + \mu_0^2)\phi^a(x') \tag{9.4}$$

and an interaction term

$$\int d^dx V[\phi^a(x)] \equiv \int d^dx \frac{\lambda_0}{8N}(\phi^a\phi^a)^2. \tag{9.5}$$

We then use the fact that J^a and ϕ^a are conjugate fields, that is

$$\frac{\delta \mathcal{W}}{\delta J^a(x)} = \frac{1}{\mathcal{Z}} \frac{\delta \mathcal{Z}}{\delta J^a(x)} = \langle \phi^a(x) \rangle_{\vec{J}}, \tag{9.6}$$

where $\langle \rangle_{\vec{J}}$ denotes the ensemble average in the presence of an external field $\vec{J}$. This allows us to write the partition function in the form

$$\mathcal{Z}[\beta, J^a] = \exp\left[-\int d^d x V \left(\frac{\delta}{\delta J^a(x)} \right) \right] \mathcal{Z}_0[\beta, J^a], \tag{9.7}$$

where $\mathcal{Z}_0$ is the partition function for non-interacting ϕ^a fields.
Next we perform the integration over ϕ^a in $\mathcal{Z}_0$ to obtain

$$\mathcal{Z} = \mathcal{C} \exp\left[-\int d^d x V \left(\frac{\delta}{\delta J^a(x)} \right) \right] \exp\left[\frac{1}{2} \int d^d x d^d y J^a(x) \Delta(x-y) J^a(y) \right], \tag{9.8}$$

where $\mathcal{C}$ is a normalization constant and $\Delta(x-y)$ is the free propagator of the ϕ^a fields, defined through the relation

$$[-\nabla^2 + \mu_0^2] \Delta(x-y) = \delta(x-y). \tag{9.9}$$

The final step is to expand the exponential of the interaction term in (9.8) in a functional Taylor series, and retain the higher order terms in 1/N. Although the expansion parameter contains a λ_0/N term, it also contains a factor of order N due to the presence of N ϕ^a fields. The number of terms at leading order in 1/N is in fact infinite. Therefore this method is inappropriate for the construction of a 1/N expansion. It is however the most commonly used procedure in the case of one scalar field.

9.3.2 The Steepest Descent Method

We can always assume that for finite N, the magnitude squared of the N-dimensional spin field and that of the external magnetic field are of order N. As a consequence the Hamiltonian density $\mathcal{H}$ is of order N and $\mathcal{H} - J^a \phi^a$ becomes a functional of the general form $\mathcal{A}/\kappa$ with $\kappa = 1/N$. This leads to the following form for the partition function:

$$\mathcal{Z}[\kappa] = \int \mathcal{D}\phi^a \exp\left[-\int d^d x \mathcal{A}(\phi^a(x))/\kappa \right]. \tag{9.10}$$

For simplicity we set $\mathcal{A} \equiv A(x)$ where $x \in \mathbb{R}$ and $A(x)$ is a real valued analytic function in the interval [a, b]. Accordingly $\mathcal{Z} \equiv \mathcal{I}(\kappa)$ where

$$\mathcal{I}(\kappa) = \int_a^b dx \exp\left(-A(x)/\kappa \right). \tag{9.11}$$

We now want to approximate $\mathcal{I}$ for $\kappa \to 0^+$, Using the *steepest descent method* Ref. [4].

The dominant contribution to (9.11) corresponds to the minimum of $A(x)$. Let the absolute minimum be at $x^c \in (a, b)$. Then the integral can be approximated by limiting the integration interval to a small neighborhood of x^c, $[x^c - \varepsilon, x^c + \varepsilon]$. The maximum error E is then

$$E = (b-a)\exp\left(-A''(x^c)\varepsilon^2/2\kappa\right) \tag{9.12}$$

which suggests a suitable change of variables

$$x \mapsto y \equiv (x - x^c)/\sqrt{\kappa}. \tag{9.13}$$

We can now expand A/κ around the minimum as

$$A/\kappa = A(x^c)/\kappa + \frac{1}{2}A''(x^c)y^2 + \frac{1}{6}\sqrt{\kappa}A'''(x^c)y^3 + \frac{1}{24}\kappa A^{(4)}(x^c)y^4 + O(\kappa^{3/2}). \tag{9.14}$$

At leading order in κ, $\mathcal{I}(\kappa)$ becomes

$$\mathcal{I}(\kappa) \approx \sqrt{\kappa}\exp\left(-A(x^c)/\kappa\right)\int_{-\varepsilon/\sqrt{\kappa}}^{\varepsilon/\sqrt{\kappa}} dy \exp\left(-A''(x^c)y^2/2\right). \tag{9.15}$$

Since κ is small, we can extend the interval of integration to the whole real axis. The fact that $A''(x^c) > 0$ ensures that the contribution of the integrand at infinity is negligible. Thus (9.15) reduces simply to

$$\mathcal{I}(\kappa) \approx \sqrt{2\pi\kappa/A''(x^c)}\exp\left(-A(x^c)/\kappa\right). \tag{9.16}$$

An extension to higher orders is obtained by expanding the exponential of the higher order terms in a Taylor series. This will result in a sum of terms of increasing order in $\sqrt{\kappa}$. Odd powers of $\sqrt{\kappa}$ vanish under integration, thus leading to a sum over powers of κ with coefficients corresponding to expectation values of a Gaussian distribution:

$$\mathcal{I}(\kappa) \approx \sqrt{2\pi\kappa/A''(x^c)}\exp\left(-A(x^c)/\kappa\right)J(\kappa), \tag{9.17}$$

where

$$J(\kappa) = 1 + \sum_{l=1}^{\infty} J_l\kappa^l. \tag{9.18}$$

This series is asymptotic, that is there is no disk around $\kappa = 0$ in the complex plane where it converges, because it diverges for $\kappa < 0$. However for small enough κ, the partial L-sums approximate $J(\kappa)$ within an error proportional to $L!\kappa^L$.

In conclusion, the steepest descent method is the appropriate technique to expand the partition function $\mathcal{Z}[\kappa]$ (κ =1/N) in 1/N. The procedure presented in this section will be extended to functional integrals in Sec. 9.4 and Sec. 9.5.

9.4 Spontaneous Symmetry Breaking

The aim of this section is to establish whether spontaneous symmetry breaking occurs in the Ginzburg-Landau-Wilson model for dimension d=1,2,3,4 at leading order in 1/N. For this, we will calculate the ensemble average of the spin field $\langle\phi^a\rangle_{\vec{J}}$ in the thermodynamic limit as the external magnetic field $\vec{J}\to 0$ and to verify whether a non-vanishing solution exists.

In our particular case when symmetry breaking occurs the state of thermodynamic equilibrium (or ground state) is no more invariant under a reflection in spin space about the space perpendicular to the direction of magnetization. Therefore, only the O(N-1) subgroup of the O(N) invariance group of the Hamiltonian is preserved by the ground state. At first one might argue that such an asymmetric state is not stable, because a priori the direction of magnetization is totally arbitrary. However stability is supported by the following consideration: once a specific direction is chosen, the probability that the magnetization reorients itself corresponds to the probability that all spins at all lattice sites reorient simultaneously. This would require a time of the order of a Poincaré cycle [5].

Instead of computing $\langle\phi^a\rangle_{\vec{J}}$ directly from the partition function and taking the limit $\vec{J}\to 0$ it is much more convenient to introduce the effective action Γ which is essentially the negative Helmholtz free energy. We can exploit its property of being maximal at equilibrium for any mechanically isolated system at constant temperature. Before introducing Γ, it is convenient to rename $\langle\phi^a\rangle_{\vec{J}}\equiv\phi^a_c$ where the subscript c stands for classical field, and $\langle\phi^a\rangle_{\vec{J}\to 0}\equiv\langle\phi^a\rangle$.

9.4.1 The effective action

The effective action $\Gamma[\phi^a_c]$ is the negative Legendre transform of $\mathcal{W}[J^a]$:

$$\Gamma[\phi^a_c]\equiv\mathcal{W}[J^a]-\int d^dx J^a(x)\phi^a_c(x) \tag{9.19}$$

which follows directly from (9.6). From the properties of $\mathcal{Z}$ and $\mathcal{W}$ mentioned in Sec. 9.2, Γ turns out to be the generating functional of the one-particle irreducible (1PI) n-point correlation functions $\Gamma^{(n)}$[2]. Correspondingly, the 1PI Feynman diagrams are those connected diagrams which remain connected after any of the lines joining two points is deleted.

From (9.19) it immediately follows

$$\frac{\delta\Gamma[\phi^a_c]}{\delta\phi^b_c(x)}=-J^b(x). \tag{9.20}$$

Therefore the ensemble average of the spin field $\langle\phi^a\rangle$ extremalizes Γ, that is

$$\left.\frac{\delta\Gamma[\phi_c^a]}{\delta\phi_c^b(x)}\right|_{\langle\phi^b\rangle} = 0. \tag{9.21}$$

Since Γ is essentially the negative Helmholtz free energy, we can assert that, if the extremum is an absolute maximum, $\langle\phi^a\rangle$ corresponds to a state of thermodynamic equilibrium and that otherwise it is not an absolute extremum. Indeed, if this were the case thermodynamic equilibrium would not exist and the energy would be unbounded from below. Thus our task is to determine the nature of the extremum.

In order to simplify this analysis we demand that the classical field is a constant function of the space coordinates. Therefore we require the spins to be distributed uniformly throughout space. In this case the effective action reduces to a real valued function of N real variables. It is customary to introduce the effective potential $V(\phi_c^a)$ which is defined through the relation

$$\Gamma(\phi_c) = -\Omega V(\phi_c), \tag{9.22}$$

where Ω is the volume of space (lattice) and goes to infinity as the thermodynamic limit is reached. The analysis of the extremum then reduces to that of the Hessian of V. In order to understand what the Hessian of V corresponds to, we consider the Taylor expansion of Γ as a functional of one scalar field ϕ_c, around $\langle\phi\rangle$. We define the shifted field $\varphi = \phi_c - \langle\phi\rangle$ and write

$$\Gamma[\varphi] \equiv \sum_{n=0}^{\infty}\frac{1}{n!}\int d^dx_1...d^dx_n\Gamma^{(n)}(x_1,...,x_n)\varphi(x_1)...\varphi(x_n). \tag{9.23}$$

In Fourier representation, (9.23) becomes

$$\Gamma[\varphi] = \sum_{n=0}^{\infty}\frac{1}{n!}\int d^dp_1...d^dp_n\delta^d(p_1+...+p_n)\Gamma^{(n)}(p_1,...,p_n)\tilde{\varphi}(p_1)...\tilde{\varphi}(p_n). \tag{9.24}$$

Note that we have used the same notation for the n-point correlation functions and their respective Fourier transforms. This convention will be adopted throughout the text and will not lead to any confusion.

For a constant field ϕ_c we can then write $V(\varphi)$ in the form

$$V(\varphi) = -\sum_{n=0}^{\infty}\frac{1}{n!}\varphi^n\Gamma^{(n)}(p_i=0) \tag{9.25}$$

and derive

$$\left.\frac{\delta^2 V}{\delta\phi_c^2}\right|_{\langle\phi\rangle} = -\Gamma^{(2)}(0) = \left(G^{(2)}(0)\right)^{-1}. \tag{9.26}$$

For the case of N scalar fields Eq. (9.26) becomes

$$\left.\frac{\delta^2 V}{\delta\phi_c^a \delta\phi_c^b}\right|_{\langle\phi^a\rangle} = -\Gamma_{ab}^{(2)}(0) = \left(G_{ab}^{(2)}(0)\right)^{-1} \equiv M_{ab}^2, \tag{9.27}$$

where M_{ab}^2 is the physical square mass tensor that corresponds to the inverse susceptibility tensor $(\chi_{ab})^{-1}$ in statistical mechanics.

If M_{ab}^2 is positive semi-definite, the extremum of V is a plausible ground state (state of thermodynamic equilibrium). Otherwise tachyons appear, that is particles with imaginary mass, hence they are faster than the speed of light (as their name suggests). The appearance of these particles is symptomatic for an instability.

Therefore the first and crucial step in the investigation of the existence of symmetry breaking in our model is to compute the effective potential at leading order in 1/N. We follow Ref. [6].

We choose the external magnetic field $\vec{J}$ such that $J^a = 0$ for all $1 < a \leqslant N$ and $J^1 = J$. The partition function (9.2) then takes the form

$$\mathcal{Z}[J] = \mathcal{N} \int \mathcal{D}\phi^a \exp\left(-\int d^d x \frac{1}{2}\phi^a(-\nabla^2 + \mu_0^2)\phi^a + \frac{\lambda_0}{8N}(\phi^a\phi^a)^2 - J\phi^1 \right). \tag{9.28}$$

The calculation can be simplified by using the Hubbard-Stratanovich transformation:

$$\exp\left(-\frac{\lambda_0}{8N}\int d^d x (\phi^a\phi^a)^2 \right) \propto \int \mathcal{D}\Psi \exp\left(\int d^d x \left[N\frac{\Psi^2}{2} - \frac{\Psi}{2}(\phi^a\phi^a)\sqrt{\lambda_0} \right] \right). \tag{9.29}$$

We now apply the steepest descent method. For this, we bring the partition function to the form of (9.11). This is readily achieved by rewriting the partition function as

$$\mathcal{Z}[J] = \mathcal{N} \int \mathcal{D}\Psi\mathcal{D}\phi^a \exp\left(-N\int d^d x \left[\frac{1}{2N}\phi^a(-\nabla^2 + \mu_0^2 - \sqrt{\lambda_0}\Psi)\phi^a - \frac{\Psi^2}{2} \right] \right). \tag{9.30}$$

Integration over the ϕ^a fields with $1 < a \leqslant N$ reduces $\mathcal{Z}$ to the form

$$\begin{aligned}\mathcal{Z}[J] = \mathcal{N} \int \mathcal{D}\phi^1\mathcal{D}\Psi \det(-\nabla^2 + \mu_0^2 - \sqrt{\lambda_0}\Psi)^{(N-1)/2} \times \\ \exp\left(-\int d^d x \left[\frac{1}{2}\phi^1(-\nabla^2 + \mu_0^2)\phi^1 + \frac{N}{2}\Psi^2 + J\phi^1 \right] \right).\end{aligned} \tag{9.31}$$

We now set $(\phi^1)^2 = \phi^a\phi^a$. From the matrix identity

$$\ln\det(A) = \operatorname{Tr}\ln(A), \tag{9.32}$$

the effective potential for $\vec{J} = 0$ at leading order in 1/N is given by

$$V(\phi^a, \chi) = \frac{1}{2}\mu_0^2\phi^2 + \frac{N}{2}\Psi^2 + \frac{1}{2}N\int \frac{d^dk}{(2\pi)^d}\ln(k^2 + \mu_0^2 - \sqrt{\lambda_0}\Psi), \tag{9.33}$$

where for convenience we have renamed $\phi_c^a \equiv \phi^a$, $\phi_c^a\phi_c^a \equiv \phi^2$.
Defining $\chi \equiv \mu_0^2 - \sqrt{\lambda_0}\Psi$, we obtain the expression given in [7]:

$$V(\phi^a, \chi) = -\frac{N}{2\lambda_0}\chi^2 + \frac{1}{2}\chi\phi^2 + \frac{N\mu_0^2}{\lambda_0}\chi + \frac{1}{2}N\int \frac{d^dk}{(2\pi)^d}\left[\ln(k^2 + \chi)\right]. \tag{9.34}$$

The stationary point of V is determined by the following two equations

$$\frac{\partial V}{\partial \chi} = 0 \tag{9.35}$$

and

$$\frac{\partial V}{\partial \phi^a} = 0. \tag{9.36}$$

Eq. (9.35) can be expressed as

$$\phi^2 = \frac{2N}{\lambda_0}\chi - \frac{2N\mu_0^2}{\lambda_0} - N\int \frac{d^dk}{(2\pi)^2}\frac{1}{k^2 + \chi}. \tag{9.37}$$

This shows that $V = V(\phi^2, \chi(\phi^2))$, and thus

$$\frac{dV}{d\phi^2} = \frac{\partial V}{\partial \phi^2} + \frac{\partial V}{\partial \chi}\frac{\partial \chi}{\partial \phi^2} = \frac{1}{2}\chi. \tag{9.38}$$

Eq. (9.36) can now be written as

$$\frac{dV}{d\phi^2}\phi^a = \chi\phi^a = 0 \tag{9.39}$$

showing that the extremum of V can be either symmetric ($\phi^a = 0$ for all a), or asymmetric ($\chi = 0$). The important consequence of this result is that in our model symmetry breaking occurs only if there is a positive solution of ϕ^2 with $\chi = 0$.

We now proceed to analyze Eq. (9.37) for each space dimension d separately. Note that the integral in $V(\phi^a, \chi)$ is divergent and the renormalization procedure depends on the dimension of space. For the cases $d = 1, 2, 3$ we follow Ref. [7] and Ref. [8] for $d = 4$.

9.4.2 DIMENSION D = 1

For dimension $d = 1$ the theory is already finite so that we do not need to renormalize either the mass or the coupling constant, hence $\mu^2 = \mu_0^2$ and $\lambda = \lambda_0$. From (9.37), the squared magnetization density ϕ^2 is simply given by

$$\phi^2 = \frac{2N}{\lambda}\chi - \frac{2N\mu^2}{\lambda} - \frac{N}{2\sqrt{\chi}} \ . \tag{9.40}$$

Clearly there is no positive value of ϕ^2 for $\chi = 0$. Whatever the value of μ^2, at $\chi = 0$ $\phi^2 = -\infty$, hence, the theory to leading order in $1/N$ does not exhibit symmetry breaking. We note that, as χ increases ϕ^2 increases and therefore also the derivative of V increases with ϕ^2. V is therefore a monotonically increasing and convex function of ϕ^2 which ensures that its minimum is at the origin as expected.

9.4.3 DIMENSION D = 2

For dimension $d = 2$ the integral in Eq. (9.37) diverges logarithmically. In order to remove this divergence we must add a logarithmically divergent counterterm. For example, we leave $\lambda \equiv \lambda_0$ and define the renormalized quantity μ^2/λ as

$$\frac{\mu^2}{\lambda} \equiv \frac{\mu_0^2}{\lambda_0} + \frac{1}{2}\int \frac{d^2k}{(2\pi)^2}\frac{1}{k^2 + M^2}, \tag{9.41}$$

where M^2 is a regularization parameter with dimensions of mass squared. The introduction of this mass term is completely analogous to setting an upper bound Λ to the momentum (see Sec. 9.2). No further renormalization is needed. From Eq. (9.37) we derive

$$\phi^2 = \frac{2N}{\lambda}\chi - \frac{2N\mu^2}{\lambda} + \frac{N}{4\pi}\ln(\chi/M^2). \tag{9.42}$$

We recognize that Eq. (9.42) has the same features as Eq. (9.40). In particular, for any positive value of M^2 there is no $\phi^2 > 0$ for $\chi = 0$, so that we can conclude that in two dimensions there is no spontaneous symmetry breaking at leading order in 1/N. These results for $d = 1$ and 2 are consistent with the Mermin-Wagner theorem.

9.4.4 DIMENSION D = 3

In three dimensions the theory contains an ultraviolet divergence which is fully absorbed in the renormalized parameter μ^2/λ defined as

$$\frac{\mu^2}{\lambda} \equiv \frac{\mu_0^2}{\lambda_0} + \frac{1}{2}\int \frac{d^3k}{(2\pi)^3}\frac{1}{k^2}, \tag{9.43}$$

leaving $\lambda \equiv \lambda_0$. From Eq. (9.37) we set

$$\phi^2 = \frac{2N}{\lambda}\chi - \frac{2N\mu^2}{\lambda} + \frac{N}{4\pi}\sqrt{\chi}. \tag{9.44}$$

This case is no longer trivial as for the lower dimensions. We remark that $\lambda = \lambda_0 > 0$ to ensure the existence of a ground state (see Sec. 9.2). Two cases must be considered:

i) $\mu^2 \geqslant 0$ which implies that there is no $\phi^2 > 0$ for $\chi = 0$ and that the minimum is at the origin ($\phi^2 = 0$).

ii) $\mu^2 < 0$ which admits the existence of an asymmetric minimum located at

$$\langle\phi\rangle^2 = -\frac{2N\mu^2}{\lambda}. \tag{9.45}$$

To the right of the minimum the effective potential is monotonically increasing and convex since its derivative is monotonically increasing. To the left of the minimum we enter an unphysical region, because from Eq. (9.44), $Im(\chi) \neq 0$. This implies that the derivative of V w.r.t. ϕ^2 is complex and therefore also V.

In conclusion, at leading order in 1/N symmetry breaking does occur in three dimensions.

9.4.5 DIMENSION D = 4

The investigation of symmetry breaking in four dimensions is more subtle. Indeed a puzzle emerged from the conclusions drawn in Ref. [7]. On the one hand, by applying the method adopted for lower dimensions, the authors predicted the existence of an asymmetric minimum and argued that symmetry breaking exists for $d = 4$ at leading order in 1/N. On the other hand, when analyzing the poles of the 1PI 2-point correlation functions around that minimum (see Sec. 9.4.1), tachyons appeared. It was then speculated that there was a sickness in the theory at leading order in 1/N. However there was a subtlety in the analysis of [7] which was pointed out and resolved in Ref. [8] without having to invoke a different method. Here we follow the treatment in Ref. [8].

As for the lower dimensions, the first step consists of eliminating the divergences in the saddle point equation (9.37) by introducing the following renormalized mass and coupling constant

$$\frac{\mu^2}{\lambda} \equiv \frac{\mu_0^2}{\lambda_0} + \frac{1}{2}\int \frac{d^4k}{(2\pi)^4}\frac{1}{k^2} \tag{9.46}$$

and

$$\frac{1}{\lambda} \equiv \frac{1}{\lambda_0} + \frac{1}{2}\int \frac{d^4k}{(2\pi)^4}\frac{1}{k^2(k^2+M^2)}\ . \tag{9.47}$$

Next we rewrite the saddle point equation in terms of the renormalized parameters

$$\chi = \mu^2 + \frac{\lambda}{2}\left(\frac{\phi^2}{N}\right) + \frac{\lambda}{32\pi^2}\chi \ln(\chi/M^2). \tag{9.48}$$

At this point it is worthwhile rewriting (9.48) in terms of renormalization invariant quantities. In this way we eliminate the complication of dealing with arbitrary M. One such renormalization invariant quantity is certainly μ^2/λ (see Eq. (9.46)). Another is

$$\chi_0 \equiv M^2 \exp(32\pi^2/\lambda), \tag{9.49}$$

which is obtained from the condition that $\frac{1}{\lambda_0}(M) = \frac{1}{\lambda_0}(M')$ for all M and M'. In order to further simplify our analysis we introduce the quantity ρ through the relation

$$\chi \equiv \chi_0\rho. \tag{9.50}$$

The saddle-point equation now takes the renormalization invariant form

$$\rho\ln\rho = -\frac{32\pi^2}{\chi_0}\left(\frac{\mu^2}{\lambda}\right) - \frac{16\pi^2}{\chi_0}\left(\frac{\phi^2}{N}\right), \tag{9.51}$$

from which one realizes that $\exists\ \phi_b^2$ such that for any value $\phi^2 > \phi_b^2$ and for any value of μ^2/λ, $Im(\rho\ln\rho)$ and therefore $Im(\rho)$ is different from zero. This is due to the fact that $\rho\ln\rho$ has a finite minimum value for real positive ρ, which also defines ϕ_b^2 through the relation

$$\rho\ln\rho(\phi_b^2) = \min_{\rho\geqslant 0}\rho\ln\rho. \tag{9.52}$$

Since ρ is proportional to the derivative of V w.r.t. ϕ^2 (see Eqs. (9.38), (9.50)), for $\phi^2 > \phi_b^2$ $V(\phi^2)$ is complex and therefore unphysical.
For $0 \leqslant \phi^2 < \phi_b^2$, $V(\phi^2)$ is a real double valued function. This results directly from the fact that ρ is a double valued function of $\rho\ln\rho$. Futher analysis shows that for any value of μ^2/λ, one of the two branches (*branch I*) of V is symmetric i.e. its minimum is at $\phi^2 = 0$, while the other (*branch II*) is asymmetric for $\mu^2/\lambda < 0$ (see Fig. 9.1).

This result is very important, because depending on whether *branch II* is more energetically favorable than *branch I*, symmetry breaking may or may not occur. Indeed the authors of Ref. [7] had only realized the existence of *branch II* which led them to the conclusion that symmetry breaking occurs in four dimensions.

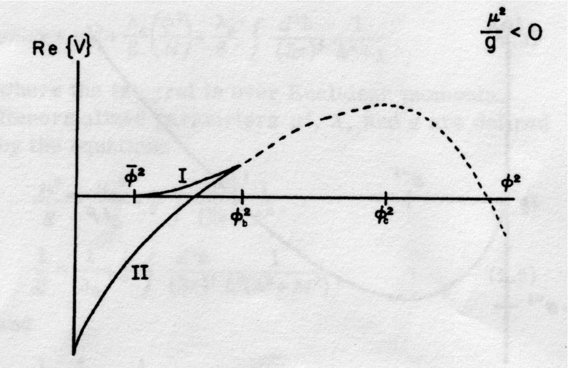

Figure 9.1: $ReV(\phi^2)$ vs. ϕ^2 for $\mu^2/\lambda < 0$. The solid line indicates the domain for which the effective potential is real, while the dashed line indicates that $ImV(\phi^2) \neq 0$ (from Ref. [8]). Note that $g \equiv \lambda$

However a simple calculation shows that *branch I* is always lower than *branch II*, whatever the value of μ^2/λ and there are no tachyons (see Ref. [8]). This means that there is (surprisingly) no spontaneous symmetry breaking at leading order in 1/N in four dimensions.

9.5 1/N EXPANSION

In this section we will outline the most important steps and give sample calculations for the construction of the 1/N expansion in a three-dimensional space, referring almost exclusively to Ref. [9] and using the steepest descent method outlined in Sec. 9.3.2. We will obtain three important formulas at next-to-leading order in 1/N: i) the so-called constraint equation relating the inverse susceptibility (renormalized square mass, see Sec. 9.4.1) to the reduced temperature; ii) the expression of the 2-point 1PI correlation function $\Gamma^{(2)}$ and iii) that of the 4-point 1PI correlation function $\Gamma^{(4)}$. These three formulas will be crucial for the construction of a Renormalization Group (RG) scheme in the subsequent section.

We start by reconsidering the Hamiltonian introduced in (9.1). From now on we will refer to the bare squared mass μ_0^2 as the mean-field reduced temperature t_0 as motivated in Landau theory. We now bring the partition function (9.2) to the form (9.11) which corresponds to the first step in the steepest descent method. This is achieved through a transformation similar to the one adopted for the calculation of the effective potential at leading order in 1/N (see (9.30)). Here we integrate over the N ϕ^a fields and obtain an expression of the partition function in terms of only one field, i.e. the auxiliary field Ψ:

$$\mathcal{Z}[\Psi] = \mathcal{N} \int \mathcal{D}\Psi \exp\left[-NH_{eff} + \frac{1}{2}\int d^3r d^3r' J^a(\vec{r})\Delta(\vec{r},\vec{r'};\Psi)J^a(\vec{r'})\right], \quad (9.53)$$

where the effective Hamiltonian H_{eff} is defined by

$$H_{eff} = \int d^3r \frac{1}{\lambda_0}\Psi^2(\vec{r}) - Tr\ln\Delta(\vec{r},\vec{r'};\Psi), \quad (9.54)$$

and the ϕ-propagator $\Delta(\vec{r},\vec{r'};\Psi)$ is defined through the relation

$$[-\nabla^2 + t_0 + i\Psi(\vec{r})]\Delta(\vec{r},\vec{r'};\Psi) = \delta(\vec{r}-\vec{r'}). \quad (9.55)$$

Next we need to calculate correlation functions in the absence of an external magnetic field. The connected 2-point correlation functions $G_{ab}(x,x')$ are given by

$$G_{ab}(\vec{r},\vec{r'}) = \delta_{ab}G^{(2)}(\vec{r}-\vec{r'}), \quad (9.56)$$

where

$$G^{(2)}(\vec{r}-\vec{r'}) = \langle\Delta(\vec{r},\vec{r'},\Psi)\rangle, \quad (9.57)$$

and the 4-point connected function is written as

$$G^{(4)}(\vec{r}_1,\vec{r}_2;\vec{r}_3,\vec{r}_4) = \langle\Delta(\vec{r}_1,\vec{r}_2,\Psi)\Delta(\vec{r}_3,\vec{r}_4,\Psi)\rangle. \quad (9.58)$$

In order to calculate ensemble averages we need to follow the next step in the steepest descent method, that is we expand H_{eff} in $N^{-1/2}$. For the particular case of the connected correlation functions (9.57) and (9.58), we will also need to find an approximate expression for the ϕ-propagator.

For the approximation of the effective Hamiltonian, we will only outline the most critical steps. We expand H_{eff} around $\langle\Psi\rangle$ which turns out to be a much more efficient procedure than the most common expansion around the saddle point. It is useful to introduce the inverse susceptibility $\tilde{t}_0$ defined through the relation

$$\tilde{t}_0 \equiv \Gamma^{(2)}(0) = G^{(2)}(0). \quad (9.59)$$

Now we can implement the change of variables (see 9.13)

$$\Psi \longmapsto \psi \equiv N^{1/2}(\Psi - \langle\Psi\rangle), \quad (9.60)$$

where $\langle\Psi\rangle$ is given by

$$\langle\Psi\rangle = -i\left(\tilde{t}_0 - t_0 - \frac{1}{N}\delta\right), \quad (9.61)$$

where δ is of order zero in 1/N and is defined through the condition $\langle\psi\rangle = 0$. Eq. (9.61) is obtained by first showing that

$$\Delta(\vec{r},\vec{r'},\langle\Psi\rangle) \approx \langle\Delta(\vec{r},\vec{r'},\Psi)\rangle \equiv \Delta(\vec{r}-\vec{r'}) = \int \frac{d^3p}{(2\pi)^3}\frac{e^{i\vec{p}\vec{r}}}{(p^2+\tilde{t}_0)}. \tag{9.62}$$

In carrying out the expansion of H_{eff} one realizes that an analogous one must be developed for $\Delta(\vec{r},\vec{r'},\Psi)$ about $\langle\Psi\rangle$.
We consider Eq. (9.55) and rewrite it using the change variables ($\Psi \longmapsto \psi$):

$$[-\nabla^2 + t_0 - N^{-1/2}(N{-}1/2\delta - i\psi(\vec{r}))]\Delta(\vec{r},\vec{r'};\Psi) = \delta(\vec{r}-\vec{r'}). \tag{9.63}$$

It is useful to express Eq. (9.63) in terms of matrix operators and define

$$-\nabla^2 + t_0 \mapsto A; \quad N^{-1/2}(N{-}1/2\delta - i\psi(\vec{r})) \mapsto \Xi \quad \textit{and} \quad \Delta \mapsto B. \tag{9.64}$$

Eq. (9.63) takes the form

$$[A-\Xi]B = 1. \tag{9.65}$$

We note that Ξ is of the form $\Xi_{ij} = \xi_i\delta_{ij}$. For sufficiently small ξ_i, B reduces to

$$\begin{aligned} B_{il} &= \left((A-\Xi)^{-1}\right)_{il} = \left((1-A^{-1}\Xi)A^{-1}\right)_{il} && (9.66)\\ &= \left(\sum_{k=0}^{\infty}\left(A^{-1}\Xi\right)^k A^{-1}\right)_{il} && (9.67)\\ &= \sum_{k=0}^{\infty}\sum_{j_1,..,j_k} A^{-1}_{ij_1}\xi_{j_1}...\xi_{j_k}A^{-1}_{j_k l}. && (9.68)\end{aligned}$$

For our case the sums over the indices are simply replaced by integrals over the reals. At this point calculating the correlation functions (9.57) and (9.58) is a simple exercise and amounts to retaining the correct orders in 1/N.
By retaining only the 1PI parts of the connected correlation functions, one obtains (see [9]) the expressions for the n-point 1PI correlation functions $\Gamma^{(n)}$. The results at next-to-leading order are

$$\Gamma^{(2)}(\mathbf{p}) = p^2 + \tilde{t}_0 + N^{-1}[\Sigma(\mathbf{p};\tilde{t}_0,\lambda_0) - \Sigma(\mathbf{0};\tilde{t}_0,\lambda_0)] \tag{9.69}$$

and

$$\Gamma^{(4)}(\mathbf{0}) = N^{-1}D(\mathbf{0}) + O(N^{-2}), \tag{9.70}$$

where

$$\Sigma(\mathbf{p};\tilde{t}_0,\lambda_0) = \frac{1}{2}\int\frac{d^3k}{(2\pi)^3}\Delta(\mathbf{k}+\mathbf{p})D(\mathbf{k}) \tag{9.71}$$

and

$$A(\tilde{t}_0, \lambda_0) = \int \frac{d^3k}{(2\pi)^3} \frac{d^3k'}{(2\pi)^3} \Delta(\mathbf{k})^2 \Delta(\mathbf{k'}) D(\mathbf{k} + \mathbf{k'}). \tag{9.72}$$

D is the propagator of the ψ field in Fourier space and its value at $\vec{k} = 0$ is $D(0) = (\lambda_0 + a\tilde{t}_0^{-1/2})$ where $a = 1/(16\pi)$.
Furthermore from the condition $\langle\psi\rangle = 0$ (see Eq. (9.60)), we obtain the so-called constraint equation

$$t_0 = \tilde{t}_0 - \frac{\lambda_0}{2} \int \frac{d^3k}{(2\pi)^3} \Delta(\mathbf{k}) + N^{-1} \left[\frac{\lambda_0}{8} A(\tilde{t}_0, \lambda_0) - \lambda_0 \Sigma(\mathbf{0}; \tilde{t}_0, \lambda_0) D(0)^{-1} \right] + O(N^{-2}) \tag{9.73}$$

which yields a relation between the inverse susceptibility $\tilde{t}_0$ and the mean field reduced temperature t_0.

9.6 RENORMALIZATION AND CRITICAL EXPONENTS

In this section we will outline a renormalization group procedure (see [9]) for the calculation of critical exponents at leading order in 1/N.
At leading order the constraint Eq. (9.73) reads

$$t_0 = \tilde{t}_0 - \frac{\lambda_0}{2} \int \frac{d^3k}{(2\pi)^3} \Delta(\mathbf{k}). \tag{9.74}$$

This expression contains a divergent integral. By using exactly the same procedure as the one adopted in the investigation of symmetry breaking in three dimensions (see Sec. 9.4.4), this divergence can be absorbed by subtracting from the mean-field reduced temperature t_0 its fluctuation correction t_{0_c}. This yields

$$t_0 - t_{0_c} = \tilde{t}_0 + 2a\lambda_0 \tilde{t}_0^{1/2}, \tag{9.75}$$

where

$$t_{0_c} = -\frac{\lambda_0}{2} \int \frac{d^3k}{(2\pi)^3} \frac{1}{k^2}. \tag{9.76}$$

From the equation above it clearly follows that t_{0_c} plays the role of the critical temperature, since as the critical point is approached, i.e. as $\tilde{t}_0 \to 0$, $t_0 \to t_{0_c}$.
From Eq. (9.75) one could immediately extract critical exponents, however in general this is not recommended and we observe that an exact power law behavior exists only in the limit $\lambda_0 \to \infty$. This suggests to introduce a renormalization scheme which ensures that the exact power law behavior occurs at finite normalized λ.
The renormalization scheme used here is very general and can be extended to

higher orders in the 1/N expansion. We start by introducing renormalized variables as follows

$$\begin{aligned}\lambda_0 &= mZ_\lambda(\lambda)\lambda, && (9.77)\\ t_0 - t_{0_c} &= m^2 Z_t(\lambda)t, && (9.78)\\ \tilde{t}_0 &= m^2\tilde{t}, && (9.79)\end{aligned}$$

where m is a scale parameter with dimensions of mass multiplying the dimensionless renormalized quantities. We call the Z functions renormalization functions. In order to determine them, we need to impose the usual renormalization conditions

$$\begin{aligned}\Gamma^{(2)}(p^2 = 0, t = 1) &= m^2 && (9.80)\\ \lim_{N\to\infty} N\Gamma^{(4)}(\mathbf{p}_i = 0, t = 1) &= m\lambda, && (9.81)\end{aligned}$$

which give

$$\begin{aligned}Z_\lambda(\lambda) &= (1 - a\lambda)^{-1} = \frac{z+a}{z}, && (9.82)\\ Z_t(\lambda) &= \frac{1+a\lambda}{1-a\lambda} = \frac{z+2a}{z}. && (9.83)\end{aligned}$$

A scaling field $z \equiv \lambda^{-1} - a$ was introduced in order to simplify the calculations in what follows.

Now that the renormalization functions are known we are ready to write down the appropriate RG equation. In particular let us consider the equation relating the unrenormalized reduced temperature to the renormalized one:

$$t_0 - t_{0_c} = m^2\left(1 + \frac{2a}{z}\right)t. \qquad (9.84)$$

the l.h.s. of this equation is renormalization invariant, namely it does not depend on the choice of m. Therefore the so called RG equation reads

$$\left[z\frac{\partial}{\partial z} - 2\tilde{t}\frac{\partial}{\partial \tilde{t}} + 2 - \frac{2a}{z+2a}\right] t(z,\tilde{t}) = 0 \qquad (9.85)$$

which is obtained by setting to zero the derivative with respect to m of the r.h.s. of equation 9.84. By solving the RG equation we obtain the scaling relations. This is done with the method of characteristics (see [10]). The characteristic equations of 9.85 are

$$\begin{aligned}z(l) &= zl; && (9.86)\\ \tilde{t}(l) &= \tilde{t}l^{-2}; && (9.87)\\ t(z(l),\tilde{t}(l)) &= l\left(\frac{zl+2a}{z+2a}\right). && (9.88)\end{aligned}$$

We can choose any parametrization we want for the renormalized parameters. Thus we might as well take l to satisfy $\tilde{t}(l) = 1$ from which the scaling relations follow

$$\begin{aligned} \tilde{t}(l) \sim \tilde{t}l^{-2-\eta} &= \tilde{t}l^{-2}; && (9.89) \\ t(l) \sim tl^{1/\nu} &= tl. && (9.90) \end{aligned}$$

Finally the critical exponents at leading order in 1/N are

$$\eta = 0; \qquad \nu = 1; \qquad \gamma = (2-\eta)\nu = 2. \tag{9.91}$$

For higher orders in 1/N the RG procedure stays the same apart from the fact that the two point correlation function needs to be renormalized and therefore $\tilde{t}_0$. The complication lies in computing the renormalization functions. However this is only a technical matter and no additional concepts must be introduced.
At next-to-leading order in 1/N, the critical exponents are

$$\begin{aligned} \eta &= 8(3\pi^2 N)^{-1} + O(N^{-2}), && (9.92) \\ \nu &= 1 - 32(3\pi^2 N)^{-1} + O(N^{-2}), && (9.93) \\ \gamma &= 2(1 - 12(\pi^2 N)^{-1}) + O(N^{-2}). && (9.94) \end{aligned}$$

It is hard to say whether the critical exponents at next-to-leading order are at all meaningful for physical N. Indeed it appears that as the order in 1/N increases, the values of the critical exponents suffer abrupt changes.

9.7 Concluding remarks

In this chapter we have introduced the Ginzburg-Landau-Wilson O(N) model, for which we have investigated the existence of spontaneous symmetry breaking for space dimensions 1 through 4, developed the 1/N expansion and presented a general RG procedure for the calculation of critical exponents. This has required in particular an outline of the so called steepest descent method and its advantage in the present context. Moreover we reviewed fundamental methods used for the investigation of symmetry breaking. We found that at leading order in 1/N spontaneous symmetry breaking exists only in three dimensions.
The O(N) model and 1/N expansion constitute one of the most frequently used theoretical approaches in the preliminary investigation of critical behavior in condensed matter systems. Two important examples are the ferromagnetic transition and superconductivity.

BIBLIOGRAPHY

[1] S. K. Ma, *The 1/n Expansion*, in *Phase transitions and critical phenomena*, edited by C. Domb and M. S. Green (Academic Press, London, 1976), vol. 6.

[2] L. H. Ryder, *Quantum Field Theory* (Cambridge University Press, Cambridge, 2005).

[3] D. J. Wallace, *The ε-Expansion for Exponents and the Equation of State in Isotropic Systems*, in *Phase transitions and critical phenomena*, edited by C. Domb and M. S. Green (Academic Press, London, 1976), vol. 6.

[4] J. Zinn-Justin, *Path Integrals in Quantum Mechanics* (Oxford University Press, Oxford, 2005).

[5] K. Huang, *Statistical Mechanics* (John Wiley & Sons, New York, 1987).

[6] J. Zinn-Justin, *Quantum Field Theory and Critical Phenomena* (Oxford University Press, Oxford, 1989).

[7] S. Coleman, R. Jackiw, and H. D. Politzer, *Spontaneous symmetry breaking in the O(N) model for large N*, Phys. Rev. D **10**, 2491 (1974).

[8] L. F. Abbott, J. S. Kang, and H. J. Schnitzer, *Bound states, tachyons, and restoration of symmetry in the 1/N expansion*, Phys. Rev. D **13**, 2212 (1976).

[9] I. D. Lawrie and D. J. Lee, *Renormalization group and 1/N expansion for the three-dimensional Ginzburg- Landau-Wilson model*, Phys. Rev. B **64**, 184505 (2001).

[10] N. Goldenfeld, *Lectures on Phase Transitions and the Renormalization Group*, Frontiers in Physics (Westview Press, 1992).

CHAPTER 10

QUANTUM PHASE TRANSITIONS AND THE BOSE-HUBBARD MODEL

ERIC MARCEL FEHR
SUPERVISOR: FABRICIO ALBUQUERQUE

In the first section the general concepts of quantum phase transitions are introduced. The study of the Bose-Hubbard model then allows to have closer look at the crucial concept of competition between different terms in the Hamiltonian. In the case of the Bose-Hubbard model these are the hopping term, which is related to superfluidity, and the on-site repulsion term, corresponding to a Mott insulating state. This is followed by a mean-field approach, from which one can easily obtain the phase diagram, which is then discussed in detail. At the end we will present the work of Greiner et.al. as they were able to realize the Bose-Hubbard model in the system of an ultra-cold bosonic gas in an optical lattice potential.

10.1 WHAT IS A QUANTUM PHASE TRANSITION?

As the temperature approaches zero a system would be in its ground state and classically, as thermal fluctuations will die out in the limit of zero temperature, no change of this is possible. But if we consider a quantum system, quantum fluctuations due to Heisenberg's uncertainty relation would always be present, even at $T = 0$. Hence it is possible that these fluctuations can drive a change in the ground state. Consider a Hamiltonian, $H(g)$, whose degrees of freedom reside on the sites of a lattice and which varies as a function of a dimensionless coupling

g. The ground state energy of $H(g)$ would, for a finite lattice, generically be a smooth, analytic function of g. The main possibility of an exception comes from the case when g couples only to a conserved quantity:

$$H(g) = H_0 + gH_1\,, \tag{10.1}$$

where H_0 and H_1 commute. Therefore H_0 and H_1 can be simultaneously diagonalized and so, even though the eigenvalues vary with g, the eigenfunctions are independent of g. This means that there can be a level-crossing where an excited level becomes the ground state at $g = g_c$, creating a point of non-analyticity of the ground state energy as a function of g.[1] So we can look at these non-analyticities in the ground state energy of the infinite lattice system as the quantum critical points.

For the two limits $g \gg g_c$ and $g \ll g_c$ it is clear that the system would be in one of the two ground states. But for g approaching g_c the two terms would start to compete each other, hence we will call them the competing terms in the Hamiltonian, and the system would undergo a phase transition.

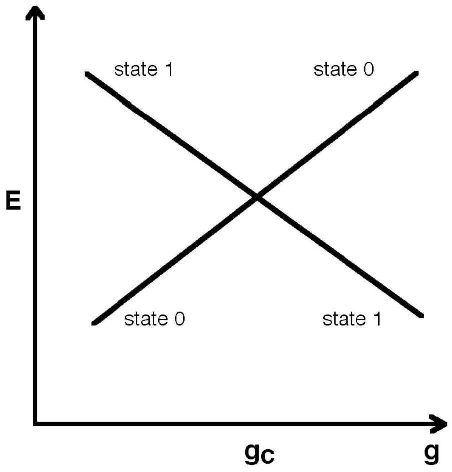

Figure 10.1: Sketch of a level-crossing where an excited state becomes the new ground state.

We will now only consider second order quantum phase transitions. Loosely speaking these are transitions at which the characteristic energy scale of fluctuations above the ground state (Δ), we will call it energy gap if it is nonzero, vanishes as g approaches g_c, meaning that we get a real level-crossing as sketched in figure 10.1. In most cases Δ vanishes as a power law

---

[1] It is possible to treat avoided level-crossings in a similar way.

$$\Delta \sim J|g - g_c|^{z\nu}\,, \tag{10.2}$$

where J is the energy scale of a characteristic microscopic coupling and $z\nu$ is a *critical exponent* (its value is *universal* and independent of microscopic details of the Hamiltonian $H(g)$). This behavior of (10.2) holds both for $g > g_c$ and for $g < g_c$ with the same value of $z\nu$ but different constants of proportionality.
Today one knows of some materials which show such quantum critical behavior, for example:

$\mathbf{LiHoF}_4$: The low-lying magnetic excitations of this insulator consist of fluctuations of the Ho ions between two spin states that are aligned parallel and anti-parallel to a particular crystalline axis. One can think of a two-state "Ising" spin sitting on each Ho ion. At $T = 0$ all these spins would be aligned parallel and hence it would be a ferromagnet. If this material is placed in a magnetic field transverse to the magnetic axis there would be quantum tunneling induced between the two states of the Ho ions. For sufficiently strong tunneling rate the long range order would be destroyed and a quantum paramagnet is formed.

$\mathbf{CeCu}_{6-x}\mathbf{Au}_x$: This heavy fermion material has a magnetically ordered ground state, with the magnetic moments on the Ce ions arranged in a spin density wave with an incommensurate period (this simply means that the expectation value of the spin operator oscillates in a wave-like manner with a period that is not a rational number times a period of the crystalline lattice). This order is present at large values of the doping x. By decreasing the value of x or by applying pressure on the crystal it is possible to destroy the magnetic order and in a second order quantum phase transition the ground state becomes a Fermi liquid.

Two-dimensional electron gas in semiconductor heterostructures : This has a very rich phase diagram with a large number of quantum phase transitions. Imagine bringing two ferromagnetic layers close to each other. For larger layer spacing the two would stay in their ferromagnetic order aligned in the same direction (that one of an applied field!). But for smaller spacings there turns out to be a anti-ferromagnetic exchange between the two layers, such that the ground state becomes a spin singlet.

Ultra-cold bosonic gas in an optical lattice potential : This would show a transition of second order from a superfluid to a Mott-insulator as one increases the depth of the optical lattice potential. We will see that this behavior is well described by the Bose-Hubbard model discussed below.

10.2 The Bose-Hubbard Model

We will now study these general concepts of quantum phase transitions discussed above in more detail in the Bose-Hubbard model. The Bose-Hubbard Hamiltonian (10.3) was first studied by Fisher et.al [1] in 1989 and reads:

$$H_B = -w \sum_{\langle i,j \rangle} \left(\hat{b}_i^\dagger \hat{b}_j + \hat{b}_j^\dagger \hat{b}_i \right) - \mu \sum_i \hat{n}_i + \frac{U}{2} \sum_i \hat{n}_i (\hat{n}_i - 1) \ . \tag{10.3}$$

Here $\hat{b}_i^\dagger$ and $\hat{b}_i$ are creation and annihilation operators for bosons at site i, $\hat{n}_i = \hat{b}_i^\dagger \hat{b}_i$ being the occupation number operator at the same site. The creation and annihilation operators act as follows on the eigenstates of the single-site occupation number operator

$$\hat{b}_i^\dagger \left| n_i \right\rangle = \sqrt{n_i + 1} \left| n_i + 1 \right\rangle \qquad \hat{b}_i \left| n_i \right\rangle = \sqrt{n_i} \left| n_i - 1 \right\rangle \tag{10.4}$$

and fulfill the commutation relations,

$$\left[\hat{b}_i, \hat{b}_j^\dagger \right] = \delta_{ij} \qquad \text{and} \qquad \left[\hat{b}_i, \hat{b}_j \right] = \left[\hat{b}_i^\dagger, \hat{b}_j^\dagger \right] = 0 \ \ \forall i, j \ . \tag{10.5}$$

We can easily verify that the Hamiltonian H_B shown in Eq. (10.3) is invariant under a global U(1) phase transformation under which $\hat{b}_i \rightarrow \hat{b}_i e^{i\phi}$. The first term is called the *hopping term* and describes the hopping of the particles from one site to its nearest-neighbor sites ($\langle i, j \rangle$ denotes that we sum up only over pairs of nearest neighbors) hence accounting for the delocalization of particles in the lattice. Therefore this term can be seen as the kinetic part of the Hamiltonian. The last term is the *on-site repulsion* denoting the repulsion between two particles at the same site. The term with the chemical potential μ allows to control the total density of particles in the system. Comparing the hopping and the on-site repulsion we can see that, while the former favors states in which the particles are delocalized throughout the lattice, the latter makes multiple occupied sites energetically expensive and favors states in which the particles are well localized. We can expect that both terms will compete in the intermediate coupling regime, when μ is small enough, and, following the arguments presented in the Introduction, we can expect a quantum phase transition. However, before going into a mean-field analysis of H_B, which will allow us to verify that this is indeed the case, it is instructive to analyze the two limits $\frac{w}{U} \rightarrow 0$ (where on-site repulsion dominates) and $\frac{w}{U} \rightarrow \infty$ (where hopping dominates).

10.2.1 Limit of zero Hopping

In the limit of $\frac{w}{U} \rightarrow 0$ the Hamiltonian reduces to (10.6)

$$H_{\text{on-site}} = -\mu \sum_i \hat{n}_i + \frac{U}{2} \sum_i \hat{n}_i(\hat{n}_i - 1) \tag{10.6}$$

This Hamiltonian is just a sum of single-site Hamiltonians and therefore the ground state is just the tensor product of well defined single-site eigenstates. We can therefore look at a single site. There we know, we must have integer filling. Considering a state with n_0 particles at this site, we get an energy contribution of this site like

$$E_{ss}^{(n)} = \frac{U}{2} n_0(n_0 - 1) - \mu n_0 \ . \tag{10.7}$$

This would be minimal for $n_0 = \frac{1}{2} + \frac{\mu}{U}$ but casted to an integer value, meaning that the value of n_0 changes only for integer values of $\frac{\mu}{U}$. As this result is independent of the lattice site, we know that we have a commensurate filling of the lattice and the total density would be pinned at an integer value for a whole range of the chemical potential. This means that the ground state is incompressible, as the compressibility is defined as $\kappa = \frac{d\rho}{d\mu}$, where ρ is the density.
As we will be interested in the particle correlations in momentum space, when, later on, analyzing the experimental results for quantum atomic gases, we now want to examine the distribution of particles in momentum space. Hence we have to derive the expectation value for the number of particles at a certain momentum p in the ground state of (10.6). We therefore introduce $\hat{b}_q^\dagger$ and $\hat{b}_q$ as the creation and annihilation operators for particles at momentum q, which are given by the Fourier transform of the corresponding real space operators as

$$\hat{b}_q^\dagger = \frac{1}{\sqrt{M}} \sum_{i=1}^{M} \hat{b}_i^\dagger \, e^{-i\mathbf{q}\mathbf{r}_i} \qquad \textit{and} \qquad \hat{b}_q = \frac{1}{\sqrt{M}} \sum_{i=1}^{M} \hat{b}_i \, e^{i\mathbf{q}\mathbf{r}_i} \ , \tag{10.8}$$

where M denotes the total number of sites. The expectation value of $\hat{n}_q = \hat{b}_q^\dagger \hat{b}_q$ then can be written as

$$\langle \hat{b}_q^\dagger \hat{b}_q \rangle_{gs} = \frac{1}{M} \langle \sum_{i,j=1}^{M} \hat{b}_i^\dagger \hat{b}_j \, e^{-i\mathbf{q}(\mathbf{r}_i - \mathbf{r}_j)} \rangle_{gs} \ . \tag{10.9}$$

The sum and also the phase factor can be taken out of the expectation brackets, such that we get the sum over the expectation values $\langle \hat{b}_i^\dagger \hat{b}_j \rangle_{gs}$ but this would be zero for $i \neq j$, as the ground state is a product of single-site wave functions. Hence it follows

$$\langle \hat{b}_q^\dagger \hat{b}_q \rangle_{gs} = \frac{1}{M} \sum_{i,j=1}^{M} n\,\delta_{ij}\,e^{-i\mathbf{q}(\mathbf{r}_i - \mathbf{r}_j)} = \frac{1}{M} \sum_{i=1}^{M} n = n\ , \tag{10.10}$$

and n has no index as we have commensurate filling of the lattice. We see that this expectation value is independent of q (featureless) and hence every momentum is covered with the same weight, which denotes the total delocalization in Fourier space and therefore the strict localization in real space. In particular, in this limit, there will not be any phase coherence and a momentum space pattern won't show any substructure such as interference fringes. Also the energy spectrum of this state has a well defined gap $\Delta = 2Un - \mu$ from the ground state to its lowest excitations. A material having this properties is termed a *Mott insulator* (**MI**).

10.2.2 LIMIT OF DOMINANT HOPPING

In this case the Hamiltonian (10.3) reduces to

$$H_{hopp} = -w \sum_{\langle i,j \rangle} \left(\hat{b}_i^\dagger \hat{b}_j + \hat{b}_j^\dagger \hat{b}_i \right)\ . \tag{10.11}$$

We will first rewrite this Hamiltonian in Fourier space. For that we need the Fourier-back-expansion

$$\hat{b}_i^\dagger = \frac{1}{\sqrt{M}} \sum_{\mathbf{q}} \hat{b}_q^\dagger\, e^{i\mathbf{q}\mathbf{r}_i} \qquad \textit{and} \qquad \hat{b}_i = \frac{1}{\sqrt{M}} \sum_{\mathbf{q}} \hat{b}_q\, e^{-i\mathbf{q}\mathbf{r}_i}\ . \tag{10.12}$$

Rewritten in Fourier space this would give us

$$H'_{hopp} = -\frac{w}{M} \sum_{\langle i,j \rangle} \sum_{\mathbf{q},\mathbf{k}} \left(\hat{b}_q^\dagger \hat{b}_k\, e^{i(\mathbf{q}\mathbf{r}_i - \mathbf{k}\mathbf{r}_j)} + \text{h.c.} \right)\ . \tag{10.13}$$

As we consider only nearest neighbors, we can write $\mathbf{r}_j = \mathbf{r}_i + \hat{\mathbf{a}}$, where $\hat{\mathbf{a}}$ is a unitary vector connecting nearest-neighbor sites. The summation over i would then give us $M \times \delta_{\mathbf{qk}}$ and the left phase factor with $\hat{\mathbf{a}}$ just can be expressed as a cosine.

$$H'_{hopp} = -w \sum_{\mathbf{q},\mathbf{k},\hat{\mathbf{a}}} \hat{b}_q^\dagger \hat{b}_k\, \delta(\mathbf{q} - \mathbf{k})\, \left(e^{-i\mathbf{k}\hat{\mathbf{a}}} + e^{i\mathbf{k}\hat{\mathbf{a}}} \right) = -2w \sum_{\mathbf{q},\hat{\mathbf{a}}} \hat{n}_q \cos(\mathbf{q}\hat{\mathbf{a}}) \tag{10.14}$$

A system of free bosonic particles will, at $T = 0$, form a perfect condesate and hence all particles would occupy the state with lowest available energy. As w is positive the ground state of this Hamiltonian would be at $q = 0$ and therefore the particles occupying the ground state would have zero momentum ($\langle \hat{b}^{\dagger}_{q}\hat{b}_{q}\rangle_{gs} = \delta_{\vec{q},\vec{0}}$, only one momentum contributes) and hence they are well localized at one particular point in momentum space. This means, the particles in this state are spread out over the whole lattice in real space and they have a constant phase equal $\forall i$ (phase coherence). Important to note: Fixing such a constant phase is clearly a sign that this state is no longer invariant under a global U(1) phase transformation. This denotes that the U(1)-symmetry of the Hamiltonian H_B, and hence of H'_{hopp}, is broken.

Using a terminology widely used in literature we will refer to this state as a *superfluid* (**SF**). However, we should have in mind that, although everybody expects all bose-condensed systems to display superfluid behavior, there is no proof and this cannot always be tested experimentally.

10.2.3 MEAN-FIELD APPROACH AND SPONTANEOUS SYMMETRY BREAKING

Following the original work of Fisher [1, 2] we introduce a mean-field approximation of the Bose-Hubbard model. Within this approach, we can decouple the original Hamiltonian and write it as a sum of single-site operators

$$H_{MF} = \sum_i \left(-\mu \hat{n}_i + \frac{U}{2}\hat{n}_i(\hat{n}_i - 1) - \Psi^*_B \hat{b}_i - \Psi_B \hat{b}^{\dagger}_i \right) \ . \tag{10.15}$$

It treats the interactions exactly, as it has the same on-site terms as H_B, and approximates the kinetic energy (hopping) by adding a 'field' Ψ_B representing the averaged influence of neighboring sites. The complex field Ψ_B is just a variational parameter and has to be self-consistently determined such that the ground state energy E_{MF} of H_{MF} is minimized.

The ground state wave function of H_{MF} for an arbitrary Ψ_B will simply be a product of single-site wave functions, because H_{MF} is just a sum of single-site Hamiltonians. Next we want to evaluate the expectation value of H_B in this wave function. By adding and subtracting H_{MF} from H_B, we can write the mean-field value E_0 of the ground state energy of H_B, eq. (10.3), in the form

$$\frac{E_0}{M} = \frac{E_{MF}(\Psi_B)}{M} - Zw\langle \hat{b}^{\dagger}\rangle\langle \hat{b}\rangle + \langle \hat{b}\rangle \Psi^*_B + \langle \hat{b}^{\dagger}\rangle \Psi_B \ , \tag{10.16}$$

where $E_{MF}(\Psi_B)$ is the ground state energy of H_{MF}, M is the number of sites of the lattice, Z is the number of nearest neighbors around each lattice point and the expectation values are evaluated in the ground state of H_{MF}. This can be done as the mean-field ground state wave function applies to each site separately and the expectation value is the same for each site. Further this treatment is valid for arbitrary dimensions[2].

Notice that the additional term with the fields Ψ_B in H_{MF} breaks the U(1) symmetry we had for the Hamiltonian H_B and does not conserve the total number of particles. Therefore the Hamiltonian is U(1)-symmetric whenever $\Psi_B = 0$, which should correspond to **MI** phases as seen in the limit of zero hopping (see section 10.2.1). On the other hand for $\Psi_B \neq 0$ this symmetry is broken and we have a superfluid (compare section 10.2.2). Therefore $|\Psi_B|$ can be seen as the order parameter of our phase transition and we will see later that $\Psi_B \propto \langle \hat{b} \rangle$.[3]

As one can see by numerical analysis of the system, the phase transition between the Mott insulator and the superfluid would be of second order, meaning that the order parameter Ψ_B rises continuously as one crosses into the ordered phase (superfluid phase). Therefore we can write down the Landau theory argument for the ground state energy as follows

$$E_0 = E_{00} + r\,|\Psi_B|^2 + s\,|\Psi_B|^4 \ , \tag{10.17}$$

assuming s to be positive in order to have a minimum. For $r > 0$ there is a unique ground state at $\Psi_B = 0$ (see fig. 10.3), which would be the case of the Mott insulating phase, and for $r < 0$, where the before unique ground state gets unstable, there are an infinite number of minima of the energy at a nonzero value of Ψ_B (see fig. 10.2) meaning that the symmetry is spontaneously broken and the system chooses a particular value of the phase (constant global phase) as it is the case in the superfluid phase. Hence the phase boundary must be at $r = 0$.

When a continuous symmetry is spontaneously broken it gives rise to long range order along a chosen direction in order parameter space (longitudinal), and the correlations along orthogonal directions (in order parameter space) transverse to the ordered one exhibit power law decay all over this ordered phase. The transverse correlation functions would just diverge at $k = 0$ (k being the momentum). As we have a complex, and hence two dimensional, scalar field Ψ_B as an order parameter there is just one transverse direction in order parameter space namely the angular direction of Ψ_B in polar coordinates (or the imaginary part), as we can always do a U(1) phase transformation such that the ordering of the system is along the real or radial part of Ψ_B.

---

[2] Nevertheless one has to be careful since the results obtained from such a treatment are poorer for lower dimensions.

[3] Another important assumption underlying (10.15) is that the ground state does not spontaneously break a translational symmetry of the lattice, as the mean-field Hamiltonian is the same on every site. However, in Quantum Monte Carlo simulations one has seen that such phases breaking translational symmetry do not exist in the model we consider.

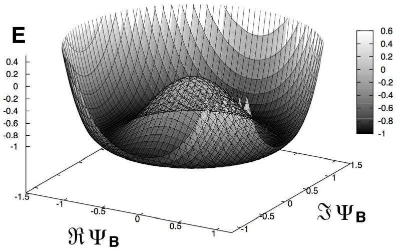

Figure 10.2: Sketch of the energy for $r < 0$. This is the broken symmetric potential with a degenerate minimum at $|\Psi_B| \neq 0$.

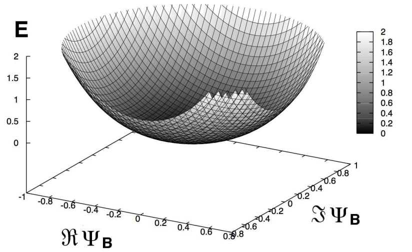

Figure 10.3: Sketch of the energy for $r > 0$. This is the symmetric potential with a unique minimum at $|\Psi_B| = 0$

Excitations in the transverse (angular) direction are gapless for vanishing momentum (meaning that they are mass-less), as they all belong to the ground state, which is degenerate.[4] The particle associated with the angular excitations is termed Goldstone-boson (Following Goldstone's theorem [3, 4]) and in the case of a superfluid it is termed phonon.

10.2.4 PHASE DIAGRAM IN THE MEAN-FIELD APPROACH

If we would numerically solve the self-consistent equation for the energy of the ground state, starting from a point in the superfluid phase, we could see that Ψ_B approaches zero continuously when one enters the Mott insulating phase. Therefore Ψ_B would be small near the phase boundary and we can do perturbation theory in Ψ_B, obtaining the mean-field ground state energy and wave function in order to be able to derive the expectation value for the ground state energy of H_B in the mean-field approach. Let's reconsider H_{MF} and treat the on-site repulsion and the chemical potential as the unperturbed part and the term containing the mean-field parameter as the perturbative part.

$$H_{MF} = \sum_i \left(\underbrace{-\mu \hat{n}_i + \frac{U}{2}\hat{n}_i(\hat{n}_i - 1)}_{H_0} - \underbrace{\Psi_B^* \hat{b}_i - \Psi_B \hat{b}_i^\dagger}_{H'} \right) \tag{10.18}$$

The ground state energy in second order perturbation theory and the ground

---

[4] Or more natively: If we look at figure 10.2 we can argue that the particle (or field) associated with the radial direction would acquire mass because of the curvature of the potential, where as the one related to the angular direction has no curvature and hence no mass.

state wave function in first order can be written in general like

$$\begin{aligned} E_n &= E_n^{(0)} + \langle n|H'|n\rangle + \sum_{k\neq n} \frac{|\langle k|H'|n\rangle|^2}{E_n^{(0)} - E_k^{(0)}} + O(|\Psi_B|^3) \\ |\tilde{n}\rangle &= |n_0\rangle + \sum_{k\neq n} |k\rangle \frac{\langle k|H'|n\rangle}{E_n^{(0)} - E_k^{(0)}} + O(|\Psi_B|^2) \end{aligned}$$

We will calculate all the terms separately and, without loss of generality, we will look only at a single-site as it would be the same for each site. Note that $\langle n|H'|n\rangle = 0$ as H' contains linear terms in $\hat{b}$ and $\hat{b}^\dagger$. Therefore

$$\begin{aligned} E_n^{(0)} &= \frac{U}{2} n(n-1) - \mu n \qquad H'_{kn} = \langle k|H'|n\rangle \\ \text{a)} \qquad & |k\rangle = |n+1\rangle \qquad H'_{kn} = \langle n+1|(-\Psi_B \hat{b}^\dagger - \Psi_B^* \hat{b})|n\rangle = -\Psi_B \sqrt{n+1} \\ & \Rightarrow |H'_{kn}|^2 = |\Psi_B|^2 (n+1) \qquad E_n^{(0)} - E_k^{(0)} = -Un + \mu \\ \text{b)} \qquad & |k\rangle = |n-1\rangle \qquad H'_{kn} = \langle n-1|(-\Psi_B \hat{b}^\dagger - \Psi_B^* \hat{b})|n\rangle = -\Psi_B^* \sqrt{n} \\ & \Rightarrow |H'_{kn}|^2 = |\Psi_B|^2 n \qquad E_n^{(0)} - E_k^{(0)} = U(n-1) - \mu \end{aligned}$$

Collecting these results in the expression of $E_n = E_0^{MF}$ and the mean-field ground state

$$\begin{aligned} \frac{E_0^{MF}}{M} &= E_n^{(0)} + |\Psi_B|^2 \left(\frac{n+1}{\mu - Un} + \frac{n}{U(n-1) - \mu} \right) = E_n^{(0)} - |\Psi_B|^2 \chi_0 + O(|\Psi_B|^3) \\ |\tilde{n}\rangle &= |n\rangle - \frac{\Psi_B \sqrt{n+1}}{\mu - Un} |n+1\rangle - \frac{\Psi_B^* \sqrt{n}}{U(n-1) - \mu} |n-1\rangle + O(|\Psi_B|^2) \ , \end{aligned}$$

where we define $\chi_0 = \frac{n+1}{Un-\mu} + \frac{n}{\mu - U(n-1)}$. From this the expectation values follow as

$$\begin{aligned} \langle \hat{b} \rangle &= \langle \tilde{n}|\hat{b}|\tilde{n}\rangle = -\Psi_B \left(\frac{n+1}{\mu - Un} + \frac{n}{U(n-1) - \mu} \right) = \Psi_B \chi_0 \\ \langle \hat{b}^\dagger \rangle &= \langle \tilde{n}|\hat{b}^\dagger|\tilde{n}\rangle = -\Psi_B^* \left(\frac{n+1}{\mu - Un} + \frac{n}{U(n-1) - \mu} \right) = \Psi_B^* \chi_0 \ , \end{aligned}$$

which are the relations we would have to use to determine Ψ_B self-consistently. Using eq. (10.16) we get the mean-field approximation of the ground state energy of the Bose-Hubbard Hamiltonian

$$\frac{E_0}{M} = E_n^{(0)} + |\Psi_B|^2 \left[\chi_0 - Zw\chi_0^2\right] \ . \tag{10.19}$$

Therefore r (compare eq. (10.17)) is the coefficient of $|\Psi_B|^2$ and from $r = 0$ we will get the phase boundary as discussed in the previous section. If we minimize eq. (10.19) with respect to χ_0 we can see that χ_0 must be positive, as Zw is positive. Therefore the sign change in r can only come from $1 - Zw\chi_0$, hence the phase boundary is given by

$$Zw = \frac{(n - \frac{\mu}{U})(\frac{\mu}{U} - n + 1)}{n(n - \frac{\mu}{U}) + (n+1)(\frac{\mu}{U} - n + 1)} \ . \tag{10.20}$$

Equation (10.20) describes the phase boundary for given n (integer density of particles). Therefore we can obtain the phase diagram by simply plotting this function in the $\frac{Zw}{U}$-$\frac{\mu}{U}$-plane, as is done in figure 10.4.

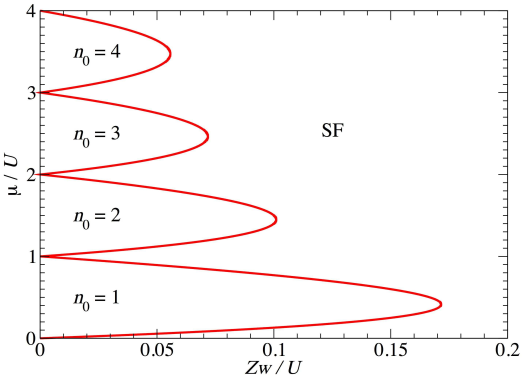

Figure 10.4: Phase diagram of H_B obtained through mean-field approach.

The limit of $w = 0$ corresponds to the Mott insulating state, as seen above, provided that $\frac{\mu}{U}$ is not equal to a positive integer. We know already that both the hopping term and the on-site term commute with the total number operator $\hat{N}_B = \sum_i \hat{n}_i$, such that both conserve the total number of bosons. Therefore, for $w = 0$ and $\frac{\mu}{U}$ at non-integer values (case of integer values would be discussed later), we have a well defined energy gap and the ground state is an eigen-state of $\hat{N}_B$ (is incompressible). As one turns on a small nonzero w the ground state will move adiabatically without undergoing any level-crossing with any other state. The perturbation arising from a nonzero w commutes with $\hat{N}_B$. Consequently the ground state will remain an eigen-state of $\hat{N}_B$ with precisely the same eigenvalue (rests incompressible) even for small nonzero w. Assuming translational invariance we get quantized values of the density (pinned at integer values). This argument also shows that the energy gap will survive everywhere within the lobe and hence we have a Mott insulating state inside the lobes. [2]

In [1] there is a nice argument how one can understand the lobe like shapes of the phase boundaries which we will recall here. Choose an arbitrary point on the μ-w plane inside one of the lobes (in the **MI**-phase) and start to increase μ while keeping w fixed. Eventually one will reach a point where the chemical potential together with the kinetic energy gained by adding an extra particle, free to hop through the lattice, would balance the associated potential energy cost (this is the level-crossing shown in fig. 10.1). Therefore, since any nonzero numbers of particles free to hop without energy cost will, at zero temperature, immediately Bose-condense and build a superfluid, such a point of energy balance defines the phase boundary for a transition between the Mott insulating and the superfluid phase. The same is true, for holes instead of particles, when one lowers μ. Now, the kinetic energy, which is account for by the hopping term, increases with w such that the balance is found earlier, meaning that the width within μ of the **MI**-phase would decrease. And this leads to the lobe like shapes shown in figure 10.4.

Note that the superfluid phase extends all the way down to $w = 0$ at integer values of $\frac{\mu}{U}$, where we have a degeneracy. This degeneracy clearly denotes that occupying the state with n bosons is energetically identical to occupying it with $n + 1$. Therefore we are free to add additional particles even at arbitrary low, but nonzero, w without energy cost, which leads to superfluidity as the additional number of bosons is free to hop through the lattice and will hence Bose-condense.[5]

It is instructive to consider the contours of constant density in the phase diagram; the lines of integer density are hereby of particular interest. For non-integer densities the constant density contours lie entirely within the superfluid phase, skirting the Mott insulating phases and terminating on the μ axis at the special point of integer value of $\frac{\mu}{U}$. But the integer density contours meet the phase boundary right at the tip of the lobes (points of maximum w on the phase boundary).

If this were not the case we would simply get a negative compressibility ($\kappa = \frac{d\rho}{d\mu}$) in the vicinity of the tips, which is a physical impossibility. That the contours for densities just slightly greater or smaller than n lie just slightly above or below the **MI**-phase with constant density n, is consistent with the assertion that the **MI-SF** transition at a generic point on the phase boundary is driven by the addition or subtraction of small numbers of particles to the incompressible **MI**-phase. Therefore the density changes continuously from its fixed integer value n

---

[5] These points of integer values of $\frac{\mu}{U}$ are in fact tri-critical points as they are facing the superfluid phase as well as two Mott insulating phases with different densities.

in the **MI** state as one crosses into the superfluid.
The transition at fixed integer density n at the tip of the **MI**-lobes on the other hand, is driven by quite different physics (other universality class): Here the density never changes, but sufficiently large w enables the bosons to overcome the on-site repulsion and hop throughout the lattice, thereby Bose-condensing. This one can see also in the power law description of the energy gap, which has different critical exponents for the two classes of transitions. But we don't want to go deeper into this (for a detailed discussion see [2]). The analysis presented here agrees with Quantum Monte-Carlo results (compare for example [5]).

10.3 ULTRA-COLD BOSONIC GAS IN AN OPTICAL LATTICE POTENTIAL

Jaksch et.al. showed in 1998 [6] that a system of cold bosonic atoms in optical lattices can be well described by the Bose-Hubbard model given by eq. (10.3). A gas of bosonic atoms is cooled down until it forms a Bose-condensate, then it is stored in a trapping potential. Afterwards an optical lattice potential is applied, which is just built by crossing standing waves induced by orthogonally arranged laser beams (see figure 10.5). The Hamiltonian of such a system is

$$\begin{aligned} H &= \int d^3x \, \psi^\dagger(\mathbf{x}) \left(-\frac{\hbar^2}{2m} \bigtriangledown^2 + V(\mathbf{x}) + V_T(\mathbf{x}) \right) \psi(\mathbf{x}) \\ &\quad + \frac{1}{2} \frac{4\pi a_s \hbar^2}{m} \int d^3x \, \psi^\dagger(\mathbf{x}) \psi^\dagger(\mathbf{x}) \psi(\mathbf{x}) \psi(\mathbf{x}) \;, \end{aligned} \tag{10.21}$$

where V is the optical lattice potential, V_T the trapping potential for the condensate. The interaction potential between the atoms is approximated by a short-range pseudopotential with a_s the s-wave scattering length and m the mass of the atoms. The wave functions ψ are Bloch wave functions, and hence can be described by a superposition of well localized Wannier functions $\psi(\mathbf{x}) = \sum_i b_i w(\mathbf{x} - \mathbf{x}_i)$. This holds if the valleys of the lattice potential are well separated from each other, as it is indeed the case for optical wavelengths. If one now keeps only the lowest vibrational states (10.21) reduces to

$$H = -w \sum_{\langle i,j \rangle} \left(\hat{b}_i^\dagger \hat{b}_j + \hat{b}_j^\dagger \hat{b}_i \right) - \sum_i \varepsilon_i \hat{n}_i + \frac{U}{2} \sum_i \hat{n}_i (\hat{n}_i - 1) \;, \tag{10.22}$$

where w is the integral over the kinetic term and the optical lattice potential, ε_i the integral over the trapping potential and U comes from the simplified particle-particle interaction. This reduced Hamiltonian would lead to the Bose-Hubbard

Hamiltonian if we assume the trapping potential to be flat in the region observed, such that we can assume the ε_i to be independent of the lattice sites and hence take them out of the sum.

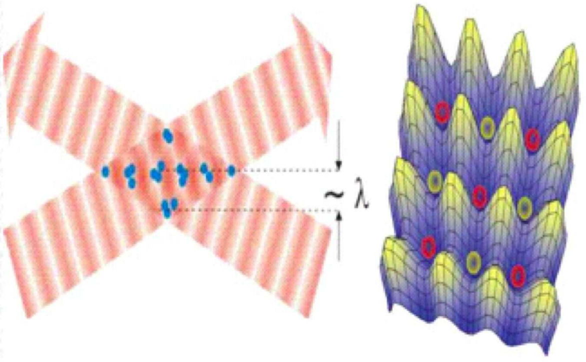

Figure 10.5: Sketch of an optical lattice built by crossing standing waves.

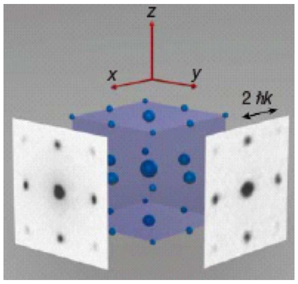

Figure 10.6: Schematic experimental apparatus, 3D interference pattern with measured absorption images, obtained after ballistic expansion from a lattice with potential depth of $V_0 = 10E_r$ and a time of flight of 15 ms.

Such an ultra-cold bosonic gas in an optical lattice potential, as proposed by Jaksch et. al. [6], was realized in the lab by Greiner et.al. in 2002 [7]. They controlled the hopping rate w by tuning the intensity of the laser beams (changing the depth of the optical potential, measured in terms of recoil energy E_r) and studied the effect of the depth of the optical lattice potential on the coherence of the state. They measured coherence just by ramping up the optical potential to the desired depth and suddenly releasing the particles from the combined trap and lattice potential, such that the wave functions could expand freely and interfere with each other. They made absorption images along two orthogonal directions of these interference pattern (see figure 10.6).

In the superfluid regime they obtained interference pattern with sharp maxima. Increasing the potential depth further (meaning decreasing the hopping rate w) also higher order interference maxima appeared as effects due to the presence of the lattice. However, at a potential depth of 13 E_r the interference maxima no longer increased. Instead an incoherent background of atoms gained more and more strength until at a potential depth of 22 E_r, no interference pattern was visible at all (compare with figure 10.7). This is just what we have seen in section 10.2.1 and 10.2.2.

A remarkable feature they observed during the evolution from the coherent to

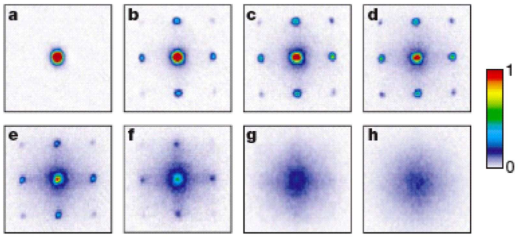

Figure 10.7: Absorption images of multiple matter wave interference patterns. These were obtained after suddenly releasing the atoms from an optical lattice potential with different potential depths V_0 after a time of flight of 15 ms. Values of V_0 were: **a**, 0 E_r; **b**, 3 E_r; **c**, 7 E_r; **d**, 10 E_r; **e**, 13 E_r; **f**, 14 E_r; **g**, 16 E_r; **h**, 22 E_r.

the incoherent state was that when the interference pattern was still visible no broadening of the interference peaks could be detected until they completely vanished in the incoherent background. This behavior can be explained on the basis of the superfluid-Mott insulator phase diagram. In fact the trapping potential is not that flat as we have assumed[6] and therefore the system, after it has crossed the quantum critical point, will evolve into alternating regions of incoherent Mott insulator domains and coherent superfluid domains (compare with [6]), where the superfluid fraction continuously decreases for increasing ratios U/w.

We have to mention that Greiner et.al. were also able to restore coherence after being in the Mott insulator state when they lowered the potential depth, here they also did measurements on the energy gap and discovered that it vanished at the same potential depth were the interference pattern reappeared.

At the end one can conclude that theory and experiment are in good agreement with each other. Nevertheless their realization of the Bose-Hubbard model with an atomic gas now allows the study of strongly correlated many-body quantum mechanics with unprecedent control of parameters.

---

[6] The system is hence in-homogeneous.

BIBLIOGRAPHY

[1] M. P. A. Fisher, P. B. Weichman, G. Grinstein, and D. S. Fisher, *Boson localization and the superfluid-insulator transition*, Phys. Rev. B **40**, 546 (1989).

[2] S. Sachdev, *Quantum Phase Transitions* (Cambridge University Press, Cambridge, 1999).

[3] J. Goldstone, , Nuovo cimento **19**, 154 (1961).

[4] J. Goldstone, A. Salam, and S. Weinberg, *Broken Symmetries*, Phys. Rev. **127**, 965 (1962).

[5] G. G. Batrouni, R. T. Scalettar, and G. T. Zimanyi, *Quantum Critical Phenomena in One-Dimensional Bose Systems*, Phys. Rev. Lett. **65**, 1765 (1990).

[6] D. Jaksch, C. Bruder, J. I. Cirac, C. W. Gardiner, and P. Zoller, *Cold Bosonic Atoms in Optical Lattices*, Phys. Rev. Lett. **81**, 3108 (1998).

[7] M. Greiner, O. Mandel, T. Esslinger, T. W. Hänsch, and I. Bloch, *Quantum phase transition from a superfluid to a Mott insulator in a gas of ultracold atoms*, Nature **415**, 39 (2002).

CHAPTER 11

QUANTUM FIELD THEORY AND THE DECONFINEMENT TRANSITION

YVES BARMAZ
SUPERVISOR: URS WENGER

Several gauge field theories show a phase transition between a low temperature confining phase and a high temperature deconfining phase. We introduce the lattice formalism for studying the behavior of pure gauge theories, in particular the interaction of static quarks. We show some criterion for confinement. We analyze how the so-called center symmetry is related to the phase transition, and how one can use this relation to make predictions about the critical behavior of the gauge theory.

11.1 INTRODUCTION

Some gauge field theories present a phase transition between a confining phase and an non-confining one, the most important example being the quantum chromodynamics (QCD), which describes the strong interaction of the Standard Model. We will try to study this phenomenon here, with the restriction to pure gauge theories. The introduction of dynamical fermions would involve different symmetries between the phases, and consequently different symmetry breaking mechanisms. We will begin with a recall of a few notions of field theories, at both zero and finite temperature, mostly taken from [1].

11.2 GAUGE FIELD THEORIES

Quantum field theories usually lead to divergent quantities, due to the infinite number of degrees of freedom. One way to regularize these quantities is to introduce a space-time lattice. The continuum version of the action, $S = \int d^4x\, \mathcal{L}$, is replaced by a sum over lattice elements (e.g. sites or plaquettes, which are elementary loops of the lattice). While the scalar fields and Dirac fields are assigned to the lattice points, vector fields (such as gauge fields) live on the links between the sites.

In a gauge field theory, one can show that the local gauge invariance can be implemented via the introduction of link variables $U_\mu(n)$ related to the gauge potential as

$$U_\mu(n) \equiv U_{n,n+\hat{\mu}} = e^{ieaA_\mu(n)}. \tag{11.1}$$

Gauge transformations are described by an element $G(n)$ of a gauge group assigned to each lattice site. To ensure gauge invariance, the link variables transform as follows under a local gauge transformation:

$$U_\mu(n) \to G(n)U_\mu(n)G^{-1}(n+\hat{\mu}) = e^{ieaA_\mu^G(n)}, \tag{11.2}$$

where $A_\mu^G(n)$ is a discretized version of $A_\mu(x) - \frac{1}{e}\partial_\mu\Lambda(x)$, and $\hat{\mu}$ is a unit vector in the μ-direction.

In a pure gauge theory, the only term in the action is the kinetic term of the gauge field. For simplicity we consider the case where the gauge group is $U(1)$. The corresponding Lagrangian density is given by

$$\mathcal{L}(x) = F_{\mu\nu}(x)F_{\mu\nu}(x) \tag{11.3}$$

where a summation over repeated indices is understood, and $F_{\mu\nu}$ describes the field-strength tensor. Here we work with the Euclidean time version of the action, and the indices μ, ν are taken in $\{1,2,3,4\}$.

To get a lattice version of this kinetic term, from the structure $F_{\mu\nu}F_{\mu\nu}$ it is clear we can consider the smallest loops, e.g. a plaquette in the μ-ν-plane:

$$U_{\mu\nu}(n) := U_\mu(n)U_\nu(n+\hat{\mu})U_\mu^\dagger(n+\hat{\nu})U_\nu^\dagger(n). \tag{11.4}$$

The link variables are path-ordered. This will become important when we will consider non-Abelian theories. Inserting (11.1), one finds

$$U_{\mu\nu}(n) = e^{iea^2F_{\mu\nu}(n)}, \tag{11.5}$$

where $F_{\mu\nu}(n) = \frac{1}{a}\left[(A_\nu(n+\hat{\mu}) - A_\nu(n)) - (A_\mu(n+\hat{\nu}) - A_\mu(n))\right]$ is the discretized version of the field-strength tensor. For a small lattice constant a, one can show that

$$\frac{1}{e^2}\sum_n\sum_{\mu<\nu}\left[1-\frac{1}{2}\left(U_{\mu\nu}(n)+U^\dagger_{\mu\nu}(n)\right)\right]\approx\frac{1}{4}\sum_{n,\mu,\nu}a^4F_{\mu\nu}(n)F_{\mu\nu}(n).$$

Thus the lattice action for the gauge potential is given by

$$S_G\left[U\right]=\frac{1}{e^2}\sum_P\left[1-\frac{1}{2}\left(U_P+U_P^\dagger\right)\right] \tag{11.6}$$

where U_P (plaquette variable) stands for the product of link variables around the boundary of a plaquette "P" taken in the counterclockwise direction.

Our formula for the pure gauge action can be generalized for $SU(N)$ gauge theories,

$$S_G^{(SU(N))}\left[U\right]=\beta\sum_P\left[1-\frac{1}{N}\mathrm{Re}\,\mathrm{Tr}\,U_P\right],\quad \beta=\frac{2N}{g_0^2}, \tag{11.7}$$

where the sum extends over all distinct plaquettes, and U_P stands for the path-ordered product of link variables along the boundary of the plaquette. This action is invariant under the gauge transformation on the lattice described above.

At this point we should mention that the gauge action contains highly non-trivial interaction terms, due to the non-Abelian character of the theory. This self-coupling of the gauge potentials is believed to be responsible for quark confinement.

Knowing the lattice expression for the $SU(N)$ gauge action, we can now compute correlation functions:

$$\langle U^{cd}_{\mu_1}(n_1)\dots\rangle=\frac{\int\mathcal{D}U\,U^{cd}_{\mu_1}(n_1)\dots e^{-S_G}}{\int\mathcal{D}U\,e^{-S_G}}. \tag{11.8}$$

Here the integration measure $\mathcal{D}U$ will be a product over the lattice links of Haar measures of $SU(N)$, which are gauge invariant. This choice hence guarantees that quantum fluctuations will not break the gauge invariance of the whole theory.

11.3 Wilson Loop and Static $q\overline{q}$-Potential

As we will see, the Wilson loops allow to describe the potential of two interacting static quarks. In particular, their counterpart in finite temperature field theories will provide a criterion to decide whether quarks are confined or not.

We consider a heavy quark (Q) and an antiquark ($\overline{Q}$) introduced in the ground state of a quantum system described by the Abelian gauge action (11.6). We want to study the energy of this (infinitely) heavy pair. We consider the gauge invariant state

$$|\phi_{\alpha\beta}(\mathbf{x},\mathbf{y})\rangle=\overline{\Psi}^{(Q)}_\alpha(\mathbf{x},0)U(\mathbf{x},0;\mathbf{y},0)\Psi^{(Q)}_\beta(\mathbf{y},0)|\Omega\rangle, \tag{11.9}$$

with $|\Omega\rangle$ describing the ground state and

$$U(\mathbf{x},t;\mathbf{y},t) = P\exp\left(ie\int_{\mathbf{x}}^{\mathbf{y}} dz^i A_i(\mathbf{z},t)\right), \tag{11.10}$$

where the integration is performed along a straight line joining $\mathbf{x}$ and $\mathbf{y}$. The P in front of the exponential stands for the path-ordering operation. This is of course irrelevant if we consider an Abelian gauge theory. $\Psi^{(Q)}$ is a Dirac field operator describing the heavy quarks, with its Dirac indices denoted by α or β. The vector fields A_i are taken in the Lie algebra of the gauge group (up to multiplication by $ie\,dz^i$). $|\phi_{\alpha\beta}\rangle$ is not an eigenstate of the Hamiltonian, but it serves as a trial state to find the lowest energy of states with non-vanishing projection onto it. We will study the propagation of $|\phi_{\alpha\beta}\rangle$ to extract this energy. The evolution of this state is described by the Green function

$$\begin{gathered} G_{\alpha'\beta',\alpha\beta}\,(\mathbf{x}',\mathbf{y}';\mathbf{x},\mathbf{y};t) = \\ \langle\Omega|T\left(\overline{\Psi}^{(Q)}_{\beta'}(\mathbf{y}',t)U(\mathbf{y}',t;\mathbf{x}',t)\Psi^{(Q)}_{\alpha'}(\mathbf{x}',t)\overline{\Psi}^{(Q)}_{\alpha}(\mathbf{x},0)U(\mathbf{x},0;\mathbf{y},0)\Psi^{(Q)}_{\beta}(\mathbf{y},0)\right)|\Omega\rangle \end{gathered} \tag{11.11}$$

In the limit of infinite quark masses, the positions are frozen, and in the continuation to imaginary times, $t \to -iT$, with the limit $T \to \infty$, the contributions of states with energy higher than the one of the ground state vanish exponentially, so we expect

$$G_{\alpha'\beta',\alpha\beta}\,(\mathbf{x}',\mathbf{y}';\mathbf{x},\mathbf{y};-iT) \to \delta^{(3)}(\mathbf{x}-\mathbf{x}')\delta^{(3)}(\mathbf{y}-\mathbf{y}')C_{\alpha'\beta',\alpha\beta}(\mathbf{x},\mathbf{y})e^{-E(R)T}, \tag{11.12}$$

where $C_{\alpha'\beta',\alpha\beta}$ is a function describing the overlap of the trial state (11.9) with the ground state(s) of the Hamiltonian in the presence of the static pair, and $E(R)$ is the ground state energy of the static pair separated by a distance $R = |\mathbf{x}-\mathbf{y}|$, which includes the self-energy. To compute this energy, we need a path integral representation of the Green function (11.11), which is given by

$$\frac{1}{Z}\int \mathcal{D}A\mathcal{D}\psi^{(Q)}\mathcal{D}\overline{\psi}^{(Q)}\left(\overline{\psi}^{(Q)}_{\beta'}(\mathbf{y}',t)\ldots\psi^{(Q)}_{\beta}(\mathbf{y},0)\right)e^{iS}, \tag{11.13}$$

where

$$\begin{aligned} S &= S_G\,[A] + S_Q\left[\psi^{(Q)},\overline{\psi}^{(Q)},A\right] \\ S_Q\left[\psi^{(Q)},\overline{\psi}^{(Q)},A\right] &= \textstyle\int d^4x\,\overline{\psi}^{(Q)}(x)\,(i\gamma^\mu D_\mu - M_Q)\,\psi^{(Q)}(x). \end{aligned} \tag{11.14}$$

The last term S_Q represents the gauge-invariant Dirac action for the heavy quarks. Notice that the path-integral involves here in the continuum formulation the gauge fields A_μ instead of the link variables $U_\mu(n)$ in the lattice formulation.

We now set $x = (\mathbf{x}, 0)$, $x' = (\mathbf{x}', t)$, $y = (\mathbf{y}, 0)$ and $y' = (\mathbf{y}', t)$. Since we are in the static case, dropping the spatial derivatives in the action still gives a good approximation. After some calculation, one gets

$$\lim_{M_Q \to \infty} G_{\alpha'\beta',\alpha\beta} = \delta(\mathbf{x}-\mathbf{x}')\delta(\mathbf{y}-\mathbf{y}')\,(P_+)_{\alpha\alpha'}\,(P_-)_{\beta\beta'}\,e^{-2iM_Q t}\langle \exp\left(ie \oint dz^\mu A_\mu(z)\right)\rangle, \tag{11.15}$$

where the integral is to be performed along the boundary of a rectangle with corners at x, x', y and y', $\langle\cdot\rangle$ denotes the ground state expectation value in the absence of the static quark-antiquark source, and the matrices $P_\pm$ are defined by $P_\pm = (1 \pm \gamma^0)$. Once again we make the continuation to imaginary times, and we get

$$\lim_{M_Q \to \infty} \left[G_{\alpha'\beta',\alpha\beta}\right]_{t \to iT} = \delta(\mathbf{x}-\mathbf{x}')\delta(\mathbf{y}-\mathbf{y}')\,(P_+)_{\alpha\alpha'}\,(P_-)_{\beta\beta'}\,e^{-2M_Q t}\langle W_C\,[A]\rangle_{eucl}, \tag{11.16}$$

where the Wilson loop is defined by

$$W_C\,[A] = \exp\left(ie \oint_C dz_\mu A_\mu(z)\right), \tag{11.17}$$

the integration being performed along a rectangular contour in the Euclidean space-time with corners given by $(\mathbf{x}, 0)$, $(\mathbf{x}, T)$, $(\mathbf{y}, 0)$ and $(\mathbf{y}, T)$, and its Euclidean expectation value by

$$\langle W_C\,[A]\rangle_{eucl} = \frac{\int \mathcal{D}A\, W_C\,[A]\, e^{-S}}{\int \mathcal{D}A\, e^{-S}}. \tag{11.18}$$

To get the static $q\bar{q}$-potential, it suffices to study the behavior for large T of $W(R,T) \equiv \langle W_C\,[A]\rangle_{eucl}$:

$$\lim_{T \to \infty} W(R,T) = F(R)e^{-E(R)T}. \tag{11.19}$$

$F(R)$ reflects the overlap between the ground state(s) and our trial state. The interaction energy follows simply as

$$E(R) = -\lim_{T \to \infty} \frac{1}{T} \ln\langle W_C\,[A]\rangle_{eucl}. \tag{11.20}$$

So far we have used the continuum formulation, which has only a formal meaning. To define it, and in order to be able to compute this energy, we need the lattice formulation. The Wilson loop can simply be replaced by a product of link variables

$$W_C\,[U] = \prod_{l \in C} U_l, \tag{11.21}$$

taken along a temporal rectangular contour C on the lattice, with ground state expectation value

$$W(\hat{R},\hat{T}) \equiv \langle W_C\,[U]\rangle = \frac{\int \mathcal{D}U\, W_C\,[U]\, e^{-S}}{\int \mathcal{D}U\, e^{-S}}. \tag{11.22}$$

Calculations show that the inter-quark potential rises linearly with separation of the quarks in QCD, which indicates confinement at zero temperature, while QED leads to a Coulomb potential.

11.4 Quantum Field Theories at Finite Temperature

To study the thermodynamic properties of quantum field theories, the path integral formalism allows to express partition functions and other expectation values of thermodynamic observables in an elegant and simple way. Phase transitions taking place of course at finite temperatures, we will need this formalism, that we are briefly introducing here.

11.4.1 Path Integral Representation of the Partition Function in Quantum Mechanics

Before turning our attention to complicated systems of fields, it is easier to begin with the simple case of statistical quantum mechanics. The partition function is given there by

$$Z = \mathrm{Tr}\, e^{-\beta H}, \tag{11.23}$$

where $\beta = \frac{1}{k_B T}$ as usual and H stands for the Hamiltonian of the system. We set $k_B = 1$. Let n be the number of degrees of freedom. In the following, we describe with

$$|q\rangle = |q_1, \ldots, q_n\rangle \tag{11.24}$$

the simultaneous eigenstates of the coordinate operators Q_i with eigenvalues q_i. The partition function then reads

$$Z = \int \prod_{\alpha=1}^{n} dq_\alpha \langle q|e^{-\beta H}|q\rangle. \tag{11.25}$$

We notice a certain similarity of the integrand with the Euclidean time propagator

$$\langle q'|e^{-H(\tau'-\tau)}|q\rangle \approx \int \mathcal{D}q\mathcal{D}p\, e^{ip_\alpha^{(l)}\left(q_\alpha^{(l+1)}-q_\alpha^{(l)}\right)} e^{-\epsilon H(q^{(l)},p^{(l)})}, \tag{11.26}$$

where $\mathcal{D}q\mathcal{D}p = \prod_{\beta=1}^{n}\prod_{l=1}^{N-1} dq_\beta^{(l)} \prod_{l=0}^{N-1}\frac{dp_\beta^{(l)}}{2\pi}$, $q^{(0)} = q$ and $q^{(N)} = q'$, and where the equality is reached in the limit $N \to \infty$. To get the partition function from this propagator, it suffices to replace the Euclidean time interval $\tau' - \tau$ with the inverse temperature β, identify the coordinates at "time" $\tau = 0$ with the ones at $\tau = \beta$, and perform the integration over q ($= q^{(0)}$ in the following). Our partition function then gets the form

$$Z = \lim_{\substack{N\to\infty \\ \epsilon\to 0 \\ N\epsilon=\beta}} \int \mathcal{D}q\mathcal{D}p\, e^{i\phi[q,p]} e^{-\sum_{l=0}^{N-1}\epsilon H\left(q^{(l)},p^{(l)}\right)}\big|_{q^{(N)}=q^{(0)}}, \tag{11.27}$$

where $\mathcal{D}q\mathcal{D}p = \prod_{l=0}^{N-1}\prod_\alpha \frac{dq_\alpha^{(l)}dp_\alpha^{(l)}}{2\pi}$ and $\phi\left[q,p\right] = \sum_{l=0}^{N-1}\sum_\alpha p_\alpha^{(l)}\left(q_\alpha^{(l+1)} - q_\alpha^{(l)}\right)$, as well as a (formal) continuum version

$$Z = \int_{\mathrm{per}} \mathcal{D}q \int \mathcal{D}p\, e^{-\int_0^\beta d\tau\left[\sum_\alpha ip_\alpha(\tau)\dot{q}_\alpha(\tau) - H(q(\tau),p(\tau))\right]}, \tag{11.28}$$

where "per" (for periodic) reminds the reader that coordinates at "time" $\tau = 0$ and $\tau = \beta$ are to be identified. We now have a path integral representation for the partition function, and we remark that three features make a distinction from the classical partition function:

1. The phase-space measure involves coordinates and momentum variables associated with every Euclidean time support on the discretized interval $[0, \beta]$ (and not only at one fixed time)

2. The Boltzmann factor is replaced by

$$\exp\left(-\beta\overline{H}\right),$$

where $\overline{H} = \frac{1}{N}\sum_{l=0}^{N-1} H\left(q^{(l)}, p^{(l)}\right)$ is the "time" averaged Hamiltonian defined at discrete time supports.

3. The phase-space measure multiplied by the phase factor depends on coordinates and momenta, and couples coordinates at neighboring lattice sites on the time (temperature) axis.

We notice that the integrand in the partition function (11.27) involves the phase $e^{i\phi[q,p]}$, and hence this is not a probability distribution in the phase space.
If the Hamiltonian has the form $H = \frac{1}{2}\sum_{\alpha=1}^{n} p_\alpha^2 + V(q)$, then performing the Gauss integration on momenta, one finds that

$$\int_{\mathrm{per}} [dq]\, e^{-\int_0^\beta d\tau\, L_E(q,\dot{q})}, \tag{11.29}$$

where$[dq] = \prod_{l=0}^{N-1}\prod_{\alpha=1}^{n}\frac{dq_\alpha^{(l)}}{\sqrt{2\pi\epsilon}}$, $L_E(q^{(l)},\dot{q}^{(l)}) = \sum_\alpha \frac{1}{2}\dot{q}_\alpha^{(l)2} + V(q^{(l)})$, with $q = q^{(0)}$. We can conclude that within the path integral framework, temperature is introduced by restricting the Euclidean time to the compact interval $[0,\beta]$ and imposing periodic boundary conditions on the coordinate degrees of freedom.

11.4.2 SCALAR BOSONS

Following the prescription we just found to introduce temperature into a system, we describe now the formalism of the finite temperature field theories with the example of the scalar field. Although we will not use this kind of field later, this remains the simplest kind of field, and hence gives rise to the simplest partition function. To find this partition function, we simply start from the quantum mechanics version, and we replace the coordinates $q_\alpha(\tau)$ by fields $\phi_{\mathbf{x}}(\tau) := \phi(\mathbf{x},\tau)$. With the Lagrangian

$$\begin{aligned} L_E[\phi,\dot{\phi}] &= \int d^3x \mathcal{L}_E(\phi,\partial_\mu\phi), \\ \mathcal{L}_E &= \frac{1}{2}\partial_\mu\phi\partial_\mu\phi + \frac{1}{2}M^2\phi^2, \end{aligned} \tag{11.30}$$

we find the path integral representation of the partition function

$$Z_0 = \mathcal{N}\int_{\text{per}} \mathcal{D}\phi\, e^{-\int_0^\beta d\tau \int d^3x \mathcal{L}_E[\phi,\dot{\phi}]}. \tag{11.31}$$

The scalar field has to satisfy periodic boundary conditions $\phi(\mathbf{x},0) = \phi(\mathbf{x},\beta)$. The partition function can thus be interpreted as a weighted sum over all field configurations living on a Euclidean space-time surface compactified along the time-direction.

11.4.3 NON-PERTURBATIVE $SU(N)$ GAUGE THEORY AT FINITE TEMPERATURE

We want to study the behavior of hadronic matter at finite temperature as described by a pure $SU(N)$ theory, which corresponds to a QCD without dynamic quarks. In particular, we would like to know if this model predicts a phase transition from a low temperature confining phase to a high temperature where quarks and gluons are deconfined, and if this is the case, we would like to find the critical temperature and the order of the transition. The non-perturbative framework provided by the lattice form of QCD should give answers to these questions.

To compute thermodynamical observables, we need a non-perturbative formulation of the partition function. From the above discussion, we guess that

$$Z = \int \mathcal{D}U\, e^{S[U]}. \tag{11.32}$$

The action now takes the form

$$S = \sum_n \mathrm{Re} \left\{ \beta_t \sum_i \mathrm{Tr}\,(U_{4i}(n)) + \beta_s \sum_{i<j} \mathrm{Tr}\,(U_{ij}(n)) \right\} \tag{11.33}$$

where $U_\mu(n)$ are link variables subjected to periodic boundary conditions, and $U_{\mu\nu}(n)$ the corresponding path-ordered products around plaquettes starting at the lattice site n following the two directions μ and ν. The sum over n is meant over all lattice sites, and over roman indices i and j from 1 to 3. β_t and β_s are independent couplings for "time-like" and "space-like" plaquettes, which depend on the temperature and the conventional bare coupling $\frac{2}{g^2}$, explicitly

$$\begin{array}{rcl} \frac{2}{g^2} & = & a^{3-d}\sqrt{\beta_s\beta_t}, \\ T & = & \frac{\sqrt{\beta_s/\beta_t}}{N_t a}, \end{array} \tag{11.34}$$

where a is the space-like lattice spacing, $(N_t T)^{-1}$ the time-like spacing, and d the spatial dimension. Notice that for $d = 3$, the coupling constant becomes dimensionless.

11.5 THE WILSON LINE OR POLYAKOV LOOP

Since the lattice is periodic in time, in addition to the topologically trivial Wilson loops defined above (which may be shrunk to a point), there exist topologically non-trivial loops which wind around the lattice along the time direction. For example, the "Wilson line" or "Polyakov loop" $L(\mathbf{x})$ at some spatial location $\mathbf{x}$ is defined by

$$L(\mathbf{x}) = \mathrm{Tr} \prod_{n=1}^{\hat{\beta}} U_4(\mathbf{x} + n\hat{t}). \tag{11.35}$$

Its expectation in the ensemble (11.32) determines the free energy of a single static quark relative to the vacuum,

$$e^{-F_q/T} = \langle L(\mathbf{x}) \rangle \tag{11.36}$$

and the correlation function of two Wilson lines yields the static quark-antiquark free energy

$$e^{-F_{q\bar{q}}(\mathbf{x}-\mathbf{y})/T} = \langle L(\mathbf{x}) L^\dagger(\mathbf{y}) \rangle, \tag{11.37}$$

as one could guess from the similarity with the Wilson loop in the case of zero temperature. Static quarks will be confined if this correlation function vanishes when $|\mathbf{x} - \mathbf{y}| \to \infty$. Provided cluster decomposition holds, that is

$$\lim_{|\mathbf{x}-\mathbf{y}|\to\infty} \langle L(\mathbf{x}) L^\dagger(\mathbf{y}) \rangle = |\langle L \rangle|^2, \tag{11.38}$$

this condition is equivalent to $L(\mathbf{x}) = 0$, which shows that inserting a single static quark requires infinite energy. On the other hand, if $\langle L \rangle \neq 0$, the free energy will go to a constant as the quarks are separated, which indicates that there is no confinement. Accordingly, the expectation value of the Wilson line evaluated in a pure gluonic medium serves as an order parameter for distinguishing a confined phase from a deconfined one in the pure $SU(3)$ gauge theory. Following [2], we can now use this order parameter to study the deconfinement transition.

11.6 SPONTANEOUS BREAKDOWN OF THE CENTER SYMMETRY AND THE DECONFINEMENT PHASE TRANSITION

11.6.1 THE CENTER SYMMETRY

In statistical mechanics, phase transitions are usually associated with the breakdown of a global symmetry. This is also expected in the $SU(3)$ gauge theory. The lattice action (11.33) is not only invariant under periodic gauge transformation, but also possesses a further symmetry which is not shared with the Wilson line. Recall that the center $\mathcal{C}$ of a group G is the subgroup

$$\mathcal{C} = \left\{ z \in G | zgz^{-1} = g \; \forall g \in G \right\}. \tag{11.39}$$

For example, the center of $SU(3)$ is

$$Z_3 = \left\{ e^{\frac{2\pi i l}{3}} \in \mathbb{C} | l = 0, 1, 2 \right\}. \tag{11.40}$$

We assume now that the center is not trivial. If we multiply all time-like oriented link variables U_4 between two neighboring spatial sections of the lattice by an element of the center,

$$U_4(\mathbf{n}, n_4) \to z\, U_4(\mathbf{n}, n_4), \;\; n_4 \text{ fixed}, \;\; z \in \mathcal{C} \text{ fixed } \forall \mathbf{n} \in \mathbb{Z}, \tag{11.41}$$

our action is kept invariant. But the Wilson line is not invariant, since it contains exactly one element that does not transform trivially:

$$L(\mathbf{x}) \to zL(\mathbf{x}). \tag{11.42}$$

If the ground state of the quantum system respects the symmetry of the classical action, then link configurations related with the center symmetry will occur with the same probability, therefore the same numbers of configurations will yield the values $L_l = e^{2\pi il/3}L$, $(l = 0, 1, 2)$ for the Wilson line. Consequently, its expectation value will vanish, but this was interpreted as a signal for confinement. Thus we expect that the center symmetry is realized in the low temperature, confining phase of the pure $SU(3)$ gauge theory. On the other hand, if $\langle L\rangle \neq 0$, then the center symmetry is broken. So we expect further that the deconfinement transition is accompanied by a breakdown of the center symmetry, and that the phases of the Polyakov loops cluster around one of the Z_3 roots.

These considerations are valid for the pure gauge sector, or equivalently, in the infinite quark mass limit, which is of course unphysical. However the study of the pure $SU(3)$ gauge theory provides us with important information on the role played by the non-Abelian gauge fields for quark confinement.

11.6.2 HIGH TEMPERATURES

In the action (11.33), the couplings obey $\beta_t \sim T$ and $\beta_s \sim 1/T$. Thus in the limit of high temperatures the contribution of any configuration with non-zero electric flux ($U_{n,4i} \neq 1$) becomes arbitrarily small compared to the configurations with vanishing electric flux (remember that the trace of a unitary matrix is maximal for the unit matrix). Therefore for high temperatures the partition function is highly peaked about configurations in which the spatial link variables are static up to a gauge transformation,

$$U_i(\mathbf{n}) = U_4(\mathbf{n})U_i(\mathbf{n}+\hat{t})U_4(\mathbf{n}+\hat{i})^\dagger. \tag{11.43}$$

Moreover periodicity in the time direction requires $U_i(\mathbf{n}) = U_i(\mathbf{n}+N_t\hat{t})$. These two conditions imply that the twists

$$\Omega_{\mathbf{x}} = \prod_{n=1}^{\hat{\beta}} U_4(\mathbf{x}+n\hat{t}) \tag{11.44}$$

must satisfy the condition

$$\Omega_{\mathbf{x}} = U_i(\mathbf{x})\Omega_{\mathbf{x}+\hat{\imath}}U_i(\mathbf{x})^\dagger. \tag{11.45}$$

For almost all configurations of spatial link variables, this relation requires the twists to equal a constant element of the center, $\Omega_{\mathbf{x}} = z$, $z \in \mathcal{C}$. Consequently, the Wilson lines being the traces of twists, we have that $\langle L(\mathbf{x})L^\dagger(\mathbf{y})\rangle \neq 0$ in the limit $|\mathbf{x}-\mathbf{y}| \to \infty$.

Similarly, small symmetry-breaking perturbations (such as a "magnetic field" term $h\sum_{\mathbf{x}} \mathrm{ReTr}\,\Omega_{\mathbf{x}}$) will cause the only significant contributions to come from a neighborhood of configurations for which $\Omega_{\mathbf{x}} = 1$.

Therefore at sufficiently high temperatures we have $\langle L(\mathbf{x})\rangle \neq 0$ and we are in a non-confining phase of the theory.
Nevertheless we should notice that this result of symmetry breaking is valid only in the infinite volume limit. In finite volumes, finite potential barriers do not prevent tunneling between the ground states, the symmetry is then reestablished, and the expectation value of the Wilson line vanishes, $\langle L(\mathbf{x})\rangle = 0$. In practice one then consider the expectation value of the modulus of the Wilson line, $\langle |L|\rangle$ (small in the symmetric phase, large in the phase of broken symmetry), or the distribution of phases of the Wilson lines in numerical simulations.

11.6.3 PHASE TRANSITIONS

If now the zero-temperature theory is in a confining phase, then there must be at least one phase transition to separate this phase from the high temperature non confining phase. $L(\mathbf{x})$ will be an order parameter for this phase transition where the global center symmetry is spontaneously broken.
If the transition is continuous, then the critical behavior will be due to long-range fluctuations in the Wilson line $L(\mathbf{x})$. Specifically, integrating out the spatial gauge fields should produce only short-range interactions in the resulting effective field theory for $L(\mathbf{x})$.
The dynamics of spatial gauge fields are qualitatively the same at high and low temperatures. In particular spatial Wilson loops obey an area-law behavior at all temperatures, and both high and low temperature limits of the theory can be shown to predict short range interactions. It is consistent to expect a similar behavior for all temperatures, and we will assume this is the case. Integrating out all degrees of freedom except the Wilson lines (whose behavior is temperature dependent) should thus produce an effective theory with short range interactions which is invariant under the center symmetry,

$$L(\mathbf{x}) \to zL(\mathbf{x}), \quad z \in \mathcal{C}. \tag{11.46}$$

The corresponding partition function was calculated [3] as

$$Z = \int \mathcal{D}L \, \exp\left[-S_{\text{eff}}\right] \tag{11.47}$$

with the effective action

$$\begin{aligned} S_{\text{eff}}(L) = {} & \beta_{\text{eff}} \sum_{\mathbf{x},i} |L(\mathbf{x}) - L(\mathbf{x}+\hat{\imath})|^2 \\ & + \sum_{\mathbf{x}} \left\{ -\frac{1}{2} \ln\left[27 - 18|L(\mathbf{x})|^2 + 8\mathrm{Re}\, L(\mathbf{x})^3 - |L(\mathbf{x})|^4\right] - 6\beta_{\text{eff}}|L(\mathbf{x})|^2 \right\} \end{aligned} \tag{11.48}$$

If, as a function of T, this theory has a continuous transition, then one could in principle locate the renormalization group fixed point which governs the critical behavior. And if, in the space of d-dimensional theories with short-range interactions invariant under the center symmetry, there exists only a singe fixed point, then the critical behavior of the original $(d+1)$-dimensional finite temperature gauge theory will be the same as that of simple d-dimensional spin models invariant under the same global symmetry. As a matter of fact, in many cases only one single fixed point in a given class of theories is known, so that one can use the critical behavior of spin models to predict the critical behavior in finite temperature gauge theories. [2]

We emphasize that these predictions depend on the assumption of a continuous transition. It is in general difficult to rule out the possibility of a first order transition occurring before.

11.6.4 PREDICTIONS

We are now equipped to make predictions about phase diagrams (g^2, T), g^2 being the coupling, T the temperature, and phase transitions of finite temperature gauge theories.

At $T = 0$, the confining phase extends from ∞ to some critical coupling g^2_{cr}, which may vanish (this happens for asymptotically free theories), depending on the dimension of the theory and the gauge group.

- In the confining phase, where the center symmetry is unbroken, Wilson line correlation function takes the form

  $$\Gamma(\mathbf{x}) \equiv \langle L(0) L^\dagger(\mathbf{x})\rangle \sim \exp\left[-\sigma|\mathbf{x}|/T\right], \quad \text{as } |\mathbf{x}| \to \infty, \tag{11.49}$$

  which corresponds to a linear static quark-antiquark potential, $F_{q\bar{q}} \sim \sigma|\mathbf{x}|$, where the string tension σ depends on g_{cr} and T.

- In the high-temperature phase, the center symmetry is broken, and two cases are to be considered.

  - If the center $\mathcal{C}$ is continuous, like for an Abelian group, this phase must contain massless Goldstone bosons, and the correlation function of Wilson lines

    $$\Gamma(\mathbf{x}) \sim M^2 \left(1 + \frac{e^2}{T|\mathbf{x}|^{d-2}}\right), \quad \text{as } |\mathbf{x}| \to \infty \tag{11.50}$$

    corresponds to a static Coulomb potential, $F_{q\bar{q}} \sim -e^2/|\mathbf{x}|^{d-2}$ with renormalized charge e^2.

- If the center is discrete, this phase can have a non-zero mass gap, whence

  $$\Gamma(\mathbf{x}) \sim M^2 \left(1 + \mathcal{O}\left(e^{-\mu|\mathbf{x}|}\right)\right), \quad \text{as } |\mathbf{x}| \to \infty. \tag{11.51}$$

  In this case, the short-range static potential $F_{q\bar{q}} \sim \mathcal{O}\left(e^{-\mu|\mathbf{x}|}\right)$ is similar to the Debye screening of an electric plasma.

The strong coupling limit of any of the gauge theories we consider may be shown to reduce exactly to an equivalent spin-system with nearest neighbor ferromagnetic couplings invariant under the center symmetry. The low temperature phase (11.49) corresponds to the disordered phase of the spin system while the high temperature phase (11.50-11.51) is analogous to the ordered phase. This is an example of inverse symmetry breaking, where the symmetry is broken in the high temperature phase. Note that the correlation length ξ in the disordered spin model yields the string tension in the gauge theory via $\sigma = (\xi T)^{-1}$.

11.6.5 Examples

In $(3+1)$ dimensions, the $SU(2)$ gauge theory with its center group Z_2 is expected to show the same critical behavior as the $3d$ Ising model, while the phase transitions of the $SU(N)$ gauge theories for $N \geq 3$ are first order.
In $(2+1)$ dimensions, the transition of the $SU(2)$ gauge theory now corresponds to the one of the $2d$ Ising model, and the $SU(3)$ theory to the $2d$, $q = 3$ Potts model. It is not clear whether the $SU(4)$ theory has a second order or a very weak first order phase transition. For $N = 5$, and presumably for all $N > 5$, the phase transitions of the $SU(N)$ theories are first order. Finally the expected critical behavior of the $U(1)$ gauge theory is the one of the 2-dimensional XY model, with its Berezinsky-Kosterlitz-Thouless transition.

11.7 Discussion of the Deconfinement Phase Transition in the Pure $SU(3)$ Gauge Theory

Here we will discuss some results of numerical simulations, without going into deep explanations on the methods used. These simulations aim at determining characteristics of the phase transitions such as the critical temperature, the nature of the transition, or critical exponents if they exist.

Numerical simulations are performed on a small lattice, but large enough to avoid finite volume effects.
The deconfinement transition in the pure $SU(3)$ gauge theory is supposed to be associated with the breakdown of the Z_3 center symmetry, and predicted to be first order. The order parameter that distinguishes the two phases is the expectation value of the Wilson line. In the infinite volume limit, the first order deconfining phase transition would appear as a discontinuity in the Wilson line or in the energy density. However, on a finite lattice this discontinuity will be smoothed out, but a rapid variation should be seen, and is indeed seen. Nevertheless, such a variation does not exclude the possibility that the transition is second order. To reach a definitive result, one can then consider a few characteristics of a first order transition, for example the coexistence of phases at the critical temperatures: In Monte Carlo simulations, this should manifest itself in the more or less frequent flip of the system between the "ordered" and "disordered" phases.
To determine the critical temperature, if the transition is first order, as it is the case here, and spatial lattice volume large enough, then localizing the discontinuity should suffice. Alternatively, one may test the Z_3 symmetry directly by looking at the distribution of real and imaginary parts of Polyakov loops, measured on a large number of link configurations, as a function of the temperature.

- In the Z_3 symmetric phase, configurations related by Z_3 symmetry operations occur with equal probability.

- In the Z_3-broken phase the system will spend a substantial simulation time in one of the three vacua, before tunnelling between the vacua will restore the Z_3 symmetry.

We conclude this section with some orders of magnitude. The critical temperature for QCD is in the range of $10^{12}\,$K, or 270 MeV, a temperature that the universe reached some $10^{-6}\,$s after the Big Bang. Once more we should emphasize that these results are valid only for pure Yang-Mills theories. The presence of dynamical quarks would break the center symmetry. This would weaken the transition, which would then be only a cross-over. This happens for example in the QCD of the Standard Model, where a cross-over takes place at 170 MeV.

BIBLIOGRAPHY

[1] H. J. Rothe, *Lattice gauge theories : an introduction* (World Scientific, New Jersey, 2005).

[2] B. Svetitsky and L. G. Yaffe, *Critical behavior at finite-temperature confinement transitions*, Nucl. Phys. B **210**, 423 (1982).

[3] A. D. Kennedy, J. Kuti, S. Meyer, and B. J. Pendleton, *Where is the continuum in lattice quantum chromodynamics?*, Phys. Rev. Lett. **54**, 87 (1985).

CHAPTER 12

THE PHASES OF QUANTUM CHROMODYNAMICS

BELA BAUER
SUPERVISOR: DR. URS WENGER, DR. PHILIPPE DE FORCRAND

The purpose of this work is to explore the phase diagram of matter as described by Quantum Chromodynamics. Interest in these phases is caused by the wish to understand the high-temperature universe fractions of a second after the Big Bang, and by the desire to understand high-density matter, which can be found in the core of neutron stars.
The various phase transitions that occur in the T-μ-plane are described. Exotic high density phases, such as the colour flavour locking phase, are discussed in more detail. Finally, a short introduction to relativistic heavy ion collisions (RHIC), which is an experimental tool to explore these phases, is given.

12.1 INTRODUCTION

In the first section of this report, some necessary foundations of QCD are introduced, where it is assumed that the reader is at least in very general terms familiar with the concept of a field theory. Special emphasis is put on the chiral symmetry (breaking) in QCD and the physical consequences of spontaneous symmetry breaking, as seen in the Goldstone theorem and the Higgs mechanism. In the second part, the phase transitions in the T-μ-plane are described. In the third section, an exotic phase that occurs in high-density matter, colour superconductivity, will be described. In the last section, relativistic heavy ion collisions will be introduced very quickly.

12.1.1 QFT AND THERMODYNAMICS

PARTITION FUNCTION IN QFT

In order to make the connection between quantum field theory and statistical mechanics, we consider the partition function of a statistical system, which, for the canonical ensemble, is given as

$$Z = \sum_{\text{all states}} e^{-\beta E}, \tag{12.1}$$

where $\beta = 1/T$. We will now try to connect this expression to quantum field theory. For a quantum system, we can rewrite the above using

$$e^{-\beta E} \rightarrow \langle \alpha | e^{-\beta H} | \alpha \rangle \tag{12.2}$$

for some state $|\alpha\rangle$ with energy expectation value E. From the path integral representation of quantum field theory we know that the transition amplitude between two field configurations ϕ_a and ϕ_b is given by

$$\langle \phi_b(x) | e^{-iHt} | \phi_a(x) \rangle \ = \int_{\phi(x,0)=\phi_a(x), \phi(x,t)=\phi_b(x)} \mathcal{D}\phi \ \exp\left[i \int_0^t d^4x \mathcal{L} \right] \tag{12.3}$$

where $\mathcal{L} = \frac{1}{2}(\partial_\mu \phi)^2 - V(\phi)$. We now switch to imaginary time (Euclidian time/action) with $\tau = it$, yielding $\int_0^t d^4x \mathcal{L} \rightarrow i \int_0^\tau d^4x \mathcal{L}_E$ in the exponent. We then find our final result

$$Z = \int_{\phi(0)=\phi(\beta)} \mathcal{D}\phi \ \exp\left[- \int_0^\beta d^4x \mathcal{L}_E \right]. \tag{12.4}$$

Here, the sum over all states was incorporated into the functional integral. We only consider diagonal matrix elements, i.e. $\langle \phi | e^{-iHt} | \phi \rangle$, and replace iHt by βH, therefore the boundary condition on the integral in (12.3) becomes $\phi_a(x) = \phi_b(x) = \phi(x, 0) = \phi(x, \beta)$.

CHEMICAL POTENTIAL AND THE GRAND CANONICAL ENSEMBLE

In the canonical ensemble used above the total particle number is kept constant. In a relativistic field theory, particle number conservation is not a useful concept anymore:

- The theory is no longer formulated in terms of particles, but in terms of fields. Particle number is not an obvious property of these fields. However, a particle number operator counting the number of particles can be applied.
- The creation of particle-antiparticle pairs can occur. Therefore, a conserved quantity can only be defined through the number of particles minus the number of antiparticles.

A more convenient way is to choose an ensemble where the particle number is allowed to fluctuate and then introduce a weight factor in a similar fashion to the Gibbs factor above. This will also prove to be useful later in the discussion.
This ensemble is called the grand canonical ensemble. The partition function is given as

$$Z = \sum_{\text{all states } \alpha} e^{-\beta E_\alpha} e^{\beta \mu N_\alpha}. \tag{12.5}$$

The quantity μ is called the *chemical potential* associated with the total charge N. It causes a shift in the energy of each energy level which is proportional to a charge N.
Closely related to this is the grand (canonical) potential (also referred to as Helmholtz free energy), which, if the partition function is chosen as a starting point, can be defined to be

$$\Omega(T, \mu) = -T \ln Z. \tag{12.6}$$

It can be shown that this potential has the following properties:

$$\begin{aligned} \Omega &= E - TS - \mu N && (12.7)\\ &= -pV. && (12.8) \end{aligned}$$

In equilibrium, this potential will be minimized.

Chemical potential in path integrals and the $U(1)_B$ symmetry

Now, the concept of a chemical potential will be incorporated into the path integral formalism. Two arguments will be demonstrated, which yield the same result. First, the chemical potential will be considered as a change in the energy of a given state. A global time-dependent phase factor to the field,

$$\psi \to \psi e^{i\mu t}, \tag{12.9}$$

which changes the Lagrangian only through the time derivative, has an effect equivalent to changing the frequency of the phase rotation of the field, which is equivalent to a change in the energy, since $|\alpha(t)\rangle = e^{-iEt}|\alpha(0)\rangle$. This can be used to account for the chemical potential in the Lagrangian by using a replacement

$$\frac{\partial}{\partial t}\psi \to \left(\frac{\partial}{\partial t} + i\mu\right)\psi \tag{12.10}$$

which is equivalent to the aforementioned phase factor. This leads to the following Lagrangian (not Euclidian time!), which is invariant under (12.9):

$$\begin{aligned}\mathcal{L} &= -\overline{\psi}\left[i\gamma^\mu(\partial_\mu + \delta_{0\mu}i\mu) - m\right]\psi &(12.11)\\ &= -\overline{\psi}\left[i\gamma^\mu\partial_\mu - m\right]\psi + \mu\overline{\psi}\gamma^0\psi. &(12.12)\end{aligned}$$

The other argument is that the chemical potential should couple to the baryon density. Since $\overline{\psi}\gamma^0\psi$ represents the charge density in the Lagrangian, it can be seen that the last term couples this density to the chemical potential in the desired way. The symmetry (12.9) is a global, continuous symmetry referred to as $U(1)_B$ and due to Noether's theorem, it is connected to the conserved baryon number.

Variables of the phase diagram

When talking about a phase diagram, one needs to define what the parameters of the phase diagrams, i.e. the variables along its axes, are. Generally, one would like to choose variables that, in equilibrium, are constant throughout the system — even in different phases — and that are intensive, i.e. independent of the system size. In the phase diagram we want to consider for QCD, the obvious variables would be the temperature and the density. The second, however, does not fulfill the above properties, since, in a regime of phase coexistence at a first order phase transition, it is not constant throughout the system. From basic thermodynamics, however, it is known that in such a phase coexistence region, the chemical potential is constant across the phase boundaries. Therefore, it is chosen as the second parameter of the phase diagram along with the temperature.

12.1.2 Example: Partition function for fermions

Instead of using the path integral formulation, a simpler approach can be used in the case of fermions without interaction. It will be used as a quick way to calculate the particle density as a function of the chemical potential for low temperatures. Take, as an example, a system with two momentum states that, if occupied by a particle, have an energy contribution $\omega_{\vec{p}} - \mu = \sqrt{\vec{p}^2 + m^2} - \mu$ and $\omega_{\vec{p}} + \mu$ if occupied by an anti-particle. Each state is degenerate due to spin-up and spin-down particles. We therefore have

$$\begin{aligned}
Z &= \sum_{\text{all states}} e^{-E/T} && (12.13)\\
&= e^{-E(|0,0\rangle)/T} + e^{-E(|\uparrow,0\rangle)/T} + e^{-E(|0,\bar{\uparrow}\rangle)/T} + \ldots && (12.14)\\
&= 1 + e^{-(\omega_{\vec{p}_0}-\mu)/T} + e^{-(\omega_{\vec{p}_1}+\mu)/T} + \ldots && (12.15)\\
&= \prod_{\vec{p}} (1+e^{-(\omega_{\vec{p}}-\mu)/T})^2 (1+e^{-(\omega_{\vec{p}}+\mu)/T})^2 && (12.16)
\end{aligned}$$

We can now find the particle density (using $q(\vec{p}) = (1+e^{-(\omega_{\vec{p}}-\mu)/T})^2(1+e^{-(\omega_{\vec{p}}+\mu)/T})^2$)

$$\begin{aligned}
N &= -\frac{\partial \Omega}{\partial \mu} = -\frac{\partial Z}{\partial \mu}\frac{\partial \Omega}{\partial Z} = -\frac{T}{Z}\frac{\partial Z}{\partial \mu} && (12.17)\\
&= -\frac{T}{Z}\sum_{\vec{p}} \left(\prod_{\vec{p}' \neq \vec{p}} q(\vec{p}) \right) \frac{\partial}{\partial \mu} q(\vec{p}) && (12.18)\\
&= -T \sum_{\vec{p}} \left(\frac{1}{q(\vec{p})} \right) \left\{ (1+e^{-(\omega_{\vec{p}}+\mu)/T})^2 2 (1+e^{-(\omega_{\vec{p}}-\mu)/T}) e^{-(\omega_{\vec{p}}-\mu)/T} (-\frac{1}{T}) + \ldots \right\} && (12.19)\\
&= 2 \sum_{\vec{p}} \left\{ \frac{1}{e^{(\omega_{\vec{p}}-\mu)/T}+1} - \frac{1}{e^{(\omega_{\vec{p}}+\mu)/T}+1} \right\}. && (12.20)
\end{aligned}$$

The two terms in (12.20) show the well-known Fermi distribution for particles and antiparticles, which has the appearance of a step function for low temperatures. The Fermi momentum, i.e. the momentum up to which all states are occupied in the ground state, is

$$p_F = \sqrt{\mu^2 - m^2}. \qquad (12.21)$$

Replacing the sum over $\vec{p}$ by an integral over phase space for the infinite volume where $\vec{p}$ becomes continuous and and assuming that the temperature is low and the occupied states form a Fermi sphere with volume $\frac{4\pi}{3}p_F^3$ in momentum space, we find for the density of charge

$$n = \frac{N}{V} = \frac{8\pi}{3}(\mu^2 - m^2)^{3/2}. \qquad (12.22)$$

It can be seen that for $\mu < m$, there will be no occupied states. The function n is therefore not analytic at $\mu = m$. It can be used as order parameter for a phase transition at this point. This is closely analogous to the situation in QCD for low temperatures.

12.1.3 QCD AND SYMMETRIES

CHIRAL SYMMETRY

Consider a simple fermionic field described by the Dirac equation

$$(i\gamma^\mu\partial_\mu - m)\psi(x) = -i\partial_\mu\overline{\psi}\gamma^\mu - m\overline{\psi} = 0. \tag{12.23}$$

In the following, we will use the Weyl representation where

$$\gamma^5 = \begin{pmatrix} -1 & 0 \\ 0 & 1 \end{pmatrix}, \psi(x) = \begin{pmatrix} \psi_L(x)' \\ \psi_R(x)' \end{pmatrix} \tag{12.24}$$

$$\begin{aligned} \psi_L(x) &= \frac{1-\gamma^5}{2}\psi(x) & (12.25)\\ \psi_R(x) &= \frac{1+\gamma^5}{2}\psi(x). & (12.26) \end{aligned}$$

ψ'_L and ψ'_R are 2-component Weyl spinors and represent left-handed and right-handed components of the field and therefore eigenstates of the helicity operator with eigenvalue ±1. Now consider the following currents corresponding to the symmetry transformations $U(1)_B:\ \psi(x) \rightarrow e^{i\alpha}\psi(x)$ and $\psi(x) \rightarrow e^{i\alpha\gamma^5}\psi(x)$,

$$j^\mu(x) = \overline{\psi}(x)\gamma^\mu\psi(x) \text{ and } j^{\mu5}(x) = \overline{\psi}(x)\gamma^\mu\gamma^5\psi(x), \tag{12.27}$$

and their divergences

$$\begin{aligned} \partial_\mu j^\mu &= (\partial_\mu\overline{\psi})\gamma^\mu\psi + \overline{\psi}\gamma^\mu\partial_\mu\psi & (12.28)\\ &= (im\overline{\psi})\psi + \overline{\psi}(-im\psi) & (12.29)\\ &= 0 & (12.30)\\ \partial_\mu j^{\mu5} &= (\partial_\mu\overline{\psi})\gamma^\mu\gamma^5\psi(x) + \overline{\psi}\gamma^\mu\gamma^5\partial_\mu\psi & (12.31)\\ &= (im\overline{\psi})\gamma^5\psi - \overline{\psi}\gamma^5(-im\psi) & (12.32)\\ &= 2im\overline{\psi}\gamma^5\psi, & (12.33) \end{aligned}$$

where we have used the anticommutation relation $\{\gamma^5, \gamma^\mu\} = 0$. It can be seen that for $m = 0$, the *axial vector current* $j^{\mu5}$ is conserved. We can now define left-handed and right-handed currents as

$$\begin{aligned} j^\mu_L &= \overline{\psi_L}\gamma^\mu\psi_L &&= \psi^\dagger\frac{1-\gamma^5}{2}\gamma^0\gamma^\mu\frac{1-\gamma^5}{2}\psi, & (12.34)\\ j^\mu_R &= \overline{\psi_R}\gamma^\mu\psi_R &&= \psi^\dagger\frac{1+\gamma^5}{2}\gamma^0\gamma^\mu\frac{1+\gamma^5}{2}\psi. & (12.35) \end{aligned}$$

We then find that (using the anticommutation and $\gamma^5\gamma^5 = I$)

$$\begin{aligned} j_L^\mu + j_R^\mu &= j^\mu, && (12.36)\\ \partial_\mu j_L^\mu = \partial_\mu j_R^\mu &= 0. && (12.37) \end{aligned}$$

This shows that (for zero quark masses) the currents for left-handed and right-handed quark fields are separately conserved.

Chiral symmetry breaking in QCD and dynamical quark masses

In the case of QCD with two massless quark flavours, we denote by Q the doublet of light quarks,

$$Q = \begin{pmatrix} u \\ d \end{pmatrix} = Q_L + Q_R, \tag{12.38}$$

where, just as above,

$$Q_L = \frac{1-\gamma^5}{2}\begin{pmatrix} u \\ d \end{pmatrix},\ Q_R = \frac{1+\gamma^5}{2}\begin{pmatrix} u \\ d \end{pmatrix} \tag{12.39}$$

These transform as

$$Q_L \to U_L Q_L,\ Q_R \to U_R Q_R, \tag{12.40}$$

where U_L and U_R are transformations realizing the isospin symmetry separately for left-handed and right-handed quarks, hence

$$U_L, U_R \in SU(2). \tag{12.41}$$

The chiral flavour symmetries of QCD would therefore be $SU(2)_L \times SU(2)_R$. In a theory with more massless quark flavours, this symmetry becomes $SU(N_f)_L \times SU(N_f)_R$, where N_f is the number of quark flavours. With the additional colour (gauge) symmetry $SU(3)_C$ and the symmetry that, due to Noether's theorem, induces baryon number conservation, the full symmetry group of QCD with N_f massless quark flavours is

$$SU(3)_C \times SU(N_f)_L \times SU(N_f)_R \times U(1)_B. \tag{12.42}$$

It is known for QCD that the coupling between quarks and antiquarks becomes very strong at large distances, while, in our theory of massless quarks, the creation of a quark-antiquark-pair is connected to only a very small energy cost. Hence we can expect the vacuum to be populated by such pairs. Since, however, the overall momentum and angular momentum, i.e. spin, of the vacuum needs to be 0, they carry net helicity charge. Considering that the creator of a left-handed quark is the annihilator of a right-handed antiquark (and vice versa), we find a vacuum with the non-vanishing expectation value for $\overline{Q}Q$

$$\begin{aligned}\langle 0|\overline{Q}Q|0\rangle &= \langle 0|\overline{Q_L}Q_L + \overline{Q_R}Q_R + \overline{Q_L}Q_R + \overline{Q_R}Q_L|0\rangle && (12.43)\\ &= \langle 0|\overline{Q_L}Q_R + \overline{Q_R}Q_L|0\rangle && (12.44)\\ &\neq 0. && (12.45)\end{aligned}$$

If we now apply the symmetry transformations of (12.41) and require the vacuum to be unaffected, we find the condition

$$\langle 0|\overline{Q_L}Q_R + \overline{Q_R}Q_L|0\rangle = \langle 0|\overline{Q_L}U_L^\dagger U_R Q_R + \overline{Q_R}U_R^\dagger U_L Q_L|0\rangle \qquad (12.46)$$

which can only be fulfilled if $U_L = U_R$. Therefore, it appears that the dynamic creation of quark-antiquark pairs in the vacuum that mixes left-handed and right-handed quarks breaks the full symmetry down to $SU(2)_V$!

The Goldstone theorem and the Higgs mechanism

In 1961, it was shown by Goldstone ([1], [2, Ch. 11.1]) that in the absence of long-range interactions, the spontaneous breaking of a continuous symmetry is always associated with the appearance of a massless particle, called a Goldstone boson. By a spontaneous symmetry breaking, we denote a situation where the Lagrangian of the field theory has a symmetry which is not realized in the ground state. A short proof for classical scalar field theories will be given here. Consider a theory with several fields $\phi^a(x)$ with a Lagrangian

$$\mathcal{L} = D\phi - V(\phi) \qquad (12.47)$$

where D is some differential operator on $\phi(x)$. If the potential V is minimized by a field $\phi_0^a(x)$ such that

$$\left(\frac{\partial}{\partial\phi^a}V\right)(\phi_0^a) = 0, \qquad (12.48)$$

we can expand the potential about this field up to second order, finding

$$V(\phi) = V(\phi_0) + \frac{1}{2}(\phi-\phi_0)^a(\phi-\phi_0)^b\left(\frac{\partial^2}{\partial\phi^a\partial\phi^b}V\right)(\phi_0) \qquad (12.49)$$

The coefficient of the quadratic term is a symmetric matrix whose eigenvalues, due to formal analogy with ordinary mass terms, can be identified with the masses of the fields. A massless particle would therefore correspond to a vanishing eigenvalue of this matrix. Assuming that the Lagrangian has a continuous symmetry, which takes the form

$$\phi^a \to \phi^a + \alpha\Delta^a(\phi), \qquad (12.50)$$

and assuming that the fields are constant such that $D\phi = 0$, we find that the potential must realize the symmetry:

$$V(\phi^a) = V(\phi^a + \alpha\Delta^a(\phi)) = V(\phi^a) + \alpha\Delta^a(\phi)\frac{\partial}{\partial\phi^a}V(\phi) \tag{12.51}$$

Differentiating this with respect to a second field ϕ^b, we find at $\phi = \phi_0$

$$0 = \left(\frac{\partial\Delta^a}{\partial\phi^b}\right)(\phi_0)\left(\frac{\partial V}{\partial\phi^a}\right)(\phi_0) + \Delta^a(\phi_0)\left(\frac{\partial^2}{\partial\phi^a\partial\phi^b}V\right)(\phi_0). \tag{12.52}$$

The first term vanishes due to (12.48). In the second term, we recognize the coefficient matrix of (12.49). Since we assumed that the ground state does not respect the symmetry, i.e. $\Delta^a(\phi_0) \neq 0$, we see that

$$\Delta^a(\phi_0)\left(\frac{\partial^2}{\partial\phi^a\partial\phi^b}V\right)(\phi_0) = \Delta^a(\phi_0)\cdot 0, \tag{12.53}$$

hence $\Delta^a(\phi_0)$ is an eigenvector of the coefficient matrix with eigenvalue 0. This proves Goldstone's theorem.

It can be shown that this extends to general field theories, i.e. beyond the classical scalar case shown above. If, however, spontaneous symmetry breaking occurs in a gauge theory, where the local gauge symmetry has led to the occurrence of gauge vector bosons, by a mechanism called Higgs mechanism these vector bosons acquire mass. This will be demonstrated for the case of a complex scalar field with the Lagrangian

$$\mathcal{L} = -\frac{1}{4}(F_{\mu\nu})^2 + |D_\mu\phi|^2 - V(\phi),\ D_\mu = \partial_\mu + ieA_\mu \tag{12.54}$$

which couples the field to itself and an electromagnetic field. This is invariant under a local $U(1)$ transformation,

$$\phi \to e^{i\alpha(x)}\phi(x),\ A_\mu(x) \to A_\mu(x) - \frac{1}{e}\partial_\mu\alpha(x) \tag{12.55}$$

We now choose the potential in such a way that the ground state acquires a non-vanishing expectation value and expand the Lagrangian about that vacuum state ϕ_0 using $\phi(x) = \phi_0(x) + \frac{1}{\sqrt{2}}(\phi_1(x) + i\phi_2(x))$. We find for the kinetic term (cutting off cubic and quartic terms)

$$|D_\mu\phi|^2 = \frac{1}{2}(\partial_\mu\phi_1)^2 + \frac{1}{2}(\partial_\mu\phi_2)^2 + \sqrt{2}e\phi_0 A_\mu\partial^\mu\phi_2 + e^2\phi_0^2 A_\mu A^\mu. \tag{12.56}$$

The last term can be written as

$$\Delta\mathcal{L} = \frac{1}{2}m_A^2 A_\mu A^\mu \tag{12.57}$$

and obviously assigns a mass to the gauge bosons given by the gauge fields A_μ. This calculation can be extended to non-Abelian gauge theories, where the same effect is observed. The Goldstone boson that is associated with the symmetry breaking does not appear as a physical particle. In a certain sense, however, it can be understood as giving the gauge vector bosons a longitudinal component, which does not appear as linearly independent component for the massless vector bosons of the theory with full symmetry in the ground state.

12.1.4 Simplifications of QCD

Throughout this report, we will mainly consider a stripped-down version of QCD, which is supposed to make the considerations a lot easier. The simplifications made to standard QCD are:

- The electroweak interactions are not taken into consideration.
- We will consider the two lightest quarks, u and d, as massless, and there will be no other quarks. The action then takes on a global $SU(2)_L \times SU(2)_R \times U(1)_B$ symmetry which is broken down to $SU(2)_V \times U(1)_B$ for low temperatures, as seen above.

In the following, the term QCD will mostly be used synonymously for QCDLite. The full theory of QCD will be referred to as QCD+.

In the path integral formalism introduced above, this theory can be written with a grand canonical partition function

$$Z = e^{\Omega(T,\mu)/T} = \int \mathcal{D}A \, \mathcal{D}\overline{\psi} \, \mathcal{D}\psi \; e^{-S_E} \tag{12.58}$$

with the Euclidian action

$$S_E = \int_0^{1/T} dx_0 \int d^3x \left[\frac{1}{2g^2} Tr(F_{\mu\nu}F_{\mu\nu}) - \sum_{f=1}^{N_f} \overline{\psi}_f \left(\partial\!\!\!/ + igA\!\!\!/ + \frac{\mu}{N_c}\gamma_0 \right) \psi_f \right] \tag{12.59}$$

Here, $N_f = 2$ is the number of quark flavours and $N_c = 3$ is the number of colours.

12.1.5 The MIT Bag Model

Currently, the dynamics of QCD are far from being solved even in the simplest cases. A simplified treatment of nucleons, based on the concepts of confinement and asymptotic freedom, is the so-called Bag Model ([3]). Here, the quarks are assumed to be massless and move non-interactingly in a spherical “bag” of radius R, which has a constant energy density $3B \approx 3 \cdot 175\text{MeV fm}^{-3}$, which can be found by fitting results of the model to observed data for nucleons. This constant energy causes an inwards-acting pressure that confines the quarks to the “bag”. Due to the asymptotic freedom inside the bag, the condensate which breaks chiral symmetry is not present and therefore, chiral symmetry is restored.

12.2 THE QCD PHASE DIAGRAM

Current research interest is directed towards two regions in the phase diagram: the region of low temperatures and high densities, and the region of high temperatures and low densities. In the case of high densities, research is motivated by the occurence of exotic phases and the relevance for astrophysics (neutron stars). The method used is mainly that of analytic calculations, since lattice simulations become very difficult for large fermion numbers due to the sign problem. In the region of high temperatures, the quark-gluon plasma is being studied very carefully. For theoretical investigations, lattice simulations are the primary tool here, since little analytic results can be found. Experimentally, the QGP can be studied through heavy-ion collisions. The third region of the phase diagram, where both T and μ are finite and large, is very difficult to study both theoretically and experimentally and therefore less research activity is directed towards this. An overview over the phase diagram is given in figure 12.1.

12.2.1 LOW TEMPERATURE AND FINITE DENSITY

THE GROUND STATE $T = 0$ First, the case of $T = 0$, i.e. the ground state, will be considered. It will be found that there are various phase transitions along the axis of finite chemical potential in the phase diagram. Considering the partition function again,

$$Z = \sum_{\text{all states } \alpha} \exp\left(-\frac{E_\alpha - \mu N_\alpha}{T}\right), \tag{12.60}$$

it is obvious that for $T = 0$ the state which minimizes $E_\alpha - \mu N_\alpha$ dominates the sum. For $\mu = 0$, this is the vacuum with $N = E = 0$, where the baryon number $n(\mu) = 0$. If we increase μ, this remains true as long as $E_\alpha - \mu N_\alpha > 0$ for all excited states α. When $E_\alpha - \mu N_\alpha = 0$, the vacuum is no longer the dominating state. Therefore, at $\mu = \mu_0$, where

$$\mu_0 := \min_\alpha \left(\frac{E_\alpha}{N_\alpha}\right), \tag{12.61}$$

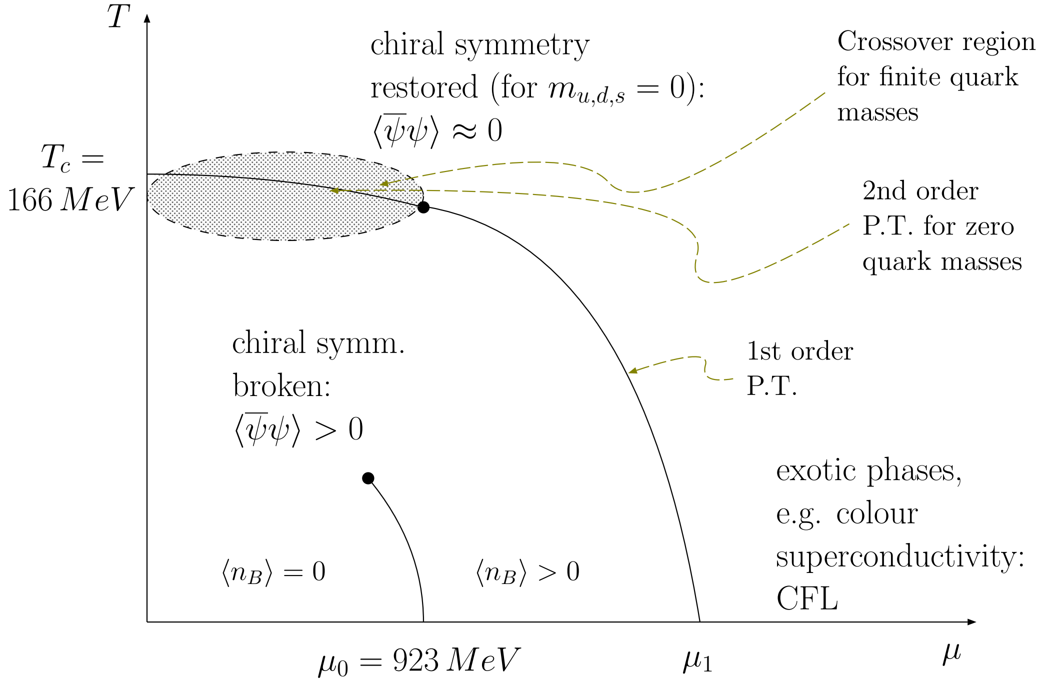

Figure 12.1: Phase diagram of QCD

we expect the transition to a phase where $n(\mu) > 0$. This behaviour was seen before in (12.20) for the case of free fermions. In both cases, $n(\mu)$ can be used as order parameter which is not analytical at $\mu = \mu_0$. In the case of the free fermions, this transition is at $\mu_0 = m$. In the case of QCD, it is somewhat more difficult to estimate the value of μ_0. Using

$$\frac{E}{N} = m_N - \frac{Nm_N - E}{N}, \tag{12.62}$$

where m_N is the nucleon mass, it becomes obvious that the state which minimizes E/N is the state that maximizes the second term $\epsilon = \frac{Nm_N-E}{N}$, which is the binding energy per nucleus. Using empirical data on the binding energy in atomic nuclei and the Weizsacker formula (neglecting electromagnetic terms), it is found that for a nucleus with an infinite number of nucleons, which is a situation similar to what we have here, this energy saturates to (see [4, p. 213]) $\epsilon \approx 16$ MeV. We therefore conclude that for the reduced QCD we are using there is a first-order phase transition at

$$\mu_0 \approx m_N - 16 \text{ MeV} \approx 923 \text{ MeV} \tag{12.63}$$

This phase can be characterized as a nuclear liquid with a density of about $n_0 \approx 0.16$ fm^{-3}. In a full theory including Coulomb forces, the situation is changed: the proposed nucleus with an infinite number of nucleons becomes unstable due to Coulomb repulsion. Since iron nuclei have the highest binding energy, they are energetically favoured; adding electrons to ensure electric neutrality, a phase transition at $\mu_0 \approx m_N - 8$ MeV ≈ 931 MeV to the density of iron solid is expected. At sufficient chemical potential corresponding to very high pressures, neutron matter becomes stable (i.e. gravitational compression in a neutron star). The phases along this axis of the phase diagram therefore correspond to the phases occuring in a neutron star.

For values of μ in the region of $\mu_0 < \mu < 200\text{MeV} + \mu_0$, very little is known about the phases. Speculations are that there might be crystallization of nuclear matter, superconducting phases, kaon condensation and strange-quark matter, but this is not very well-understood.

If μ becomes large on a QCD scale, i.e. $\mu \gg \mu_0 + 200\text{MeV}$, the increasing density of particles forces these to occupy high momentum states due to Fermi statistics[1]. A high density of quarks causes a screening of the interaction forces and they are asymptotically free for high momenta. Hence, one can expect the quark-antiquark condensate of the ground state which breaks the chiral symmetry to vanish. Therefore, we expect a phase transition at $\mu = \mu_1$ where the chiral symmetry is restored! However, there are speculations that this naive approach does not describe the true phase diagram. Exotic phases, where the chiral symmetry is again broken by some completely different mechanism, have been proposed and will be treated in section 12.3.

THE SITUATION FOR LOW TEMPERATURES Generally, it can be assumed that the phase transition at $T = 0$, $\mu = \mu_1$ extends as a line of phase transitions into the T-μ-plane, since the argument of asymptotic freedom persists. Since this phase transition is not very well understood, the properties of such a line of phase transitions are also largely unknown. More discussion of this will be found in sect. 12.2.3.

The situation at $\mu = \mu_0$ is much easier. Since, for $T > 0$, the baryon density

---

[1] As a matter of fact, this argument is not entirely correct but just a heuristic way to make the transition more plausible. As was said in the beginning, compactification of the time component imposes periodic boundary conditions in the time direction, which become antiperiodic boundary conditions for fermions. If one now applies a spectral decomposition of the fields with regard to the time direction, one finds a discrete spectrum (Matsubara frequencies), i.e. a discrete spectrum in momentum space. Antiperiodicity however requires those frequencies to be odd multiples of πT, i.e. a ground state momentum $p = 0$ cannot be occupied. Increasing chemical potential drives the lowest Matsubara frequency to even higher values, so that eventually all momentum states are asymptotically free. Therefore, the Fermi sphere argument is not valid in the sense that the Fermi sphere is in fact not filled, but rather a "Fermi shell". Nevertheless, the argument will be used in the following for its intuitive clarity

$n(\mu) > 0$ even for $\mu < \mu_0$, this cannot be used as an order parameter to predict a phase transition at $\mu = \mu_0$ in this situation. For first order phase transitions, however, it can be argued from thermodynamics that such a transition does not appear as a point, but rather as a line of first-order phase transitions. Therefore we expect a first-order phase transition to be a point in a line of phase transitions, generally terminated by a critical point. The slope of this line is described by the Clausius-Clapeyron equation, which in this case reads

$$\frac{dT}{d\mu} = -\frac{\Delta n}{\Delta s}. \tag{12.64}$$

Using this, we can use the analogy to a normal liquid-gas transition to find properties of this line of phase transitions.

- Due to the third law of thermodynamics (Nernst theorem), the entropy should be minimal for $T \to 0$. Therefore, at $T = 0$, there can be no change in the entropy, $\Delta s = 0$, and therefore the slope is infinite at that point.
- We expect the phase corresponding to a gas, i.e. that of higher temperature, to have a lower particle density than the "liquid" phase, $\Delta n < 0$. Since the system absorbs latent heat at a first order phase transition, $\delta Q < 0$, and thereby $\Delta s < 0$. Therefore, with $\frac{\Delta n}{\Delta s} > 0$, we find that $\frac{dT}{d\mu} < 0$.
- A line of first-order phase transitions can be expected to end in a point where the two phases merge and cannot be distinguished, a critical point. There are estimates that the critical point is found at a temperature similar to the binding energy in the nuclear matter phase, i.e. at $T_0 \approx 16$ MeV.

If the phase transition at $\mu = \mu_1$ is of first order, a similar argument would apply there.

12.2.2 Quark-gluon-plasma at high temperatures

In this section, the phases of QCD will be considered as the temperature is raised while the chemical potential remains at $\mu = 0$. The transition here is between a phase in which the pions — as lightest mesons — dominate the hadronic matter, and a phase where quarks and gluons form a high-energy plasma. For both phases, we make the approximation that interactions between particles can be neglected; we also assume that no other hadrons except pions are formed in the low-temperature phase. In fact, lattice simulations show that this is not a good approximation, but it will lead to a rough estimate for the transition temperature.

It is well-known that the radiation pressure of a field is given by $P = \frac{1}{3}\epsilon$, where ϵ is the energy density. The energy density of a bosonic free field is given by

$$\epsilon = 3P = n_f \frac{\pi^2}{30} T^4 \tag{12.65}$$

where n_f is the number of degrees of freedom in the field. For the case of pions, $n_f = 3$ since there are three types of pions, π^+, π^-, π^0. For the quark gluon plasma, we have

- Gluons:
  - One octet, carrying colour and anti-colour
  - Two spin states
- Quarks:
  - Three colours,
  - two spins,
  - two flavours,
  - particles and anti-particles for the quarks, and a factor of $\frac{7}{4}$ for the different (Fermi) statistics in the calculation of the energy density.

Hence, we have

$$\begin{aligned} P_{\text{hadronic}} &= 3 \cdot \frac{\pi^2}{90} T^4 && (12.66) \\ P_{\text{QGP}} &= 37 \cdot \frac{\pi^2}{90} T^4 - B. && (12.67) \end{aligned}$$

Here, B is the bag constant defined in sect. 12.1.5 and accounts for the change in pressure due to the energy density in quark matter, which is assumed to coincide with that inside a nucleon. It describes in a simple way the interactions between the quarks, which, in the hadronic phase, are encapsulated into the pions. We know from thermodynamic considerations that $p = -\frac{\partial \Omega}{\partial V} = -\frac{\Omega}{V}$ (Ω is extensive) and therefore

$$\Omega = -pV. \tag{12.68}$$

Since the system, in equilibrium, chooses the state that minimizes this potential, we can conclude that at constant volume, the state with the highest pressure will be realized. The above expressions for the pressure in the different phases hence tells us that the phase transition occurs when $P_{\text{hadronic}} = P_{\text{QGP}}$, which leads to

$$T_c = \left(\frac{45}{17\pi^2}\right)^{1/4} B^{1/4} \approx 150\text{MeV} \tag{12.69}$$

Using the above, we can also find the energy density of the plasma phase:

$$\epsilon_{\text{QGP}} \approx 850 \ \frac{\text{MeV}}{\text{fm}^3} \tag{12.70}$$

The order of the phase transition from hadronic matter to the quark-gluon plasma has recently been a topic of discussion. While originally, it was expected to be of strong first order (the above argument even allows to estimate the latent heat), this behaviour was not seen experimentally. Currently, the most accepted view is the following:

- In the case of zero quark masses, the transition is of second order.
- In the case of non-zero quark masses, the chiral symmetry is never an exact symmetry, hence there is no symmetry breaking connected to the transition. Therefore, the expectation is that there is no phase transition at all but instead a crossover region.

DEBYE SCREENING IN QGP An important effect in the QGP is Debye screening of the quark interactions. Debye screening is an effect that QGP has in common with classical (nuclear matter) plasmas, where electric field screening occurs. In order to heuristically derive the Debye screening ([5]) for the case of QGP, consider an external colour potential ϕ^a (i.e. in a hypothetical colour capacitor). If the space is filled with mobile colour charges of (constant) density ρ^a, the system is described up to first order by the Poisson equation

$$\Delta\phi^a = -g\rho^a, \tag{12.71}$$

where g is the effective coupling. The external potential induces a non-vanishing colour density, which can be calculated to be

$$\rho^a(\phi) \approx -m_D^2\phi^a. \tag{12.72}$$

Here, m_D denotes the Debye screening mass, which is gT for gluons and $gT/\sqrt{6}$ for each quark flavour. If we now consider a test charge at the origin, of colour charge $t^a\delta(r)$, we find the system to be described by the screened Poisson equation

$$\left[\Delta - gm_D^2\right]\phi^a = -gt^a\delta(r). \tag{12.73}$$

Generally, a screened Poisson equation $[\Delta - \lambda^2]\,u(r) = -f(r)$ has the solution $u(r) = \int d^3r' \frac{e^{-\lambda|r-r'|}}{4\pi|r-r'\text{“}|} f(r')$. In our case, we therefore find

$$\phi^a(r) = t^a\frac{g}{4\pi r}e^{-gm_Dr} \tag{12.74}$$

Hence, the colour potential seen by a single colour charge decreases exponentially. The Debye mass m_D obviously defines a length scale, the Debye screening length λ_D, as a significant length scale for the potential.

12.2.3 High temperature and chemical potential

As discussed above, there are two lines of first order phase transitions along the axis of zero temperature and finite chemical potential, and a phase transition of second order in the case of zero quark masses or a crossover for finite quark masses along the axis of low densities and high temperatures. In the high-temperature QGP and the high-density phase, the quark-antiquark condensate $\langle Q\overline{Q}\rangle$, which was used as order parameter for the phase transition between phases with and without chiral symmetry, vanishes (despite the fact that chiral symmetry might be broken again in CFL, as discussed below). It can therefore be expected that in the case of zero quark masses, where the transition from hadronic matter to QGP is connected to the breaking of an exact symmetry, the regions of $\langle Q\overline{Q}\rangle = 0$ and of $\langle Q\overline{Q}\rangle \neq 0$ are separated by one single line of phase transitions, i.e. that the line of second order phase transitions at high temperatures and the line of first order phase transitions at high densities merge. The point where the two lines meet is a tricritical point.

If the quark masses are not exactly zero, the chiral symmetry is never exactly restored and the line of second order phase transitions to QGP becomes a crossover region. In this case, the aforementioned tricritical point does not exist and is replaced by a (bi-)critical point.

Properties of the tricritical point A tricritical point is a point where three disctinct phases merge into one, i.e. where a line of three-phase coexistence phase transitions merges into a second order phase transition where no coexistence is possible. Such points exist in other physical systems and have been studied there, so that some properties of this tricritical point can be deduced from universality.

In order to understand the tricritical point in this case, an additional parameter has to be introduced into the phase diagram. The quark mass m can be used for this. The sign of the quark mass can be chosen arbitrarily, since it corresponds to the multiplication of the fields by γ^5. Accordingly, opposite signs of the quark mass m lead to opposite signs of the chiral condensate $\langle \overline{Q}Q\rangle$. Phase transitions along the axis of the quark mass occur because finite quark masses explicitly break the chiral symmetry.

The line of first-order transitions starting at $\mu = \mu_1$, which distinguishes a high-density and a low-density phase, can now be extended to finite m to form surfaces of first order phase transitions, i.e. surfaces of coexistence of the high- and low-density phases. The regions of low density and temperature under each such surface are separated at the $m = 0$ plane by opposite signs of the chiral

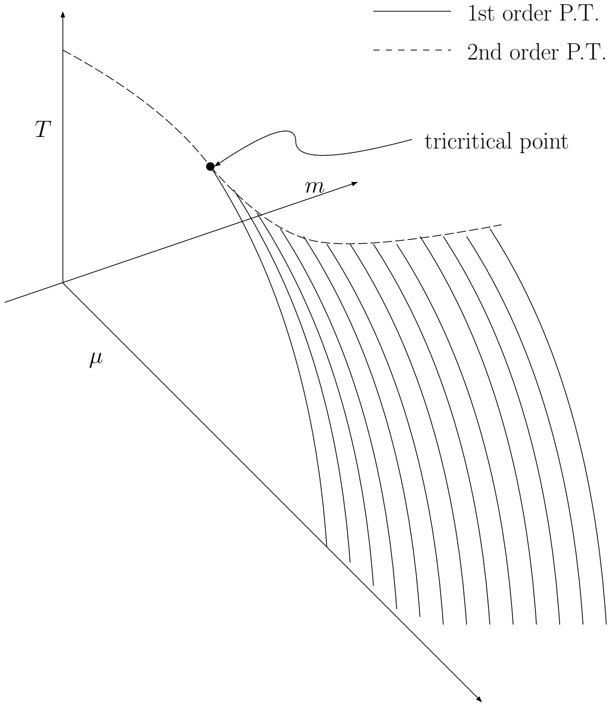

Figure 12.2: Schematic T-μ-m phase diagram and the tricritical point

condensate, i.e. the T-μ-plane under these surfaces corresponds to a plane of first order phase transitions between chiral condensates of opposite sign. Since chiral symmetry is explicitly broken for $m \neq 0$, the high- and low-T/μ phase need not necessarily be separated by a phase transition — a crossover is a also possible. It is therefore possible that the surfaces of first order transitions have bounding lines of second order phase transitions. These lines merge into one line of second-order phase transitions for $m = 0$ at the tricritical point.
The three phases that merge at the critical point therefore are:

- The high-temperature and high-density phase with vanishing chiral condensate.
- The two low-T and low-μ phases with opposite sign of the chiral condensate.

An illustration of the above can be found in figure 12.2.

12.3 Colour superconductivity and colour flavour locking

For low temperatures and high chemical potentials, a mechanism called colour superconductivity has been proposed. A variety of phases can be predicted using this mechanism; the two most important ones are:

Two-flavour colour superconductivity This phase, also referred to as 2SC, appears under the assumption of only two quark flavours whose masses are very small on the energy scales of the problem and can therefore be ignored.

Colour flavour locking If the theory of 2SC is extended to three quark flavours, one finds CFL. Interest in this phase is particularly strong due to the fact that it breaks the chiral symmetry, but by a completely different mechanism than by which it is broken in QCD for low densities.

The only currently known way to create such densities is by gravitational collapse, which takes place in neutron stars. Hence, at least some of these phases, especially CFL, are expected to play an important role in the physics of neutron stars. For example, the specific heat capacity of quark matter, which is linked to the cooling rate of neutron stars, is affected by colour superconductivity effects. Currently, however, there are plans to build collision experiments to explore these phases in more detail.

Throughout this discussion, it will be assumed that the coupling between quarks is weak. Since, as was mentioned before, the high chemical potential in dense matter forces the quarks to occupy high-momentum states, i.e. the Fermi momentum is increased as μ increases. Since the quarks at the Fermi surface are the relevant degrees of freedom for dynamic processes, it can be assumed that those are asymptotically free. As a consequence, perturbative calculations provide valid results in the high-density regime.

12.3.1 Symmetry breaking due to colour superconductivity

CFL

In the case of a theory with three quarks, (u, d, s), a phase commonly referred to as *colour flavour locking* appears. The attractive force that causes the formation of a condensate of quark pairs is provided by the single gluon exchange, which, at weak coupling, dominates the quark interaction. Knowing this, it can be deduced

([6, 7]) that the ground state has nonvanishing condensates

$$\langle \psi^{a\alpha}_{iL}(\vec{p})\psi^{b\beta}_{jL}(-\vec{p})\epsilon_{ab}\rangle = -\langle \psi^{a\alpha}_{iR}(\vec{p})\psi^{b\beta}_{jR}(-\vec{p})\epsilon_{ab}\rangle \propto \epsilon^{\alpha\beta A}\epsilon_{ijA}. \qquad (12.75)$$

Here, indices (α, β) refer to colour, (i, j) to flavour and (a, b) to spin; for A, summation convention applies. Using the identity

$$\epsilon^{\alpha\beta A}\epsilon_{ijA} = \delta^{\alpha}_{i}\delta^{\beta}_{j} - \delta^{\alpha}_{j}\delta^{\beta}_{i} \qquad (12.76)$$

we see that in the condensate (12.75), colour and flavour indices are linked; the condensate is therefore not symmetric under separate rotations of colour or flavour, but only under rotations that simultaneously modify colour and flavour indices.

The full symmetry group of QCD with 3 massless quarks (12.42) was $SU(3)_c \times SU(3)_L \times SU(3)_R \times U(1)_B$. With the above condensates, the $SU(3)_L$ and $SU(3)_R$ chiral symmetries become locked to the colour symmetry $SU(3)_c$. Hence, the full symmetry group of the CFL phase is reduced to

$$SU(3)_{\text{color,L,R}} \times Z_2. \qquad (12.77)$$

Though the condensates do not mix right-handed and left-handed fermions, as it is the case in low-density, low-temperature QCD, the chiral symmetry is effectively broken due to CFL! The baryon number $U(1)_B$ symmetry is also broken: the condensate of quark pairs in the ground state, $\langle QQ'\rangle$, is not invariant under a $U(1)_B$ transformation $Q \to e^{i\alpha}Q$, since $\langle QQ'\rangle \neq e^{2i\alpha}\langle QQ'\rangle$ except for $e^{i\alpha} = -1$, which corresponds to Z_2. This, however, does not imply that baryon number is not conserved. A physical interpretation of the reduced symmetry would be that the quantum number to which it refers (baryon number in this case, electric charge in the case of ordinary superconductivity) can easily be transported within the sample, which directly relates to superconductivity.

In general, a gauge-invariant order parameter is difficult to find for the case of a broken gauge symmetry. For example, in the electroweak theory, such a parameter cannot be found. In the case of CFL, however, order parameters can be found for the breaking of the global symmetries, i.e. the breaking of the chiral $SU(3)_L \times SU(3)_R$ and the $U(1)_B$ baryon number symmetry.

2SC

If the three massless quarks of CFL are replaced by just two, a state called 2SC can be found. Again, an attractive force leading to a BCS instability is provided by the single gluon exchange. However, in this case, the resulting condensate is of a different structure. It is found to be

$$\langle \epsilon_{\alpha\beta 3}\epsilon^{ij}\psi_i^\alpha \psi_j^\beta \rangle \neq 0. \tag{12.78}$$

Again, (α, β) are colour and (i, j) are flavour indices. It can be seen that one colour is distinguished from the others (in this case 3 or blue). This breaks the local $SU(3)_C$ gauge symmetry down to a $SU(2)_C$ symmetry. The ground state condensate also doesn't mix left-handed and right-handed fermions, therefore the chiral $SU(2)_L \times SU(2)_R$ symmetry is not broken in the 2SC phase. Since $U(1)_B$ is also unbroken, no global symmetries are broken. Hence, a symmetry breaking distinguishes the 2SC phase from the phase of low densities and temperatures, where chiral symmetry is dynamically broken. It has been shown that the transition is of first order.

12.3.2 Energy gap in the excitation spectrum

In an ordinary solid, the electron gas description, i.e. the description as an ideal, non-interacting Fermi gas, becomes more and more valid as temperature is decreased since the phonon-electron scattering becomes less and less important. In some materials, however, there is a critical temperature T_c at which the existence of a weak, interacting force leads to the formation of electron bound states, which condensate as so-called Cooper pairs. This is one of the central predictions of the BCS theory of type I superconductivity. For the case of an ordinary superconductor, this attractive interaction is mediated by a dynamical deformation of the ion lattice.

In the case of very dense quark matter, where high-momentum states up to some Fermi momentum p_F are occupied leading to weak coupling in the limit of asymptotic freedom, one might intuitively think (and it was generally accepted for a long time) that the system can be described as a Fermi gas, too. As in the case of the electron gas, there is a screening mechanism, which for the case of QCD has been described in sect. 12.2.2 when referring to the high-temperature QGP. Yet again there are attractive interactions between the quarks, which lead to formation of Cooper pairs.

In the case of colour superconductivity, the well-known effects of superconductivity (of colour charge) and the Meissner-Ochsenfeld effect, i.e. the expulsion of (colour) fields, do apply but have no observable consequences. The most relevant physical aspect therefore is the fact that for a binding energy of E in such a quark pair, the quark energy spectrum has a gap between the ground state and the first excited state which is equal to $\Delta = -\frac{E}{2}$. This affects thermodynamics properties of such high-density quark matter.

The central question therefore would be to calculate this energy gap. For a long time, it was thought that the binding energy is very low around 1 MeV ([8]). In the late 1990s, non-perturbative effects have been proposed ([9]) leading to much higher energy gaps on the order of 100 MeV.

12.3.3 PHYSICAL CONSEQUENCES OF CFL

PSEUDO-GOLDSTONE BOSONS We saw that in the case of CFL, $SU(3)_c \times SU(3)_L \times SU(3)_R$ is reduced to $SU(3)_{\mathrm{c,L,R}}$. From sect. 12.1.3, we know that for each broken global continuous symmetry, a massless Goldstone boson occurs and for each broken gauge symmetry, the gauge vector boson acquires a finite mass. Due to the breaking of the colour symmetry, which is the gauge group, we expect the gauge bosons, i.e. the gluons, to acquire mass.

Of the Goldstone bosons due to broken chiral symmetry, an octet appears as oscillations of the diquark condensates (12.75), which can be described by an effective Lagrangian. If the masses of the light quarks are assumed to take non-zero values, the symmetry is not exact any more, so that pseudo-Goldstone bosons are created which, as opposed to normal Goldstone bosons, have a finite mass. In the case of the CFL bosons, they can be considered as physical mesons and masses can be calculated, giving, for example

$$m_{\pi^\pm}^2 = \frac{2c}{f_\pi^2} m_s(m_u + m_d), \ m_{K^\pm}^2 = \frac{2c}{f_\pi^2} m_d(m_u + m_s), \tag{12.79}$$

where c, f_π are coefficients of the effective Lagrangian. Due to the weak coupling at asymptotically high densities in CFL, analytic calculations for these coefficients are possible and give estimates of the mass of, for example, the kaons, in the range of $m_{K^\pm} \approx 5 \ldots 20\mathrm{MeV}$ for $\mu = 400\mathrm{MeV}$.

Additionally, the breaking of $U(1)_B$ to Z_2 is associated with the appearance of a singlet Goldstone boson, which is responsible for the superconductive transport of colour charge.

NEUTRON STAR COOLING A neutron star is the result of a supernova created by a star with a mass between 1.44 and 3 times the mass of the sun. For such stars, the supernova collapses after it is "dead“, but the mass is not high enough to create a black hole. Neutron stars are objects of extraordinary density, which is around 10^{12} kg/cm^3 in the core. Their radius is about 10 km.

One of the observable properties of a neutron star is its cooling, which, at least during some parts of its life cycle, is dominated by neutrino emission and the heat

capacity of the star. Since the heat capacity is affected by the physical situation at the Fermi surface, colour superconductivity will have some effect on the cooling rate. In the CFL phase, all quarks have a gap in the excitation spectrum with $\Delta \gg T$, hence their thermal excitation is very low, $\propto \exp(-\Delta/T)$.
Hence, there is no contribution to the specific heat from the quarks; the bulk of the specific heat is due to the electrons, with some contributions by the pseudo-Goldstone-bosons discussed in the last paragraph. The core is therefore only cooled by contact to the outer, hadronic-matter-shell of the neutron star.

12.4 Relativistic Heavy-Ion Collisions

The way to experimentally study the quark-gluon plasma, i.e. QCD at high temperatures and low, yet finite chemical potentials, is through relativistic heavy-ion collisions ([4, Ch. 8.5], [10, Ch. 4]). In these collisions, particle accelerators are used to collide heavy nuclei such as sulphur, lead or gold with very high energies. The first experiments, for example SPS at CERN, had center of mass (CM) energies in the range $2A \ldots 18A$ GeV, where A is the number of nucleons in the nucleus. Current experiments, such as the RHIC collider in Brookhaven, NY, reach energies of $200A$ GeV. At the LHC in CERN, expected CM energies are $5500A$ GeV. There are plans to build collider experiments that could explore the region of high densities at low temperatures, using even heavier nuclei such as uranium, but using lower collision energies. One facility where this is planned is CBM/FAIR at GSI, Darmstadt.

12.4.1 Stages of a RHI collision

Relativistic heavy ion collisions are usually described in four phases (see also fig. 12.3), where the exact distinction between phases differs between authors. This roughly follows [5], with additional input from [4].

- In the first phase, the ultra-relativistic nuclei, which are deformed in the center-of-mass system due to relativistic length contraction, approach each other and partons initially scatter from each other. Phase-space density is very high and the system can be approximated by classical fields. Interactions at this stage occur at a very short timescale, $t_{\text{int}} \approx 0.1 - 0.3$ fm/c. In this step, according to current calculations, energy densities of up to 20 GeV fm^{-3} occur.

- The equilibration or thermalization of the system takes place through multiple parton scattering. Thermalization times are estimated to be around

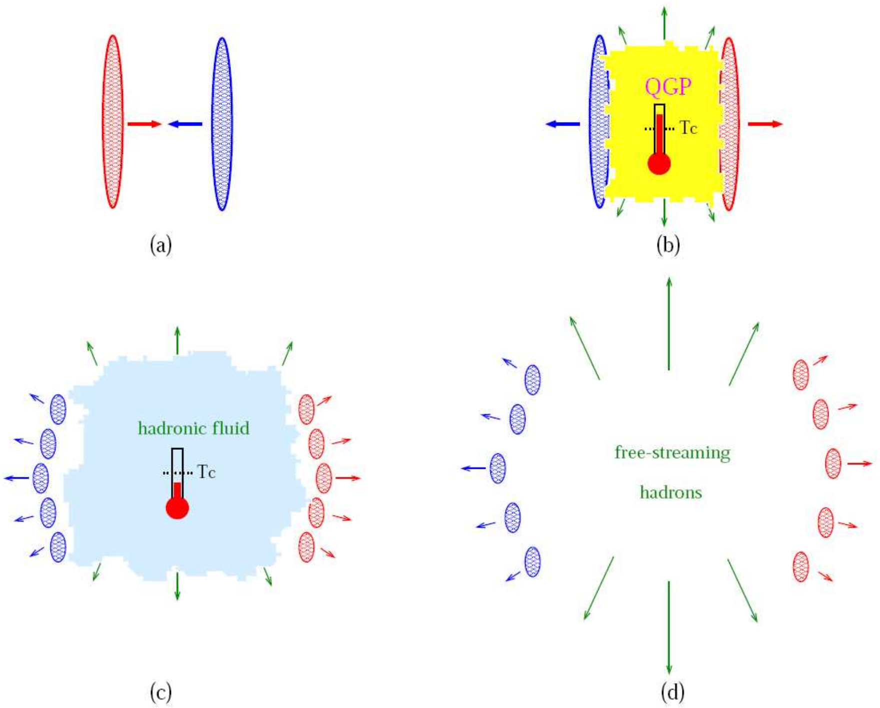

Figure 12.3: Phases of a RHI collision: a) approaching nuclei, b) thermalization and formation of the plasma, c) hydrodynamic expansion, d) hadron formation. Plot taken from [10, p. 20].

$t_{\text{therm}} \approx 0.5 - 1.0$ fm/c.

- The expansion of the quark-gluon plasma can be described through relativistic fluid dynamics. The flow is expected to be centered around the collision axis, i.e. the expansion is a one-dimensional process. The cooling law can be predicted be $T(t) \propto t^{-1/3}$, and the expanding plasma remains thermalized for $t_{\text{dec}} \approx 10$ fm/c.
- Finally, T drops below T_c and hadrons are formed. The timescale of this process is still an open question.

12.4.2 Signatures of the QGP in RHIC

Since the dynamics of QGP are very difficult to treat theoretically, it is also very difficult to obtain information about the QGP from the observed hadrons and leptons in a collision. Out of the many signatures of QGP that are expected to be seen in experimental data of RHI collisions, only two will be described below which relate directly to what has been said in sect. 12.2.2.

J/Ψ SUPPRESSION

One physical signature of QGP creation that was hoped to be observable in RHI collisions is the suppression of J/Ψ ($c\bar{c}$) production. The relatively long decay time of the J/Ψ, which is the reason for the appearance of a sharp and high resonance peak in non-QGP collisions, i.e. $p\bar{p}$, is caused by two facts:

- Due to confinement, i.e. the linearly increasing potential between the two constituents of the meson, these constituents are not free to pair with other particles.

- Since the mass of the J/Ψ, 3096.9 MeV, is lower than that of two mesons containing a charm and a light quark, e.g. the various types of D (mass $\approx$ 1870 MeV), a process in which it is broken up into two such mesons with continuous quark lines is not possible. It therefore has to decay via quark-antiquark annihilation and production of gluons, which is suppressed.

In 1986, it was proposed ([11]) that the creation of the J/Ψ is suppressed by the creation of QGP. The reason for this was thought to be the effect of deconfinement in a high-temperature plasma and the screening of the attractive forces as described in sect. 12.2.2 ([10, 12, 4]). If the screening length λ_D falls below the radius of the J/Ψ, the pair can dissociate and the isolated heavy quarks can create mesons with light quarks as well. This should in principle extend to other heavy mesons.

The effect of heavy meson suppression has been measured experimentally, as seen in fig. 12.4.2. Recently, however, lattice simulations have shown that heavy mesons are more stable than expected — this is still an area of open discussion.

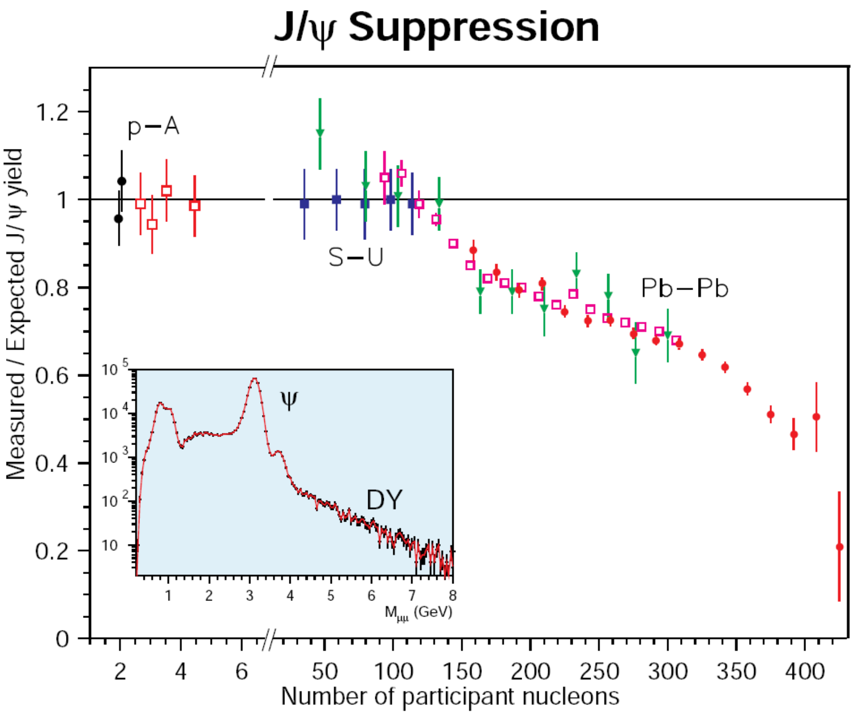

Figure 12.4: Heavy meson production suppression in RHIC experiments at SPS. Plot taken from [10, p. 22].

Bibliography

[1] J. Goldstone, A. Salam, and S. Weinberg, Phys. Rev. **127**, 965 (1962).

[2] M. Peskin and D. Schroeder, *An Introduction to Quantum Field Theory* (Addison-Wesley, 1995).

[3] A. Chodos, Phys. Rev. D **9**, 3471 (1974).

[4] J. Kogut and M. Stephanov, *The Phases of Quantum Chromodynamics* (Cambridge University Press, 2004).

[5] B. Müller, *Large Hadron Phenomenology* (Taylor & Francis, 2004), Scottish Graduate Series.

[6] K. Rajagopal and F. Wilczek (2000), hep-ph/0011333.

[7] M. Alford and F. Wilczek, *Color-flavor locking and chiral symmetry breaking in high density qcd*, Phys. Lett. B **537**, 443 (1999), hep-ph/9804403.

[8] D. Bailin and A. Love, Phys. Rep. **81**, 325 (1984).

[9] R. Rapp, T. Schäfer, E. Shuryak, and M. Velkovsky, Phys. Rev. Lett. **81**, 53 (1998).

[10] S. Hands, *The phase diagram of qcd*, Contemp. Phys. **42**, 209 (2001).

[11] T. Matsui and H. Satz, Phys. Lett. B **178**, 416 (1986).

[12] F. Karsch, *Deconfinement and quarkonium suppression*, Eur. Phys. J. C **43**, 35 (2005), hep-lat/0502014.

Chapter 13

BCS theory of superconductivity

Thomas Burgener
supervisor: Dr. Christian Iniotakis

In this chapter BCS theory for conventional superconductors will be presented. Starting with a discussion of the Cooper problem I continue by introducing a model hamiltonian and solving it with a Bogoliubov-Valatin transformation. After having found a solution of the hamiltonian I'm going to calculate the critical temperature, the temperature dependence of the order parameter and some thermodynamic quantities. At the end I briefly introduce the difference between type I and type II superconductors.

13.1 Introduction

In 1957 John Bardeen, Leon N. Cooper and John R. Schrieffer [1] published their work about superconductivity. For this work they received the Nobel prize in 1972. The theory is today called the BCS theory, coming from the first letters of the names of its inventors. The theory is formulated in terms of a mean-field theory and was the first "working" *microscopic* theory for superconductors. In its original form the theory was only applied to conventional superconductors.

In this chapter I'd like to present the main features of the BCS theory. Most of the things I show here are from the book of Tinkham [2].

13.2 Cooper Pairs

The basic concept for understanding superconductivity within the context of BCS theory is the formation of Cooper pairs. I will first discuss how these bound pairs of electrons are formed and then explain how an attractive interaction between two electrons can occur.

13.2.1 Bound Pairs of Electrons

The basic idea that even a weak attraction can bind pairs of electrons into a bound state goes back to Cooper [3]. He showed that the Fermi sea of electrons is unstable against the formation of at least one bound pair, regardless of how weak the interaction is, so long as it is attractive. This result is a consequence of the Fermi statistic and of the existence of the Fermi sea background.

To show how the binding comes about, we consider a simple model of two electrons added to a filled Fermi sea at $T = 0$, with the assumption, that the extra electrons interact with each other but not with the electrons in the sea, except via the exclusion principle. Therefore we are looking for a two-particle wavefunction. We expect the lowest-energy state to have zero momentum. Including the antisymmetric singlet spin function suggests building up a wavefunction of the sort

$$\Psi_0(\mathbf{r}_1, \mathbf{r}_2) = \sum_{\mathbf{k}} \left(g_{\mathbf{k}} e^{i\mathbf{k}\cdot\mathbf{r}_1} e^{-i\mathbf{k}\cdot\mathbf{r}_2} \right) \left(|\uparrow\downarrow\rangle - |\downarrow\uparrow\rangle \right). \tag{13.1}$$

Taking into account the antisymmetry of the total wavefunction with respect to exchange of the two electrons leads to the condition

$$g_{\mathbf{k}} \overset{!}{=} g_{-\mathbf{k}}$$

for the coefficients in the wavefunction. By inserting (13.1) into the Schrödinger equation of the problem, one can show that the weighting coefficients $g_{\mathbf{k}}$ and the energy eigenvalue E are to be determined by solving

$$(E - 2\epsilon_{\mathbf{k}}) g_{\mathbf{k}} = \sum_{k > k_f} V_{\mathbf{k}\mathbf{k}'} g_{\mathbf{k}'}. \tag{13.2}$$

In this expression, the $\epsilon_{\mathbf{k}}$ are unperturbed plane-wave energies and the $V_{\mathbf{k}\mathbf{k}'}$ are the matrix elements of the interaction potential

$$V_{\mathbf{k}\mathbf{k}'} = \frac{1}{\Omega} \int V(\mathbf{r}) e^{i(\mathbf{k}'-\mathbf{k})\cdot\mathbf{r}} d\mathbf{r}, \tag{13.3}$$

where $\mathbf{r} = \mathbf{r}_1 - \mathbf{r}_2$ and Ω is the normalization volume. If a set of $g_{\mathbf{k}}$ satisfying (13.2) with $E < 2E_F$ can be found, then a bound pair state exists.

Since it is hard to analyze this situation for general $V_{\mathbf{kk}'}$, Cooper introduced the very serviceable approximation of the interaction potential as a step function

$$V_{\mathbf{kk}'} = \begin{cases} -V & , E_F < \epsilon_{\mathbf{k}}, \epsilon_{\mathbf{k}'} < E_F + \hbar\omega_c \\ 0 & , \text{otherwise} \end{cases} , \tag{13.4}$$

where E_F is the Fermi energy and $\hbar\omega_c$ is a cutoff energy. Then from (13.2) we get

$$g_{\mathbf{k}} = V \frac{\sum g_{\mathbf{k}'}}{2\epsilon_{\mathbf{k}} - E}. \tag{13.5}$$

Summing up both sides and canceling $\sum g_{\mathbf{k}}$ gives

$$\frac{1}{V} = \sum_{k > k_F} \frac{1}{2\epsilon_{\mathbf{k}} - E}. \tag{13.6}$$

When we replace the summation by an integration, with $N(0)$ denoting the density of states at the Fermi level for electrons of one spin orientation, this becomes

$$\frac{1}{V} = N(0) \int_{E_F}^{E_F + \hbar\omega_c} \frac{d\epsilon}{2\epsilon - E} = \frac{1}{2} N(0) \ln \frac{2E_F - E + 2\hbar\omega_c}{2E_F - E}. \tag{13.7}$$

In most classic superconducters, it is found that $N(0)V < 0.3$ and this allows use of the so-called *weak-coupling approximation*, valid for $N(0)V \ll 1$, in which the solution to the preceding equation can be written as

$$E \approx 2E_F - 2\hbar\omega_c e^{-\frac{2}{N(0)V}}. \tag{13.8}$$

Thus, there *is* a bound state with negative energy with respect to the Fermi surface made up entirely of electrons with $k > k_F$. The contribution of the attractive potential leads to binding regardless how small V is. Note that the form of the binding energy is not analytic at $V = 0$; i.e. it cannot be expanded in powers of V. As a result, it cannot be obtained by perturbation theory, a fact that greatly delayed the genesis of the theory.

13.2.2 Origin of the Attractive Interaction

We now have to understand the origin of the negative $V_{\mathbf{kk}'}$ needed for superconductivity.

To get a negative $V_{\mathbf{kk}'}$ we have to take the electron-lattice interactions into account. The physical idea is that the first electron polarizes the medium by attracting positive ions; these excess positive ions in turn attract the second electron, resulting in an effective attractive interaction between the electrons. If this attraction is strong enough to override the screened Coulomb interaction, it gives rise to a net attractive interaction, and superconductivity results. Historically, the importance of the electron-lattice interaction in explaining superconductivity was first suggested by Fröhlich [4] in 1950. This suggestion was confirmed experimentally by the discovery [5], [6] of the *isotope effect*, i.e. the proportionality of the critical temperature T_c and the critical magnetic field H_c to $M^{-1/2}$ for isotopes with mass M of the same element.[1]

Obviously, these lattice deformations are correlated to the characteristic phonon frequencies of the material. From momentum conservation, we can see that if an electron is scattered from $\mathbf{k}$ to $\mathbf{k}'$, the relevant phonon must carry the momentum $\mathbf{q} = \mathbf{k} - \mathbf{k}'$, and the characteristic frequency must then be the phonon frequency $\omega_{\mathbf{q}}$. It is plausible that the phonon contribution to the screening function is proportional to $(\omega^2 - \omega_{\mathbf{q}}^2)^{-1}$. This resonance denominator gives a *negative* sign if $\omega < \omega_{\mathbf{q}}$, corresponding to the physical argument above; for higher frequencies, i.e. electron energy difference larger than $\hbar\omega_{\mathbf{q}}$, the interaction becomes repulsive. Thus, the cutoff energy $\hbar\omega_c$ of Cooper's attractive matrix element $-V$ is expected to be of the order of the Debye energy $\hbar\omega_D = k\Theta_D$, which characterizes the cutoff of the phonon spectrum.

13.3 BCS Theory

I'd like to present now the BCS theory for conventional superconductors. I start with introducing the model hamiltonian, which will be solved using a Bogoliubov-Valatin-Transformation. At the end of the section I will calculate the condensation energy and show, that the superconducting state is energetically more favorable.

13.3.1 The Model Hamiltonian

We have seen that the Fermi sea is unstable against the formation of a bound Cooper pair when the net interaction is attractive. Clearly we must then expect

---

[1] The critical temperature and the critical field will be introduced and discussed later in the chapter.

pairs to condense until an equilibrium state is reached. Because we work now with a system of many electrons, we have to find a smart way to handle the many-body wavefunction. This can be done by using second quantisation: Let's introduce the creation operator $c^\dagger_{\mathbf{k}\sigma}$, which creates an electron of momentum $\mathbf{k}$ and spin σ, and the correspondig annihilation operator $c_{\mathbf{k}\sigma}$. These operators obey the standard anticommutation relations for fermions:

$$\{c_{\mathbf{k}\sigma}, c^\dagger_{\mathbf{k}'\sigma'}\} \equiv c_{\mathbf{k}\sigma} c^\dagger_{\mathbf{k}'\sigma'} + c^\dagger_{\mathbf{k}'\sigma'} c_{\mathbf{k}\sigma} = \delta_{\mathbf{k}\mathbf{k}'}\delta_{\sigma\sigma'} \tag{13.9}$$

$$\{c_{\mathbf{k}\sigma}, c_{\mathbf{k}'\sigma'}\} = 0 = \{c^\dagger_{\mathbf{k}\sigma}, c^\dagger_{\mathbf{k}'\sigma'}\}. \tag{13.10}$$

Additionally the particle number operator $n_{\mathbf{k}\sigma}$ is defined by

$$n_{\mathbf{k}\sigma} \equiv c^\dagger_{\mathbf{k}\sigma} c_{\mathbf{k}\sigma}. \tag{13.11}$$

With these operatos we can write down our *pairing hamiltonion*:

$$\mathcal{H} = \sum_{\mathbf{k}\sigma} \epsilon_{\mathbf{k}} n_{\mathbf{k}\sigma} + \sum_{\mathbf{k}\mathbf{l}} V_{\mathbf{k}\mathbf{l}} c^\dagger_{\mathbf{k}\uparrow} c^\dagger_{-\mathbf{k}\downarrow} c_{-\mathbf{l}\downarrow} c_{\mathbf{l}\uparrow}. \tag{13.12}$$

The first sum corresponds to the kinetic part for (single/unpaired) electrons and the second sum describes the annihilation of a Cooper pair $c_{-\mathbf{l}\downarrow}c_{\mathbf{l}\uparrow}$ and the creation of another one $c^\dagger_{\mathbf{k}\uparrow}c^\dagger_{-\mathbf{k}\downarrow}$. Clearly this hamiltonian omits many other terms which involve electrons not paired as $(\mathbf{k}\uparrow, -\mathbf{k}\downarrow)$. Such terms have zero expectation value in the BCS ground-state wavefunction but may be important in other applications. To regulate the mean number of particles $\bar{N}$, we add a term $-\mu\mathcal{N}$, where μ is the chemical potential and $\mathcal{N}$ is the particle-number. Mathematically this is equivalent to taking the zero of kinetic energy to be at μ (or E_F). The hamiltonian then reads as

$$\mathcal{H} - \mu\mathcal{N} = \sum_{\mathbf{k}\sigma} \xi_{\mathbf{k}} n_{\mathbf{k}\sigma} + \sum_{\mathbf{k}\mathbf{l}} V_{\mathbf{k}\mathbf{l}} c^\dagger_{\mathbf{k}\uparrow} c^\dagger_{-\mathbf{k}\downarrow} c_{-\mathbf{l}\downarrow} c_{\mathbf{l}\uparrow}. \tag{13.13}$$

We now apply mean-field theory to this hamiltonian. We first note that because of coherence, operators such as $c_{-\mathbf{k}\downarrow}c_{\mathbf{k}\uparrow}$ can have nonzero expectation values $b_{\mathbf{k}}$ in the superconducting state, rather than averaging to zero as in a normal metal, where all phases are random. Moreover, because of the large numbers of particles involved, the fluctuation about these expectation values should be small. This suggests that it will be useful to express such a product of operators formally as

$$c_{-\mathbf{k}\downarrow}c_{\mathbf{k}\uparrow} = b_{\mathbf{k}} + (c_{-\mathbf{k}\downarrow}c_{\mathbf{k}\uparrow} - b_{\mathbf{k}}) \tag{13.14}$$

and subsequently neglect quantities which are bilinear in the presumably small fluctuation term in parantheses. By inserting (13.14) in our pairing hamiltonion

(13.13), we obtain the so-called *model hamiltonian*

$$\mathcal{H}_M - \mu\mathcal{N} = \sum_{\mathbf{k}\sigma} \xi_{\mathbf{k}} c^\dagger_{\mathbf{k}\sigma} c_{\mathbf{k}\sigma} + \sum_{\mathbf{kl}} V_{\mathbf{kl}} (c^\dagger_{\mathbf{k}\uparrow} c^\dagger_{-\mathbf{k}\downarrow} b_{\mathbf{l}} + b^*_{\mathbf{k}} c_{-\mathbf{l}\downarrow} c_{\mathbf{l}\uparrow} - b^*_{\mathbf{k}} b_{\mathbf{l}}), \tag{13.15}$$

where the $b_{\mathbf{k}}$ are to be determined self-consistently, so that

$$b_{\mathbf{k}} \equiv \langle c_{-\mathbf{k}\downarrow} c_{\mathbf{k}\uparrow} \rangle . \tag{13.16}$$

We define further

$$\Delta_{\mathbf{k}} = -\sum_{\mathbf{l}} V_{\mathbf{kl}} b_{\mathbf{l}} = -\sum_{\mathbf{l}} V_{\mathbf{kl}} \langle c_{-\mathbf{l}\downarrow} c_{\mathbf{l}\uparrow} \rangle , \tag{13.17}$$

which will turn out to be the order parameter. In terms of $\Delta_{\mathbf{k}}$, the model hamiltonian becomes

$$\mathcal{H}_M - \mu\mathcal{N} = \sum_{\mathbf{k}\sigma} \xi_{\mathbf{k}} c^\dagger_{\mathbf{k}\sigma} c_{\mathbf{k}\sigma} - \sum_{\mathbf{k}} (\Delta_{\mathbf{k}} c^\dagger_{\mathbf{k}\uparrow} c^\dagger_{-\mathbf{k}\downarrow} + \Delta^*_{\mathbf{k}} c_{-\mathbf{k}\downarrow} c_{\mathbf{k}\uparrow} - \Delta_{\mathbf{k}} b^*_{\mathbf{k}}), \tag{13.18}$$

which now only consists of terms with products of two operators.

13.3.2 Bogoliubov-Valatin-Transformations

We now have to diagonalize the hamiltonian (13.18). This can be done by applying a suitable linear transformation to define new Fermi operators $\gamma_{\mathbf{k}}$. As shown independently by Bogoliubov [7] and by Valatin [8], the appropriate transformation is specified by

$$c_{\mathbf{k}\uparrow} = u^*_{\mathbf{k}} \gamma_{\mathbf{k}\uparrow} + v_{\mathbf{k}} \gamma^\dagger_{-\mathbf{k}\downarrow} \tag{13.19a}$$

$$c^\dagger_{-\mathbf{k}\downarrow} = -v^*_{\mathbf{k}} \gamma_{\mathbf{k}\uparrow} + u_{\mathbf{k}} \gamma^\dagger_{-\mathbf{k}\downarrow}, \tag{13.19b}$$

where the numerical coefficients $u_{\mathbf{k}}$ and $v_{\mathbf{k}}$ are complex numbers and satisfy $|u_{\mathbf{k}}|^2 + |v_{\mathbf{k}}|^2 = 1$. Substituting these new operators into the model hamiltonian (13.18), and carrying out the indicated products taking into account the noncommutivity of the operators, we obtain

$$\begin{aligned}
\mathcal{H}_M - \mu\mathcal{N} \;=\; & \sum_{\mathbf{k}} \xi_{\mathbf{k}} \Big((|u_{\mathbf{k}}|^2 - |v_{\mathbf{k}}|^2)(\gamma^\dagger_{\mathbf{k}\uparrow}\gamma_{\mathbf{k}\uparrow} + \gamma^\dagger_{-\mathbf{k}\downarrow}\gamma_{-\mathbf{k}\downarrow}) \\
& + 2|v_{\mathbf{k}}|^2 + 2u^*_{\mathbf{k}} v^*_{\mathbf{k}} \gamma_{-\mathbf{k}\downarrow}\gamma_{\mathbf{k}\uparrow} + 2u_{\mathbf{k}} v_{\mathbf{k}} \gamma^\dagger_{\mathbf{k}\uparrow}\gamma^\dagger_{-\mathbf{k}\downarrow} \Big) \\
& + \sum_{\mathbf{k}} \Big((\Delta_{\mathbf{k}} u_{\mathbf{k}} v^*_{\mathbf{k}} + \Delta^*_{\mathbf{k}} u^*_{\mathbf{k}} v_{\mathbf{k}})(\gamma^\dagger_{\mathbf{k}\uparrow}\gamma_{\mathbf{k}\uparrow} + \gamma^\dagger_{-\mathbf{k}\downarrow}\gamma_{-\mathbf{k}\downarrow} - 1) \\
& + (\Delta_{\mathbf{k}} {v^*_{\mathbf{k}}}^2 - \Delta^*_{\mathbf{k}} {u^*_{\mathbf{k}}}^2)\gamma_{-\mathbf{k}\downarrow}\gamma_{\mathbf{k}\uparrow} \\
& + (\Delta^*_{\mathbf{k}} v^2_{\mathbf{k}} - \Delta_{\mathbf{k}} u^2_{\mathbf{k}})\gamma^\dagger_{\mathbf{k}\uparrow}\gamma^\dagger_{-\mathbf{k}\downarrow} + \Delta_{\mathbf{k}} b^*_{\mathbf{k}} \Big) .
\end{aligned} \tag{13.20}$$

Now, if we choose $u_{\mathbf{k}}$ and $v_{\mathbf{k}}$ so that the coefficients of $\gamma_{-\mathbf{k}\downarrow}\gamma_{\mathbf{k}\uparrow}$ and $\gamma^\dagger_{\mathbf{k}\uparrow}\gamma^\dagger_{-\mathbf{k}\downarrow}$ vanish, the hamiltonian is diagonalized; e.g. it is carried into a form containing only constants plus terms proportional to the occupation numbers $\gamma^\dagger_{\mathbf{k}\uparrow}\gamma_{\mathbf{k}\uparrow}$. The coefficients of both undesired terms are zero if

$$\begin{aligned}
& 2\xi_{\mathbf{k}}u_{\mathbf{k}}v_{\mathbf{k}} + \Delta^*_{\mathbf{k}}v^2_{\mathbf{k}} - \Delta_{\mathbf{k}}u^2_{\mathbf{k}} = 0 \qquad \Big| \cdot \frac{\Delta^*_{\mathbf{k}}}{u^2_{\mathbf{k}}} \\
\Rightarrow \quad & \left(\frac{\Delta^*_{\mathbf{k}}v_{\mathbf{k}}}{u_{\mathbf{k}}}\right)^2 + 2\xi_{\mathbf{k}}\left(\frac{\Delta^*_{\mathbf{k}}v_{\mathbf{k}}}{u_{\mathbf{k}}}\right) - |\Delta_{\mathbf{k}}|^2 = 0 \\
\Rightarrow \quad & \frac{\Delta^*_{\mathbf{k}}v_{\mathbf{k}}}{u_{\mathbf{k}}} = \underbrace{\sqrt{\xi^2_{\mathbf{k}} + |\Delta_{\mathbf{k}}|^2}}_{\equiv E_{\mathbf{k}}} - \xi_{\mathbf{k}} \equiv E_{\mathbf{k}} - \xi_{\mathbf{k}} \qquad (13.21)
\end{aligned}$$

Using the normalization condition $|u_{\mathbf{k}}|^2 + |v_{\mathbf{k}}|^2 = 1$ we can solve for the coefficients and find

$$|v_{\mathbf{k}}|^2 = 1 - |u_{\mathbf{k}}|^2 = \frac{1}{2}\left(1 - \frac{\xi_{\mathbf{k}}}{E_{\mathbf{k}}}\right). \qquad (13.22)$$

The phases of $u_{\mathbf{k}}$, $v_{\mathbf{k}}$ and $\Delta_{\mathbf{k}}$ are related by (13.21) since $\Delta^*_{\mathbf{k}}v_{\mathbf{k}}/u_{\mathbf{k}}$ is real. That is, the phase of $v_{\mathbf{k}}$ relative to $u_{\mathbf{k}}$ must be the phase of $\Delta_{\mathbf{k}}$. There is no loss in generality in choosing all the $u_{\mathbf{k}}$ to be real and positive. If we do so, $v_{\mathbf{k}}$ and $\Delta_{\mathbf{k}}$ must have the same phase.

13.3.3 CALCULATION OF THE CONDENSATION ENERGY

Next we like to calculate the condensation energy. Therefore we need the ground state wavefunction of the superconducting state. BCS took an ansatz for the ground state of the following form

$$|\Psi_G\rangle = \prod_{\mathbf{k}}(u_{\mathbf{k}} + v_{\mathbf{k}}c^\dagger_{\mathbf{k}\uparrow}c^\dagger_{-\mathbf{k}\downarrow})\,|0\rangle \qquad (13.23)$$

where $|u_{\mathbf{k}}|^2 + |v_{\mathbf{k}}|^2 = 1$. This form implies that the probability of the pair $(\mathbf{k}\uparrow, -\mathbf{k}\downarrow)$ being occupied is $|v_{\mathbf{k}}|^2$, whereas the probability that it is unoccupied is $|u_{\mathbf{k}}|^2 = 1 - |v_{\mathbf{k}}|^2$. It is important to note, that first $|\Psi_G\rangle$ does not conserve the particle number[2], and second it is the vacuum state for the γ operators, e.g.

$$\gamma_{\mathbf{k}\uparrow}\,|\Psi_G\rangle = 0 = \gamma_{-\mathbf{k}\downarrow}\,|\Psi_G\rangle\,. \qquad (13.24)$$

---

[2] However, the actual particle number is very sharply peaked about an averaged value $\bar{N}$. For details see section 3.3 of [2]

We first calculate the energy of the ground state in the superconducting phase to be

$$\begin{aligned}\langle\Psi_G|\,\mathcal{H}-\mu\mathcal{N}\,|\Psi_G\rangle &= 2\sum_{\mathbf{k}}\xi_{\mathbf{k}}v_{\mathbf{k}}^2+\sum_{\mathbf{kl}}V_{\mathbf{kl}}u_{\mathbf{k}}v_{\mathbf{k}}u_{\mathbf{l}}v_{\mathbf{l}}\\ &= \sum_{\mathbf{k}}\left(\xi_{\mathbf{k}}-\frac{\xi_{\mathbf{k}}^2}{E_{\mathbf{k}}}\right)-\frac{\Delta^2}{V} \qquad (13.25)\end{aligned}$$

where we again used the approximativ potential introduced in 13.2. The normal state at $T=0$ corresponds to the BCS state with $\Delta=0$, in which case $E_{\mathbf{k}}=|\xi_{\mathbf{k}}|$. Thus the energy of the normal state is given by

$$\langle\Psi_n|\,\mathcal{H}-\mu\mathcal{N}\,|\Psi_n\rangle=\sum_{|\mathbf{k}|<k_F}2\xi_{\mathbf{k}}. \qquad (13.26)$$

By taking the difference of these two energies we get an expression for the condensation energy to be

$$\begin{aligned}\langle E\rangle_s-\langle E\rangle_n &= \sum_{|\mathbf{k}|>k_F}\left(\xi_{\mathbf{k}}-\frac{\xi_{\mathbf{k}}^2}{E_{\mathbf{k}}}\right)+\sum_{|\mathbf{k}|<k_F}\left(-\xi_{\mathbf{k}}-\frac{\xi_{\mathbf{k}}^2}{E_{\mathbf{k}}}\right)-\frac{\Delta^2}{V}\\ &= 2\sum_{|\mathbf{k}|>k_F}\left(\xi_{\mathbf{k}}-\frac{\xi_{\mathbf{k}}^2}{E_{\mathbf{k}}}\right)-\frac{\Delta^2}{V}\\ &= \left(\frac{\Delta^2}{V}-\frac{1}{2}N(0)\Delta^2\right)-\frac{\Delta^2}{V}=-\frac{1}{2}N(0)\Delta^2. \qquad (13.27)\end{aligned}$$

This shows us that the superconducting state has lower energy than the normal state.

13.4 FINITE TEMPERATURES

So far we looked only at the ground state properties of our superconductor. In this section I'd like to discuss finite temperature effects, including the interpretation of $\Delta_{\mathbf{k}}$ as an energy gap in the excitation spectrum, the determination of the critical temperature T_c and the calculation of some thermodynamic quantities.

13.4.1 EXCITATIONS AND THE ENERGY GAP

If we insert (13.22)) in the model hamiltonian (13.18) we get

$$\mathcal{H}_M-\mu\mathcal{N}=\sum_{\mathbf{k}}(\xi_{\mathbf{k}}-E_{\mathbf{k}}+\Delta_{\mathbf{k}}b_{\mathbf{k}}^*)+\sum_{\mathbf{k}}E_{\mathbf{k}}(\gamma_{\mathbf{k}\uparrow}^\dagger\gamma_{\mathbf{k}\uparrow}+\gamma_{-\mathbf{k}\downarrow}^\dagger\gamma_{-\mathbf{k}\downarrow}). \qquad (13.28)$$

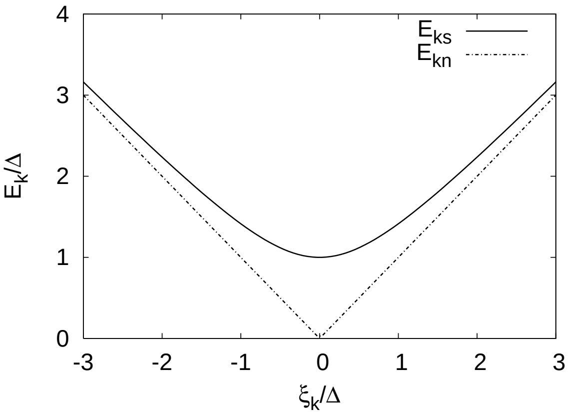

Figure 13.1: Energies of elementary excitations in the normal and superconducting states as functions of $\xi_{\mathbf{k}}$.

The first sum is simply a constant and the second sum gives the increase in energy above the ground state in term of the number operators $\gamma^\dagger_{\mathbf{k}\sigma}\gamma_{\mathbf{k}\sigma}$. Thus, the $\gamma^\dagger_{\mathbf{k}\sigma}$ operators describe the elementary quasi-particle excitations of the system[3]. The energies of these excitations are given by

$$E_{\mathbf{k}} = \sqrt{\xi^2_{\mathbf{k}} + |\Delta_{\mathbf{k}}|^2}. \tag{13.29}$$

A plot of the excitation spectrum is given in Figure 13.1. This also shows us that $\Delta_{\mathbf{k}}$ plays the role of an energy gap or minimum excitation energy since even at the Fermi surface, where $\xi_{\mathbf{k}} = 0$, $E_{\mathbf{k}} = |\Delta_{\mathbf{k}}| > 0$.

We can compute the energy gap $\Delta_{\mathbf{k}}$ by rewriting (13.17) in terms of the γ operators:

$$\begin{aligned}
\Delta_{\mathbf{k}} &= -\sum_{\mathbf{l}} V_{\mathbf{kl}} \langle c_{-\mathbf{l}\downarrow} c_{\mathbf{l}\uparrow} \rangle \\
&= -\sum_{\mathbf{l}} V_{\mathbf{kl}} u^*_{\mathbf{l}} v_{\mathbf{l}} \left\langle 1 - \gamma^\dagger_{\mathbf{l}\uparrow}\gamma_{\mathbf{l}\uparrow} - \gamma^\dagger_{-\mathbf{l}\downarrow}\gamma_{-\mathbf{l}\downarrow} \right\rangle \\
&= -\sum_{\mathbf{l}} V_{\mathbf{kl}} u^*_{\mathbf{l}} v_{\mathbf{l}} (1 - 2f(E_{\mathbf{l}})) \\
&= -\sum_{\mathbf{l}} V_{\mathbf{kl}} \frac{\Delta_{\mathbf{l}}}{2E_{\mathbf{l}}} \tanh \frac{\beta E_{\mathbf{l}}}{2}.
\end{aligned} \tag{13.30}$$

---

[3] Such quasi-particles are coherent particle-hole excitations: With (13.19) the $\gamma^\dagger_{\mathbf{k}\sigma}$ operators always consist of an electron creation and annihilation operator, and coherence comes from condition (13.21).

At the third equality we used that the γ operators describe fermions and therefore we can replace the expectation values of the number operators by the Fermi function f. Using again our approximated potential we find

$$\frac{1}{V} = \frac{1}{2}\sum_{\mathbf{k}} \frac{\tanh(\beta E_{\mathbf{k}}/2)}{E_{\mathbf{k}}}. \tag{13.31}$$

From this formula we can determine T_c and the temperature dependence of $\Delta(T)$.

13.4.2 DETERMINATION OF T_c AND $\Delta(0)$

The critical temperature T_c is the temperature at which $\Delta(T) \to 0$. In this case, $E_{\mathbf{k}} \to |\xi_{\mathbf{k}}|$, and the excitation spectrum becomes the same as in the normal state. Thus, T_c is found by replacing $E_{\mathbf{k}}$ with $|\xi_{\mathbf{k}}|$ in (13.31) and solving. After changing the sum to an integral, taking advantage of the symmetry of $|\xi_{\mathbf{k}}|$ about the Fermi level, and changing to a dimensionless variable of integration, we find that this condition becomes

$$\frac{1}{N(0)V} = \int_0^{\beta_c \hbar\omega_c/2} \frac{\tanh x}{x} dx = \ln\left(\frac{2e^{\gamma}}{\pi}\beta_c \hbar\omega_c\right), \tag{13.32}$$

where $\gamma = 0.577...$ is the Euler constant. Consequently,

$$kT_c = \beta_c^{-1} \approx 1.13\hbar\omega_c e^{-1/N(0)V}. \tag{13.33}$$

For small temperatures (13.31) can be rewritten as

$$\frac{1}{N(0)V} = \int_0^{\hbar\omega_c} \frac{d\xi}{(\xi^2+\Delta^2)^{1/2}} \tag{13.34}$$

$$\Rightarrow \Delta(T=0) = \frac{\hbar\omega_c}{\sinh(1/N(0)V)} \approx 2\hbar\omega_c e^{-1/N(0)V}, \tag{13.35}$$

which gives us a relation of T_c and $\Delta(0)$:

$$\frac{\Delta(0)}{kT_c} \approx \frac{2}{1.13} \approx 1.764. \tag{13.36}$$

13.4.3 TEMPERATURE DEPENDENCE OF THE GAP

We can also determine the temperature dependence of the energy gap from (13.31). By inserting the expression for $E_{\mathbf{k}}$ and rewriting the sum as an integral we get

$$\frac{1}{N(0)V} = \int_0^{\hbar\omega_c} \frac{\tanh \frac{1}{2}\beta(\xi^2+\Delta^2)^{1/2}}{(\xi^2+\Delta^2)^{1/2}} d\xi. \tag{13.37}$$

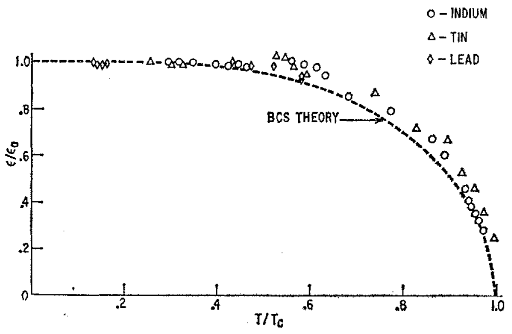

Figure 13.2: Temperature dependence of the energy gap compared with experimental data [9].

This formula has to be evaluated numerically. A plot of the results together with some experimental data is shown in Figure 13.2. We see that the theoretical value fits the experimental one quite good. The reason why mean-field theory gives that good result here is, that the effective number of nearest neighbors of a Cooper pair is big.

Near T_c we can find approximately

$$\frac{\Delta(T)}{\Delta(0)} \approx 1.74 \left(1 - \frac{T}{T_c}\right)^{1/2}, \quad T \approx T_c, \tag{13.38}$$

which shows the square-root dependence of the order parameter, which is typical for a mean-field theory.

13.4.4 Thermodynamic Quantities

With $\Delta(T)$ determined, the temperature dependent set of fermion excitation energies $E_{\mathbf{k}} = \sqrt{\xi_{\mathbf{k}}^2 + \Delta(T)^2}$ is fixed. These energies determine the quasi-particle occupation numbers $f_{\mathbf{k}} = (1 + e^{\beta E_{\mathbf{k}}})^{-1}$, which in turn determine the electronic entropy in the usual way for a fermion gas, namely,

$$S_{es} = -2k \sum_{\mathbf{k}} ((1 - f_{\mathbf{k}}) \ln(1 - f_{\mathbf{k}}) + f_{\mathbf{k}} \ln f_{\mathbf{k}}). \tag{13.39}$$

A plot of this formula for the normal and superconducting state is shown in Figure 13.3.

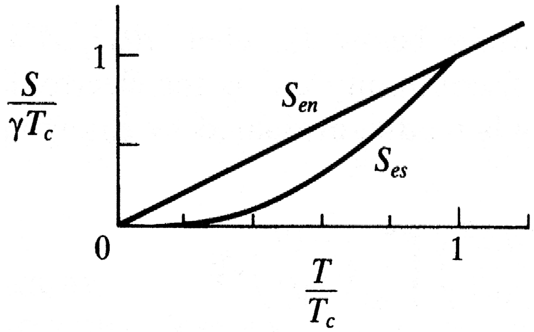

Figure 13.3: Electronic entropy in the normal and superconducting state.

Given $S_{es}(T)$, the specific heat can be written as

$$\begin{aligned} C_{es} &= T\frac{dS_{es}}{dT} = -\beta\frac{dS_{es}}{d\beta} \\ &= 2\beta k\sum_{\mathbf{k}} -\frac{\partial f_{\mathbf{k}}}{\partial E_{\mathbf{k}}}\left(E_{\mathbf{k}}^2 + \frac{1}{2}\beta\frac{d\Delta^2}{d\beta}\right). \end{aligned} \tag{13.40}$$

The first term is the usual one coming from the redistribution of quasi-particles among the various energy states as the temperature changes. The second term is more unusual and describes the effect of the temperature dependent gap in changing the energy levels themselves.

For the normal state the electronic specific heat is given by

$$C_{en} = \gamma T = \frac{2\pi^2}{3}N(0)k^2T. \tag{13.41}$$

It is important to note, that at T_c we will observe a jump in $C(T)$ because the derivative $\frac{d\Delta^2}{d\beta}$ is finite below T_c and 0 above. This jump can be calculated and gives

$$\begin{aligned} \Delta C &= \left.(C_{es} - C_{en})\right|_{T_c} = N(0)k\beta^2\int_{-\infty}^{\infty}\left(-\frac{\partial f}{\partial|\xi|}\right) \\ &= N(0)\left.\left(-\frac{d\Delta^2}{dT}\right)\right|_{T_c} \approx 9.4N(0)k^2T_c \end{aligned} \tag{13.42}$$

A plot together with experimental results is shown in Figure 13.4. Again BCS theory gives very good predictions.

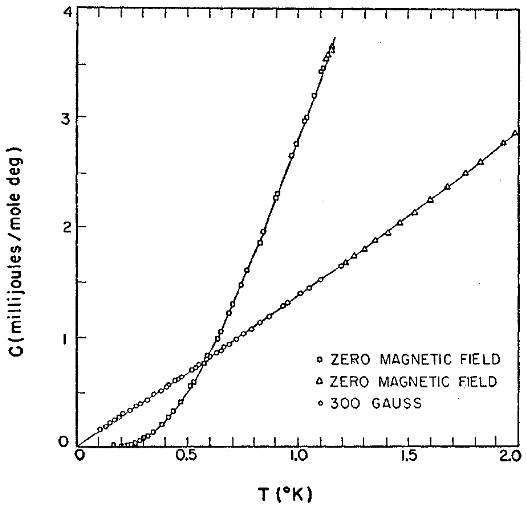

Figure 13.4: Temperature dependence of the specific heat compared with experimental data [10].

13.5 TYPE II SUPERCONDUCTORS AND THE VORTEX STATE

So far we did not talk about the electrodynamic properties of a superconductor, especially we did not look how a supercunductor reacts in a magnetic field. For example one quite radical thing that occurs in superconductors is the so-called Meissner-Ochsenfeld effect where an external magnetic field will be excluded completely from the superconductor. At the border of the superconductor the field drops down exponentially fast. A side-effect is a reduction of the critical temperature T_c. If we now further increase the magnetic field, we will find a critical magnetic field H_c at which superconductivity will disappear. A qualitative plot of the phase diagramm is given in Figure 13.5.

Alexei A. Abrikosov [11] studied the electromagnetic properties of superconductors more closely[4] by applying Ginzburg-Landau theory[5]. If one does so, we find two characteristic length scales in our theory:

1. The Landau penetration depth for external magnetic fields λ that describes how fast an magnetic field will decay and

---

[4] For this work Abrikosov received the Nobel prize in 2003.

[5] Even if the Ginzburg-Landau theory was first introduced as a phenomenological theory L. P. Gor'kov [12] showed that under certain approximations this theory can be derived from BCS theory.

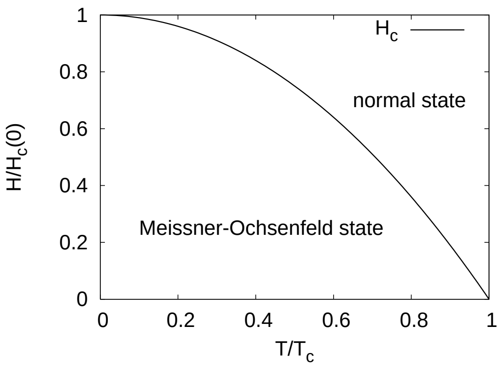

Figure 13.5: Phase diagram of a type I superconductor.

2. the Ginzburg-Landau coherence length ξ, which characterizes the distance over which the order parameter ψ can typically vary.

With these two length scales we are able to define the Ginzburg-Landau parameter κ as

$$\kappa \equiv \frac{\lambda}{\xi}. \tag{13.43}$$

For a lot of superconductors κ is small. Abrikosov now asked what would happen if κ becomes large? By linearizing the GL equations near T_c he found a threshold for κ and introduced the differentiation of Type I and Type II superconductors:

- $\kappa < \frac{1}{\sqrt{2}}$: Type I superconductor
- $\kappa > \frac{1}{\sqrt{2}}$: Type II superconductor.

Type I superconductors now have the electromagnetic property of expelling the external magnetic field completely as discussed above. But in type II superconductors we have to introduce two new critical magnetic fields different from H_c. The upper critical field $H_{c2} > H_c$ separates the normal and the superconducting state. The second critical field $H_{c1} < H_c < H_{c2}$ divides the superconducting phase in two diffentent states. For external fields smaller than H_{c1} we will again observe a Meissner-Ochsenfeld state. For fields between H_{c1} and H_{c2} we will find vortices in our superconductor where superconductivity is locally destroyed. Therefore the external magnetic field can penetrate the superconductor and the total flux is quantized in units of the magnetic flux quantum

$$\Phi_0 = \frac{hc}{2e} = 2.07 \times 10^{-7}\ \mathrm{G/cm^2}. \tag{13.44}$$

The phase diagram for type II superconductors is shown in Figure 13.6.

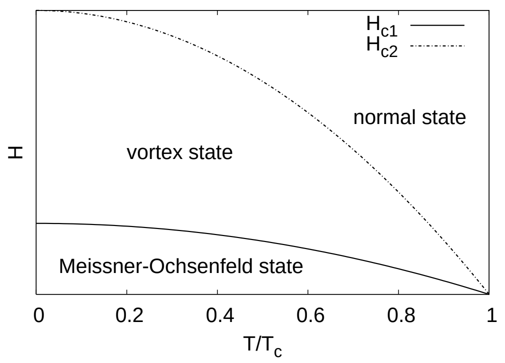

Figure 13.6: Phase diagram of a type II superconductor.

An important feature of the vortices is, that they reject each other. Therefore it's somehow clear, that they will arange themselves in a certain way and form a vortex lattice. There are different solutions of Ginzburg-Landau theory representing different symmetries of the vortex lattice. One family of solutions can be written as [13]

$$\begin{aligned}\Psi(x,y) &= \frac{1}{\mathcal{N}}\sum_{n=-\infty}^{\infty}\exp\left(\frac{\pi(ixy-y^2)}{\omega_1\Im\omega_2}+i\pi n\right.\\ &\qquad\left.+\frac{i\pi(2n+1)}{\omega_1}(x+iy)+i\pi\frac{\omega_2}{\omega_1}n(n+1)\right)\end{aligned}$$

with

$$\mathcal{N}=\left(\frac{\omega_1}{2\Im\omega_2}\exp\left(\pi\frac{\Im\omega_2}{\omega_1}\right)\right)^{1/4}.$$

By choosing the parameters ω_1 and ω_2 in an adequate way we get the solutions for the square and a triangular lattice symmetry. Some plots are shown in Figure 13.7. In a perfect superconductor the triangular symmetry is energetically more favorable but the difference between the two states is quite small[6]. Therefore one can observe both symmetries in nature. The reason for that can be found in the symmetry of the ion lattice or in the specific shape of the real Fermi surface.

---

[6] In his original work Abrikosov made a numerical mistake and identified the square lattice as the lowest energy solution.

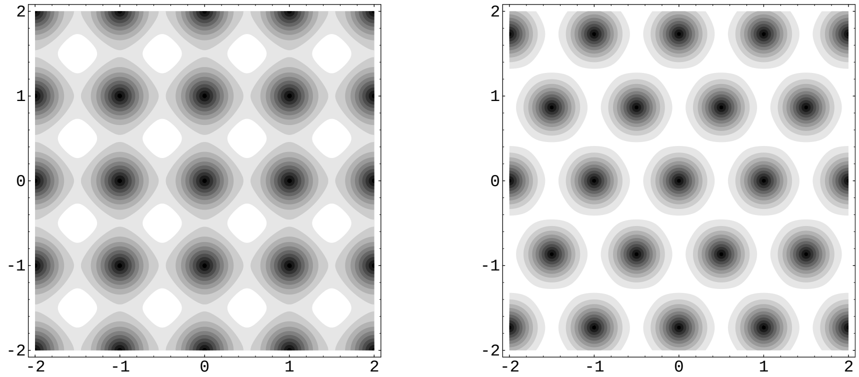

Figure 13.7: Square and triangular symmetry of the vortex lattice in type II superconductors.

Bibliography

[1] J. Bardeen, L. N. Cooper, and J. R. Schrieffer, *Theory of Superconductivity*, Phys. Rev. **108**, 1175 (1957).

[2] M. Tinkham, *Introduction to Superconductivity, Second Edition* (Dover, New York, 1996).

[3] L. N. Cooper, *Bound Electron Pairs in a Degenerate Fermi Gas*, Phys. Rev. **104**, 1189 (1956).

[4] H. Fröhlich, *Theory of the Superconducting State. I. The Ground State at the Absolute Zero of Temperature*, Phys. Rev. **79**, 845 (1950).

[5] E. Maxwell, *Isotope Effect in the Superconductivity of Mercury*, Phys. Rev. **78**, 477 (1950).

[6] C. A. Reynolds, B. Serin, W. H. Wright, and L. B. Nesbitt, *Superconductivity of Isotopes of Mercury*, Phys. Rev. **78**, 487 (1950).

[7] N. N. Bogoliubov, Nuovo Cimento **7**, 794 (1958).

[8] J. G. Valatin, Nuovo Cimento **7**, 843 (1958).

[9] I. Giaever and K. Megerle, *Study of Superconductors by Electron Tunneling*, Phys. Rev. **122**, 1101 (1961).

[10] N. E. Phillips, *Heat Capacity of Aluminum between 0.1K and 4.0K*, Phys. Rev. **114**, 676 (1959).

[11] A. A. Abrikosov, Zh. Eksp. Teor. Fiz. **32**, 1442 (1957).

[12] L. P. Gor'kov, Zh. Eksp. Teor. Fiz. **36**, 1918 (1959).

[13] T. Dahm, S. Graser, C. Iniotakis, and N. Schopohl, *Spectrum of low-energy excitations in the vortex state: Comparison of the Doppler-shift method to a quasiclassical approach*, Phys. Rev. B **66**, 144515 (2002).

CHAPTER 14

BOSE EINSTEIN CONDENSATION

VOLKER SCHLUE
SUPERVISOR: FABRICIO ALBUQUERQUE

The phenomenon of Bose-Einstein-Condensation in dilute gases *is exposed in its historical context as well as studied with view on more recent experiments with trapped atomic clouds. The* Gross-Pitaevskii Equation *is discussed.*

14.1 INTRODUCTION

In 1924 D. BOSE gave a deduction of Planck's Law of Black Body Radiation, relying on no classical concepts whatsoever [1]. Up to this point, the prefactor of the formula

$$\rho(\nu, T) = \frac{8\pi\nu^2}{c^3}\frac{h\nu}{e^{\frac{h\nu}{kT}} - 1}$$

resulted from an electromagnetic treatment. The new method divides the phase space of a light quantum into "cells" of size h^3, and counts the number of ways (W) a certain occupation state can be realized. The occupation numbers of each cell, however, should be as such, that this number maximizes the entropy of the macroscopic system, related by *Boltzmann's law*:

$$S \propto \log(W)$$

From this all thermodynamic properties can be deduced. A. EINSTEIN expected the analogy between gases of quanta and gases of molecules to be complete. Consequently, he developed the quantum theory of the one-atomic ideal gas [2], wherein not only the occupation density, i.e. the Bose distribution function, is given explicitly,

$$n = \frac{1}{e^{\alpha + E/kT} - 1} ,$$

but it is also found that the new equations of state allow only for a maximal number of particles for given volume and temperature; or, for fixed particle number and temperature the volume may not be reduced arbitrarily. In practice, however, the density of particles may always be increased, and it is immediately suggested, that the over-counting particles "*condense*" in the lowest quantum state, that of zero kinetic energy, (the particles therefore condense in momentum space). It is shown that the condensate is in thermodynamic equilibrium with the gas.

The papers of BOSE and EINSTEIN employed a method of counting, in which the quanta could not be thought of as statistically independent anymore. Today this "mutual influence" is understood in terms of *correlation functions* (cf. section 14.4), which could also be used to establish a criterion for condensation in interacting systems; it reads[1]

$$\lim_{|\vec{r}-\vec{r}'|\to\infty} \rho(\vec{r},\vec{r}') = \frac{\langle N_0 \rangle}{V} ,$$

where $\langle N_0 \rangle$ denotes the expectation value of the occupation number of the zero-momentum state, and $\rho(\vec{r},\vec{r}') = \langle \psi^\dagger(\vec{r}')\psi(\vec{r}) \rangle$ denotes the one-particle density matrix.

In the following we will limit ourselves to *Bose-Einstein condensation in dilute gases* [3]. Experimental breakthroughs in the last decade, namely the trapping of atoms using laser cooling, enable the investigation of Bose-Einstein condensation as a *macroscopic quantum phenomenon*, e.g. through the measurement of the density distribution, $n(\vec{r}) = N|\phi_0(\vec{r})|^2$, reflecting the shape of the single-particle ground state wave function (of the trap), provided all atoms are condensed, and are non-interacting.

14.2 THE NON-INTERACTING BOSE GAS

For an ideal gas of non-interacting bosons in thermodynamic equilibrium [4], the thermodynamic potential Ω_ν of all particles occupying a given quantum state $|\nu\rangle$ with energy ε_ν is given by

---

[1] In a homogeneous Bose gas the density matrix and the correlation function are proportional for distances large compared to the de Broglie scale.

$$\Omega_\nu = -k_B T \log \sum_{n_\nu=0}^{\infty} e^{n_\nu(\mu-\varepsilon_\nu)/k_B T} \; .$$

To ensure convergence, we must have $\mu < 0$; then the distribution function is obtained as follows:

$$n_\nu = -\frac{\partial \Omega_\nu}{\partial \mu} = \frac{1}{e^{\frac{\varepsilon_\nu-\mu}{k_B T}} - 1} \; . \tag{14.1}$$

For $N = \sum_\nu (e^{(\varepsilon_\nu-\mu)/k_B T} - 1)^{-1}$ here the chemical potential μ is a function of the (fixed) particle number N and the temperature T. If we exclude from the above sum the term ν corresponding to the lowest energy level ε_ν we obtain the number of excited particles N_{ex} – the *transition temperature* T_C will then be the lowest temperature allowing for all particles to be in excited states, at $\mu = 0$:

$$N = N_{ex}(T_C, \mu = 0) \; . \tag{14.2}$$

We shall now calculate this temperature in the case of a *harmonic trap* [3]. The gas will then be subject to the potential

$$V(\vec{r}) = \sum_{i=1}^{3} \frac{1}{2} m \omega_i^2 r_i^2 \tag{14.3}$$

and the energy levels are $\varepsilon_\nu = \varepsilon(n_1, n_2, n_3) = \sum_{i=1}^{3}(n_i + 1/2)\hbar\omega_i$. For large particle numbers and temperatures, that is $N^{1/3} \gg 1, T \gg \hbar\omega_i/k_B$, it is common to treat the energy spectrum as a continuum, hence replacing sums by integrals in the calculation of N_{ex}. For large energies, that is $\epsilon \gg \hbar\omega_i$, we may further neglect the zero point energy, to find that there are approximately

$$\frac{1}{\prod_{i=1}^{3} \hbar\omega_i} \int_0^{\varepsilon} \mathrm{d}\varepsilon' \int_0^{\varepsilon-\varepsilon'} \mathrm{d}\varepsilon'' \int_0^{\varepsilon-\varepsilon'-\varepsilon''} \mathrm{d}\varepsilon''' \; 1 = \frac{1}{6} \frac{\varepsilon^3}{\prod_{i=1}^{3} \hbar\omega_i}$$

states with energies less or equal to ε, yielding a density of states given by $(2 \prod_{i=1}^{3} \hbar\omega_i)^{-1} \varepsilon^2 = c\varepsilon^2$. Consequently,

$$N_{ex}(T_C, \mu = 0) \approx \int_0^{\infty} \mathrm{d}\varepsilon \, c\varepsilon^2 \frac{1}{e^{\varepsilon/k_B T_C} - 1} = c(k_B T_C)^3 \Gamma(3)\zeta(3) \tag{14.4}$$

resulting in, by means of (14.2),

$$T_C \approx \frac{\hbar\overline{\omega} N^{1/3}}{k_B \zeta(3)^{1/3}} \; ; \tag{14.5}$$

where $\overline{\omega} = (\omega_1\omega_2\omega_3)^{1/3}$ and $\zeta(3)^{-1/3} \approx 0.94$. From equations (14.4), (14.5) we easily obtain the number of particles in the condensate,

$$N_0 = N - N_{ex}(T, \mu = 0) \approx N(1 - (\frac{T}{T_C})^3) \,. \tag{14.6}$$

This dependence is characteristic for thermally driven *phase transitions*, and we will now study the specific heat of the gas, near T_C, in order to determine that it is a *second order* phase transition[2], with a discontinuously changing quantity near the critical point. First, the energy for $T < T_C(\mu = 0)$, is given by

$$E \approx \int_0^\infty \mathrm{d}\varepsilon \, c\varepsilon^2 \frac{\varepsilon}{e^{\varepsilon/k_BT} - 1} = c\Gamma(4)\zeta(4)(k_BT)^4 \,,$$

(only the particles in the excited states contribute), therefore $C_v \approx 4E/T$. Expressed in terms of the number of particles N and the transition temperature T_C, we have, using (14.5),

$$E \approx 3\frac{\zeta(4)}{\zeta(3)}Nk_B\frac{T^4}{{T_C}^3}$$

and $C_v \approx 12(\zeta(4)/\zeta(3))Nk_B(\frac{T}{T_C})^3$.
Secondly, for $T > T_C(\mu \neq 0)$, we simply note the more general expressions

$$N \approx \int_0^\infty \mathrm{d}\varepsilon \, c\varepsilon^2 \frac{1}{e^{(\varepsilon-\mu)/k_BT} - 1} \tag{14.7}$$

$$E \approx \int_0^\infty \mathrm{d}\varepsilon \, c\varepsilon^3 \frac{1}{e^{(\varepsilon-\mu)/k_BT} - 1} \,. \tag{14.8}$$

Thirdly, a discontinuity of the specific heat at $T = T_C$, can be seem as follows: $\frac{\mathrm{d}E}{\mathrm{d}T} = (\frac{\partial E}{\partial T})_\mu + (\frac{\partial E}{\partial \mu})_T\frac{\partial \mu}{\partial T}$. Since we assume $\mu = \partial\mu/\partial T|_{T=T_C}(T - T_C)$ $(T \gtrsim T_C)$ the second term is non-vanishing and causes a discontinuity,

$$\Delta C|_{T=T_C} = (\frac{\partial E}{\partial \mu})_T\frac{\partial \mu}{\partial T}|_{T=T_C} \,.$$

The equations (14.8) imply on one hand

$$(\frac{\partial E}{\partial \mu})_T \overset{p.I.}{=} 3N \,,$$

while $(\frac{\partial \mu}{\partial T})_N = -(\frac{\partial N}{\partial T})_\mu(\frac{\partial N}{\partial \mu})_T^{-1}$, so that on the other,

$$(\frac{\partial N}{\partial T})_\mu \overset{p.I.}{=} \int_0^\infty \mathrm{d}\varepsilon \frac{2c\varepsilon\frac{\varepsilon-\mu}{T} + c\varepsilon^2\frac{1}{T}}{e^{\frac{\varepsilon-\mu}{k_BT}} - 1} \overset{(T\to T_C,\mu\to 0)}{\longrightarrow} \frac{3N}{T_C}$$

---

[2] In fact this–Bose-Einstein Condensation in three dimensions–is the *only* phase transition that can take place in a non-interacting system.[5]

and

$$(\frac{\partial N}{\partial \mu})_T \overset{p.I.}{=} \int_0^\infty \mathrm{d}\varepsilon \frac{2c\varepsilon}{e^{\frac{\varepsilon-\mu}{k_BT}}-1}$$
$$\xrightarrow{(T\to T_C,\mu\to 0)} \int_0^\infty \mathrm{d}\varepsilon \frac{2c\varepsilon}{e^{\frac{\varepsilon}{k_BT_C}}-1} = \frac{2c\Gamma(1)\zeta(2)(k_BT_C)^3}{k_BT_C} \overset{(14.5)}{=} \frac{\zeta(2)}{\zeta(3)}\frac{N}{k_BT_C} .$$

Therefore

$$\Delta C|_{T=T_C} = -9N\frac{\zeta(3)}{\zeta(2)}k_B \approx -6.58Nk_B .$$

It is to be remarked that the above results hold only for a density of states $\propto \varepsilon^2$ corresponding to the harmonic trap. If the quadratic dependence is replaced by a more general exponent $\alpha - 1$, the analogous calculation yields $\Delta C \propto \frac{\zeta(\alpha)}{\zeta(\alpha-1)}$ so that $\Delta C \longrightarrow 0$ as $\alpha \searrow 2$; $\alpha = 3/2$ is the case of the free, homogeneous Bose gas. However, it can be shown [4], that the derivative of the specific heat, w.r.t. temperature remains discontinuous at $T = T_C$, the jump being $\Delta(\frac{\partial C}{\partial T})_v \cong -3.66\frac{N}{T_C}$.

14.3 The Bose Gas with Hard Cores in the Mean Field Limit

We expect a dilute interacting Bose Gas to be effectively described by the Hamiltonian

$$H = \sum_i \left[\frac{\vec{p}_i^2}{2m} + V(\vec{r}_i)\right] + U_0 \sum_{i<j} \delta(\vec{r}_i - \vec{r}_j) . \tag{14.9}$$

For a zero temperature calculation we adopt the *Hartree approximation*, consisting of finding the single particle wave function ϕ which minimizes the energy expectation value of (14.9) in the state

$$\Psi(\vec{r}_1, \ldots, \vec{r}_N) = \prod_{i=1}^N \phi(\vec{r}_i) , \tag{14.10}$$

under the constraint that ϕ remains normalized. Hence we must have

$$\delta\mathcal{F}[\phi] \overset{!}{=} 0 , \tag{14.11}$$

where $\mathcal{F}[\phi] = \langle\Psi|H|\Psi\rangle - \mu N\langle\phi|\phi\rangle$. The calculation of $\mathcal{F}$ gives

$$\mathcal{F}[\phi] = N \int \mathrm{d}\vec{r}\, \phi^*(\vec{r}) \left(\frac{\vec{p}^2}{2m} + V(\vec{r}) + \frac{1}{2}U_0(N-1)|\phi(\vec{r})|^2 - \mu\right) \phi(\vec{r})$$

so that for the variation we obtain

$$\delta\mathcal{F}[\phi] = N\int \mathrm{d}\vec{r}\,\left(\delta(\phi^*)\frac{\vec{p}^2}{2m}\phi(\vec{r}) + \phi^*(\vec{r})\frac{\vec{r}^2}{2m}\delta(\phi) + \cdots - \mu\phi^*(\vec{r})\delta(\phi)\right).$$

In the case $\delta\phi = 0$, (14.11) can only be satisfied if

$$\frac{\vec{p}^2}{2m}\phi(\vec{r}) + V(\vec{r})\phi(\vec{r}) + U_0(N-1)|\phi(\vec{r})|^2\phi(\vec{r}) - \mu\phi(\vec{r}) = 0\,.$$

Replacing ϕ by $\Psi = \sqrt{N}\phi$, the wave function of the condensed state, and noting $N - 1 \approx N$ we arrive at the *Gross-Pitaevskii equation*

$$-\frac{\hbar^2}{2m}\triangle\psi + V\psi + U_0|\psi|^2\psi = \mu\psi\;; \tag{14.12}$$

the Lagrange multiplier μ in $\mathcal{F}$ may therefore be interpreted as the chemical potential.

For a slowly varying external potential (as the harmonic trap) the Bose Gas should locally be uniform, and excited particles, which are not in the zero kinetic energy state, may be neglected in the sense that the first term in (14.12) can be dropped in the determination of the groundstate wave function. Noting that $|\psi(\vec{r})|^2 = n(\vec{r})$ is the particle density of the gas, we immediately get

$$n(\vec{r})U_0 + V(\vec{r}) = \mu\,, \tag{14.13}$$

expressing that the condensed particles distribute such that the energy to add a new particle is the same at each point. Due to the analogy to the theory of Fermi Gases and atoms, one refers to the above as the *Thomas-Fermi approximation.*

We now consider a few properties of the harmonic trap (14.3) [3]. As we see from (14.13) the boundary of the cloud is given by $V(\vec{r}) = \mu$, in this case an ellipsoid with semi-axes $R_i = \sqrt{2\mu/m\omega_i^2}$. Using (14.13) and (14.3) we have

$$N = \int_{V(\vec{r})\le\mu} \mathrm{d}\vec{r}\,n(\vec{r}) = \frac{8\pi}{15}\left(\frac{2\mu}{m\overline{\omega}^2}\right)^{\frac{3}{2}}\frac{\mu}{U_0}$$

which establishes a relationship between the chemical potential and the number of particles, namely $\mu \propto N^{\frac{2}{5}}$; in particular, since $\partial E/\partial N = \mu$, the energy per particle is

$$\frac{E}{N} = \frac{5}{7}\mu\,.$$

It should be remarked, both interaction and finite temperatures will in fact deplete the zero-momentum state, thus making the ansatz (14.10) invalid. The wave function taking care of these excitations is rather

$$\Psi = \frac{N_1! \cdots N_k!}{N!} \sum_{[\pi]\in S_n} \prod_{i_1=1}^{N_1} \phi_{\varepsilon_1}(\vec{r}_{\pi^{-1}(i_1)}) \cdots \prod_{i_k=N_1+\cdots+N_{k-1}+1}^{N_1+\cdots+N_k} \phi_{\varepsilon_k}(\vec{r}_{\pi^{-1}(i_k)})$$

where ϕ_{ε_j} is the (excited) state of energy ε_j occupied N_j times. A treatment starting from this wave function corresponds to a *Hartree-Fock-approximation*. Therein the reduction of the transition temperature in the presence of interactions was investigated.

14.4 THE WEAKLY INTERACTING BOSE GAS IN THE CRITICAL REGIME

In an interacting system the concept of Bose-Einstein Condensation retains: it is the macroscopic occupation of a single-particle state, (which is not necessarily the zero-momentum state). The transition temperature experiences a change, but even the determination of the sign of the shift is non-trivial: in fact, for repulsive interactions it increases linearly with the s-wave scattering length [6]. We shall now be interested in correlations, in particular the *correlation length*, in the gas, as its behavior near the critical point determines the *critical exponent* ν.[3] Correlations are expressed by the off-diagonal elements of the one-body density matrix $\langle \Psi^\dagger(\vec{r})\Psi(\vec{r}')\rangle$, while it is assumed, that in thermodynamic equilibrium, this is only a function of the distance $s = |\vec{r} - \vec{r}'|$,

$$n(s) = \langle \Psi^\dagger(\vec{r})\Psi(\vec{r}')\rangle \ .$$

Then in the presence of a condensate (here at $\vec{p} \approx 0$), where in momentum space $n(\vec{p}) = N_0\delta(\vec{p}) + \tilde{n}(\vec{p})$ we have

$$n(s) = \frac{1}{V}\int \mathrm{d}\vec{p}\, n(\vec{p}) e^{i\vec{p}\cdot s\vec{e}/\hbar} \xrightarrow{s\to\infty} \frac{N_0}{V}$$

since in normal systems $\tilde{n}$ is smooth. Thus typically $n(s)$ falls off to zero quickly for $T > T_C$, while it approaches a plateau for $T < T_C$.

From an experimental point of view, the correlation function is essentially determined by evaluating the interference pattern of two matter waves originating from spatially separated regions of a trapped gas [7]. Rubidium atoms can be prepared in the hyperfine ground state $|J = 1, m_J = -1\rangle$ in a magneto-optical trap, and further cooled to the desired temperature by radio-frequency induced

---

[3] In fact only ν and α have been determined experimentally, because the order parameter is not directly accessible.

evaporation. A virtual double slit is created using a radio-wave field with two frequency components, inducing spin-flip transitions into the magnetically untrapped atomic state $|J=2, m_J=0\rangle$. The emitted atoms are accelerated downwards, as subjected to gravity, and overlap outside the trap. From the visibility of the interference pattern the spatial coherence is deduced. The correlation function thus quantifies the phase coherence of the atoms, on which the formation of the interference pattern depends. The *order parameter* is the condensate wave function itself.

Closely above T_C the decay of $n(s)$ is characterized by the *correlation length* ξ,

$$\langle \Psi^\dagger(\vec{r})\Psi(\vec{r}')\rangle \propto \frac{1}{s}\exp(-\frac{s}{\xi})|_{s=|\vec{r}-\vec{r}'|}$$

for a homogeneous Bose Gas (and $s > \lambda_{\mathrm{dB}} = \sqrt{2\pi\hbar^2/mk_BT}$).

The theory of critical phenomena predicts a singularity of ξ as a function of T near the critical point (see also Fig.14.1)of the form

$$\xi \propto |\frac{T_C}{T-T_C}|^\nu \; .$$

More recent measurements in this regime [8], using the same method as referred to above, found this to be satisfied, if $\nu = 0.67 \pm 0.13$. This directly supports the classification of Bose-Einstein-Condensation in weakly interacting gas to the same *universality class* as the 3D XY-Model. The correlation length reflects the scale of regions of equal phase, its divergence corresponds to the governing of long-range *fluctuations* of the system, already indicating the onset of the condensed phase.

From the theoretical point of view it is precisely this generation of a large scale (the scale set by the correlation length), at which the properties of the system become independent of the details of the microscopic structure, which allowed for the *renormalization group idea*: the generation of a scale-dependent effective hamiltonian.[4] In this context—the renormalization group analysis of a field theory—the above critical exponent can be predicted [9]. Since the order parameter of the system is, as we have seen, the condensate wave function, which is given by its modulus and its phase, the critical phenomena should be encaptured by the *2-vector model*, which is a $(\phi^2)^2$ field theory with an effective ($O(2)$-invariant-) hamiltonian of the form

$$\mathcal{H}(\phi) = \int \left(\frac{1}{2}(\partial_\mu\phi)^2 + \frac{1}{2}(r_C+t)\phi^2 + \frac{1}{4!}g\Lambda^\varepsilon(\phi^2)^2\right) \mathrm{d}^d x \tag{14.14}$$

---

[4] Universality then relies upon the existence of IR fixed points in hamiltonian space.

where ϕ is a 2-vector (t is the reduced temperature, g is a function of temperature which plays the role of a coupling constant, Λ has to be thought of as a large momentum cutoff, r_C is a critical value). Universal quantities are calculated by the method of ε-*Expansion*, which is a formal dimensional continuation to a critical theory in $d = 4 - \varepsilon$ dimensions where infrared divergences appear, for a critical field theory does not exist for a dimension smaller than four. The Renormalization Group Equations then determine the critical behavior of the corresponding correlation functions, and allow for a systematic determination of the critical exponents. For the case of interest to us, $\varepsilon = 1$, the summed expansion yields

$$\nu = 0.671 \pm 0.005$$

in good agreement with experiment, which is also a confirmation of RG ideas, and the concept of universality.

14.5 SPONTANEOUS SYMMETRY BREAKING IN THE BOSE GAS

The condensation of atoms into the lowest quantum state locks their phase[5], as all condensed atoms are described by the same wavefunction. Since the interactions in alkali gases (as considered in 14.4) are short range, there is then an infinite wavelength zero-momentum excitation, which changes the overall phase. The situation is comparable to a ferromagnet, in which all spins line up at $T = 0$, and only interact via the short-range exchange interaction: the corresponding excitation is a spin wave carrying no energy. Both is a consequence of *Goldstone's theorem*, which may be stated as follows [10]: *If a continuous symmetry of the Lagrangian is spontaneously broken, and if there are no long-range forces, then there exist zero-frequency excitations at zero momentum.* These are also called *Goldstone bosons.*

---

[5] The continuous $O(2)$-symmetry of (14.14) is broken.

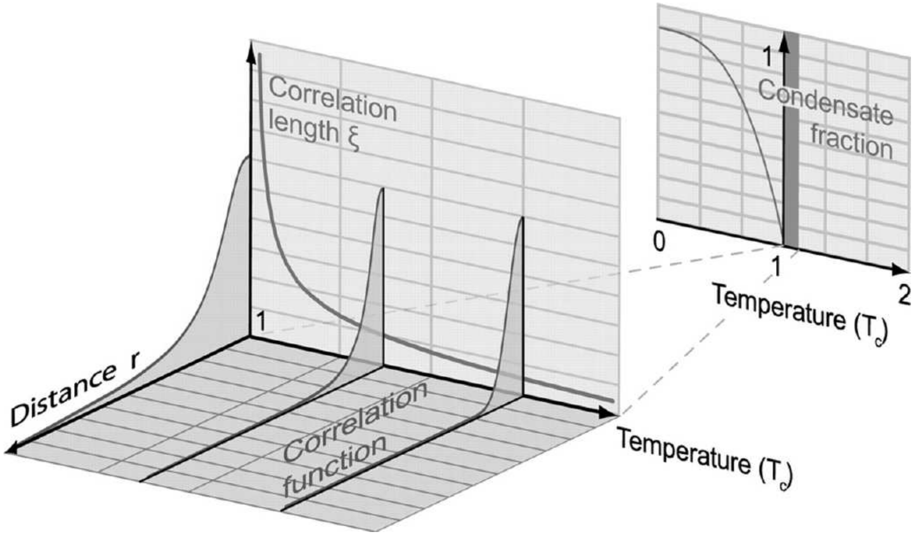

Figure 14.1: Schematics of the correlation function and the correlation length close to the phase transition temperature. Source: [8]

Bibliography

[1] D. Bose, *Plancks Gesetz und Lichtquantenhypothese*, Zeitschrift für Physik **26** (1924).

[2] A. Einstein, *Quantentheorie des einatomigen idealen Gases. Erste und zweite Abhandlung*, Sitzungsberichte der preussischen Akademie der Wissenschaften: physikalisch-mathematische Klasse (1924).

[3] C. Pethick and H. Smith, *Bose-Einstein Condensation in Dilute Gases* (Cambridge University Press, 2002).

[4] L. Landau and E. Lifshitz, *Statistical Physics, Part 1* (Pergamon, Oxford, 1980).

[5] I. Herbut, *A modern Approach to Critical Phenomena* (Oxford University Press, 2007).

[6] G. Baym, J.-P. Blaizot, M. Holzmann, F. Laloë, and D. Vautherin, *The transition Temperature of the Dilute Interacting Bose Gas*, Physical Review Letters **83**, 9 (1999).

[7] I. Bloch, T. Hänsch, and T. Esslinger, *Measurement of the spatial coherence of a trapped Bose gas at the phase transition*, Nature **403**, 166 (2000).

[8] T. Donner, S. Ritter, T. Bourdel, A. Öttl, M. Köhl, and T. Esslinger, *Critical Behavior of a Trapped Interacting Bose Gas*, Science **315**, 1556 (2007).

[9] J. Zinn-Justin, *Quantum Field Theory and Critical Phenomena* (The International Series of Monographs on Physics, Oxford, 1993).

[10] J. Kapusta and C. Gale, *Finite-Temperature Field Theory: Principles and Applications* (Cambridge University Press, 2006).

Chapter 15

Superfluidity and Supersolidity

Lars Bonnes
supervisor: Lode Pollet

The first part of this report covers the superfluid behavior of ^{4}He, *the Two-fluid model, Bose-Einstein condensation (BEC) and quantized vortices. The second part will discuss the phenomenon of superflow in crystalline Helium by reviewing the important experiments (Kim-Chan etc.) and the theoretical approaches of zero-point vacancies and crystalline disorder.*

15.1 Superfluid Helium

15.1.1 Motivation

Helium is the lightest noble gas. Its stable isotopes are ^{3}He ($0,000137\,\%$ natural concentration) and ^{4}He ($99,999863\,\%$ natural concentration) which obeys Bose statistics.

Experiments carried out with ^{4}He in 1938 observed a drop in the viscosity of liquid Helium (a decrease of at least a factor of 1500) below a certain temperature, later known as "lambda temperature" T_λ at approximately $2.17\,K$. For this nonviscous fluid the term "superfluidity" was introduced and the new phase of Helium is named "He II" besides the normal phase is referred to as "He I". The phase diagram is drawn in Fig. 15.1.

An ideal Bose-Einstein gas of ^{4}He will condensate below $T_c = 3.3\,K$. Although the assumptions of an ideal Bose-Einstein gas are very rough T_c and T_λ are similar and the question was if superfluidity is related to condensation.

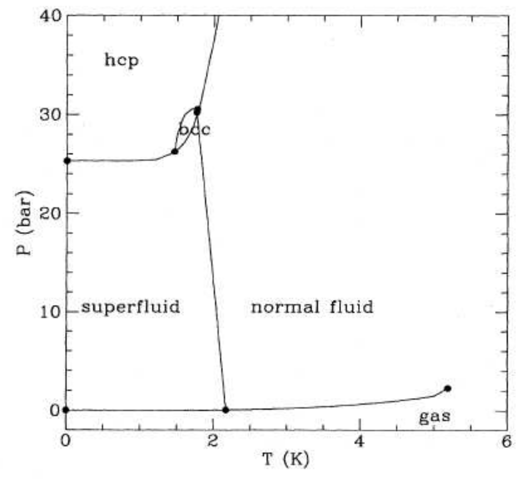

Figure 15.1: Phase diagram of Helium from katen from Ref. [1].

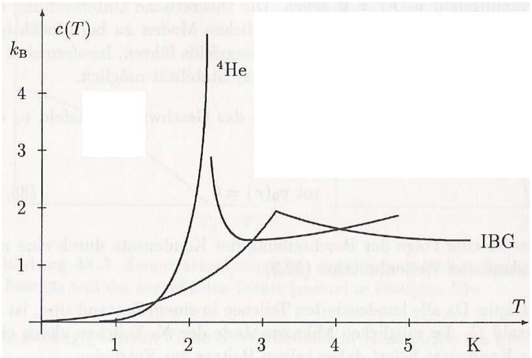

Figure 15.2: Specific heat of an ideal Bose gas (IBG) and He II. Figure adapted from Ref. [2].

In fact both phenomena show qualitative similarities but their quantitative effects differ a lot as one can see in Fig. 15.2 where the specific heat of Helium and an ideal Bose gas are shown.

15.1.2 TWO-FLUID MODEL

We follow the approach of Ref. [3]. The Two-fluid model is able to explain the effects observed in the experiments (frictionless flow etc.) and gives quantitative predictions for $T \sim 0\,K$.

ANSATZ

Assume liquid ^{4}He of mass density ρ flowing through a capillary with a velocity v (parallel to the walls) at a certain time t_0 and assume furtherly $T = 0$. Its energy density in the laboratory frame is $E = \frac{\rho v^2}{2}$. By a Galilean transformation to the rest frame of the Helium the walls move with $-v$ relative to the liquid. Excitations (i.e., phonons etc.) will occur in the liquid in the case of friction. Assume one elementary excitation with momentum $\vec{p}$ and an energy $\epsilon(\vec{p})$ where ϵ is an arbitrary relation of dispersion. The energy is given by

$$E = \underbrace{\epsilon(\vec{p}) + \vec{p}\vec{v}}_{\Delta E} + \frac{\rho v^2}{2}. \tag{15.1}$$

This formula can be derived by applying a Galilean transformation $S = e^{-iG}$ with $G = \frac{m}{\hbar}\vec{v}\sum_j \vec{r}_j$ to the Hamiltonian with translation invariant potential.[1] If energy dissipates from the Helium, then $\Delta E < 0$ is required and thus

$$v > \frac{\epsilon(\vec{p})}{p} \tag{15.2}$$

if $\vec{v}$ and $\vec{p}$ are assumed to be antiparallel. This is a necessary condition for the appearance of friction induced elementary excitations.

If, in particular, Eq. (15.2) can not be fullfilled for a given v the flow is frictionless. For a finite temperature close to $T = 0$ the liquid already contains thermal excitations[2]. They are assumed to form a gas of quasi particles distributed via the function $n(\epsilon)$ (particle density function) and moving with a velocity $\vec{v'}$ relatively to the liquid. The distribution function in the rest frame of the gas is displaced by $-\vec{p}\vec{v'}$ $(n(\epsilon - \vec{p}\vec{v'}))$.

The momentum per unit volume of the gas of quasi particles is calculated via

$$\vec{P} = \int d\tau \; \vec{p} n(\epsilon - \vec{p}\vec{v'}) \tag{15.3}$$

with the measure $d\tau = \frac{d^3p}{(2\pi\hbar)^3}$. Since $\vec{p}\vec{v'}$ is small[3] one Taylor expands $n(\epsilon - \vec{p}\vec{v'})$ to first order in $\vec{p}\vec{v'}$. By averaging over the three spatial dimensions $\vec{p}\vec{v'} \approx \frac{1}{3}p\hat{p}\vec{v'}$

---

[1] $e^{-iG}He^{iG} = H - i[G,H] - \frac{1}{2}[G,[G,H]] + ...$ By explicit calculation one finds $[G,H] = -\hbar\vec{v}\sum_j \hat{P}_j$ where $\hat{P}_j$ is the operator of momentum, $[G,[G,H]] = -M\vec{v}^2$ and that higher terms vanish in this expansion.

[2] The concept of a gas of quasi-particles representing elementary excitations does not hold for large temperatures near T_λ.

[3] In the low temperature regime we are dealing with, the momenta of the excitations are small. Since the COM movement of this gas of quasi particles will vanish when taking the average over all times its variation resulting from interaction with the thermal radiation field v' is small aswel.

where $\hat{p}$ is the unit vector parallel to $\vec{p}$, one obtains directly

$$\vec{P} = \vec{v'} \underbrace{\int d\tau \frac{1}{3} p^2 \left(-\frac{dn(\epsilon)}{d\epsilon} \right)}_{\rho_n} . \tag{15.4}$$

This flow carries mass and by comparison with the form $\vec{P} = \vec{v'}\, \rho_n$ one determines the mass density to

$$\rho_n = \int d\tau \frac{1}{3} p^2 \left(-\frac{dn(\epsilon)}{d\epsilon} \right) . \tag{15.5}$$

The particles in this excitation gas may scatter inelastically with the capillary walls and thus induce friction into our system even if the velocity v of the liquid Helium does not fulfill Eq. (15.2).

The result of the calculations above is that the fraction $\frac{\rho_n}{\rho}$ of the total liquid will have friction with the walls and so one makes the ansatz of dividing the total mass density into a normal part (ρ_n) that behaves like a normal liquid (He I) and a superfluid part (ρ_s) that has no friction with

$$\rho = \rho_n + \rho_s . \tag{15.6}$$

Hence the current is given by

$$\vec{j} = \rho_n \vec{v}_n + \rho_s \vec{v}_s . \tag{15.7}$$

The normal and the superfluid part interpenetrate without interaction. This model was firstly introduced by Tisza and Landau.

Quantitative Description

The spectrum of liquid Helium is shown in Fig. 15.3. For small momenta it is parameterized as $\epsilon(p) = cp$ where c is the speed of sound and the quasi particles in this regime are called phonons. For larger p the linearity does not hold but in the regime of the local minimum it is parameterized as $\epsilon(p) = \Delta + \frac{(p-p_0)^2}{2m'}$. One refers to the quasi particles in this regime as rotons.

With knowledge of the spectrum one can derive the densities for the normal and superfluid part via Eq. (15.5) and (15.6).

The phonons are distributed by the Bose distribution $n(p) = [e^{(\frac{\epsilon(p)}{T}} - 1)]^{-1}$. Since the energy gap $\Delta = 8.7\, K$ of the roton excitation is large[4] one can approximate their distribution by Boltzmann law $n(p) = e^{-\frac{\epsilon(p)}{T}}$.

---

[4] The calculations in the previous part were made under the assumption that we were close to zero temperature. Close to lambda temperature the concentration of quasi particles becomes that large that its concept breaks down.

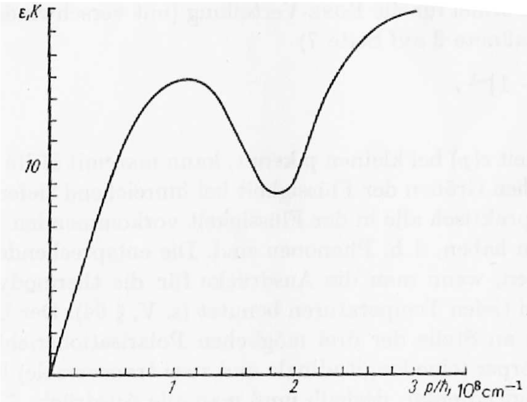

Figure 15.3: Spectrum of liquid Helium.[3]

We now calculate the normal and superfluid density component using the results from the two-fluid model.

Phonon part: Substitute $\frac{dn}{d\epsilon} = \frac{1}{c}\frac{dn}{dp}$ in Eq. (15.5) and perform a partial integration. The energy off all phonons can be calculated analogously to the black body radiation but with a factor $\frac{1}{3}$ because of only one polarization direction to $E_{Ph} \propto T^4$. The result is

$$(\rho_n)_{ph} = \frac{4E_{ph}}{3c^2}T^4 \tag{15.8}$$

Roton part: Use $\frac{dn}{d\epsilon} = -\frac{n}{T}$ and use the approximations that the main contribution of rotons has a momentum $p = p_0$ since the energy gap is large and only rotons with the lowest momentum will be excited. The number of rotons can be derived by minimizing the free energy $F = -NT\ \ln\left[\frac{eV}{N}\int d\tau e^{-\frac{\epsilon(p)}{T}}\right]$ with respect to the particle number N. Finally, with $N_{rot} \propto \sqrt{T}e^{-\frac{\Delta}{T}}$,

$$(\rho_n)_{rot} = \frac{\bar{p}^2}{3T}\frac{N_{rot}}{V}\frac{1}{\sqrt{T}}e^{-\frac{\Delta}{T}}. \tag{15.9}$$

15.1.3 GENERAL BEC

The superfluid phase of Helium is characterized by “generalized BEC”[4]. This is defined as one can find at any time a complete orthonormal basis set of single particle wave functions such that one and only one is occupied with a number of atoms of order[5] N whereas the occupation numbers of all others is of order 1. This will be illustrated in a simple basis set.

---

[5] N is a macroscopic large number of particles of Helium in the order of 10^{23}.

As an expamle how to derive long range order in a condensed system, the boson field operator is written in a basis of plane waves

$$\hat{\Psi}(t,\vec{r}) = \frac{1}{\sqrt{V}} \sum_{\vec{p}} \hat{a}_p e^{\frac{i}{\hbar}\left[\vec{p}\vec{r} - \frac{p^2}{2m}t\right]} \tag{15.10}$$

and the condensation takes place at $p = 0$. The occupation of this state is $\hat{a}^\dagger \hat{a} = N_0$ where $N_0 \sim N$ and thus consistent with the concept of generalized BEC.

As $N \gg 1$ the commutator $[\hat{a}_0, \hat{a}_0^\dagger] = \hat{a}_0 \hat{a}_0^\dagger - \hat{N} = (N+1) - N \approx N - N = 0$ can be approximated to be zero and since the operators commute one can treat them like classical numbers. In a physical sense one can argue that if a particle is added to the macroscopically occupied ground state the state will not be altered. Define $\hat{\Xi} = \frac{\hat{a_0}}{\sqrt{V}}$. For full mathematical rigour the assumptions only hold in the thermodynamic limit

$$\lim_{N\to\infty} < m, N|\hat{\Xi}|m, N+1 >= \Xi \tag{15.11}$$

$$\lim_{N\to\infty} < m, N+1|\hat{\Xi}^\dagger|m, N >= \Xi^*, \tag{15.12}$$

with $\frac{N}{V} = const$ where N is the occupation number of the ground state and m denotes such other quantum number as the occupation numbers of the other levels.

So the Boson field operator can be separated by

$$\hat{\Psi} = \underbrace{\hat{\Xi}}_{condensate} + \underbrace{\hat{\Phi}}_{uncondensed}, \tag{15.13}$$

whereas the uncondensed operator in the thermodynamic limit vanishes since

$$\lim_{N\to\infty} < m, N|\hat{\Phi}|m, N+1 >= 0 \tag{15.14}$$

$$\lim_{N\to\infty} < m, N+1|\hat{\Phi}^\dagger|m, N >= 0. \tag{15.15}$$

The density matrix $N\rho(t;\vec{r}_1,\vec{r}_2) =< m, N|\hat{\Psi}^\dagger(t,\vec{r}_2)\hat{\Psi}(t,\vec{r}_1)|m, N >$ can be written with use of Eq. (15.13)

$$N\rho(\vec{r}_1,\vec{r}_2) = n_0 + N\rho'(\vec{r}_1,\vec{r}_2). \tag{15.16}$$

With help of Eq. (15.10) one sees

$$\rho'(\vec{r}_1,\vec{r}_2) = \sum_{p\neq 0} \hat{a}_p^\dagger \hat{a}_p e^{\frac{i}{\hbar}\vec{p}(\vec{r_2}-\vec{r_1})} \to \int_{p\neq 0} d\tau n_{\vec{p}} e^{\frac{i}{\hbar}\vec{p}(\vec{r_2}-\vec{r_1})} \tag{15.17}$$

for $V \to \infty$ and thus $\rho'(\vec{r}_1, \vec{r}_2) \to 0, |\vec{r_1} - \vec{r_2}| \to \infty$.
Since ρ is finite and non zero in the limit of $|\vec{r_1} - \vec{r_2}| \to \infty$ the liquid will have long range ordering.
It is very important to note that the condensate density mn_0 and the superfluid density ρ_s do not correspond. For superfluid Helium at $T = 0$ one finds $\frac{n_0}{n} \sim 10\%$ whereas $\frac{\rho_s}{\rho} = 1$ because of Galilean invariance.

15.1.4 PHASE TRANSITION

As seen before Helium undergoes condensation into a single particle wave function below T_λ. Thus the phase relation between the particles in the condensate is fixed and by choosing a phase for the condensate wave function the $U(1)$ symmetry of the system is spontaneously broken in the phase transition.
When having superfluid flow the BEC can not be claimed to be in the $p = 0$ wave function. So Ξ will now become a function of space and time and can be written as

$$\Xi(t, r) = \sqrt{n_0(t, r)} e^{i\phi(t,r)} \tag{15.18}$$

and can be considered as a wave function for the condensate. Since $\Xi(t, r) \equiv 0$ for $T > T_\lambda$ this quantity is the ordering parameter[6]. It goes to zero continuously hence the phase transition will be of second order.
The ordering parameter is complex and the phase transition is of in λ-transition universality class as the three dimensional XY model.
The critical exponent describing the behavior of the specific heat in the vicinity of the phase transition α ($C_v \propto (T - T_\lambda)^{-\alpha}$) for this phase transition is ought to be best measured by a space shuttle experiment [5] to $\alpha = -0.01285 \pm 0.00038$, which is very close to theoretical predictions by perturbation theory [6] that calculate it to $\alpha = -0.01294 \pm 0.00060$, i.e. the specific heat remains finite at T_λ.

15.1.5 SUPERFLUID VELOCITY

The mass current $\vec{j}_{con}$ can be calculated via

$$\vec{j} = \frac{i\hbar}{2m}(\Xi^* \nabla \Xi - \Xi \nabla \Xi^*) = n_0 \frac{\hbar}{m} \nabla \phi. \tag{15.19}$$

With Eq. (15.18) one defines the superfluid velocity to be proportional to this current thus

$$\vec{v}_s := \frac{\hbar}{m} \nabla \phi. \tag{15.20}$$

---

[6] Both its real and imaginary part are ordering parameters.

The potential of the velocity is the phase of the condensate wave function thus it is an irrotational flow ($\nabla \times \vec{v}_s = 0$). The amplitude of the condensate wave function (the amount of particles that undergo BEC) is not important for the effect of superfluidity.
The superfluidity itself is not an observable but the current $\vec{j} = \vec{v}\rho = \vec{v}_s\rho_s + \vec{v}_n\rho_n$ is.
The superflow in Helium is a response to the phase of the condensate and, in three spatial dimension, both phenomena go hand in hand. There are Bose-Einstein condensates that do not show a superfluid response and, in the two dimensional case, superfluidity occurs without condensation.

ONSANGER-FEYNMAN QUANTIZATION

Calculating the flux $\oint \vec{v}_s d\vec{l} = \frac{\hbar}{m}\Delta\phi$ and taking into account that the phase of the wave function is just defined modulus $2\pi n, n \in \mathbb{Z}$, one derives the Onsanger-Feynman quantization

$$\oint \vec{v}_s d\vec{l} = n\frac{h}{m}. \tag{15.21}$$

For a simply connected region it follows that $n = 0$.
In a normal fluid the vorticity as defined in Eq. (15.21) can take any value whereas its value in the superfluid case has to be multiples of $\frac{h}{m}$. This has important consequences.

VORTICES

The case $n \neq 0$ in Eq. (15.21) can only be realized only in a not simply connected area. One introduces vortices (either closed loops or ending at the surfaces) where the velocity field has a divergence ($v_s \propto \frac{1}{r}$ where r is the distance to the vortex [3]) but the wave function is vanishing so this divergence does not cause any problems thus we define v_s in every point outside the vortex. From a macroscopical viewpoint the vortex is infinitely small.
Consider a rotating cylinder with radius R with liquid Helium inside rotating at $\vec{\omega} = (0, 0, \omega)$ parallel to the symmetry axis. The energy in the rest frame of the Helium is given by

$$E_{rot} = E - M\omega. \tag{15.22}$$

The goal is to find a ω_c such that for $\omega > \omega_c$ the appearance of vortices is favored. Because of the symmetry of the system the vortex has to be parallel to the symmetry axis. The energy difference in the presence of a vortex is given by the increase in kinetic energy due to the motion of the superfluid,

$$\Delta E_V = \int \frac{\rho_s v_s^2}{2} d^3r = L\rho_s \pi \left(\frac{nh}{m}\right)^2 \ln\frac{R}{a} \tag{15.23}$$

where L is the length of the vortex, a is its diameter[7] of a vortex.
The increase in angular momentum decreases E_{rot} and is given by

$$M_s = \int \rho_s v_s r d^3r = L\pi R^2 n \frac{\hbar}{m} \rho_s. \tag{15.24}$$

ω_c is obtained by solving $M\omega_c = \Delta E_V$. One finds

$$\omega_c = n^2 \frac{\hbar}{mR^2} \ln\frac{R}{a}. \tag{15.25}$$

Vortices with $|n| > 1$ are metastable because $\Delta E_V \sim n^2$ but $M_s\omega \sim n$ thus two vortices with vorticity 1 will be favourable for an vortex with vorticity 2.
Fig. 15.4 shows photographs of the of vortices in liquid Helium.

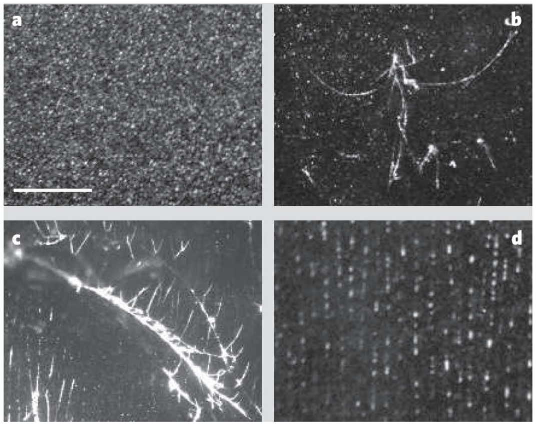

Figure 15.4: Visualization of vortices in liquid Helium with hydrogen particles of size $\sim 2.7\mu m$[7]. $T > T_\lambda$: a) The particles are uniformly distributed in the liquid. $T < T_\lambda$: b) - c) Tens of millikelvin below T_λ and the hydrogen particles accumulate at the cores of vortices (that are thermally excited). d) The vortices are grouping in equally spaced lines parallel to the rotational axis. The axis of rotation is in the image plane parallel from top to bottom. White bar in a) is the scale ($1\,mm$).

Consider now a gedankenexperiment where liquid Helium flows in an annular channel between two cylinders with radii $r_1 < r_2$ rotating with $\vec{\omega}$ parallel to

---

[7] $a \sim 10^{-10}m$. It is important that it has a finite value due to the finiteness of ΔE_V and can no longer be assumed to be 0.

its symmetry axis. The scalar velocities in the following are the circumferential components of the vectors.

For $T > T_\lambda$ the liquid behaves like a classical one with a velocity field $v_n(r) = \omega r$ where the velocity of the liquid at the boundary equals the boundaries velocity $v_n(r_2) = v_{wall}$. The moment of intertia is $I_{cl}\omega$.

Consider cooling down below T_λ. The region is not simply connected thus $n \neq 0$ is possible even if there are no vortices present. i.e. $\omega < \omega_c$.

The angular velocity of the superfluid is measured in units of $\omega' = \frac{\hbar}{mR^2}$ ($n = 1$ in Eq. (15.21).). Since the quantization of the circulation in Eq. (15.21) the superfluid velocity can not build a velocity field similar the the normal component. It is found that the angular velocity of the superfluid Helium will be given by $\omega_s = n\omega'$ where n is determined as the integer closest to $\frac{\omega}{\omega'}$. The angular velocity of the superfluid can even exceed the one of the cylinders, e.g. if $\omega = 0.75\omega'$[4].

The total angular of momentum when cooling below the critical temperature is reduced by $\frac{\rho_n(T)}{\rho}$. Hence, one can tune the angular momentum of the configuration by varying T.

This effect is known as the “Hess-Fairbank” effect.

15.2 Supersolid Helium

At pressures above $\sim 26\,bar$ Helium can form a crystal, as shown in Fig. 15.1. In the following the hcp (hexagonal close packing) phase will be discussed. The hcp structure is drawn schematically in Fig. 15.5.

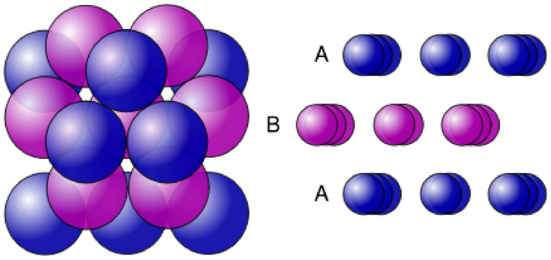

Figure 15.5: Schematic drawing of the hcp structure.

15.2.1 Observations / Experiments

Kim-Chan Experiment

In analogy to the Andronikashvili experiments (disks rotating in superfluid Helium) the response of solid Helium to a rotation is observed. E. Kim and E. W.

H. Chan (KC)[8] carried out such experiments in 2004.
The setup is shown in Fig. 15.6. Helium of ultra high purity (^{3}He of 0.3 ppm[8]) is filled into the annular channel of a torsion cell and is solidified. The nonclassical rotational inertia fraction (NCRIF) is the difference in the moment of inertia divided by the classical moment $\frac{\Delta I}{I_c}$. The result is shown in Fig. 15.7. As one can see the NCRIF is equal to zero for $T > 200\,mK$ and then rapidly increases until it saturates at $T \approx 40\,mK$. The experiment was carried out at different maximal velocities (v_{max} is the maximal velocity at the maximum radius of the annular channel).
This can be interpreted as some part of the solid decouples from the motion. For small velocities the NCRIF saturates at the same value. So one can assume that there exists a critical velocity under which the decoupling can take place; thus the NCRIF for small velocities can be interpreted as the fraction of the supersolid and the total density because $I \propto \rho$ thus $\frac{\Delta I}{I_c} = \frac{\rho_s}{\rho}$.

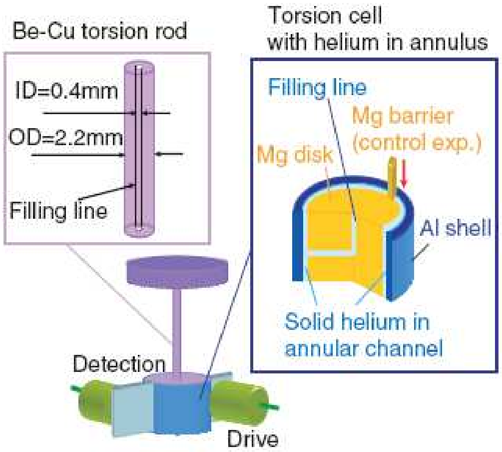

Figure 15.6: Setup of KC experiment.[8]

To make sure that this observation is related to a superflow decoupling from the rotation a control experiment with a blocked annulus is carried out and the NCRIF is suppressed.
So the phase diagram is amended as drawn in Fig. 15.8 under the assumption that there is a phase transition from a normal crystal to one with a new ground state featuring superflow.
The transition temperature shows only a weak dependence on pressure in the limits of $315\,mK$ ($26\,bar$) and $230\,mK$ ($40\,bar$) with supersolid fractions of $1 - 10\,\%$.

---

[8] It turns out that this effect is very sensible to the impurity due to ^{3}He.

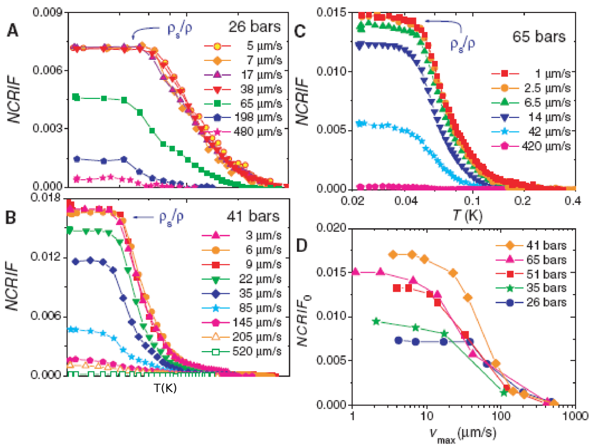

Figure 15.7: A-C: Measurement of NCRIF of Kim and Chan as a function of temperature. The different lines correspond to different maximal velocities. D: Measurement of NCRIF as function of maximal velocity v_{max}[8]

Quality of the Crystal

The KC experiment was repeated by other experimentalists. It was observed that the appearance of NCRIF was related to the quality of the crystal. If it was annealed (melted, refrozen, etc.) the supersolid behavior was weakened and vanished for a fully annealed crystal[9].

This leads to the conjecture that supersolidity is not an universal property but that one can create samples of solid Helium that do not show non-classical behavior in torsional experiments.

Communicating Vessels

Further investigation on the depedence of the quality of the crystal are carried out by relaxation of a crystal with different hights. The experimental setup[10] consists of a certain volume with a tube in it. In this volume and the tube solid Helium is in equilibrium with its liquid phase but the levels in the tube and the rest of the volume differ ($h(t)$) as drawn in Fig. 15.9; the top of the tube is closed. If mass is able to flow frictionless the levels will relax.

One observes the following (at temperatures comparable to those of the Kim-Chang experiments):

- Crystals of good quality (few grain boundaries, defects, etc.) show no mass flow. The upper bound of the velocity (due to errors) differs from the expectation by Kim-Chan by a factor of 300.

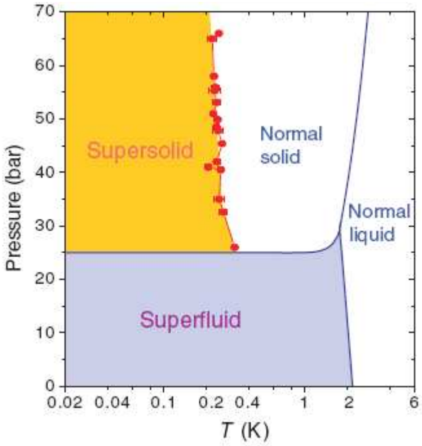

Figure 15.8: Phase diagram by Kim and Chan.[8]

- In some samples one observed cusps in this sample and relaxation took place as long as the cusps disappeared.
- If a relaxation takes place, $\dot{h}(t) = const.$ A viscous fluid would have shown an exponential decay wheres a constant flow indicates a superflow at its critical velocity.
- The more cusps the faster the relaxation.

15.2.2 Models

Zero Point Vacancies

The classic model of a crystal proposes an integer number of atoms per unit cell - the crystal is commensurate and thus insulating because it does not feature off-diagonal long range order as it is discussed below. If one drops this assumption the ground state can have vacancies (empty lattice points in the crystal) if their activation energy is not positive (gapless vacancies)[11].
Only zero-point vacancies or interstitials can make an ideal crystal supersolid. This is necessary because one must have (restricting to single-particle effects) off-diagonal long range order (ODLRO) that is defined as

$$\int n(\vec{r}, \vec{r}')d^3r \to \infty \tag{15.26}$$

in the thermodynamic limit[11] where $n(\vec{r}, \vec{r}') = \prod_{i\geq 2}^{N} \int d^3r_i \Psi_G(\vec{r}, \vec{r_i})\Psi_G(\vec{r}', \vec{r_i})$ is the single-particle density matrix with N denoting the total number of particles and Ψ_G the wave function of the ground state.

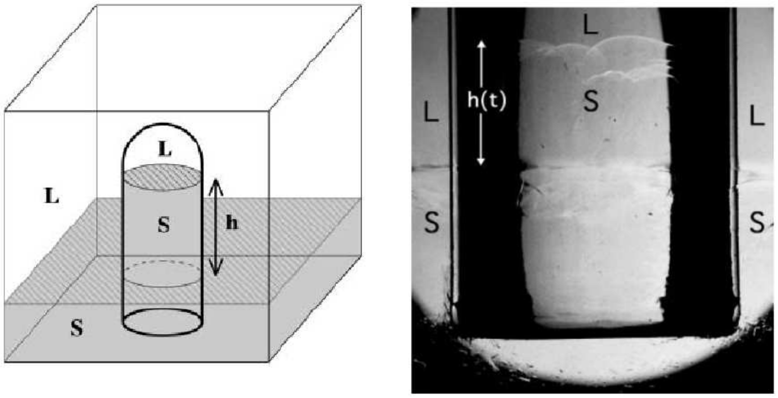

Figure 15.9: Left: Experimental setup of a crystall grown to a different height in a tube, Right: Photo of solid Helium at 1.3 K. L = liquid, S = solid phase.[10]

By using path-integral Monte Carlo simulations [11] [1] in complex time ($\tau = it$) one investigates the behavior of the density matrix and the time dependent zero-momentum Greens function G that is the two-point correlation function n in the zero-time limit via $n(\vec{r}) = G(\vec{r}, \tau \to 0_-)$.

$$G(\vec{r}, \tau) = \langle \Phi(\vec{r}, \tau) | \Phi(0, 0) \rangle \tag{15.27}$$

thus $G(k, \tau)$ is the Fourier transform of $G(\vec{r}, \tau)$. The zero-momentum value is just the integral over all positions since $G(k, \tau) \sim \int d^3r \, G(\vec{r}, \tau) e^{-i\vec{k}r}$ hence

$$G(k = 0, \tau) \sim \int d^3 r G(\vec{r}, \tau). \tag{15.28}$$

Numerical results from such simulations are shown in Fig. 15.10. Both quantities decay exponentially and the activation energy for an interstitial or a vacancy is very large ($\sim 23\,K$ for an interstitial and $\sim 13\,K$ for a vacancy) compared to the temperature of $T = 0.2\,K$ where the simulation is performed. The energy gap for creating an interstitial Δ_{I} or a vacancy Δ_{V} is calculated by fitting $G(k = 0, \tau) \propto e^{-\Delta_{\mathrm{V/I}}|\tau|}$ to the numerical data.

The possibility for the true ground state to consist of a larger number of vacancies is not ruled out by these observations but further Monte Carlo simulations in which a certain number of vacancies were forced in the crystal show a strong attraction between these vacancies so they phase separate from the bulk crystal[11]. The result of these simulations is that the true ground state of an ideal ^{4}He-crystal is the insulating and commensurate hcp-phase.

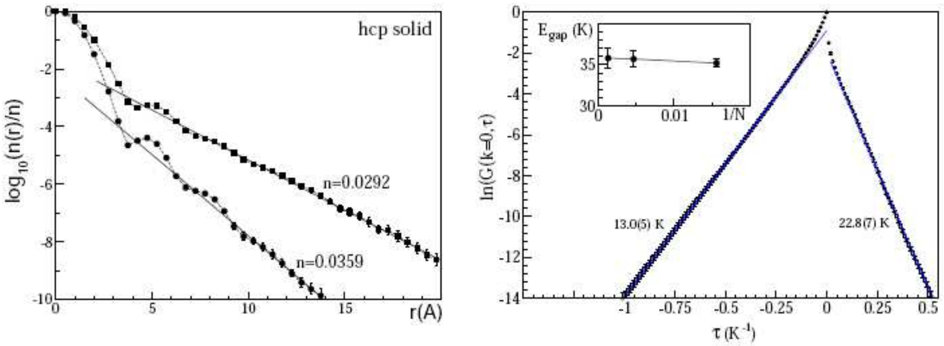

Figure 15.10: Simulation results for hcp-crystal with $N = 800$ atoms. Left: Density matrix at $P = 32\,bar$ for different particle densities ($[n] = \mathring{A}^{-3}$). Right: Zero-momentum Green function for zero momentum. The left graph represents vacancies and the right interstitial. The energy gap of an interstitial Δ_I or a vacancy Δ_V is calculated by fitting $G(k = 0, \tau)$ with the ansatz $G \sim e^{-\Delta|\tau|}$. Inset: Energy gap as $\Delta_\mathrm{I} + \Delta_\mathrm{V}$ versus system size. Since this is constant the finite and positive E_gap is not a finite size effect. [11]

Inhomogeneous Theory

Besides scenarios of a homogeneous crystal, the presence of disorder (e.g. grain boundaries, dislocations and other defects) might explain the phenomenon of supersolid Helium[12]. These approaches are strongly supported by the observation of grain boundary superflow in the communicating vessel experiment or by the experiments where the quality of the crystal was altered by annealing.
Grain boundary superfluidity in lower dimensionality might be achieved by placing two samples next to each other. A proof-of-principle study on superflow in solids due to interfaces between crystallites[12] was done numerically. It could be shown that a quantum phase transition of superfluid-insulator phases may exist.

Bibliography

[1] Ceperley, D.M. , *Path integrals in the theory of condensed helium*, Rev. Mod. Phys. **67**, 279 (1995).

[2] T. Fliessbach, *Statistische Physik, Lehrbuch zur theoretischen Physik IV* (Spektrum Akademischer Verlag, Heidelberg, Berlin, Oxford, 1995).

[3] Lifschitz, E.M. and Pitajewski, L.P. , *Lehrbuch der statistischen Physik IX, Statistische Physik, Teil 2* (Akademie-Verlag Berlin, Berlin, 1989).

[4] Leggett, A. J. , *Superfluidity*, Rev. Mod. Phys. **71**, 318 (1999).

[5] Lipa, J. A. , Swanson, D. R., Nissen, J.A., Chui, T. C. P. and Israelsson, U. E. , *Heat capacity and thermal relaxation of bulk helium very near the lambda point*, Phys. Rev. Lett. **76**, 944 (1996).

[6] Kleinert, H., *Critical exponents from seven-loop strong-coupling ϕ^4-theory in three dimensions*, Phys. Rev. D **60**, 085001 (1999).

[7] Bewley, G. P., Lathrop, D. P. and Sreenivasan, K. R. , *Visualaziation of quantized vortices*, Nature **441**, 588 (2006).

[8] Kim, E. and Chan, M. H. W., *Observation of superflow in solid helium*, Science **305**, 1941 (2004).

[9] Rittner, A. S. C., Reppy, J. D. , *Observation of Classical Rotational Inertia and Nonclassical Supersolid Signals in Solid ^{4}He below 250mK*, Phys. Rev. Lett. **97**, 165301 (2006).

[10] Sasaki, S., Ishiguro, R., Caupin, F. , Maris, H. J. and Balibar, S. , *Superfluidity of grain boundaries and supersolid behavior*, Science **313**, 1098 (2006).

[11] Prokof'ev, N.V., *What makes a crystal supersolid?* (2006), (cond-mat/0612499).

[12] Prokof'ev, N.V. and Svistunov, B.V. , *On the supersolid state of matter* (2004), (cond-mat/0409472).